38th Annual
RESEARCH DAY



Friday, November 13, 2026

The Office of Research and the Research Advisory Committee would like to thank this year's sponsors for their generous contributions to Research Day, 2026.

Presenting Sponsor

Langley Federal Credit Union

Corporate Sponsors

Illumina

Door Prize Donations:

The ODU Graduate School

Thank you!

A special note of appreciation and gratitude goes to



Alfred Abuhamad, MD
Executive Vice President of Macon & Joan Brock Virginia Health Sciences
at Old Dominion University



Judette Louis, MD, M.P.H.
Dean of Eastern Virginia Medical School
Macon & Joan Brock Virginia Health Sciences at Old Dominion University

and the Research Advisory Committee
for the Administrative and Research Community support of Research Day.

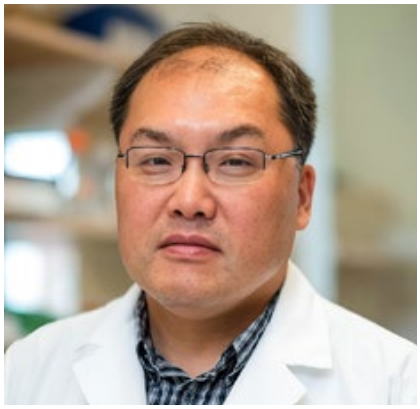
Special appreciation and gratitude
for their support of Research Day 2026
are also extended to the

Office of Research Leadership:



Milton L. Brown, MD, Ph.D., FNAI

Professor, Internal Medicine,
Sr. Associate Vice President of Research
Prudence and Louis Ryan
Endowed Chair of Research



David Mu, Ph.D.

Professor, Dept. of Biomedical
& Translational Sciences
Associate Dean for Research Administration

and the
Research Advisory Committee Leadership:



Paul Harrell, Ph.D.

Research Advisory Committee Chair
Associate Professor, Dept. of Pediatrics
Division of Community Health & Research



Lifang Yang, MD, Ph.D.

Research Advisory Committee Vice Chair
Assistant Professor,
Dept. of Biomedical & Translational Sciences,
Division of Tumor Biology
Leroy T. Cancer Jr. Cancer Research Center

Support for research travel and publications for trainees are made possible by funding mechanisms managed by the Office of Research and Medical Student Research.

Of special note, we would like to highlight the following resources:

EVMS Community Faculty Designated Student/Resident/Fellow Research Award

Travel Award: This travel award seeks to recognize and promote scholarly activity by trainees at Macon & Joan Brock Virginia Health Sciences at Old Dominion University. Up to eight awards of $1,500 each are available each fiscal year to support trainee travel to a regional, national, or international academic conference to present research. To be eligible, applicants must present at an academic conference and prepare a submission quality manuscript for publication. Those interested in being considered for this award should contact the Office of Research for more information.

Publication Award: This publication award provides funding to students, residents, and fellows at Macon & Joan Brock Virginia Health Sciences at Old Dominion University who have submitted a manuscript for publication. This award provides up to $500 in reimbursement for costs incurred while publishing, up to the maximum award amount. Those interested in being considered for this award should contact the Office of Research for more information.

Medical Student Research Award

Travel Award: Provided through the Office of Medical Student Research for any medical students looking to travel to regional, national, or international academic conferences. This award is available to 2nd–4th year medical students and runs on a structured cycle system, with active funding cycles from September 2026 through March 2027, giving students clear windows to apply as you plan conference travel. Interested students must submit the ***MSR Travel Reimbursement Request Form*** before they travel and within the appropriate cycle.

For more information about these awards or the application process, students, residents, and fellows can contact the Office of Research at ***VHS-EVMSResearch@odu.edu***.





38th Annual Research Day
Presented by Langley Federal Credit Union

November 13, 2026
Waitzer Hall
Macon & Joan Brock Virginia Health Sciences at Old Dominion University

Timeline of Events

Connection information and more on the Research Day website:
https://www.odu.edu/virginia-health-sciences/research-day

Sponsor, Service Provider, and Core Facility Exhibition

12:30 - 5:30 PM **In person:** Waitzer Hall, rooms 100 and 200

Opening Remarks, Faculty Awards, and Keynote Address

11:15 AM - 12:50 PM **In person:** Waitzer Hall, room 300 | **Pizza lunch** will be served
Remote: Join via link on the Research Day website

Opening Remarks

11:30 -11:45 AM Dr. Paul Harrell, EVMS Research Advisory Committee Chair
Dr. Alfred Abuhamad, Executive Vice President of Virginia Health Sciences at ODU
Dr. Judette Louis, Dean of Eastern Virginia Medical School

Presentation of Faculty Awards

11:45 AM -12:00 PM Early Career Research Excellence Award
Presented by Dr. Paul Harrell, Research Advisory Committee Chair

Excellence in Research Mentorship Award
Presented by Dr. Lifang Yang, Research Advisory Committee Vice Chair

Junior Clinical Investigator Program (JCIP)
Presented by Dr. David Mu, Associate Dean for Research Administration

Keynote Speaker

12 -12:45 PM Introduction of Keynote Speaker
Dr. Paul Harrell, Research Advisory Committee Chair

Larry Sanford, Ph.D.
Professor, Department of Biomedical and Translational Sciences
Macon & Joan Brock Virginia Health Sciences at Old Dominion University
Topic: ***Sleep, Stress, Learning, Memory, and the Immune System: Reflections on Complex Drivers of Health***

12:45 - 12:50 PM **Keynote Door Prize raffle drawing** and event announcements

Short Break – Visit Sponsor, Service Provider, and Core Facility Tables

12:50 - 1:00 PM **In person:** Waitzer Hall, rooms 100 and 200

Poster Session A

1:00 - 2:00 PM **In person:** Waitzer Hall, rooms 100 and 200
Refreshments served and **Raffle Tickets** distributed in both rooms

Posters 1A – 47A are in room 100, Posters 49A – 72A are in room 200

Short Break – Visit Sponsor, Service Provider, and Core Facility Tables

2:00 - 2:15 PM **In person**: Waitzer Hall, rooms 100 and 200

Platform (Oral) Presentations

2:15 - 3:35 PM **In person:** Waitzer Hall, room 300 | **Hot beverages** served
Remote: Join via link on the Research Day website

Hot Beverages Served and Door Prize Tickets Distributed beginning at 2:00 PM

Continued on next page

2:15 -2:29 PM **Nima George**, Biomedical Sciences Graduate Student
Angiotensin II receptor blockade is associated with lower cancer cachexia, while the triple-action conjugate YK-4-250 attenuates skeletal muscle atrophy in vitro
Mentor: Milton L. Brownj, MD, Ph.D.

2:30-2:44 PM **Kylie Lopez**, MD Student
Comparative Genomic Characterization of Cholangiocarcinoma and Gallbladder Adenocarcinoma
Mentor: Winifred Lo, MD

2:45-2:59 PM **Cynthia Monroe**, MD student
Multimodality Imaging of a Jugular Paraganglioma: A Case Report
Mentor: John Campbell, MD

3:00-3:14 PM **Ca Nguyen**, MD student
Digital cognitive behavioral therapy (dCBT-I) for psychiatrically acute adolescents with suicidal ideation and co-occurring insomnia: An open pilot of intervention feasibility and acceptability
Mentor: Cassie Glenn, Ph.D.

3:15-3:29 PM **Alyssa Reese, MD**, Plastic Surgery Resident
Trends in Pediatric Craniofacial Injuries Associated with Electric Bicycle and Scooter Use in the United States 2016-2025: An Emerging Public Health Challenge
Mentor: Lambros Viennas, MD

3:30 - 3:35 PM **Platform Presentations Door Prize raffle drawing** and event announcements

Short Break – Visit Sponsor, Service Provider, and Core Facility Tables

3:35 - 3:50 PM **In person:** Waitzer Hall, rooms 100 and 200

Poster Session B

3:50-4:50 PM **In person:** Waitzer Hall, rooms 100 and 200
Refreshments served and **Raffle Tickets** distributed in both rooms
Posters 1B – 48B are in room 100, Posters 49B – 74B are in room 200

Short Break – Visit Sponsor, Service Provider, and Core Facility Tables

4:50 - 5:15 PM **In person:** Waitzer Hall, rooms 100 and 200

Poster Session Raffle Drawing, Presentation of Poster Awards and Closing Remarks

5:15 - 5:30 PM **In person:** Waitzer Hall, Room 300

Announcements and Poster Session Raffle Drawing

Poster Awards
Presented by Dr. Paul Harrell and Dr. Li Fang Yang
Virginia Health Sciences Research Advisory Committee Chairs

People's Choice Poster Award
Presented by Dr. Lifang Yang
Virginia Health Sciences Research Advisory Committee Vice Chair

Closing Remarks
Dr. Paul Harrell
Virginia Health Sciences Research Advisory Committee Chair

Save the Date NOW! Research Day 2027 will be Friday, October 8, 2027.
Abstracts will be due in early late July/early August.

Research Day Etiquette

All VHS students should plan to participate in Research Day, particularly the poster session, even if not presenting. Non-presenting students should attend to support classmates' research activities – and help them to hone their communication skills – by listening to presentations and asking engaging questions about the projects.

We look forward to seeing everyone on Research Day!

Research Day Faculty Awards

On Research Day, the winners will be announced for two Research Day awards for faculty researchers as well as the new fellows for the Junior Clinical Investigator Program (JCIP).

Early Career Research Excellence Award

The Early Career Research Excellence Award is presented each fall at VHS Research Day to honor and recognize legacy EVMS early career researchers or clinician scientists who have exhibited a significant contribution to their discipline through widely disseminated and impactful research relatively early in their academic careers.

This award recognizes the individual's outstanding research achievements, innovative approaches, influence within their academic field and potential for continued excellence. It serves not only as recognition of their early accomplishments, but also as an encouragement to continue striving for research excellence throughout their academic careers.

Excellence in Research Mentorship Award

The Excellence in Research Mentorship Award is presented each fall at VHS Research Day to one mid-career or senior member of the legacy EVMS faculty who has exhibited robust excellence in research mentorship. This award recognizes the accomplishments of medical school faculty who have demonstrated exceptional mentoring in research to junior faculty, fellows, post-docs, and/or student trainees.

The Junior Clinical Investigator Program (JCIP)

The Junior Clinical Investigator Program (JCIP) is a competitive three-year training program providing career advancement opportunities to select research faculty interested in academic medicine. This year, we will recognize three new fellows accepted into this program.



2026
KEYNOTE LECTURE

Sleep, Stress, Learning, Memory, and the Immune System: Reflections on Complex Drivers of Health



Larry Sanford, Ph.D.

Professor,
Department of Biomedical and Translational Sciences
Macon and Joan Brock Virginia Health Sciences
at Old Dominion University

People's Choice Award

The People's Choice Award started in 2025 for attendees to vote for the "best" poster.

Voting Instructions

- View the poster and talk with the presenter
- Scan the unique QR code that is displayed on the board
- Complete the brief survey to provide your ratings for that poster

You may rate multiple posters, but you may only rate each poster **once**.

Wi-Fi Connection Information

ODU Students, Faculty, and Staff

Network: eduroam
Username: your ODU email address
Password: your MIDAS password

Android Users
EAP method: PEAP
Identity: your ODU email address
Password: your MIDAS password
CA certificate: don't validate

Guests
Visitors affiliated with participating eduroam institutions
Select the **eduroam** wireless network
Login with your organization's credentials

All other visitors

Wi-Fi information and credentials will be provided at the in-person event

Save the Date

Research Day is Returning to the 2nd Friday in October!

MARK YOUR CALENDARS NOW!

Research Day 2027

Will be held on
Friday, October 8, 2027

Research Day 2028

Will be held on
Friday, October 13, 2028

Abstracts will be due in late July/early August

POSTER PARTICIPANTS

Biomedical Sciences

RESEARCH (M.S.)

Joanna Marie Camacho, B.S. 15
Ashlynn Monique Knight, B.S. 16
Nicholas Richards, B.S. 17
Dominic Ray Stone, B.S. 18

MEDICAL (MED MASTER'S)

Sierra M. DePry, B.A. 19
Yuvateja Kocherla, B.S. 20
Veronika Murphy, B.S. 21

Ph.D. STUDENTS

Afia Salsabil Alam, B.S. 22
Adnan Alsamaraee, B.S. 23
Asa Renita Britton-Jenkins, M.S. 24
Alex T. Cain, B.S. 25
Paul Cheddie, B.S. 26
Alyssa Costello, B.S. 27
Nima George, B.S. 28
Yara Khodour, B.S. 29
Samantha McGuire, B.S. 30
Sara B. Palega, M.S. 31
Emilee Peterson, B.S. 32
Davin Stevenson, B.S. 33
Jonathan Edward Waldron, B.S. 34
Ryan Keon Washington, B.S. 35
Arielle Wolter, Ph.D. 36

Ellmer College of Health Sciences

Taskina Akhter, M.S. 37
Jessica S. Gebert, M.S., CF-SLP. 38
Josh Lawton, M.S. 39
Amin Mohammadi, M.S. 40
Ella Onsoriasl, M.S. 41
Reza Pousti, Ph.D., M.S. 42
Paphawee Prupetkaew, M.S. 43
Paul Sarac, M.S. 44
Ian P. Winter, M.S. 45

Joint School of Public Health

Omotomilola Jegede, M.S. 46
Amija Reed, B.S. 47

Other Graduate Students

Patricia E. Guereque, B.S. 48
Bryan A. Hawickhorst, M.S. 49
Gamanuel Jean, M.P.H. 50
Vonda M. McKeithan, B.S. 51
Mohamad Najafi, M.S. 52
Nikki B. Towns, M.P.H. 53

Postdoctoral Researchers

Abdul Ahad, MBBS 54
Jonathan M. Baker, Ph.D. 55
Shivangi Gupta, Ph.D. 56
Alina Moriarty, Ph.D. 57
Alina Moriarty, Ph.D. 58
Megan A. G. Sage, Ph.D., M.S. 59

Research Staff

Peter Scheible, B.S. 60
Keeley Yokley, MPH, B.S.W. 61

Residents and Clinical Fellows

Raeed W. Bari, MD 62
Nicholas B. D'Alessandro, MD 63
Ahmed Ismail, MD 64
Ahmed Ismail, MD 65
Mikaela Kcomt, MD 66
Mikaela Kcomt, MD 67
Karen Elizabeth Kennamer, B.S. 68
Kyle Nguyen Le, MD 69
John Paul Lyons, MD 70
Bijan Morshedi, MD 71
Juan Munoz-Moreno, MD 72
Juan Munoz-Moreno, MD 73
Yara Bassam Mohammed Nawaiseh, MD 74
Alyssa Reese, MD 75
Hira Sarfraz, MD 76
Muhammad Tamoor Shaikh, MD 77
Dillon Woody, MD 78

Medical Students

Gabriella Marie Adams, B.S. 79
Adam Akari, M.S. 80
Kevin Alterman, B.A. 81
Chase Armstrong, B.S. 82
Aravindan Balaguru, B.S. 83
Madison Baldauf, B.S. 84
Madison Baldauf, B.S. 85
Alexis Boscia, B.S. 86
Ethan S. Casto, B.S. 87
Wayne Jay Cochran, II, B.S. 88
Wayne Jay Cochran, II, B.S. 89
Avin Ryan Curtis, B.S. 90
Ethan Ding, B.S. 91
Moumen Elbakary, B.S. 92
Julia Feord, B.S. 93
Juan Emilio Ferrando, B.S. 94
Juan Ferrando, B.S. 95
Peter Andrew Gahan, B.S. 96
Jillian Gallardo, B.S. 97
Hailey M. Gauck, B.S. 98
Angela Goyal, B.S. 99
Austin Grove, B.S. 100
Elizabeth Harvie, B.A. 101
Eric C. Hayes, B.S. 102
Lauren Hill, B.S. 103
Gavin C. Hughes, B.S. 104
Emily Inzer, B.S. 105
Kirsten Johnson, M.S. 106
Ria Kapoor, B.S. 107
Ria Kapoor, B.S. 108
Alden I. Kaufman, M.S. 109
Zaid S. Khan, M.S. 110
Zaid S. Khan, M.S. 111
Sarah A. King, B.S. 112
Emily E. Lessard, B.S. 113
Shinjer Li, B.S. 114
Kylie Alise Lopez, B.S. 115
Haley Lundeen, B.S., B.A. 116
Brian Luong, B.S. 117
Camilla Macia, B.S. 118
Ryan Mancoll, B.S. 119
Baylee Marin, B.S. 120
Mariana Meade, B.S. 121
Oleksandra Melchers, M.S. 122
Cynthia L. Monroe, B.S. 123
Cynthia L. Monroe, B.S. 124
Kevin Moran, M.S. 125
Kevin Moran, M.S. 126
Joel Moses, B.A. 127
Emily Mungovan, B.A. 128
Raj Vinayak Nair, B.S. 129
Thien-Phuoc (Janesah) Dang Ngo, B.S. 130

Ca Nguyen, B.A. 131
Himali Patel, M.S. 132
Himali Patel, M.S. 133
Anjani Patibandla, B.S. 134
Katherine Pepper, B.S. 135
Christian Pfeffer-Kleemann, B.A. 136
Christian Pfeffer-Kleemann, B.A. 137
Nicholas J. Popolizio, B.A. 138
Phillip Jennings Poppas, B.S. 139
Maria Puglese, B.S. 140
Niya Lucille Rhodes, M.S. 141
Samantha D. Riley, B.S. 142
Owen Matthew Rolph, B.S. 143
Andrei Sanda, B.A. 144
Eleanor (Ellie) Schonberg, M.S. 145
Matthew Serrata, B.S. 146
Anyah Skipwith, M.S. 147
Darel Connor Snead, B.S. 148
Laura Snow, B.S. 149
Manas Tiwari, B.S. 150
Jhobani Torres-Gomez, B.S. 151
James Sajeev Vettichira, B.S. 152
Jonah Wright, B.S. 153
Ellen Wu, B.S. 154
Stefan Yu, B.S. 155
Jessica Zhang, B.A. 156

Other Presenters

Anhthu Cung, M.S. 157
Rocio Soledad Maggioni , MD 158
Chinenye Erica Udemba, B.S. 159

Cell-Surface GlycoRNAs Depletion Marks Endocrine Resistant in ER+ Breast Cancer

Investigator: Joanna Marie Camacho, B.S.
Mentor: Lifang Yang, MD, Ph.D.
Co-Authors(s):
Fanying Li, Macon & Joan Brock Virginia Health Sciences Eastern Virginia Medical School
Eric Feliberti, Sentara
Department(s): Department of Biomedical and Translational Sciences Division of Tumor Biology
Poster #: 49A

INTRODUCTION

Approximately 70-80% of diagnosed breast cancer (BC) cases present with the estrogen receptor positive (ER+) subtype. Although targeted endocrine therapies such as tamoxifen and fulvestrant are effective, a significant portion of patients experience disease recurrence due to de novo or acquired endocrine resistance. Alternations in biomolecular glycosylation (proteins and lipids) are well-known drivers of malignant progression, epithelial to mesenchymal transition (EMT), stemness, and metastasis. Recently cell-surface glycoRNAs were identified as a new class of glycosylated biomolecules with emerging roles in cell biology, including neutrophil recruitment and malignant transformation. However, the expression profile and biological significance of glycoRNAs in BC endocrine resistance remains unexplored. Here, we map the molecular landscape of glycoRNAs remodeled during the transition to endocrine resistance in ER+ BC.

METHODS

To model progressive endocrine resistance, a panel of breast cell lines including benign (MCF10A), endocrine-sensitive (MCF7), tamoxifen-resistant (MCF7-TAM1), and multi-endocrine resistant (MCF7-LCC9) were used. Cell-surface or total sialoglycoRNAs are labeled either with metabolic copper-free chemistry, or via direct periodate oxidation followed by aldehyde ligation (rPAL). Purified RNAs were isolated by TriZol or RNAzol combined with silica columns and rigorous DNA/protein digestion. The purity was validated by NanoDrop spectrophotometry and fluorometric assays. GlycoRNA size distributions, glycan structures, and enzymatic requirements were characterized using size fractionation (>200 vs <200 nts), targeted glycosidase/nuclease digestions, and Northern Blot analysis with SYBR Gold and streptavidin-conjugated fluorophores.

RESULTS

RNA with high purity (A260/280 ≥ 2.0; RIN > 9.0) was routinely isolated from all breast cell lines. SialoglycoRNAs were readily detected in benign MCF10A and endocrine-sensitive MCF7 cells but were markedly reduced or undetectable in endocrine-resistant variants (MCF7-TAM1 and MCF7-LCC9), revealing an inverse correlation between cell-surface glycoRNA abundance and endocrine resistance/malignancy. Notably, while tamoxifen-resistant MCF7-TAM1 cells retained intracellular (total) glycoRNA signals, their cell-surface display was substantially lost. Signal sensitive to RNase but not Proteinase K confirms glycoRNA identity. Size fractionation and enzymatic digestion demonstrated that glycoRNA signal is predominantly carried by small RNAs (<200 nt) bearing N-linked glycans, with distinct shifts in both N-glycan and O-glycan alterations are seen across our resistance model.

CONCLUSION

Cell-surface glycoRNAs are displayed on non-malignant and endocrine-sensitive breast cells, and their surface expression is inversely associated with malignancy and endocrine resistance. The loss of cell-surface glycoRNA display in resistant models points to a dramatic remodeling of the surface glyco-landscape. Future studies will identify specific glycoRNA transcripts lost during disease progression and elucidate their fundamental roles in maintaining breast tissue homeostasis and endocrine sensitivity.

Acknowledgements
We thank the VHS Breast Cancer Research Foundation (BCRF) funds to support this work.

Multiomic Analysis of Staphylococcus aureus lineage-specific variation in host-pathogen interactions.

Investigator: Ashlynn Monique Knight, B.S.
Mentor: Julia Sharp, Ph.D.
Co-Authors(s):
Katelyn Cranmer, Macon & Joan Brock Virginia Health Sciences Eastern Virginia Medical School
Julius Nyalwidhe, Macon & Joan Brock Virginia Health Sciences Eastern Virginia Medical School
Department(s): Department of Biomedical & Translational Sciences, Division of Microbiology & Molecular Cell Biology
Poster #: 50A

INTRODUCTION

Staphylococcus aureus is a significant human pathogen that poses serious challenges to the healthcare system due to diverse immune-evasion strategies and its propensity for antibiotic resistance. Worldwide, it is the leading cause of skin and soft-tissue infections, osteomyelitis, septic arthritis, and infective endocarditis - originating from both community and healthcare-associated environments. Individually heterogeneous/diverse, S. aureus strains with a shared central genome are classified into Clonal Complexes (CC) based on the allelic variation of seven housekeeping genes. While the association between CC and immune evasion is not yet fully understood, the surface protein and virulence factor profiles uniquely associated with lineage may help predict pathogenic potential, gene carriage, and antibiotic resistance.

METHODS

We investigated key phenotypic and genetic variances in community associated S. aureus across three dominant lineages to distinguish CC-associated pathogenic determinants influencing distinct host-pathogen interactions to support the development of targeted treatment strategies. Previously, our lab generated two data sets using S. aureus clinical isolates: 1) Whole genome sequencing (WGS) of >120 isolates; 2) Tandem Mass Tag (TMT) Proteomic analysis of cell-wall lysates, containing staphylococcal surface proteins and bound serum proteins, extracted from 15 isolates representing CC5, CC8, CC30 ($n \geq 4$) following exposure to 10% human serum. The TMT abundance data was analyzed with QIAGEN Ingenuity Pathway Analysis (IPA) to reveal key differences and commonalities among S. aureus CCs across an array of biological pathways, molecular networks, and upstream regulatory processes based on interactions with human proteins. Comparative genomic analyses were performed using the WGS data. Galaxy and Geneious Prime were used to assemble consensus sequences and annotations across the 15 isolates to characterize the genomic variation among each CC. Annotations were used to generate a pan-genome to distinguish common and lineage-specific genotypic features, differences in gene presence, and sequence variations to develop a phylogenetic tree.

RESULTS

IPA identified an immune-evasive phenotype in CC30 distinct from CC5 and CC8 in differential enrichment of pathways involving lipid metabolism, cellular transport, and immune signaling, while also validating the array of immunosuppressive features of USA300-dominant CC8. Furthermore, comparative-genomic analysis identified key variations in antibiotic gene carriage and a conserved core genome accompanied by considerable accessory genomic variation among the analyzed isolates, strongly distinguishing CC30 from CC5 and CC8.

CONCLUSION

Together, these findings suggest that CC-associated phenotypic and genetic differences contribute to distinct host-pathogen interactions, including unique immune-evasive strategies, and may contribute to S. aureus success as a pathogen. Future studies will further characterize a subset of candidates involved in cell signaling and lipid metabolism to validate observed lineage-specific differences at the transcript level.

Myeloid Specific Deletion of MAGL Reduces Nitrogen Mustard-Induced Lung Injury

Investigator: Nicholas Richards, B.S.
Mentor: Nagaraja Nagre, Ph.D.
Co-Authors(s):
Balaji Srinivas, Macon & Joan Brock Virginia Health Sciences Eastern Virginia Medical School
Ryan Washington, Macon & Joan Brock Virginia Health Sciences Eastern Virginia Medical School
Department(s): Biomedical and Translational Sciences
Poster #: 51A

INTRODUCTION
Nitrogen mustard (NM) is a potent cytotoxic vesicant and alkylating agent that can cause acute lung injury and progress to chronic pulmonary complications, including fibrosis, emphysema, and bronchiolitis obliterans. Although NM has not been used in warfare, its ease of synthesis and potential for weaponization make it a significant chemical threat. Myeloid cells play a critical role in NM-induced pathogenic responses. Previous studies have shown that inhibition of monoacylglycerol lipase (MAGL or MgII), a key enzyme of the endocannabinoid system, exerts anti-inflammatory effects. However, the role of myeloid MAGL in chemically induced lung injury remains unknown. Here, we used conditional deletion of MAGL in myeloid cells to test the hypothesis that myeloid MAGL deficiency protects against NM-induced acute lung injury.

METHODS
MAGLfl/fl, and myeloid-specific MAGL-deficient mice (MyeMAGL) were exposed to NM (0.125 mg/kg) via intratracheal administration. At 72 h post-exposure, pulmonary mechanics were assessed using FlexiVent rodent ventilator system. Bronchoalveolar lavage fluid (BALF) was collected to determine total cell counts and IL-1β concentrations by ELISA. Stat3 activation was evaluated by immunoblot analysis of phosphorylated Stat3 (P-Stat3) and total Stat3 expression in lung tissue. Lung injury was assessed by histological analysis.

RESULTS
Conditional deletion of MAGL in myeloid cells significantly attenuated NM-induced decline in lung function. Myeloid MAGL deficiency reduced BALF total cell counts, and IL-1β which were elevated following NM exposure. Immunoblot analysis showed reduced Stat3 activation in MyeMAGL lungs. Histological analysis revealed reduced lung injury in myeloid MAGL-deficient mice.

CONCLUSION
These findings demonstrate that myeloid MAGL contributes to NM-induced acute lung injury and inflammation. Targeting myeloid MAGL may represent a promising therapeutic strategy for mitigating acute pulmonary injury following NM exposure

Eradicating Chemoresistant and Metastatic Cancers by Targeting the Gatekeeper of the EGFR/K-RAS Pathway: Seven in Absentia Homolog (SIAH)

Investigator: Dominic Ray Stone, B.S.
Mentor: Amy H. Tang, Ph.D.
Co-Authors(s):
Jonathan Baker, Macon & Joan Brock Virginia Health Sciences Eastern Virginia Medical School
Andrew Howell, Macon & Joan Brock Virginia Health Sciences Eastern Virginia Medical School
Julia Wulfkuhle, George Mason University
Emanuel Petricoin III, George Mason University
Department(s): Biomedical and Translational Sciences
Poster #: 52A

INTRODUCTION

Pancreatic ductal adenocarcinoma (PDAC) and triple-negative breast cancer (TNBC) remain the deadliest forms of human cancer and represent a major unmet clinical need, particularly in the residual, relapsed, multidrug-resistant, and metastatic settings, where late-stage PDAC and TNBC are still undruggable and incurable, despite new breakthrough therapies. Targeting the most downstream gatekeeper of the oncogenic EGFR/K-RAS pathway, Seven in Absentia Homologue (SIAH), represents an innovative therapeutic strategy. Expression of a dominant-negative SIAH inhibitor of SIAHWT, hSIAH2PD, induces cell death, cellular stress, increased DNA damage response (DDR), and abolishes tumor growth in mice, i.e. xenograft and patient-derived xenograft (PDX) models of human cancer. Encouraged by these published and preliminary results, we aim to delineate the molecular mechanisms underlying tumor eradication induced by SIAH inhibition. We used reverse-phase protein array (RPPA) analysis to conduct global cancer pathway mapping and to identify statistically significant increases in DDR and apoptotic phospho-proteins/proteins. These results were validated by Immunofluorescence (IF) staining and/or Western blotting. A three-dimensional (3D) tumor growth assay in soft agar was performed to quantify the effects of SIAH inhibition on tumor growth and destruction longitudinally.

METHODS

RPPA analysis was performed in biological triplicate to identify molecular alterations in SIAH-proficient and SIAH-deficient MiaPaCa-2 and MDA-MB-231 cells. IF staining and Western blotting were performed at 3- and 7-days following DOX induction to validate statistically significant increases in several DDR- and apoptosis-associated proteins induced by SIAH inhibition. MiaPaCa-2 tumors in soft agar were grown utilizing a microplate format and subjected to longitudinal tumor tracking for 24-days utilizing the Cytation C10. ImageJ was utilized to quantify tumor volume and generate tumor growth curves. Matched brightfield and Z-stack imaging were utilized to visualize tumor morphology and GFP-tagged SIAH inhibitor expression.

RESULTS

RPPA analysis identified marked changes in DDR and apoptosis following SIAH inhibition. In MiaPaCa-2 cells, RPPA demonstrated statistically significant increases in p53S15, cleaved PARP, and cleaved caspases-3/7, which were successfully validated by IF and/or Western blotting. In MDA-MB-231 cells, RPPA analysis showed statistically significant increases in cleaved PARP and cleaved caspase-7, which were successfully validated by IF and/or Western blotting. Furthermore, longitudinal tumor tracking of MiaPaCa-2 tumoroids showed a clear tumor destruction phenotype following SIAH inhibition. Quantitative ImageJ analysis demonstrated a significant reduction in 3D tumor volume induced by SIAH inhibition ($p<0.0008$). Normalization to baseline tumor volume to account for inherent variation in initial 3D tumoroids yielded an even more statistically significant result ($p<0.000000002$).

CONCLUSION

Here, we report that SIAH inhibition activated DNA damage-associated apoptotic pathways in human cancer cell lines. Furthermore, quantitative longitudinal 3D analysis demonstrated gradual tumor destruction following SIAH inhibition in MiaPaCa-2 cells, highlighting the efficacy of the SIAH inhibitor as a new targeted therapy to eradicate oncogenic EGFR/RAS-driven cancers. Ultimately, delineating the relationship between SIAH inhibition, increased DDR, apoptotic responses, and 3D tumor destruction will further support our central hypothesis that SIAH represents a promising new therapeutic target for the treatment of "undruggable and incurable" human malignancies.

Optimization of Fluorescence Assisted Single-Synapse Long-Term Potentiation for Assessment of Synaptic Plasticity

Investigator: Sierra M. DePry, B.A.
Mentor: Richard Britten, Ph.D.
Co-Authors(s):
None listed.
Department(s): Radiation Oncology and Biophysics
Poster #: 42A

INTRODUCTION

Synaptic dysfunction is an early and significant feature of aging, neurodegenerative disease, and radiation associated neurological defects. However, measuring functional changes at the level of individual synapses remains a challenge. Fluorescence-assisted single-synapse long-term potentiation (FASS-LTP) addresses this limitation by making use of both chemically induced long-term potentiation (cLTP) and flow cytometric detection of activity dependent synaptic markers. This study aimed to establish and optimize a reproducible FASS-LTP workflow for assessing synaptic plasticity in frozen brain tissue using spectral flow cytometry.

METHODS

Synaptosomes were isolated from banked hippocampal samples that contained both non-irradiated control samples and samples from which animals were exposed to varying radiation conditions. To induce cLTP, the samples were exposed to glycine priming, followed by potassium chloride induced depolarization. Samples were immunolabeled for the α-amino-3-hydroxy-5-methyl-4-isoxazolepropionic acid receptor (AMPAR) subunit 1 (GluA1), a postsynaptic protein associated with synaptic potentiation, and neurexin-1β (Nrx1β), a presynaptic adhesion protein. Synaptosomal particles were identified using forward and side scatter characteristics with size reference beads to exclude debris. Fluorescence was used to quantify GluA1 positive, Nrx1β positive, and GluA1/Nrx1β double positive populations. Optimization focused on sample recovery, reagent preparation, stimulation conditions, immunolabeling, spectral unmixing, acquisition, and gating.

RESULTS

Initial experiments produced limited Nrx1β fluorescence and no clear distinction between basal and stimulated samples. Following optimization, it was observed that non-irradiated hippocampal samples had an increase in GluA1/Nrx1β double positive synaptosomes following cLTP induction, whereas irradiated samples showed a reduced or absent response. Although this trend was not evaluated as a complete statistical comparison, it suggests that radiation exposure may alter activity-dependent synaptic potentiation and supports further investigation using the optimized FASS-LTP workflow.

CONCLUSION

Overall, an increase in GluA1/Nrx1β double positive synaptosomes following stimulation establishes a functional workflow for evaluating synaptic potentiation in stored hippocampal tissue and identify critical specifications affecting FASS-LTP reproducibility. Although a complete comparison of irradiated and control samples was not fulfilled, this optimization provides the foundation for successive investigation of radiation associated synaptic dysfunction. More broadly, the ability to examine functional synaptic changes in frozen tissue creates opportunities to expand to regional vulnerability, disease progression, and therapeutic response across existing animal and human tissue collections.

Evaluation of YK-8-126 as a Dual-Function Fluorescent BRD4 Inhibitor for Target Visualization in Glioblastoma Cells

Investigator: Yuvateja Kocherla, B.S.
Mentor: Yali Kong, Ph.D.
Co-Authors(s):
Milton Brown, Macon & Joan Brock Virginia Health Sciences Eastern Virginia Medical School
Department(s): Biomedical and Translational Sciences
Poster #: 43A

INTRODUCTION

Glioblastoma remains a lethal central nervous system malignancy with severe therapeutic limitations, largely due to poor blood-brain barrier permeability and neurotoxicity. Bromodomain-containing protein 4 (BRD4) is an epigenetic reader that drives oncogenic transcription, making it a key therapeutic target. Here, we present the rationale and experimental framework for YK-8-126, a newly synthesized small-molecule BRD4 inhibitor designed to prevent BRD4-acetylated histone interactions. Uniquely engineered with a core fluorophore, YK-8-126 is designed to act as a dual-function theranostic, enabling simultaneous target inhibition and direct intracellular tracking without secondary labeling.

METHODS

Human U-87 glioblastoma cells will be treated with YK-8-126 to characterize intracellular localization using live-cell confocal microscopy. A time-course imaging study with 15-minute intervals will be performed to quantify cellular entry kinetics and signal persistence. Additionally, dose-dependent imaging assays will be conducted to establish key intracellular parameters, including fluorescence half-life (t1/2), concentration for half-maximal effect (EC50), duration of action, and steady-state cellular accumulation.

RESULTS

We anticipate that YK-8-126 will demonstrate rapid, dose-dependent cellular entry and clear sub-cellular fluorescence signal localization within U-87 cells. Based on preliminary chemical modeling and structural design, we project robust signal accumulation with minimal photobleaching over serial imaging intervals. Successful execution of these kinetic models is expected to confirm efficient cell membrane permeability and predictable intracellular steady-state kinetics aligned with BRD4 targeting.

CONCLUSIONS

This study establishes an integrative approach to evaluate YK-8-126 as a novel theranostic candidate for glioblastoma. Demonstrating simultaneous intracellular visualization and targeted BRD4 inhibition will validate YK-8-126 as a promising lead compound for targeted neuro-oncology therapeutics.

From Ovaries to Arteries: Modeling Menopause in Atherosclerosis

Investigator: Veronika Murphy, B.S.
Mentor: Elena Galkina, Ph.D.
Co-Authors(s):
Alina Moriarty, Macon & Joan Brock Virginia Health Sciences Eastern Virginia Medical School
Diane Duffy, Macon & Joan Brock Virginia Health Sciences Eastern Virginia Medical School
Kathleen Coleman, Macon & Joan Brock Virginia Health Sciences Eastern Virginia Medical School
Department(s): Department of Biomedical & Translational Sciences, Division of Microbiology & Molecular Cell Biology
Poster #: 44A

INTRODUCTION

Atherosclerosis is a multifactorial, chronic inflammatory disease that drives cardiovascular disease (CVD) and disproportionately affects postmenopausal women. Compared to premenopausal women and age-matched men, postmenopausal women experience accelerated cardiovascular dysfunction, but the mechanisms underlying this sex-specific vulnerability remain unclear.

Sleep is crucial for life, and fragmented sleep increases the risk of cardiovascular mortality. During the menopausal transition, declining estrogen levels coincide with increased sleep fragmentation (SF). Our studies demonstrate that SF accelerates age-associated vascular remodeling, leading to larger, unstable atherosclerotic plaques. The concurrent rise in CVD and SF in postmenopausal women suggests interactions between hormonal changes, sleep disruption, and vascular aging. However, fewer than 1% of preclinical cardiovascular studies utilize models of menopause, and even fewer examine how menopause-related sleep fragmentation drives atherogenesis, representing a critical gap in cardiovascular and women's health research.

The project aimed to investigate how reproductive aging, declining estrogen, and sleep fragmentation affect atherosclerosis development in postmenopausal women.

METHODS

We used a novel 4-vinylcyclohexene diepoxide (VCD) mouse model to selectively deplete ovarian follicles while preserving the ovary. After 12 weeks on a high-fat, high-cholesterol diet and SF, aortas were collected and stained with Oil Red O to quantify plaque burden. Aortic valve sections were stained with picrosirius red and MOVAT stain to assess plaque stability by comparing necrotic cores, fibrous caps, elastic fibers, and collagen.

RESULTS/CONCLUSION

Our data demonstrate that SF accelerates atherogenesis in postmenopausal conditions. Ongoing studies are focused on dissecting a specific mechanism behind this increased plaque burden.

From Stability to Genetic Reprogramming: What Happens When BMPR1α-Deficient Tregs Encounter Inflammation?

Investigator: Afia Salsabil Alam, B.S.
Mentor: Piotr Kraj, Ph.D., DVM
Co-Authors(s):
Jonathan Waldron, Old Dominion University
Kyle Christie, Old Dominion University
Department(s): Biological Sciences
Poster #: 49B

INTRODUCTION

Immune homeostasis requires effective host defense while preventing excessive inflammation and immune-mediated tissue damage. Regulatory T-cells (Tregs) preserve this balance through a Foxp3-directed suppressive program, yet inflammatory stress threatens their lineage stability. Although bone morphogenetic protein (BMP) signaling influences immune cell differentiation, the role of BMP receptor type 1A (BMPR1α) in maintaining mature Treg identity remains unknown. We hypothesized that BMPR1α signaling preserves Treg lineage stability by limiting proinflammatory reprogramming.

METHODS

To investigate BMPR1α function in Tregs, we generated mice with tamoxifen-inducible, Treg-specific deletion of Bmpr1a; wild-type (WT) littermates served as controls. Lymph node $CD4^+$ T-cells from both genotypes were phenotyped by flow cytometry before adoptive transfer. Yellow fluorescent protein (YFP) permanently marked cells expressing Foxp3 during tamoxifen treatment, whereas green fluorescent protein (GFP) identified current Foxp3 expression. This approach distinguished YFP^+GFP^- former Tregs, YFP^+GFP^+ lineage-traced Tregs retaining Foxp3, and YFP^-GFP^+ newly generated Tregs. Activation status and cytokine-receptor expression were compared between genotypes across all three populations. Recipients are monitored for weight loss, after which donor-derived Tregs will be recovered from lymph nodes and reanalyzed for Foxp3 stability, activation, and cytokine-receptor expression. In parallel, bulk and single-cell RNA sequencing and assay for transposase-accessible chromatin with sequencing (ATAC-seq) analyses are in progress to characterize BMPR1α-dependent molecular changes under homeostatic and inflammatory conditions.

RESULTS

Preliminary analyses indicated enhanced IL-18Rα/IL-1 signaling following BMPR1α loss, consistent with activation of inflammatory pathways capable of promoting Treg effector reprogramming. Before adoptive transfer, flow-cytometric analysis revealed increased proportions of activated cells relative to naïve cells across all three fate-mapped populations, YFP^+GFP^-, YFP^+GFP^+, and YFP^-GFP^+, in BMPR1α-deficient mice compared with their WT counterparts. Enhanced IL-18Rα/IL-1 signaling provides a potential mechanistic basis for these activation changes. Because YFP permanently records prior Foxp3 expression, whereas GFP reflects current Foxp3 expression, the concordant findings suggest that BMPR1α deficiency affects multiple Treg fate states, including former Tregs that have lost Foxp3, lineage-traced Tregs that retain Foxp3, and newly generated Tregs. We are comparing expression of cytokine and chemokine-receptors modulating inflammatory responses of treg cells between genotypes within each population in BMPR1α-deficient cells across all three fate states. Together, these findings suggest that BMPR1α deletion broadly alters Treg activation and cytokine-receptor profiles rather than selectively affecting a single fate-defined population. Adoptive-transfer experiments are underway to determine how BMPR1α-deficient Tregs respond to a Treg-depleted inflammatory environment, while bulk RNA-seq, single-cell RNA-seq, and ATAC-seq analyses are in progress to characterize the associated transcriptional and chromatin-accessibility changes related to the genetic reprogramming of Tregs.

CONCLUSION

These preliminary findings associate BMPR1α deficiency to decreased phenotypic stability Treg cell population and altered genetic reprogramming in response to inflammation. Defining how BMPR1α signaling regulates Treg stability during inflammation may uncover molecular mechanisms that could be targeted to develop new therapeutic strategies to alter Treg suppressor functions in autoimmune and chronic inflammatory diseases.

Age-associated Ndufs4 isoform remodeling impairs steroidogenesis in mouse granulosa cells

Investigator: Adnan Alsamaraee, B.S.
Mentor: Pavla Brachova, Ph.D.
Co-Authors(s):
Amanda Yermal, Macon & Joan Brock Virginia Health Sciences Eastern Virginia Medical School
Nehemiah Alvarez, Macon & Joan Brock Virginia Health Sciences Eastern Virginia Medical School
Department(s): Biomedical and Translational Sciences
Poster #: 53A

INTRODUCTION

Female reproductive aging is accompanied by progressive declines in ovarian mitochondrial function and steroidogenic capacity. We previously identified widespread age-associated alterations in alternative splicing in the mouse ovary, including isoform remodeling in genes involved in mitochondrial function, with particularly pronounced changes in granulosa cells. Among these candidates, Ndufs4, which encodes an accessory subunit of mitochondrial respiratory Complex I, exhibited increased expression of a short isoform in aged ovaries relative to a canonical long isoform. Because mitochondrial function is integral to steroid hormone biosynthesis, we investigated whether expression of the age-associated Ndufs4 isoform alters steroidogenic function in primary ovarian granulosa cells.

METHODS

Female C57BL/6J mice were stimulated with PMSG, and ovaries were collected 46 h later. Primary granulosa cells were isolated, cultured, and transfected with in vitro-transcribed mRNA encoding the canonical Ndufs4 long isoform, the age-associated Ndufs4 short isoform, or mTagBFP2 control using Lipofectamine MessengerMAX. Following transfection, cells were stimulated with 8-Br-cAMP to activate cAMP-dependent steroidogenic signaling. Steroidogenic acute regulatory protein (StAR) abundance was assessed by quantitative immunofluorescence, and progesterone secretion into conditioned media was measured by ELISA.

RESULTS

Expression of the age-associated short Ndufs4 isoform was associated with reduced StAR protein abundance compared with the canonical isoform, consistent with impaired regulation of a key mediator of mitochondrial cholesterol transport during steroidogenesis. Progesterone production following 8-Br-cAMP stimulation was also reduced in cells expressing the short isoform. Cells expressing the canonical long isoform produced 4.9 ng progesterone/well, whereas cells expressing the age-associated short isoform produced 2.7 ng/well, corresponding to a 45% reduction in progesterone production.

CONCLUSION

These preliminary findings suggest that overexpression of an age-associated Ndufs4 isoform attenuates mouse granulosa cell steroidogenic responsiveness. Reduced StAR abundance together with diminished cAMP-stimulated progesterone production support a functional link between age-associated Ndufs4 isoform remodeling and impaired granulosa cell steroidogenesis. Ongoing studies will define the isoform-specific effects of Ndufs4 and determine how age-associated transcript remodeling contributes to declining ovarian function during reproductive aging.

The Optimization of Microwave-Assisted Organic Synthesis Using Predictive Modeling

Investigator: Asa Renita Britton-Jenkins, M.S.
Mentor: Milton L. Brown, MD, Ph.D.
Co-Authors(s):
Shivangi Gupta, Macon & Joan Brock Virginia Health Sciences Eastern Virginia Medical School
Yali Kong, Macon & Joan Brock Virginia Health Sciences Eastern Virginia Medical School
David Mu, Macon & Joan Brock Virginia Health Sciences Eastern Virginia Medical School
Department(s): Internal Medicine
Poster #: 54A

INTRODUCTION

Over 50% of all breast cancers are associated with a BRCA1 mutation. In addition to its roles in DNA repair, cell cycle regulation, ubiquitination, and transcriptional activation, it modulates ERα activity by directly binding to the AF-2 (coactivator-binding) region of ERα. Additionally, BRCA1 was determined to prevent epithelial-to-mesenchymal transition (EMT) and stemness. The cancer stem cell population of the tumor microenvironment is responsible for the development of chemoresistance, radio-resistance, metastasis, invasion, and tumor recurrence. Our lab established that lead BRCA1-mimetic small molecules, A7 and A9, can inhibit ERα, and identified a novel A9 analog, ABJ-1-195, inhibits tamoxifen-resistant stem cells. Directing our novel BRCA1-mimetic, ABJ-1-195, to a breast cancer stem cell-targeting peptide is crucial for specific drug delivery to prevent or halt metastasis and reduce off-target toxicity. The present study focuses on the synthesis of a linker to connect ABJ-1-195 to our fluorescent, stem cell targeting peptide construct.

Previously, EDCI-mediated coupling and conventional heating via the Schotten-Baumann reaction proved unsuccessful in overcoming the poor nucleophilicity of the exocyclic amine in the 4-aminopyrimidines A9 and ABJ-1-195 for linker synthesis. Unlike conduction heating, microwave reactors use dielectric heating, or oscillating high-frequency electric fields, to promote collisions between particles, allowing the swift generation of high heat and low pressure within a sealed reaction tube. Dipolar rotation and ionic conduction are crucial for improving reaction rates, yields, and safety while reducing side reactions and chemical waste in microwave-assisted synthesis.

METHODS

In this study, our lab explored the use of predictive modeling to identify relevant parameters to increase the yield of the Schotten-Baumann reaction of A9 and ABJ-1-195 under microwave irradiation. A dataset was compiled from 22 Schotten-Baumann reactions using A9 or ABJ-1-195 performed under microwave conditions with variations in molar equivalent of starting materials, the molecular weights of starting material, the use of a catalyst, the molar equivalent of catalyst used, the dielectric constant of solvent, the dielectric loss of the solvent, the pKa of the used base, pressure applied to the reaction vial, reaction temperature, and reaction time. Additionally, approximately 120 published Schotten-Baumann reactions were also added to this dataset to evaluate the effects of these parameters on predicting reaction yield.

RESULTS

Our model predictions indicate that reaction temperature, the inclusion of a catalyst, and the amount of the selected catalyst are relevant parameters for improving the reaction yield. We successfully incorporated the linker into A9 under the highest-yield microwave conditions, affording 48%.

CONCLUSION

Predictive modeling is a useful method for identifying relevant parameters to improve the yield of microwave-assisted Schotten-Baumann reactions with poor nucleophiles, A9 and ABJ-1-195. This work supports the synthesis of a novel peptide drug conjugate to target the breast cancer stem cell population. Ultimately, this work connects targeted drug delivery methods and machine learning to advance therapeutic strategies against drug-resistant cancers.

The miR-888 Cluster as a Therapeutic Target for Aggressive Prostate Cancer

Investigator: Alex T. Cain, B.S.
Mentor: Aurora Kerscher, Ph.D.
Co-Authors(s):
Katherine Routon Stanton, Macon & Joan Brock Virginia Health Sciences Eastern Virginia Medical School
Vishal Kasina, University of Connecticut
Raman Bahal, University of Connecticut
Department(s): Biomedical Sciences
Poster #: 50B

INTRODUCTION

Metastatic prostate cancer (PCa) represents an unmet treatment need, with a 5-year survival rate of only 30%. MicroRNAs (miRNAs) are small ~24-nucleotide noncoding RNAs with potential as clinical tools for PCa. The Kerscher lab identified miR-888 and miR-891a as preferentially enriched in metastatic PCa cell lines and prostatic fluids from patients with high-grade PCa. These miRNAs promote PCa growth and aggressiveness in vitro and tumor growth in mice, while inhibition reverses these activities, highlighting their potential as anti-miRNA targets for PCa. Synthetic antisense oligonucleotides designed to bind and sequester miRNAs (antimiRs) are valuable tools for inhibiting miRNA function, but current antimiR therapies require high doses and suffer from poor tissue specificity. To improve tumor-specific antimiR delivery and efficacy, we collaborated with Dr. Raman Bahal (UConn) to test peptide nucleic acid (PNA) antimiRs targeting miR-888 and miR-891a conjugated to the acid-sensing pH low insertion peptide (pHLIP). This work tested the hypothesis that pHLIP-PNA antimiRs would facilitate delivery to PCa cells under acidic conditions and to prostate tumors in vivo, resulting in inhibition of aggressive phenotypes and tumor growth. This work also evaluated the potential of miR-888/891a as targets for treatment in the neuroendocrine (NE) PCa pathology, which represents a major unmet need.

METHODS

qRT-PCR was carried out to establish miR-888/891a expression levels across a panel of PCa cell lines including RWPE-1 (nonmalignant), LNCaP (low aggression), PC3-N (low aggression), PC3-ML (high aggression), NCI-H660 (low aggression, NE), and LASCPC-01(high aggression, NE). Cell culture assays were performed to evaluate the effects of pHLIP-PNA-antimiR-888/891a treatment on PC3-ML proliferation (WST-1) and anchorage-independent growth (soft agar). NOD/SCID mice were inoculated with PC3-ML cells; following tumor formation, mice were injected via tail vein with either CY5-labeled pHLIP delivery peptide (1 mg/kg) or pHLIP-PNA-antimiR-888/891a (1 mg/kg). pHLIP-CY5-injected mice were sacrificed 24h post-injection and organs and tumors were harvested and imaged to determine drug localization. Mice receiving pHLIP-PNA-antimiR treatment were monitored for tumor growth rate until day 25 of the study, after which they were sacrificed. Organs and tumors were harvested for downstream analysis. qRT-PCR was carried out to determine tumor miR-888/891a expression and western blotting was carried out to determine expression levels of miR-888/891a target TIMP2.

RESULTS

qRT-PCR analysis showed that miR-888/891a expression increases in step with aggressiveness, with NE lines showing highly elevated expression. AntimiR-888 alone had minimal effects (contrary to previous experiments with other batches), indicating potential variability in reagent potency, whereas combined antimiR-888/891a treatment produced additive growth inhibition. Colony formation assays showed similar trends for individual antimiRs, while combined treatment demonstrated synergy (Bliss analysis, $p<0.001$). In vivo, Cy5-pHLIP efficiently localized to PC3-ML xenograft tumors, with additional retention in kidney and liver.

AntimiR-891a showed a nonsignificant trend toward reduced overall tumor burden (Mann-Whitney U, $p=0.190$), while linear mixed-effects modeling demonstrated significantly reduced tumor growth rate over time ($p=0.00847$).

CONCLUSION

Together, these studies demonstrate the feasibility of pHLIP-mediated PNA-antimiR delivery to prostate tumors and provide evidence that targeting miR-891a can inhibit aggressive PCa phenotypes and tumor growth, supporting further reagent development for advanced and castration-resistant PCa.

Uncovering CDCP1-Siglec Interactions in Triple-Negative Breast Cancer

Investigator: Paul Cheddie, B.S.
Mentor: Lifang Yang, MD, Ph.D.
Co-Authors(s):
Fanying Li, Macon & Joan Brock Virginia Health Sciences Eastern Virginia Medical School
Linsong Zhang, Macon & Joan Brock Virginia Health Sciences Eastern Virginia Medical School
Kara Friend, Macon & Joan Brock Virginia Health Sciences Eastern Virginia Medical School
Rebecca Martin, Macon & Joan Brock Virginia Health Sciences Eastern Virginia Medical School
Eric Feliberti, Macon & Joan Brock Virginia Health Sciences Eastern Virginia Medical School
Department(s): Biomedical and Translational Sciences
Poster #: 55A

INTRODUCTION

Triple-negative breast cancer (TNBC) is characterized by an immunosuppressive, myeloid-rich tumor microenvironment. Sialic acid-binding immunoglobulin-like lectins (Siglecs), specifically the inhibitory receptors Siglec-7, -9, -10, and -15 on myeloid cells, promote immune evasion by binding tumor-surface sialoglycans. Although cell-surface sialoglycoproteins like CD24, MUC1, and GPNMB have been identified for several of these Siglecs, the dominant glyco-immune checkpoints driving local immunosuppression remains largely unexplored. CDCP1 is an oncogenic transmembrane glycoprotein overexpressed in TNBC and associated with TNBC migration, metastasis, and adverse patient outcomes. This study aims to evaluate Siglec-binding heterogeneity across TNBC lines and the functional role of CDCP1 as a Siglec ligand.

METHODS

Because Siglec recognition is influenced by sialic acid linkage and glycan context, CDCP1 glycosylation was characterized by PNGase F and neuraminidase digestion followed by immunoblotting. Sialylation was further assessed by metabolic labelling with Ac4ManNAz followed by copper-free click chemistry and streptavidin enrichment. To investigate linkage-associated sialylation, SNA (α2,6) and MAL-II (α2,3) lectin affinity pulldown was performed, with enriched CDCP1 proteoforms identified by immunoblotting. To determine whether Siglec-binding profiles differ between TNBC cell lines, baseline Siglec-7, -9, -10 and -15 binding was assessed by flow cytometry using Siglec-Fc chimeras in malignant (BT-549, HCC1143, MDA-MB-231) and non-malignant (MCF10A) cell lines. CRISPR-Cas9 ribonucleoproteins were utilized to knock out CDCP1 in MDA-MB-231 cells. Clones were screened by Western blotting for total CDCP1 expression and flow cytometry for surface CDCP1 expression relative to a CRISPR-SHAM control. Verified KO clones with near-background surface expression were evaluated for changes in Siglec-Fc binding relative to CRISPR-SHAM controls. Direct physical engagement between CDCP1 and Siglecs was determined via Siglec pulldown followed by Western blotting for CDCP1 detection.

RESULTS

Enzymatic deglycosylation revealed extensive N-glycosylation and terminal sialylation of CDCP1, while metabolic labelling and copper-free click chemistry independently demonstrated the incorporation of sialic acid into CDCP1 proteoforms. Notably, both full-length (~135 kDa) and cleaved (~70 kDa) CDCP1 were recovered in SNA- and MAL-II-enriched fractions, supporting the presence of α2,6- and α2,3-linked sialylated glycans on both proteoforms. The relative enrichment of these proteoforms varied across cell lines, revealing heterogeneity in CDCP1 sialylation that provides a biochemical foundation for its subsequent investigation as a candidate Siglec ligand. Siglec-Fc binding profiles were highly heterogeneous. MDA-MB-231 exhibited significantly higher baseline Siglec-9 and Siglec-15 binding compared to other lines. Western blot screening of CDCP1-disrupted MDA-MB-231 clones identified five clones with altered total CDCP1 expression. Subsequent flow cytometry confirmed near-background cell-surface CDCP1 levels in three of these clones (E4, B3, and D6). Preliminary Siglec-binding analysis showed CRISPR-mediated CDCP1 deletion significantly reduced Siglec-9 binding in two KO clones compared to SHAM controls, while one clone exhibited variable binding. Siglec-7 binding remained unaltered. Paradoxically, Siglec-15 binding was consistently increased across all three CDCP1-KO clones relative to SHAM controls.

CONCLUSION

These results demonstrate Siglec-binding profiles are heterogeneous in TNBC and identified CDCP1 as a potentially functional ligand for the inhibitory receptor Siglec-9. Furthermore, the unexpected upregulation of Siglec-15 binding upon CDCP1 loss may suggest a compensatory glycan-remodeling or receptor-compensatory mechanism. These findings highlight the complex, dynamic nature of the tumor glycoproteome and glyco-immune

Triggering ferroptosis in bladder cancer

Investigator: Alyssa Costello, B.S.
Mentor: Michael Henry, Ph.D.
Co-Authors(s):
Marion Dykstra, Macon & Joan Brock Virginia Health Sciences Eastern Virginia Medical School
Department(s): Biomedical and Translational Science
Poster #: 56A

INTRODUCTION

Urinary bladder carcinoma is the fifth most common cancer among men in the United States, with an estimated 64,730 new cases and 12,640 deaths in 2026. High reoccurrence rate and continual monitoring make it one of the most expensive malignancies to treat. These factors drive an urgent need for novel targeted therapies to combat bladder cancer. Inhibiting glutathione peroxidase 4 (GPX4) to induce ferroptosis—an iron-dependent, non-apoptotic cell death pathway—presents a novel therapeutic strategy. While expression of ZEB1, an epithelial-to-mesenchymal transition transcription factor, correlates with GPX4 inhibitor (GPX4i) sensitivity in several cancers, its role in bladder cancer remains uncharacterized. We hypothesized that ZEB1 expression drives sensitivity to GPX4i induced ferroptosis in bladder cancer by altering iron availability.

METHODS

We used a panel of eight bladder cancer cell lines (T24, TCCSUP, SW780, RT4, 5637, HT1376, UMUC3, HT1197) to characterize sensitivity to GPX4i compounds RSL3 and ML210. Ferroptosis specificity was confirmed using the ferroptosis inhibitor liproxstatin-1. Protein expression of ZEB1, CDH1, GPX4, ferritin heavy chain (FtH), and ferritin light chain (FtL) were measured by western blot. Baseline labile iron pool (LiP) levels were quantified using FerroOrange fluorescent probe to determine if ZEB1 expression correlates with iron availability.

RESULTS

RSL3 demonstrated high potency, yielding nanomolar IC50 values in six of eight cell lines. ML210 demonstrated moderate potency, with nanomolar IC50 values in four of eight cell lines. Liproxstatin-1 rescued cell viability in seven of eight cell lines, confirming GPX4-induced ferroptosis in those lines. Contrary to expectations, GPX4i sensitivity did not significantly correlate with ZEB1 expression or GPX4, FtH, and FtL protein levels. Baseline LiP levels varied widely across bladder cancer cell lines, with ZEB1 low lines exhibiting higher LiP levels than ZEB1 high lines.

CONCLUSION

We characterized sensitivity to GPX4i-induced ferroptosis in a panel of bladder cancer cell lines, identifying RSL3 as a potent compound and confirming that bladder cancer is susceptible to GPX4i. Unexpectedly, ZEB1 expression is not always associated with ferroptosis sensitivity. UMUC3 had the highest ZEB1 expression, but liproxstatin-1 did not rescue viability, indicating that these cells are not dying from ferroptosis. Conversely, HT1197 had low ZEB1 expression and the highest sensitivity to RSL3. Cell lines SW780, RT4, and 5637 also have low ZEB1 expression yet are sensitive to GPX4i. These contradictions suggest a ZEB1-independent mechanism of ferroptosis induction. ZEB1 also did not correlate with FtH or FtL protein expression, suggesting that ZEB1 does not affect iron storage capacity of bladder cancer cells. ZEB1 expression was anti-correlated with LiP, refuting our hypothesis. Higher LiP in ZEB1 low cell lines could explain GPX4i sensitivity and ferroptosis induction. It also suggests that ZEB1 could be suppressing LiP as a preventative measure against ferroptosis. These findings broaden the potential patient population for GPX4-targeted therapies to include ZEB1 low non-mesenchymal tumors and highlight baseline LiP as an important factor in ferroptosis susceptibility. Future work includes establishing a ZEB1 knockout cell model to study the role of ZEB1 in bladder cancer iron metabolism.

Angiotensin II receptor blockade is associated with lower cancer cachexia, while the triple-action conjugate YK-4-250 attenuates skeletal muscle atrophy in vitro

Investigator: Nima George, B.S.
Mentor: Milton L. Brown, MD, Ph.D.
Co-Authors(s):
Kan Wang , Macon & Joan Brock Virginia Health Sciences Eastern Virginia Medical School
Yali Kong, Macon & Joan Brock Virginia Health Sciences Eastern Virginia Medical School
David Mu, Macon & Joan Brock Virginia Health Sciences Eastern Virginia Medical School
Department(s): Department of Internal Medicine
Poster #: 51B

INTRODUCTION

Cancer cachexia affects approximately 50% to 80% of patients with advanced cancer and contributes to an estimated 20% to 30% of cancer-related deaths. Cachexia develops when catabolic muscle-protein degradation exceeds anabolic protein synthesis, resulting in progressive skeletal muscle loss. Angiotensin II (Ang II) is elevated in patients with cancer and has been implicated in muscle wasting associated with cardiac cachexia. Ang II-driven oxidative and inflammatory signaling may activate nuclear factor κB (NF-κB) and signal transducer and activator of transcription 3 (STAT3), increase the muscle-specific ubiquitin ligases MuRF1 and atrogin-1, and suppress anabolic IGF-1/Akt/mTOR signaling. We evaluated the association between angiotensin receptor blocker use and coded cachexia in patients with cancer and tested telmisartan, tempol, and YK-4-250, a telmisartan-tempol conjugate designed to simultaneously target AT1 receptor signaling, reactive oxygen species, and PPARγ activity as a potential triple-action strategy against cachexia-associated muscle wasting.

METHODS

A retrospective cohort study was conducted using the TriNetX Global Collaborative Network, including approximately 180 healthcare organizations. Adults with neoplasms receiving angiotensin receptor blockers were compared with patients receiving calcium channel blockers as an active comparator. Cohorts were balanced using 1:1 propensity-score matching, and coded cachexia was evaluated over 5 years. A secondary head-to-head analysis compared telmisartan with losartan. For the preliminary in vitro study, differentiated C2C12 myotubes were assigned to untreated control, Ang II-only, or intervention groups. All Ang II-exposed wells, including intervention wells, received Ang II at 500 nM. Intervention wells additionally received pretreatment with YK-4-250 at 1 or 10 μM, telmisartan at 1 μM, or Tempol at 100 μM. Myotube diameter was measured from brightfield images, with 36 myotubes evaluated per condition in a single experimental well.

RESULTS

After matching, 1,140,036 angiotensin receptor blocker users and 1,136,253 calcium channel blocker users were analyzed. At 5 years, coded cachexia occurred in 0.6% and 1.1% of patients, respectively (OR, 0.533; 95% CI, 0.517 to 0.549; log-rank $P < 0.001$). Telmisartan was associated with 28.5% lower odds of coded cachexia than losartan (OR, 0.715; 95% CI, 0.527 to 0.970; log-rank $P = 0.037$). In C2C12 myotubes, Ang II reduced mean diameter from 27.28 μm in untreated cells to 18.33 μm in Ang II-only cells. Mean diameters were 25.31 and 26.13 μm after YK-4-250 at 1 and 10 μM, respectively, compared with 26.99 μm after telmisartan and 26.85 μm after tempol. Telmisartan and YK-4-250 restored Ang II-reduced myotube diameter toward untreated values, with YK-4-250 producing comparable rescue at lower tested concentrations than tempol.

CONCLUSION

Angiotensin receptor blocker use was associated with 46.7% lower odds of coded cachexia, while telmisartan was associated with 28.5% lower odds than losartan. Telmisartan and YK-4-250 attenuated Ang II-induced myotube narrowing, and YK-4-250 demonstrated a promising efficacy-to-dose profile relative to Tempol. These findings support a potential triple-target strategy combining AT1 receptor blockade, PPARγ modulation, and ROS scavenging. Such complementary mechanisms may reduce muscle catabolism and could contribute to improved clinical outcomes, including survival. Replicated studies will evaluate MuRF1, atrogin-1, NF-κB, STAT3, IGF-1/Akt/mTOR signaling, and oxidative-stress endpoints.

Characterizing Stem Cell Responses to Localized Niche Cues at the Single-Cell Level Through Spatially Controlled 3D Bioprinting

Investigator: Yara Khodour, B.S.
Mentor: Robert D. Bruno, Ph.D.
Co-Authors(s):
None listed.
Department(s): Medical Diagnostics and Translational Sciences
Poster #: 57A

INTRODUCTION

The stem cell niche is the microenvironment where stem cells reside and receive specific cues. These cues can be cell to cell or cell to extracellular matrix (ECM) interactions and signals in which they influence the stem cell behavior, determine its fate, and facilitate asymmetric divisions [1]. This process remains poorly understood, highlighting the need for improved model systems. To address this, we present a novel 3D bioprinting system that enables the study of this niche at a single-cell level [2]. We demonstrate that the system allows for the printing of single cells in grids and large arrays in both 3D and 2D by injecting into hydrogels or directly onto glass slides using nanoliter droplets. Subsequently, we assessed whether the system could be employed to unravel differential signaling between stem cells and various ECMs.

METHODS

Single mouse embryonic stem cells (mESCs) were printed in different ECMs to uncover the influence of different matrices on the redirection of the stem cell fate. Our results showed that the ESCs fate and proliferation were different when different ECMs were used. We then evaluated if our system could be used to generate artificial niches using immobilized growth factors to drive asymmetric divisions. To achieve this, we conjugated Epidermal growth factor (EGF) and Fibroblast growth factor 2 (FGF-2), growth factors required for the self-renewal of neural stem cells (NSCs), to fluorescent FluoSpheres™. The EGF/FGF tagged FluoSpheres were incubated with NSCs and either cultured or bioprinted into arrays under differentiation conditions.

RESULTS

We show that the interaction with the EGF/FGF beads protects NSCs from differentiating using the NSC marker Nestin. Our results therefore demonstrate that the FGF/EGF beads could serve as an artificial niche to protect NSCs from differentiation and drive asymmetric divisions.

CONCLUSION

Collectively, our results demonstrate that our bioprinting system is a unique and robust tool that aids in mimicking the microenvironment where stem cells thrive, while also enabling the study of stem cell-niche interactions at a single-cell level using precision 3D bioprinting techniques.

References

1. Ferraro, F., C.L. Celso, and D. Scadden, Adult stem cels and their niches. Adv Exp Med Biol, 2010. 695: p. 155-68.

2. Reid, J.A., et al., A 3D bioprinter platform for mechanistic analysis of tumoroids and chimeric mammary organoids. Sci Rep, 2019. 9(1): p. 7466.

Spatial Characterization of Epithelial Cytokines Associated with Foam Cell Formation in Benign Prostatic Hyperplasia

Investigator: Samantha McGuire, B.S.
Mentor: Petra Popovics, Ph.D., M.S.
Co-Authors(s):
Nehemiah Alvarez, Macon & Joan Brock Virginia Health Sciences Eastern Virginia Medical School
Ilya Sobol, Sentara
Department(s): Biomedical and Tranlational Sciences
Poster #: 52B

INTRODUCTION

Benign Prostatic Hyperplasia (BPH) is a multifactorial disease characterized by the non-malignant enlargement of the prostate gland, leading to urethral compression. This disease manifests as lower urinary tract symptoms, which can significantly impair quality of life. There are currently no treatment options for BPH that target underlying disease mechanisms; therefore, it is imperative to identify new therapeutic targets beyond symptom management. Previously our lab had identified the presence of CD68+ macrophages migrating into the prostatic lumen and differentiating into lipid laden foam cells. We believe that epithelial cytokines promote this translocation and provide a target for inhibiting foam cell formation (FCF). Therefore, this research aims to uncover new targets driving FCF as well as characterizing BPH tissue microenvironments using spatial transcriptomics.

METHODS

BPH prostate tissue was obtained from individuals who underwent Holmium Laser Enucleation of the Prostate (HoLEP) surgery. The tissue was fixed in formalin, embedded in paraffin and sectioned at 8 µm for probe-based spatial transcriptomics using 10x Genomics Visium HD Spatial Gene Expression method. Sections were deparaffinized, permeabilized, and hybridized with gene specific probes. After amplification, spatial transcriptomic libraries were generated and sequenced. Data were processed using the 10x Genomics Space Ranger pipeline in Cloud Analysis, including spatial barcode and UMI processing, gene assignment, image registration, and tissue detection. Gene expression data were aggregated into 8-µm spatial bins. Osteopontin (Spp1) was used to identify foam cell rich (FCR) and foam cell sparse (FCS) regions of epithelium and adjacent stroma, followed by differential gene expression analysis.

RESULTS

Differential gene analysis showed significant upregulation of inflammatory cytokines CXCL8 ($p = 1.01E^{-22}$), CXCL6 ($p = 1.17E^{-20}$), CXCL1 ($p = 1.41E^{-9}$), immune cell activator IL32 ($p = 4.29E^{-22}$) and CCL2 ($p = 7.62E^{-11}$), and efferocytosis gene ANXA1($p = 3.07E^{-17}$) in FCR epithelium. FCR stromal regions had increased expression of inflammatory chemokines, CXCL8, ($p = 2.89E^{-27}$), CXCL6 ($p = 1.77E^{-6}$), and CCL2 ($p = 4.89E^{-5}$) compared to FCS stroma. Additionally, there was increased expression of extracellular matrix (ECM) remodeling genes, including COMP ($p = 4.93E^{-25}$), MMP10 ($p = 1.31E^{-9}$), FN1 ($p = 2.08E^{-14}$), ELN ($p = 7.05E^{-15}$), POSTN ($p = 2.95E^{-7}$), and LTBP2 ($p = 2.86E^{-9}$ in FCR stromal areas.

CONCLUSION

Spatial transcriptomics identified several candidates for epithelial cytokines in the FCR regions that may promote macrophage translocation. In addition, elevated expression of ECM genes suggest that FCR regions undergo active remodeling. Feature studies will provide validation with fluorescent in situ hybridization and utilize transurethral installation of selected cytokine candidates to test their role in macrophage translocation.

Epigenetic Regulation of Radiation-Induced Senescence in Pulmonary Fibrosis

Investigator: Sara B. Palega, M.S.
Mentor: Yan Sanders, MD
Co-Authors(s):
Jennifer Zhou, Macon & Joan Brock Virginia Health Sciences Eastern Virginia Medical School
Department(s): Biomedical and Translational Sciences
Poster #: 53B

INTRODUCTION

Pulmonary fibrosis is an age-related, progressive disease that can develop following thoracic radiation therapy. Radiation-induced lung fibrosis is associated with chronic inflammation and impaired tissue repair. An increasingly recognized driver of pulmonary fibrosis is cellular senescence, which is characterized by stable cell-cycle arrest and a potent pro-inflammatory 'senescence-associated secretory phenotype,' or 'SASP'. Senescent cells accumulate with age and repeated injury, and are recognized as a critical link between aging and age-related diseases, including pulmonary fibrosis. Previously, the euchromatin mark H4K16ac was reported to promote profibrotic gene expression in lung fibrosis. Here, we will establish clinically relevant, repeated low-dose radiation-induced senescence model in ex vivo 3D organoid and 2D cellular models to determine whether radiation-induced senescence is mediated by H4K16ac.

METHODS

IMR90 human lung fibroblasts were exposed to repeated low-dose radiation (1 or 2Gy every 2–3 days for 10 days) to model fractionated radiation exposure. Senescence was assessed by growth arrest, SA-βgal staining, apoptosis resistance, and p16 and p21 expression. Inflammatory gene expression was evaluated by mRNA profiling. To extend these findings to a 3D lung tissue environment, we established a mouse precision-cut lung slice (PCLS) model and evaluated radiation-induced changes by mRNA profiling and immunofluorescence. The active histone mark, H4K16ac, levels are examined in the 3D model by immunofluorescence, and the occupancy of H4K16ac at SASP-associated genes in lung fibroblasts was examined in 2D model following radiation by chromatin immunoprecipitation (ChIP) assays.

RESULTS

Repeated low-dose radiation induced a senescent phenotype in IMR90 fibroblasts, with upregulation of inflammatory SASP-associated genes. In our PCLS model, radiation increased mRNA markers of senescence, inflammation, and fibrosis, along with increased p21 and H4K16ac by immunofluorescence. H4K16ac is enriched in lung fibroblasts following radiation and at promoters of key inflammatory SASP genes (IL-1B, IL-6). These findings demonstrate that repeated low-dose radiation induces senescence, inflammatory, and fibrotic changes in lung tissue and supports a potential role for H4K16ac in this response. Ongoing studies aim to identify other SASP-related genes that are linked to H4K16Ac in radiation-induced senescence.

CONCLUSION

We have established complementary fibroblast and PCLS models for investigating senescence induced by fractionated radiation exposure. The euchromatin mark H4K16Ac is enriched in lung tissue following irradiation and mediates the up-regulation of key SASP-related inflammatory genes. Ongoing studies to define the role of H4K16ac in radiation induced SASP-related gene transcription. Establishing these mechanisms may identify pathways that contribute to persistent lung injury and provide potential targets for limiting radiation-induced pulmonary fibrosis.

A 3D Bioprinting Tumoroid Model: iPSC-derived Extracellular Vesicles Modulate Breast Cancer Growth

Investigator: Emilee Peterson, B.S.
Mentor: Patrick Sachs, Ph.D.
Co-Authors(s):
None listed.
Department(s): Medical Diagnostics and Translational Sciences
Poster #: 58A

INTRODUCTION

The regenerating mammary microenvironment has the unique ability to redirect non-mammary and cancer cells to a normal cell fate (1, 2). These redirected non-mammary cell types displayed normal mammary epithelial characteristics and contributed to the regeneration of a functional mammary gland epithelial tree. Our group has recently shown that mitochondrial transfer from mammary epithelial cells contributes to the microenvironmental redirection of breast cancer cells (3). We hypothesized that mitochondrial transfer from other cell types could contribute to cell fate redirection, as studies have shown that embryonic stem cells (ESCs) can redirect cancer cells and suppress tumorigenic phenotypes without the mammary niche present (4). Previously in our laboratory, breast adipose-derived stem cells (bASCs) were isolated from mammary fat tissue and reprogrammed into induced pluripotent stem cells (iPSCs), an embryonic-like stem cell. Our aim is to investigate if the intercellular transfer of mitochondria from iPSCs can redirect cancer cells through direct contact and extracellular vesicles (EVs).

METHODS

We studied mitochondrial transfer in 2D and 3D cocultures using our novel 3D bioprinting system to generate 3D chimeric tumoroid models of mammary cancer cells and iPSCs in collagen hydrogels. iPSC-derived EVs were isolated through differential centrifugation and microfiltration, then transferred to the 3D tumoroid models.

RESULTS

The iPSCs transferred their mitochondria to mammary cancer cells in 2D and 3D, and coculture experiments resulted in decreased cancer growth rates. The iPSCs did not induce apoptosis or alter the metabolic profile of the cancer cells. Similarly, iPSC-derived EVs transferred mitochondria and decreased tumoroid growth in 3D.

CONCLUSION

iPSCs have the capability to suppress tumorigenicity in mammary cancer cells, with a possibility of cancer redirection. Concentrated iPSC-derived EVs can mimic the anti-proliferative effects of the parent cells in 3D in vitro models, expanding the potential for cell-free approaches in cancer research.

Optimization of a 3D Extracellular Matrix Environment for Mammary Epithelial Organoid Formation

Investigator: Davin Stevenson, B.S.
Mentor: Robert D. Bruno, Ph.D.
Co-Authors(s):
None listed.
Department(s): Medical Diagnostic and Translational Science
Poster #: 59A

INTRODUCTION
Three-dimensional (3D) bioprinting provides an important approach for modeling mammary gland development and epithelial morphogenesis in a physiologically relevant environment. Mammary epithelial cells have a strong response to their extracellular matrix (ECM), which can influence cell organization, proliferation, polarity, and tissue-like structure formation (1, 2). The murine mammary epithelial cell line EpH4 provides a useful model for researching these processes. Combining 3D bioprinting with tunable hydrogel environments allows for the precise placement of these mammary cells within a defined matrix while evaluating ECM conditions that promote organoid formation.

METHODS
We hypothesize that incorporation of a basement membrane such as Geltrex will promote epithelial cell polarization and improve the efficiency of luminal organoid formation compared to collagen alone. To test this hypothesis, EpH4 cells were 3D bioprinted within hydrogel constructs, with initial experiments using rat-tail collagen as a matrix lacking basement membrane components. Cell morphology and organization were evaluated following printing. Geltrex will subsequently be evaluated as an alternative matrix condition.

RESULTS
The preliminary experiments using rat-tail collagen demonstrate that EpH4 cells can establish 3D cellular structures within the printed matrix. However, the cultures have not consistently developed the organized, branching morphologies characteristic of a mammary organoid model. These findings provide a foundation for determining whether addition of a basement membrane matrix improves luminal organoid formation.

CONCLUSION
Establishing an optimized 3D culture environment will provide a reproducible platform for investigating mammary epithelial morphogenesis along with the cellular and extracellular mechanisms that regulate tissue organization. This system could support studies of mammary gland development, epithelial remodeling, and disease-associated changes in tissue architecture.

Bone morphogenic protein receptor 1a deletion cause increased spontaneous paralysis in 2D2 EAE model

Investigator: Jonathan Edward Waldron, B.S.
Mentor: Piotr Kraj, Ph.D., DVM
Co-Authors(s):
None listed.
Department(s): Biology
Poster #: 54B

INTRODUCTION

Central tolerance eliminates self-reactive T cells preventing the T cell's large receptor repertoire from recognizing self-antigens. Central tolerance is not complete allowing some self-reactive cells to survive and populate peripheral organs where tolerance mechanisms such as T regulatory cells (Tregs) ensure immune homeostasis and enforce quiescence of self-reactive cells. However, cell intrinsic mechanisms may change quiescent status of effector T cells and cause their proliferation and autoimmune disease. These self-reactive cells can be studied by using 2D2 mice, where T cells express a transgenic T cell receptor specific for the neural peptide myelin oligodendrocyte glycoprotein (MOG). 2D2 cells cause experimental autoimmune encephalomyelitis (EAE), which results in progressive paralysis. According to the literature without immunization with MOG and adjuvant about 4% will spontaneously develop paralysis. Paralysis occurs significantly higher in BMPR1α deficient 2D2 mice. Bone Morphogenic Proteins (BMPs) are a part of the TGF-β superfamily known for their essential cellular functions such as differentiation, proliferation, adhesion, migration and apoptosis. More recent evidence links their role in regulating immunological functions.

METHODS

For BMPR1α analysis conditional knockout mice were bred by crossing BMPR1αfl/fl mice with CD4cre, then GFP reporter mice. Genotyping mice was from DNA extracted in toe biopsies, was followed by PCR analysis of CD4cre, floxed alleles and GFP reporter constructs. Blood analysis included staining of CD4/CD8, Foxp3-GFP, and Ly5.1/Ly5.2 congenic markers to ensure 2D2 phenotype (Vα3.2 and Vβ11), and allow donor/recipient tracking. Impact of BMP signalling in 2D2 T cells was studied by depleting environment of BMP ligands. This was achieved by adaptive transfer of dendritic cells expressing Noggin or Gremlin.

RESULTS

The phenotype and functional status of 2D2 cells was analysed in recipient animals by flow cytometry. In vitro cultures assessed 2D2 cell proliferation and cell surface markers when cultured with MOG, spinal cord lysate, or bacterial lysate.

CONCLUSION

BMPs have been shown to be regulatory proteins and here we show that they influence onset of autoimmune disease. These data point to the importance of BMPR1α signalling for maintaining immune homeostasis.

LEI-515-mediated MAGL Inhibition Protects Against Ventilator Induced Lung Injury in Mice

Investigator: Ryan Keon Washington, B.S.
Mentor: Nagaraja Nagre, Ph.D.
Co-Authors(s):
Terrie Lynch, Macon & Joan Brock Virginia Health Sciences Eastern Virginia Medical School
Nicholas Richards, Macon & Joan Brock Virginia Health Sciences Eastern Virginia Medical School
Alan Abhilash, Macon & Joan Brock Virginia Health Sciences Eastern Virginia Medical School
Department(s): Biomedical and Translational Sciences
Poster #: 60A

INTRODUCTION

Acute respiratory distress syndrome (ARDS) is a life-threatening form of Acute Lung Injury (ALI) that affects (ARDS stats). Mechanical Ventilation is a life-saving intervention for ARDS, but the various stresses it puts on the lung can exacerbate lung injury, leading to ventilator-induced lung injury (VILI), for which pharmacologic therapies are limited. Endocannabinoids are a family of molecules that interact with cannabinoid receptors. The most abundant endocannabinoid, 2-arachidonoylglycerol (2-AG), is a potent regulator of inflammatory responses. The abundance of 2-AG is tightly regulated by an enzyme known as monoacylglycerol-lipase (MAGL). Degradation of 2-AG releases free-fatty acid and arachidonic acid (AA). AA is a precursor for the production of eicosanoids, another class of molecules that regulate inflammatory responses. Inhibition of MAGL has been demonstrated to confer protection against inflammatory and mechanical tissue injury. Based on this rationale, we tested the hypothesis that pharmacological inhibition of MAGL attenuates VILI by decreasing the abundance of eicosanoids.

METHODS

A two-hit murine lung injury model was employed using intratracheal injection of lipopolysaccharide (LPS) followed by high tidal volume (30 ml/kg, 2h, 3cm H2O positive end-expiratory pressure, with room air) mechanical ventilation. C57BL/6J mice received peripherally restricted MAGL inhibitor LEI-515 (20 mg/kg, i.p) after LPS exposure and before ventilation. At the end of ventilation, the total cell number and protein content in the bronchoalveolar lavage fluid (BALF) were determined. Neutrophil population and CD63 expression in neutrophils were assessed by flow cytometry. The levels of IL-1β, CXCL2, and arachidonic acid (AA) in the BALF were determined by ELISA. Lung injury was assessed by histology, and inflammatory signaling in the lung was assessed by immunoblot analysis of lung homogenate. Neutrophil extracellular traps (NETS) release was assessed by immunoblot analysis of CitH3 and H2B in the BALF.

RESULTS

MAGL inhibition with LEI-515 significantly reduced BALF total cell counts and protein content, which were increased in response to VILI. BALF levels of IL-1β, CXCL2, TNF-α, and AA were significantly reduced in LEI-515-treated mice. Flow cytometry analysis revealed that mice treated with LEI-515 had lower neutrophil populations and reduced neutrophil surface CD63 expression. Histological analysis showed that LEI-515 treated mice had lower tissue injury. Immunoblot analysis revealed lower expression of NOX4, p-IKB, 5-LOX, and COX2 in LEI-515 treated mice. In addition, immunoblot analysis of BALF samples revealed that CitH3 and H2B levels were significantly reduced in LEI-515 treated mice.

CONCLUSION

These findings suggest that MAGL inhibition exerts a protective effect against ventilator-induced lung in part by reducing arachidonic acid mediated inflammation, oxidative stress, and neutrophil activation.

Development of a Biomimetic Mammary Microenvironment for Spatially Organized 3D Bilayer Tissue Constructs

Investigator: Arielle Wolter, Ph.D.
Mentor: Patrick Sachs, Ph.D.
Co-Authors(s):
None listed.
Department(s): Biomedical and Translational Sciences
Poster #: 55B

INTRODUCTION

The mammary gland microenvironment is dynamic, undergoing structural and biochemical changes throughout development and adult life. These changes aid in the regulation of ductal luminal epithelial and myoepithelial cell fate and the organization required for normal tissue development and function [2]. Recent studies have further demonstrated that the surrounding microenvironment can influence cellular fate and differentiation [1]. However, current *in vitro* models remain limited in reproducing both the biochemical composition and organized tissue architecture of the mammary gland.

METHODS

To address this limitation, we developed a biomimetic mammary model that integrates tissue-derived extracellular cues with spatial control of cellular organization. We combine mammary-derived decellularized extracellular matrix (dECM) with precision 3D bioprinting to provide a biochemical and structural microenvironment for the formation and organization of mammary organoids. Here, we investigate how the biochemical and structural properties of the microenvironment influence mammary cell phenotype, organization, and the formation of bilayer tissue structures. Cellular organization and phenotype are evaluated throughout organoid development to determine how closely these structures represent characteristics of native mammary tissue.

RESULTS

Prior studies have established culture conditions supporting mammary cell viability and phenotype in 2D culture, as well as aggregation and three-dimensional organization in organoid culture. Current studies incorporate these cellular populations within the engineered microenvironment using 3D bioprinting and evaluate their capacity to develop organized mammary tissue structures.

CONCLUSION

Here, we aim to establish a biomimetic mammary organoid model that combines biochemical and spatial control of tissue organization. Reproducible luminal–myoepithelial organization could provide a model for studying mammary gland development and later examining hormonal and disease-associated changes within the tissue microenvironment.

Physical Activity Fragmentation and the Association with Cardiovascular Health- Preliminary Findings in Older Adults

Investigator: Taskina Akhter, M.S.
Mentor: Leryn J. Reynolds, Ph.D.
Co-Authors(s):
Patricia Guereque, Old Dominion University
William Lowe, James Madison University
Department(s): Exercise Science
Poster #: 39A

INTRODUCTION

Physical activity (PA) promotes cardiovascular (CV) health in older adults; however, traditional measures such as moderate-to-vigorous physical activity (MVPA) and steps/day do not capture PA accumulation throughout a day. Activity fragmentation may predict behavior patterns associated with CV health. The aim of the study is to determine whether daily PA fragmentation can predict CV health in older adults (≥ 55 years). We hypothesize that the Active to Sedentary Transition Probability (ASTP) will be more closely correlated to CV health compared to non-fragmented PA measures.

METHODS

Adults (≥ 55 years) wore a physical activity monitor for 7 days to measure MVPA, steps/day, and ASTP. Heart rate variability (HRV) and brachial artery flow-mediated dilation (FMD) were assessed after 7-days using a Polar H10 heart rate monitor and Doppler Ultrasound, respectively.

RESULTS

Sixteen participants (Age: 63±9.0y, Sex: 4 male and 12 female; Body Mass Index (BMI): 25.26±4.40 Kg/m^2, %Fat: 31.06±9.81) were recruited. MVPA and steps/day were poorly correlated to Root Mean Square of Successive Differences (RMSSD) (MVPA: r=0.288, Steps/day: r=0.370), Standard Deviation of Normal-to-Normal intervals (SDNN) (MVPA: r=0.173, Steps/day: r=0.206), and FMD (MVPA: r=0.349, Steps/day: r=0.313). ASTP showed very poor correlations with these CV measures (RMSSD: r=0.208, SDNN: r=0.167, FMD: r= -0.073).

CONCLUSION

These preliminary data demonstrate activity fragmentation has weaker correlation to CV measures than traditional PA. Given the limited sample size, these findings should be interpreted cautiously.

fMRI Outcomes of Melodic Intonation Therapy for Aphasia: A Systematic Review

Investigator: Jessica S. Gebert, M.S., CF-SLP
Mentor: Stacie M. Raymer, Ph.D., CCC-SLP
Co-Authors(s):
Rachel Johnson, Old Dominion University
Department(s): Speech-Language Pathology
Poster #: 33A

INTRODUCTION
Many individuals with aphasia following a left-hemisphere stroke retain the ability to sing despite limited spontaneous verbal output. Researchers leveraged these capabilities to develop Melodic Intonation Therapy (MIT), a systematic prosodic and rhythmic method to foster recovery of verbal expression in individuals with nonfluent aphasia. Several reviews have summarized the evidence for the effects of MIT for language recovery, reporting positive outcomes for repetition, naming, and verbal fluency. Likewise, researchers have explored the neural correlates of MIT, anticipating right-hemisphere mediation of language recovery. Recent reviews have summarized neuroimaging outcomes following aphasia treatment, with few including MIT. The purpose of the current project was to systematically review the functional magnetic resonance imaging (fMRI) literature to explore neuroplastic changes associated with MIT. By restricting to one neuroimaging approach, we endeavored to constrain variables and better represent this complex dynamic recovering neural system.

DISCUSSION
We searched four databases and reference lists for studies that implemented fMRI following MIT in adults with aphasia following left-hemisphere stroke. We identified seven that met inclusion criteria: five case studies and two group studies. We implemented a 20-item fMRI appraisal checklist to consider the quality of fMRI methods and statistical analyses. Reviewers extracted data across studies pertaining to aphasia participants, treatment outcomes, fMRI methods, and post-treatment activation patterns. We found that over time, fMRI methodology has improved, increasing confidence in neuroimaging findings across studies. The seven fMRI studies reported on 30 adults with aphasia (22 male, 8 female; 6 subacute, 24 chronic), all reporting improvements on language measures. The two group studies indicated considerable right-hemisphere activation post-MIT, with a laterality index in one study favoring the right in five of eight patients, more so for those with subacute aphasia, and therapy language outcomes positively correlated with right inferior frontal gyrus (IFG) increases in another. Following MIT, all five case studies reported increased right-hemisphere activation, especially in IFG and superior temporal gyrus (STG) areas. However, three of five case studies also noted increased post-MIT left activation, particularly in prefrontal and inferior parietal regions. Two case studies showed decreased left activation post-MIT, one IFG and one "perisylvian," and one with decreased right cerebellar activation. Our right-hemisphere prediction was largely supported, as two group studies and five case studies reported increased activation in right perisylvian regions following MIT, particularly the IFG and STG. These findings are counterbalanced by findings of increased left-hemisphere activation following MIT in several studies. However, in examining left-hemisphere activation in the cases more closely, we noted discrepancies that would explain left engagement. For example, one study used a passive lexical decision task in the scanner in a patient with relatively preserved left frontal cortex, and another study delivered MIT simultaneously with 'conventional speech therapy,' which likely would engage left hemisphere capacities.

CONCLUSION
Our review suggests that important observations are evident as findings are coalesced across case studies. Group studies are particularly informative for correlating language improvements with neural changes. Overall, the preponderance of the fMRI evidence of this review supports primarily right-hemisphere mediation of successful response to MIT.

Acute effects of repetitive subconcussive soccer heading on stepping in place gait and arm swing variability

Investigator: Josh Lawton, M.S.
Mentor: Chris Rhea, Ph.D.
Co-Authors(s):
Eric Schussler, Old Dominion University
Department(s): Associate Dean for Research & Innovation
Poster #: 34A

INTRODUCTION

Repetitive subconcussive head impacts alter gait and postural control, including reduced stepping-in-place variability hours after exposure. Laboratory-based repetitive soccer heading also produces significant postural control changes. What remains unknown is the extent to which arm swing during gait may also exhibit changes in dynamics after head impacts. If so, wearables such as smartwatches could be used to monitor neuromotor changes. The purpose of this study was to examine the acute changes in stepping-in-place gait variability and arm swing variability following repetitive soccer heading.

METHODS

Ten college aged participants completed baseline stepping-in-place assessments under three conditions: eyes open, eyes closed, head shake. The participants then performed ten soccer headers from nine meters at approximately 25 mph, followed immediately by performing the same three stepping-in-place tasks. Variability was quantified as the coefficient of variation (CoV) of peak thigh and arm flexion, measured using a validated custom Android application called AccWalker. Hedges g was used due to the small sample size.

RESULTS

For leg swing, moderate effects were observed across conditions: eyes open (pre: 0.911 +/- 2.166; post: 1.270 +/- 0.524; g = 0.561), eyes closed (pre: 1.576 +/- 1.343; post: 1.339 +/- 0.883; g = 0.670) and head shake (pre: 1.293 +/- 0.658; post: 1.417 +/- 1.078; g = 0.569). For arm swing, effect sizes were moderate: eyes open (pre: 1.092 +/- 0.229; post: 1.189 +/- 0.361; g = 0.605), eyes closed (pre: 1.116 +/- 0.314; post: 1.035 +/- 0.239; g = 0.641), and head shake (pre: 1.065 +/- 0.232; post: 1.028 +/- 0.249; g = 0.551).

CONCLUSION

Decreased variability following repetitive subconcussive impacts in the leg swing eyes closed condition aligns with prior research, whereas increases during the leg swing eyes open and head shake condition are not supported by previous findings. Differences between arm and leg swing variability suggest that arm swing using AccWalker requires further validation. These findings support prior evidence of acute postural control/gait changes following repetitive soccer heading and highlight the need for further evaluations of arm swing and eyes open CoV to determine if they are valid markers of postural control/gait variability after subconcussive head impacts.

Time-to-Boundary Responses Across Sensory Conditions in Adults with and Without Chronic Ankle Instability

Investigator: Amin Mohammadi, M.S.
Mentor: Ryan S. McCann, Ph.D.
Co-Authors(s):
Reza Pousti, Old Dominion University
Saeed Eshghi, Old Dominion University
Eric Schussler, Old Dominion University
Department(s): Rehabilitation Sciences
Poster #: 40A

INTRODUCTION

Chronic ankle instability (CAI) is associated with sensorimotor impairment, altered postural control, and fear-related movement burden. Time-to-boundary (TTB) quantifies postural safety margins by estimating the time available before the center of pressure reaches the boundary of the base of support. However, it remains unclear whether TTB differentiates individuals with CAI from controls during sensory-challenging balance tasks. Therefore, this pilot study compared TTB outcomes between adults with and without CAI across six Clinical Test of Sensory Interaction and Balance (CTSIB) conditions and explored associations between TTB, physical activity, and fear-related outcomes within the CAI group.

METHODS

Twenty middle aged adults (40-59 years old) were included: CAI (n = 10) and control (n = 10). Participants completed six double-leg CTSIB conditions while standing on a force plate: firm surface with eyes open (T1), eyes closed (T2), and visual conflict (T3), and foam surface with eyes open (T4), eyes closed (T5), and visual conflict (T6). Center-of-pressure data were used to calculate absolute minimum TTB in the mediolateral (ML) and anteroposterior (AP) directions for each condition. Physical activity variables included moderate-to-vigorous physical activity, steps, and energy expenditure which were collected using a waist-worn ActiGraph wGT3X-BT accelerometer (ActiGraph LLC, Pensacola, FL, USA). Fear-related outcomes included the Tampa Scale of Kinesiophobia and Fear-Avoidance Beliefs Questionnaire. Separate 2 × 6 repeated-measures ANOVAs examined the effects of group and condition on ML and AP TTB. Exploratory Spearman correlations examined associations among TTB, physical activity, and fear-related outcomes within the CAI group.

RESULTS

TTB varied significantly across CTSIB conditions in both directions. ML TTB demonstrated a significant main effect of condition (Pillai's Trace = 0.872, $F(5,14) = 18.998$, $p < 0.001$, $\eta p^2 = 0.872$), but no significant group effect, ($F(1,18) = 0.594$, $p = 0.451$, $\eta p^2 = 0.032$) or condition × group interaction (Pillai's Trace = 0.165, $F(5,14) = 0.555$, $p = 0.733$, $\eta p^2 = 0.165$). AP TTB also demonstrated a significant main effect of condition Pillai's Trace = 0.869, $F(5,14) = 18.572$, $p < 0.001$, $\eta p^2 = 0.869$), but no significant group effect ($F(1,18) = 0.053$, $p = 0.820$, $\eta p^2 = 0.003$) or condition × group interaction (Pillai's Trace = 0.373, $F(5,14) = 1.663$, $p = 0.208$, $\eta p^2 = 0.373$). TTB generally decreased as sensory demands increased, particularly during foam and visual-conflict conditions. In exploratory CAI-only analyses, TTB was associated with physical activity and fear-related outcomes. Greater moderate-to-vigorous physical activity and energy expenditure were associated with higher AP TTB during firm eyes-open standing ($\rho = 0.685–0.794$, $p = 0.006–0.029$). Higher kinesiophobia and fear-avoidance were associated with lower TTB across sensory-challenging conditions ($\rho = -0.644$ to -0.911, $p < 0.001–0.044$).

DISCUSSION

TTB varied significantly across sensory conditions, indicating that sensory difficulty influenced postural safety margins. However, adults with and without CAI did not differ in ML or AP TTB during double-leg CTSIB testing, suggesting that double-leg TTB may be more sensitive to sensory task demands than CAI group status in this pilot sample. Lower TTB appears to contribute to greater kinesiophobia and fear-avoidance as well as lower moderate-to-vigorous physical activity in people with CAI.

MENOPAUSAL SYMPTOMS, PSYCHOSOCIAL FACTORS, AND PHYSICAL ACTIVITY AMONG PHYSICALLY ACTIVE MIDLIFE FEMALES

Investigator: Ella Onsoriasl, M.S.
Mentor: Natalie Yarish, Ph.D.
Co-Authors(s):
Heather Hamilton, Old Dominion University
Kristin Heron, Old Dominion University
Department(s): Exercise Science
Poster #: 35A

INTRODUCTION

Menopausal symptoms are common during midlife and may influence women's physical activity (PA) participation and their experience of being active. However, relationships between menopausal symptom severity, PA, confidence and enjoyment, social support (SS), exercise identity, and quality of life (QOL) remain unclear. This study examined associations between menopausal symptoms, PA, and psychosocial factors among physically active midlife women.

METHODS

This cross-sectional study included 151 women aged 40–60 years who reported engaging in intentional PA at least once per week. Participants completed an online survey including the Menopause Rating Scale (MRS), Self-Administered Modifiable Activity Questionnaire (SMAQ), Physical Activity and Social Support Scale (PASSS), Social Support for Exercise Survey (SSES), Exercise Identity Scale (EIS), and 12-Item Short Form Health Survey (SF-12). Spearman correlations and regression analyses were used to examine associations among menopausal symptoms, SS, exercise identity, QOL, and self-reported PA. Perceived effects of menopausal symptoms on PA were also summarized descriptively.

RESULTS

Contrary to the hypothesis, greater menopausal symptom severity was not associated with lower PA. Instead, symptom severity demonstrated a weak positive association with PA and was the only variable significantly associated with PA in the multiple regression model. Menopausal symptoms were highly prevalent and were commonly perceived as negatively affecting PA confidence, enjoyment, intensity, and ease of participation. SS was positively associated with PA at the bivariate level but was not significant after accounting for other variables in the multiple regression model. Exercise identity and QOL were also not significantly associated with PA in the multiple regression model.

CONCLUSION

These findings suggest that midlife women may remain physically active even while experiencing symptoms that make activity feel more difficult, less enjoyable, or less confidence-building, and that self-reported PA participation and the perceived experience of being active should be considered separately. Findings support the need for flexible, symptom-aware, and socially supportive approaches to PA promotion for midlife women.

RDE-GAIT: A Novel Mirror-Equilibrium Approach to 3-D Gait Symmetry

Investigator: Reza Pousti, Ph.D., M.S.
Mentor: Christopher K. Rhea, Ph.D.
Co-Authors(s):
Daniel M. Russell, Ellmer College of Health Sciences
Ashwini Kulkarni, Ellmer College of Health Sciences
Brittany S. Samulski, Ellmer College of Health Sciences
Christopher K. Rhea, Ellmer College of Health Sciences
Department(s): Kinesiology and Rehabilitation
Poster #: 36A

INTRODUCTION
Digital wearables enable large-scale, ecological gait assessment, yet many commonly used gait metrics lack mechanistic interpretability and cannot identify stride-level symmetry dynamics.

METHODS
To this end, we developed the Reza Dimensional Equilibrium for gait (RDE-GAIT) method and evaluated it using a public mobile brain-body dataset of 35 healthy young adults from Hanada, Kalabic, Ferris (2024). Using a left ankle IMU with a waist reference, we reconstructed the 3D leg vector at the forwardmost (anterior) and backward-most (posterior) locations during each gait cycle, and flipped/mirrored the posterior vector so that it could be directly compared to the anterior vector in 3D space. We defined the similarity between the vectors as p^((k)) ranging from 0 to 1, with values near 0 indicating less similarity and values near 1 indicating more similarity. Next, we normalized p^((k)) to a robust local baseline p^0 computed as a rolling median over a 200-cycle moving window, so each gait cycle is evaluated relative to nearby cycles (100 cycles before and 100 after) within the session. Lastly, an equilibrium value at each gait cycle termed E^((k)) was calculated as p^((k))/p^0, with $0.95 \leq E \leq 1.05$ indicating a consistent gait cycle relative to the surrounding gait cycles and $E<0.95$ or $E>1.05$ indicating inconsistent gait cycles (either an inconsistent gait cycle embedded within consistent gait cycles or a consistent gait cycle embedded within inconsistent gait cycles).

RESULTS
Outdoor walking sessions contained 1,326 5,739 gait cycles (median 4,632). The median proportion of consistent gait cycles was 78% (range 12.2 94.8%), and the median proportion of inconsistent gait cycles was 22% (range 5.2 44.8%). Twenty-eight participants exhibited consistency in >70% of gait cycles, with eight of those exhibiting a very high proportion of consistency in their gait cycles (>85%). On the contrary, three participants exhibited a high proportion of inconsistency in their gait cycles (>65%).

CONCLUSION
What remains an empirical question is the extent to which the similarity metric (p) and/or the equilibrium metric (E) relate to adaptive and/or functional gait patterns. Future work should explore these questions, as well as compare RDE-GAIT to traditional symmetry gait metrics across diverse locomotor tasks (e.g., running, irregular terrain, etc.).

The Effect of Attentional Focus on Walking Performance and Movement Control in Young Adults

Investigator: Paphawee Prupetkaew, M.S.
Mentor: Daniel M. Russell, Ph.D.
Co-Authors(s):
Ashwini Kulkarni, Old Dominion University
Louisa Raisbeck, University of North Carolina at Greensboro
Christopher Rhea, Old Dominion University
Department(s): Exercise Science
Poster #: 41A

INTRODUCTION
Where attention is focused influences the performance of motor skills. According to the constrained action hypothesis, internal focus of attention (IFA) on the body disrupts movement control by prompting conscious, effortful regulation of processes that are otherwise handled automatically, whereas external focus of attention (EFA) preserves automaticity by directing attention to environment. There is also evidence to suggest that far EFA from the person is better than near EFA (McNevin, Shea & Wulf, 2003). Walking is an important motor skill for everyday living, but performance deteriorates with age and neurological diseases and may alter the role of attentional focus. This study examined how IFA and EFA affect walking performance and movement control in healthy young adults to provide a basis for future research in clinical populations.

METHODS
Forty participants walked under six conditions: preferred speed walking without instruction (Pref), EFA on a distant target (EFA-Fr), EFA on the ground (EFA-Nr), internal focus on the head (IFA-He), lower back (IFA-Ba), and foot (IFA-Fo). Walking performance was measured using an instrumented walkway, while tri-axial accelerometers recorded head, lower back, and foot acceleration across anteroposterior (AP), mediolateral (ML), and vertical (VT) axes. Speed, stride length, and stride time were analyzed using one-way repeated measures ANOVA. Movement control was quantified by acceleration amplitude (RMS), log-normalized dimensionless jerk (LDJ) indicated smoothness, and sample entropy (SampEn) indicated predictability. Each analyzed using linear mixed models with walking speed included as a covariate to isolate the effect from speed changes. Bonferroni-correction was used as post hoc comparison.

RESULTS
All IFA conditions and EFA-Nr resulted in disrupted walking performance compared to EFA-Fr or Pref, which were not significantly different from each other. Focus of attention (FoA) instructions also impacted motion of the head and foot, but not the lower back. After accounting for changes in speed, FoA conditions reduced head AP and ML accelerations (RMS) compared with Pref. This was generally associated with higher LDJ (less smooth) and higher SampEn (less predictable) head AP movement. EFA-Nr resulted in lower LDJ (smoother) or lower SampEn (more predictable) AP head motion than EFA-Fr, IFA-He, and IFA-Ba. Focusing on the foot reduced foot acceleration (RMS) and increased SampEn (less predictable).

Discussion and Conclusion:
These findings partially support the constrained action hypothesis: IFA broadly disrupted movement control and walking performance. IFA on the foot reduced accelerations and predictability of foot motion and slowed walking speed. While EFA-Fr preserved walking speed but led to more constrained and regulated head motion. EFA-Nr slowed walking down, but head motion was less regulated than EFA-Fr or IFA on head or back. These findings indicate that the EFA distance effects on walking speed and movement control are not a function of constrained action, and it provides a rational for examining attentional focus effects on movement control in future gait rehabilitation research.

In-Field Muscle Oxygenation Responses During Competitive Soccer Match Play in Division I Collegiate Soccer Players

Investigator: Paul Sarac, M.S.
Mentor: Patrick B. Wilson, Ph.D.
Co-Authors(s):
Paul Sarac, Old Dominion University
Ian Winter, Old Dominion University
Department(s): School of Exercise Science
Poster #: 37A

INTRODUCTION

Athlete monitoring in soccer commonly relies on external load measures despite considerable inter-individual variation in the physiological responses elicited by similar external demands. Near-infrared spectroscopy (NIRS) provides a non-invasive method of continuously assessing local muscle oxygen saturation (SmO_2) and may provide additional insight into the physiological demands experienced during soccer. However, SmO_2 responses during full soccer match play remain poorly characterized. The purpose of this study was to characterize muscle oxygen saturation responses in NCAA Division I soccer players during a 90-min match and explore within-player changes in SmO_2 alongside external match demands.

METHODS

Three male NCAA Division I soccer players (age: 20.3 ± 1.5 y) completed a full-length soccer match while wearing a portable MOXY Monitor over the rectus femoris of the dominant leg to continuously measure SmO_2. External workload during match play was quantified using GPS-derived distance, load, top speed, sprint activity, and accelerations. Match data were segmented by half and into approximately 15-min epochs to characterize temporal changes in SmO_2 and external workload. Due to the exploratory nature and small sample size, analyses emphasized descriptive and within-player responses.

RESULTS

SmO_2 demonstrated substantial inter- and intra-individual variability throughout the 90-min game. Among players with complete match-level SmO_2 data (n=2), mean SmO_2 for time on the field was 38.9% and 40.8%. Across approximately 15-min epochs, mean SmO_2 ranged from 32.6 to 59.8% in one player and 39.6 to 42.9% in another. Importantly, changes in local muscle oxygenation did not consistently parallel changes in external workload. In one player, second-half mean SmO_2 for time on the field decreased from 40.6% to 36.5% while distance covered and GPS-derived load per time on the field increased by 17.5% and 26%, respectively, even though playing time decreased by 13 min or 28.9%. In another player, average SmO_2 remained relatively stable between halves (40.3% vs. 41.2%) despite changes in external demands, including a 35% reduction in sprint count.

CONCLUSION

Rectus femoris SmO_2 demonstrated substantial temporal and inter-individual variability during the 90-min match, and changes in SmO_2 did not consistently correspond with changes in external workload. These preliminary findings suggest that local muscular oxygenation may provide physiological information that is complementary to conventional GPS-based monitoring. Portable NIRS may therefore offer a feasible field-based approach for integrating internal physiological responses with external load monitoring in soccer to further understand training and game demands.

Content Validity of a Sodium Bicarbonate Use, Beliefs, and Knowledge Questionnaire Among Competitive Athletes via the Delphi Method

Investigator: Ian P. Winter, M.S.
Mentor: Patrick B. Wilson, Ph.D.
Co-Authors(s):
Leryn Reynolds, Old Dominion University
Lewis Gough, Birmingham City University
Department(s): Exercise Science
Poster #: 38A

INTRODUCTION

Sodium bicarbonate is a dietary supplement that can provide small but potentially meaningful improvements in high-intensity exercise performance. Despite inclusion on the International Olympic Committee's 2018 list of five dietary supplements known to directly improve performance, there remains a lack of information regarding the prevalence of use and athlete knowledge. The scarce data on sodium bicarbonate prevalence of use suggests that it is underutilized. The aims of this investigation were to develop and establish the content validity of a questionnaire assessing sodium bicarbonate supplementation practices and knowledge, and to quantify sodium bicarbonate's use and knowledge among competitive athletes.

METHODS

This investigation employed a survey-based, observational design and consisted of two phases. In phase one, the questionnaire was developed and sent to 11 sodium bicarbonate content experts (researchers and practitioners) for validation via the Delphi method. Content experts rated relevance, clarity, and simplicity of items/questions within the knowledge section using a 1-4 Likert scale. Content validity of each item was rated using the following formula: Content Validity Index = # of experts who gave a 3 or 4 rating / total # of experts. After receiving first-round feedback, items with a content validity score <0.78 were altered or omitted. Alterations were also made when several content experts provided similar feedback on a given item. In the second round, content experts were provided with statistics for each question, comments from all experts, and summaries of trends, before being sent the revised questionnaire for additional rating and feedback. In phase two, the validated questionnaire was shared with the target sample to gather data on sodium bicarbonate use patterns and knowledge. Eligible participants were ≥18 years old and had either regularly competed in sport or participated in at least one sporting competition during the previous 12 months.

RESULTS

A total of 273 athletes took part in the questionnaire. Of this sample, 48 (17.6%) reported having ever supplemented with sodium bicarbonate. Of those who reported taking dietary supplements within the last 12 months with the goal of enhancing sport performance (n=206), prevalence of ever using sodium bicarbonate increased to 23.3%. Among participants with complete data on knowledge questions (n=186), correct scores averaged 33.1% (±22.6%). A one-way ANOVA revealed an effect of athlete level on knowledge scores ($p<0.001$), with highly trained (6.5±3.6) and elite/international/world class (5.6±3.1) athletes scoring higher than recreationally active (3.7±2.9) and trained/developmental (4.4±3.3) athletes. There were no differences between men and women for knowledge (4.7±3.3 vs. 5.3±3.5, $p=.230$), but age was negatively correlated with knowledge ($\rho=-0.33$, $p<0.001$).

CONCLUSION

The lifetime prevalence of sodium bicarbonate use was relatively low (less than 25%) among this sample of competing athletes, even among those reporting using sports supplements within the past 12 months. Lack of knowledge of its potential utilization among recreational/trained/developmental and older athletes is indicated as one reason why, though primary sport may also play a large role. Targeted evidence-based education may help close the knowledge-to-practice gap and promote appropriate use among regularly competing athletes in sports that may benefit.

From Crisis to Crossroads: A Time-Series Analysis of Drug Overdose Mortality by Drug Class Across Hampton Roads, Virginia, 2018–2024

Investigator: Omotomilola Jegede, M.S.
Mentor: Michele Kekeh, Ph.D., M.S.
Co-Authors(s):
None listed.
Department(s): Joint School of Public Health
Poster #: 01B

INTRODUCTION

Greater Hampton Roads is experiencing a changing overdose epidemic that cannot be fully understood through overall death counts alone. Portsmouth recorded an overdose death rate of 95.7 per 100,000 in 2022 more than three times Virginia's statewide rate of 29 per 100,000. This study examined how overdose mortality changed across drug classes, localities, and demographic groups in Greater Hampton Roads from 2018–2024, with particular attention to fentanyl and emerging polysubstance patterns.

METHODS

A retrospective analysis used Virginia Department of Health (VDH) overdose mortality data and the Greater Hampton Roads Community Data Dashboard (2018–2024), stratified by drug class fentanyl and synthetic opioids, cocaine, heroin, prescription opioids, benzodiazepines, and psychostimulants and by locality, sex, and race/ethnicity. Interrupted time-series analysis with segmented regression assessed level and slope changes at two a priori breakpoints: March 2020 (COVID-19 pandemic onset) and Q3 2021 (post-pandemic fentanyl market acceleration). Trend differences by locality, race/ethnicity, and drug class were examined descriptively with frequency counts, crude rates, and percentage change calculations.

RESULTS

Fentanyl accounted for approximately 79% of regional overdose deaths from 2019–2023, highlighting the dominant role of illicit synthetic opioids in the regional epidemic. At the same time, the drug supply and pattern of overdose mortality shifted. Cocaine-involved deaths increased 221% among males aged 55–64 between 2018 and 2023, raising concern about fentanyl contamination of the stimulant supply. In contrast, heroin-involved deaths declined by more than 60% after 2020, consistent with displacement by illicit fentanyl. Segmented analysis identified a significant post-2021 acceleration in stimulant-involved emergency department visits (+24.3%; 95% confidence interval: 17.9–31.1). Racial disparities also persisted: in 2023, overdose mortality among non-Hispanic Black Virginians was nearly twice that of non-Hispanic White Virginians, with particularly pronounced disparities in Norfolk and Portsmouth. Although opioid-related deaths declined substantially by 2024, improvement was geographically uneven.

CONCLUSION

Greater Hampton Roads is not simply experiencing fewer overdoses; the epidemic is changing. Declining heroin and prescription-opioid mortality is occurring alongside persistent fentanyl involvement and increasing stimulant-related risk. These findings support a geographically targeted, drug-supply-informed approach to prevention and harm reduction. Priorities should include expanding naloxone availability, strengthening fentanyl test-strip access for people who use stimulants, integrating overdose prevention into behavioral health services, and directing resources toward communities experiencing the greatest disparities. A multi-drug, equity-centered public health response is urgently needed, including naloxone saturation across all seven cities, fentanyl test strip expansion targeting stimulant users among others. A declining death count is a floor, not a finish line.

Analysis of Health Services Needs for Members of the Buffalow Family and Friends Initiative

Investigator: Amija Reed, B.S.
Mentor: Michele Kekeh, Ph.D., M.S.
Co-Authors(s):
Omotomilola Jegede, Old Dominion University
Nischelle Buffalow, Buffalow Family and Friends
Brett Sierra, Old Dominion University
Department(s): Center for Global Health
Poster #: 02B

INTRODUCTION
In underserved communities, where access to care and social services may be limited, understanding health services needs by household composition is critical for designing targeted interventions to address the needs for these communities. This study examined household composition as a driver of community health needs among residents of South Norfolk, Virginia and the surrounding areas.

METHODS
A cross-sectional community health survey was conducted between September 2025 and January 2026. Graduate students from Old Dominion University conducted the data collection. Descriptive statistics and Chi-Square were used for the analysis.

RESULTS
Households included households with older adults only (41%), with adults only (26.1%), with children and adults (19.1%), intergenerational households (12.2%), and households with older adults and children (1.6%). Overall, households with older adults show the greatest needs, reporting significantly higher rates of not eating balanced meals and skipping meals than other households ($p < 0.05$). Among psychosocial outcomes, older adults reported the greatest social exclusion ($p = 0.014$) compared to other groups. Older adults reported greater needs including, dental care and physical therapy.

CONCLUSION
The results indicate that household composition is an important determinant of community health with older adults experiencing disproportionately higher levels of food insecurity and social exclusion, and health service needs. There is a need for community health policies that prioritize targeted strategies including, healthy nutrition assistance, initiatives for more connections, and age-friendly initiatives to improve the wellbeing of individuals in underserved communities, especially among older adults.

Reliability Between Finapres NOVA and Kubios Scientific Heart Rate Variability Measurements

Investigator: Patricia E. Guereque, B.S.
Mentor: Leryn J. Reynolds, Ph.D.
Co-Authors(s):
Taskina Ahkter, Old Dominion University
William Lowe, James Madison University
Department(s): Exercise Science
Poster #: 69B

INTRODUCTION
Heart rate variability (HRV) is a widely used noninvasive measure of autonomic cardiac regulation. Kubios Scientific is an established platform for HRV analysis, whereas beat-to-beat blood pressure devices such as Finapres NOVA provided an alternative method of acquiring cardiac interval data. However, difference in signal acquisition, beat detection, and processing may affect HRV outcomes. Therefore, this study aimed to evaluate the reliability between HRV measures obtained from Finapres NOVA and Kubios Scientific across commonly reported time-and frequency-domain indices.

METHODS
Single measure intraclass correlation coefficient (ICC) and the 95% confidence intervals (CI) were used to assess reliability between Finapres NOVA and Kubios Scientific measurements of Standard Deviation of Normal-to-Normal intervals (SDNN), Root Mean Square of Successive Differences (RMSSD), Low Frequency (LF), and High Frequency (HF) from the Finapres NOVA and Kubios Scientific.

RESULTS
When comparing the Finapres NOVA and Kubios Scientific, SDNN demonstrated poor reliability during both trials (Trial 1: ICC= 0.295, 95% CI -0.111-0.658; Trial 2: ICC= -0.021, 95% CI -0.361-0.404), RMSSD demonstrated good reliability during Trial 1 (ICC= 0.780, 95% CI 0.443-0.920) and moderate reliability during Trial 2 (ICC= 0.746, 95% CI 0.426-0.902), LF demonstrated good to excellent reliability (Trial 1: ICC= 0.844, 95% CI 0.606-0.943; Trail 2: ICC= 0.937, 95% CI 0.833-0.977), and HF demonstrated good reliability during both trials (Trial 1: ICC= 0.875, 95% CI 0.686-0.954; Trial 2: ICC= 0.782, 95% CI 0.490-0.918).

CONCLUSION
Finapres-derived HRV measures demonstrated good reliability with measures obtained using Kubios Scientific across multiple HRV indices. These findings suggest that Finapres NOVA may provide a reliable approach for HRV assessment. However, the variability in reliability across individual HRV measures suggests that equivalence between methods may be measure-specific.

Dynamic Modeling of Invisible Tumor Growth with Simulated Residual Disease and TNBC PDX Tumor Growth in the NSG MIce

Investigator: Bryan A. Hawickhorst, M.S.
Mentor: Amy H. Tang, Ph.D.
Co-Authors(s):
Jonathan Baker, Macon & Joan Brock Virginia Health Sciences Eastern Virginia Medical School
Daniel McWilliams, Macon & Joan Brock Virginia Health Sciences Eastern Virginia Medical School
Amy Tang, Macon & Joan Brock Virginia Health Sciences Eastern Virginia Medical School
Department(s): Biomedical and Translational Sciences
Poster #: 73B

BACKGROUND
Tumor dormancy, early relapse, and treatment resistance remain poorly understood. After neoadjuvant or adjuvant therapy, the locally advanced and systemically disseminated invisible tumor cells may persist undetected for months or years despite clean MRI or CT scans. Reported detection thresholds and residual tumor sizes vary in the literature, further complicating prognostic accuracy in patient risk stratification.

AIMS
To address this unmet clinical need, we developed the mathematical models and generated a computational algorithm to predict the time course of invisible tumor relapse, improve the predictive accuracy, and model the invisible-to-visible tumor transition within the detection limits of the MRI/CT tumor imaging tools.

METHODS
We simulated remission-to-relapse trajectories for invisible residual tumors beginning with 1, 10, 102, 103, and 104 cells, and calculated the time for each to progress into a 3 cm3 visible tumor. Exponential growth models with unrestricted doubling times from 2 to 30 days were used to capture rapid, unimpeded tumor growth. Secondly, we used the Spratt model, a modified logistic model, to model the complex tumor growth curves in vivo. A modified logistic model was then used to model the time course of invisible tumor growth in vivo, with doubling times of 5 to 30 days to reflect varying aggressiveness, tumor and tumor microenvironment interactions, and tempo-spatial-context-treatment dependence in response to varied tumor remission and extended tumor latency. To improve the mathematical modeling, we refine, verify, and authenticate several variable factors/clinicopathological parameters in experimental biology by fitting our hypothetical tumor growth models to the real-time TNBC tumor growth curves from six patient-derived xenograft (PDX) TNBC models in NSG mice.

RESULTS
By varying the clinically invisible residual tumor sizes from 10-6 mm3 to 10-2 mm3, we found that tumors relapsed rapidly once tumor growth resumed, often exceeding the clinical detection thresholds before the regularly scheduled follow-up appointments and allowable MRI/CT-imaging intervals can capture them. Our results highlight the hidden risk of residual diseases, the major challenge of invisible tumor modeling, and the lack of accuracy in relapse prediction in the clinic. Exponential and logistic model fits to the PDX tumor implantation data were complete; the model authentication, relapse prediction augmentation, and correct interpretation of these fitted models will be augmented with the new chemo-resistant PDX models in NSG mice.

CONCLUSION
This work underscores the unmet need and critical importance of modeling invisible tumor growth to improve the accuracy of tumor relapse prediction and patient risk stratification. Future work will focus on transforming this mathematical model into a companion prognostic tool in combination with our selected biomarker panel to predict tumor relapse risk, quantify therapeutic efficacy, and assist and support oncologists' decision-making in real time in the future.
Extramural Funding: DOD-BC180907, DOD-BC230520, HRBRC 2023/24, CAF Award, and NIH-1T34GM149816

Evaluating the Healthy Portsmouth Million Hearts Initiative: Reducing Hypertension Disparities Among Black Adults in Portsmouth, Virginia

Investigator: Gamanuel Jean, M.P.H.
Mentor: Amy Paulson, MPH
Co-Authors(s):
Brett Sierra, Macon & Joan Brock Virginia Health Sciences Eastern Virginia Medical School
Department(s): Pediatrics
Poster #: 74B

INTRODUCTION
Hypertension remains a leading cause of cardiovascular disease and disproportionately affects Black adults in the United States. In Portsmouth, Virginia, the rates of hypertension and associated morbidity exceed the state average, underscoring the need for equity-focused, community-based interventions. This study evaluates the implementation, reach, early outcomes, and equity impact of the Healthy Portsmouth Million Hearts Initiative.

METHODS
We conducted a mixed-methods quality improvement and implementation evaluation using blood pressure (BP) screening data and resident and stakeholder questionnaires collected through Research Electronic Data Capture (REDCap). The analytical sample included 125 Portsmouth residents who completed the resident questionnaire. Quantitative analyses included descriptive statistics and exploratory geographic analyses by ZIP code. Qualitative responses were analyzed using thematic analysis. The study was guided by Ecosocial Theory and the RE-AIM (Reach, Effectiveness, Adoption, Implementation, and Maintenance) framework.

RESULTS
The program reached a high-risk population, with 81.6% identifying as Black and 89.6% classified as having elevated, stage 1, or stage 2 hypertension. Of the participants who completed the resident questionnaire, 79.2% reported improved understanding of BP, 67.2% reported motivation to engage with a healthcare provider, and 51.2% reported that screening supported their ability to manage BP. Self-reported behavioral changes included increased confidence in managing BP (85.6%) and healthier eating behaviors (80.0%). Post-screening follow-up data showed that 29.1% of those with valid contact information completed follow-up engagement. Geographic analysis identified significant variation in structural barriers across ZIP codes. Participants in ZIP code 23704 were more likely to face at least one structural barrier and transportation issues compared with participants from other ZIP codes. Qualitative findings identified persistent structural barriers, including food access, transportation, and financial constraints, as well as implementation challenges in staffing capacity, resource availability, and partner organizations.

CONCLUSION
Community-based BP screening programs can effectively improve awareness, knowledge, and self-reported behavior among high-risk groups. However, maintaining long-term engagement after screening is shaped by structural and place-based barriers. Improving coordinated post-screening engagement strategies, expanding access to community resources, and using ZIP code-level barrier data to guide resource alignment may improve the initiative's equity impact and help reduce hypertension-related disparities in Portsmouth and similar communities.

Feasibility and Acceptability of a Mixed-Methods SDOH Screening and Case-Management Linkage Pilot in a Ryan White HIV Clinic

Investigator: Vonda M. McKeithan, B.S.
Mentor: Catherine Derber, MD
Co-Authors(s):
None listed.
Department(s): Department of Medicine, Division of Infectious Disease
Poster #: 70B

INTRODUCTION

Social determinants of health (SDOH), including housing instability, food insecurity, and transportation barriers, disrupt healthcare engagement and human immunodeficiency virus (HIV) treatment outcomes among people receiving Ryan White HIV/AIDS Program services. Standardized SDOH screening tools exist, but evidence on whether they can be feasibly integrated into routine HIV clinic workflows, alongside existing case-management resources, remains limited. This study evaluates the feasibility and acceptability of implementing a standardized SDOH screening and case-management linkage workflow in a Ryan White HIV clinic, and explores whether case-management engagement is associated with viral suppression in both a prospective screening cohort and a retrospective clinic population.

METHODS

This study uses separate prospective and retrospective components, analyzed independently. Case-management engagement for both components is assessed through CAREWare, the case-management data system used by the program; HIV viral-load outcomes for both are obtained from the electronic health record (EHR).

In the prospective component (October–December 2026), eligible patients complete an SDOH screening survey addressing domains including housing, food, transportation, employment, and social connection. Participants who identify needs may request information, referral, or connection with case-management services, including a same-day warm handoff when feasible. Patient perceptions of the screening process are also collected. Primary prospective outcomes are screening feasibility, acceptability, and case-management linkage. Viral suppression (<200 copies/mL) is evaluated as an exploratory outcome using the qualifying baseline and subsequent follow-up viral-load measures defined in the study protocol.

The retrospective component includes the Infectious Disease (ID)/Ryan White patient population from January 1 through August 31, 2026. Case-management utilization is determined from CAREWare encounter data, and the most recent qualifying viral-load result during the period is categorized as suppressed (<200 copies/mL) or not suppressed (≥200 copies/mL).

RESULTS

For the prospective cohort, results will describe screening feasibility and acceptability, the frequency and type of identified social needs, and case-management linkage. For both cohorts, results will describe exploratory patterns between case-management engagement and viral suppression. Missing follow-up laboratory results will not be interpreted as treatment failure.

CONCLUSION

This study will assess whether a brief standardized SDOH screening process can be incorporated into routine Ryan White HIV clinic care and connected to existing case-management resources without creating an impractical workflow burden. Findings may inform whether the approach is feasible for continued clinical implementation and provide preliminary information regarding its relationship with HIV viral suppression.

A Syndemic-Informed, Evidence-Linked Knowledge Graph of Adolescent Syphilis: Co-Occurring Clinical and Social Vulnerabilities in a Pilot Cohort

Investigator: Mohamad Najafi, M.S.
Mentor: Hongyun (Tracy) Fu, Ph.D.
Co-Authors(s):
Phillip Poppas, B.S., Macon & Joan Brock Virginia Health Sciences Eastern Virginia Medical School
Karen Tan, B.S., Macon & Joan Brock Virginia Health Sciences Eastern Virginia Medical School
Dylan M. Jack, B.A., Macon & Joan Brock Virginia Health Sciences Eastern Virginia Medical School
Haley Hunsaker, B.S., Macon & Joan Brock Virginia Health Sciences Eastern Virginia Medical School
Jian Wu, Ph.D., Old Dominion University
Yaohang Li, Ph.D., Old Dominion University
John W. Harrington, M.D., Children's Hospital of the King's Daughters
Kyzwana Caves, M.D., M.P.H., FAAP, Children's Hospital of the King's Daughters
Department(s): Department of Pediatrics, Division of Community Health and Research
Poster #: 72B

BACKGROUND
Adolescent syphilis is rising and rarely occurs alone. Syndemic theory holds that infections cluster and interact with behavioral-health, trauma-related, substance-use, and structural conditions within adverse social environments. Because many such factors appear only in narrative clinical notes, analyses based on structured diagnosis codes miss them. Knowledge graphs represent patients, conditions, and social factors as linked, source-anchored entities, providing a computational representation of syndemic theory. We piloted an evidence-linked knowledge graph to characterize syndemic co-occurrence in adolescents with syphilis.

METHODS
Retrospective, mixed-methods pilot of 14 adolescents (median age 18 years; 10 male; 10 Black/African American) with confirmed syphilis across 48 encounters at a coastal Eastern Virginia pediatric health system (2017-2024). Structured electronic medical record (EMR) fields (coinfections, insurance status, Area Deprivation Index) and clinical notes were mapped to a six-domain syndemic codebook: infectious coinfection, behavioral health, trauma/vulnerability, substance use, social determinants of health, and healthcare-system fragmentation. Each factor was linked to its source document; narrative factors were extracted using a locally hosted large language model (Llama-3.3-70B). Patient-level graphs were aggregated into a cohort knowledge graph.

RESULTS
Every patient had at least one syndemic domain; the mean was 3.4 of 6 domains, and 71% had three or more. Domain prevalence was: social/structural 86%, healthcare-system fragmentation 86%, infectious coinfection 50% (human immunodeficiency virus [HIV] 21%), behavioral health 50%, substance use 43%, and trauma/vulnerability 29%. Behavioral-health, substance-use, and trauma factors were documented in narrative notes for 7, 6, and 4 patients, respectively, but appeared in zero structured diagnosis codes. The cohort graph showed clustering of neighborhood deprivation, care fragmentation, behavioral health, and substance use.

CONCLUSION
An evidence-linked knowledge graph feasibly represented co-occurring clinical and social vulnerabilities in adolescent syphilis, operationalizing syndemic theory as an interpretable, auditable structure and revealing burden invisible to structured diagnosis codes. This single-site pilot cannot establish causal syndemic interaction, but it provides a validated foundation for temporal knowledge graphs and a larger adolescent HIV and sexually transmitted infection (STI) cohort.

Comparing Classification Models for Predicting Polyendocrine Metabolic Ovarian Syndrome Diagnosis

Investigator: Nikki B. Towns, M.P.H.
Mentor: Mohan Pant, Ph.D.
Co-Authors(s):
None listed.
Department(s): Department of Epidemiology, Biostatistics & Environmental Health
Poster #: 71B

INTRODUCTION
Polyendocrine metabolic ovarian syndrome (PMOS), formerly known as polycystic ovary syndrome (PCOS), is a common endocrine and metabolic condition associated with reproductive, endocrine, and metabolic abnormalities. Predictive modeling provides a data-driven approach for evaluating how multiple clinical factors may contribute to PMOS diagnosis. This study compared logistic regression, k-nearest neighbors (KNN), and support vector machine (SVM) models for predicting PMOS diagnosis using five clinical variables: age, body mass index (BMI), menstrual irregularity, testosterone level, and antral follicle count.

METHODS
A publicly available dataset containing 1,000 observations was analyzed in R/RStudio. PMOS diagnosis was used as the binary outcome variable, with 19.9% of observations classified as PMOS-positive. The data were partitioned into 75% training and 25% testing sets. The same training and testing sets were used across all three models, and predictors were centered and scaled for the KNN and SVM models. Classification performance was evaluated using accuracy, sensitivity, and specificity.

RESULTS
All three models demonstrated strong classification performance. Logistic regression achieved 89.56% accuracy, 75.51% sensitivity, and 93.00% specificity. KNN achieved 95.18% accuracy, 89.80% sensitivity, and 96.50% specificity. SVM demonstrated the strongest overall performance, achieving 96.79% accuracy and 99.00% specificity, whereas KNN produced the highest sensitivity. The SVM model correctly classified 241 of 249 observations in the testing set, with eight total misclassifications.

CONCLUSION
These findings demonstrate that the selected reproductive, endocrine, and metabolic variables were able to discriminate between PMOS-positive and PMOS-negative observations within this dataset. SVM provided the strongest overall classification performance, while KNN demonstrated greater sensitivity for identifying positive cases. Given the class imbalance and use of a single publicly available dataset, these findings should be considered exploratory and require external validation in additional and more diverse populations before clinical application.

Bidirectional Combination Therapy with SGLT2 Inhibitors and GLP-1 Receptor Agonists and Genitourinary Tract Infection Risk in Type 2 Diabetes: A Retrospective TriNetX Cohort Study

Investigator: Abdul Ahad, MBBS
Mentor: Atiq Bhatti, MD
Co-Authors(s):
Rehan Qayyum , Macon & Joan Brock Virginia Health Sciences Eastern Virginia Medical School
Department(s): Medicine
Poster #: 56B

INTRODUCTION
Sodium-glucose cotransporter-2 inhibitors (SGLT2i) and glucagon-like peptide-1 receptor agonists (GLP-1 RA) are increasingly combined in type 2 diabetes mellitus (T2DM). SGLT2i cause glycosuria and raise genitourinary tract infection risk, driven mainly by genital infection; GLP-1 RA are non-glycosuric and improve glycemic control and weight. While single-agent comparisons are well established, the literature lacks direct combination-therapy comparisons, and whether adding a second agent, and the order in which it is added, raises or lowers this risk remains debatable. We tested whether genitourinary tract infection risk tracks the glycosuric drug by examining both directions of combination therapy.

METHODS
This retrospective, new-user, active-comparator cohort study used the TriNetX US Collaborative Network. Adults aged ≥18 years with T2DM receiving metformin were included; those with type 1 diabetes, end-stage renal disease, or tirzepatide use were excluded. Two bidirectional contrasts were constructed: adding a GLP-1 RA to established SGLT2i therapy versus continued SGLT2i alone (Contrast 1), and adding an SGLT2i to established GLP-1 RA therapy versus continued GLP-1 RA alone (Contrast 2). Combination arms were indexed at initiation of the second agent, with ≥3 months of prior first-agent therapy required to align index timing; comparators lacked the second agent within this interval. Each contrast underwent separate 1:1 propensity score matching on demographics; renal, genitourinary, and cardiometabolic diagnoses; glucose-lowering and other medications; hemoglobin A1c; estimated glomerular filtration rate; and body mass index. After matching, standardized mean differences were below 0.1 for all covariates. Genital and urinary tract infections, defined separately by International Classification of Diseases, Tenth Revision, Clinical Modification codes, were assessed as incident events over 90 days. Conjunctivitis and low back pain served as negative controls. Risk ratios (RR) with 95% confidence intervals (CI) are reported.

RESULTS
After matching, Contrast 1 included 85,649 and Contrast 2 included 80,740 patients per arm. Adding a GLP-1 RA to an SGLT2i was associated with lower genital infection risk (0.4% versus 0.8%; RR 0.52, 95% CI 0.46 to 0.60). Conversely, adding an SGLT2i to a GLP-1 RA was associated with higher genital infection risk (1.0% versus 0.4%; RR 2.62, 95% CI 2.28 to 3.01). The opposite directions indicate that risk tracked the glycosuric agent rather than treatment escalation itself. Urinary infection was minimally affected, with a modest reduction in one direction (Contrast 1 RR 0.84, 95% CI 0.75 to 0.94; Contrast 2 RR 1.04, 95% CI 0.93 to 1.15). Negative control outcomes were near null (RR 0.87 to 0.97), arguing against surveillance bias.

CONCLUSION
Genitourinary tract infection risk during combination SGLT2i and GLP-1 RA therapy was determined by the glycosuric agent. Adding a GLP-1 RA to an SGLT2i roughly halved genital infection risk, whereas adding an SGLT2i to a GLP-1 RA more than doubled it, with urinary infection unaffected throughout. These findings suggest GLP-1 RA co-therapy does not compound, and may reduce, the genital infection risk of SGLT2i, whereas initiating an SGLT2i in a GLP-1 RA-treated patient markedly increases it. Confounding by indication remains a limitation.

Eradicating metastatic cancers by targeting a major tumor vulnerability of the K-RAS pathway: Seven in absentia homolog (SIAH)

Investigator: Jonathan M. Baker, Ph.D.
Mentor: Amy H. Tang, Ph.D.
Co-Authors(s):
Andrew Howell, Macon & Joan Brock Virginia Health Sciences Eastern Virginia Medical School
Ashleigh Hannah, Macon & Joan Brock Virginia Health Sciences Eastern Virginia Medical School
Julia Wulfkuhle, George Mason University
Emanuel Petricoin, George Mason University
Department(s): Biomedical and Translational Sciences
Poster #: 57B

INTRODUCTION

Persistent activation of the K-RAS pathway is multipotent: its downstream signaling networks promote tumorigenesis, drug resistance, relapse, and metastasis. Despite newly developed state-of-the-art therapies, none have yet to achieve durable antitumor efficacy. Seven in absentia homologues (SIAHs) are a conserved family of RING-domain E3 ubiquitin ligases that function as the most downstream signaling gatekeepers in the K-RAS pathway. Our preclinical studies demonstrated that SIAH inhibition leads to a tumor eradication phenotype of multiple stage IV human cancer cell lines both in vitro and in vivo. We propose SIAH is a major tumor vulnerability and actionable drug target for inhibiting K-RAS pathway activation. In this study, we aim to elucidate the molecular mechanisms underpinning the antitumor efficacy of our potent SIAH inhibitor, SIAH2PD, as a new targeted therapy to achieve tumor eradication.

METHODS

Reverse phase protein arrays (RPPAs) and principal component analysis (PCA) were used to quantify statistically significant fold-changes of 294 signaling proteins and phospho-proteins in response to SIAH blockade in five stage IV cell lines. RPPAs were performed in triplicate on MiaPaCa, MDA-MB-231, MDA-MB-468, HeLa, and A549 cell lines in which SIAH2PD expression was controlled by a doxycycline (DOX)-inducible Tet-ON/OFF system. Four experimental conditions were used: Tet-ON vector control cells without DOX (group A) and with DOX induction (group B); Tet-ON-SIAH2PD experimental cells without DOX (group C) and with DOX induction (group D). The ratios of each group were calculated in a pairwise comparison after normalization to GAPDH as an internal control. To validate putative targets of interest, immunofluorescence (IF), flow cytometry (FC), and Western blots (WB) were performed on cells for group C and D at 3-, 5-, and 7-days post-DOX-induction. Adherent and single cell suspensions were used respectively for cell-based assays in biological triplicates and normalized to α-Tubulin. Target protein expression was quantified and validated, and statistical analyses were performed by one-way ANOVA and T-tests using GraphPad Prism software.

RESULTS

The altered expression of NFkB, Caspase-3, Caspase-7, Cofilin, and PARP in response to SIAH blockade were independently validated by RPPA, WB, FC, and IF, demonstrating the roles of heightened cellular stress, apoptosis, and dysfunctional DNA damage and repair pathways induced by SIAHloss of function as mechanistic, synergistic to kill cancer cells and prevent tumor growth.

CONCLUSIONS

RPPA cancer pathway mapping provides invaluable molecular insights into cancer network rewiring in response to SIAH blockade, revealing a major tumor vulnerability. This study supports the design of anti-SIAH-based, anti-EGFR/K-RAS targeted therapies to control and eradicate incurable human cancers.

EXTRAMURAL FUNDING: DOD-BCRP-BC180907, DOD-BCRP-BC230520, NIH R01 CA140550-01A1, CHRB 274-05-22, DGH foundation, CIT-CRCF (MF14S-009-LS), and HRBBRC

AI Assisted Multi Modal Toxicity Prediction for Faster, Smarter Preclinical Drug Discovery and Development

Investigator: Shivangi Gupta, Ph.D.
Mentor: Milton L. Brown, MD, Ph.D.
Co-Authors(s):
David Mu, Macon & Joan Brock Virginia Health Sciences Eastern Virginia Medical School
Department(s): Internal Medicine
Poster #: 58B

INTRODUCTION
The ability to anticipate drug-induced toxicity prior to extensive animal experimentation remains a major unmet need in early drug discovery. Conventional preclinical toxicology workflows are resource intensive and often rely on iterative dose finding studies, motivating the development of predictive frameworks that can integrate diverse chemical, biological, and experimental information. This work introduces a multimodal, AI-assisted approach for preclinical toxicity prediction that combines chemical structure, physicochemical properties, biological drug sensitivity profiles, dosing characteristics, experimental metadata, and structural similarity.

METHODS
Using 64 oncology drugs from the Responses to Oncology Agents and Dosing Models to Aid Preclinical Studies (ROADMAPS) dataset, we integrated four toxicity classes; defined by weight loss and mortality outcomes along with NCI 60 GI50 values, molecular descriptors, physicochemical properties, and dosing variables. Missing GI50 measurements were imputed using a Generative Adversarial Imputation Network (GAIN). Chemical structures were encoded using 2048 bit Morgan fingerprints, and pairwise Tanimoto similarity was computed to capture structural relationships. Five machine learning algorithms - Gaussian Naive Bayes, K Nearest Neighbor, Random Forest, XGBoost, and Multi Layer Perceptron; were evaluated across four experiments designed to (i) establish baseline performance, (ii) quantify the contribution of structural similarity, and (iii) assess synthetic data augmentation.

RESULTS
Random Forest delivered the strongest baseline performance, achieving roughly 85% accuracy under a 95/5 train–test split and maintaining balanced sensitivity, specificity, AUC, and MCC. When Tanimoto derived structural similarity features were incorporated, the XGBoost model showed an additional ~2% improvement at an 85/15 split, demonstrating that structural context provides a meaningful discriminatory signal beyond traditional descriptor only representations. In contrast, synthetic data augmentation- including both SMOTE based oversampling and GAN generated samples did not yield measurable performance gains, reinforcing that model improvement in this setting depends more on high quality real experimental data than on synthetic expansion of limited datasets. Together, these findings highlight the value of structural similarity information and underscore the need for additional real toxicity observations to further enhance predictive robustness.

CONCLUSION
This study establishes a multi modal AI framework capable of integrating complementary chemical, biological, dosing, and structural information to enhance the prediction of preclinical drug toxicity. By enabling earlier identification of toxicity risk, the approach can inform dose selection, guide experimental prioritization, and reduce unnecessary animal use in alignment with the 3Rs - Replacement, Reduction, and Refinement. Future work should focus on validating this framework using larger, chemically diverse, and externally independent datasets to assess generalizability, robustness, and translational utility for real world preclinical drug development.

Myeloid STAT4 at the Intersection of Sleep Disruption and Hyperlipidemia: A Molecular Link Between Lifestyle Stress and Atherogenesis

Investigator: Alina Moriarty, Ph.D.
Mentor: Elena Galkina, Ph.D.
Co-Authors(s):
W. Coles Keeter, Macon & Joan Brock Virginia Health Sciences Eastern Virginia Medical School
Shelby MA, Macon & Joan Brock Virginia Health Sciences Eastern Virginia Medical School
Basudha Habisyasi, Macon & Joan Brock Virginia Health Sciences Eastern Virginia Medical School
Alex Coleman, Macon & Joan Brock Virginia Health Sciences Eastern Virginia Medical School
Nick Richards, Macon & Joan Brock Virginia Health Sciences Eastern Virginia Medical School
Nagaraja Nagre, Macon & Joan Brock Virginia Health Sciences Eastern Virginia Medical School
Larry Sanford, Macon & Joan Brock Virginia Health Sciences Eastern Virginia Medical School
Department(s): Biomedical and Translational Sciences
Poster #: 70A

INTRODUCTION

Neutrophils, crucial regulators of antimicrobial defense, also play a role in atherosclerosis. Signal transducer and activator of transcription 4 (STAT4)controls key neutrophil functions, including ROS generation, NETosis, and migration. Myeloid STAT4 deficiency reduces atherogenesis but impairs antimicrobial defense. Sleep fragmentation (SF), a widespread health concern, increases cardiovascular risk. SF accelerates atherosclerosis in a neutrophil-dependent manner by enhancing neutrophil functions.

METHODS

Myeloid-specific STAT4-deficient low-density lipoprotein receptor-deficient (Stat4ΔLysMLdlr-/-) and control (Stat4fl/flLdlr-/-) mice were fed a high Fat, high cholesterol Diet (DDC) and randomly assigned to a SF or home cage control (HC) groups for 16 weeks. Survival was evaluated using kaplan-meier analysis. Atherosclerotic lesion formation was evaluated using Oil-red-O staining. Immune profiling was conducted on the aorta, blood, bone marrow, intestine, and peritoneal cavity using spectral flow Cytometry.

RESULTS

Kaplan–Meier analysis revealed reduced survival in Stat4ΔLysMLdlr-/-mice compared to controls following SF but not in the HC controls. Oil red o staining of en face aortas showed reduced atherosclerosis Furthermore, Oil-Red-O staining of en face aortas and spectral flow cytometry analysis on circulating blood and peritoneal lavage fluid revealed that myeloid-specific STAT4 deficiency reduced neutrophil production, activation, and atherosclerosis, but also caused peritonitis and increased mortality after SF and DDC feeding in Stat4ΔLysMLdlr-/-mice vs Stat4fl/flLdlr-/-mice. Premature death was linked to peritonitis, possibly due to intestinal inflammation and barrier dysfunction, seen by increased ROS production in the small intestines and elevated plasma LPS levels.

CONCLUSION

Thus, we show that STAT4 critically balances immune responses during SF by driving inflammatory neutrophil activation that promotes atherosclerosis while simultaneously preserving essential host defense mechanisms, underscoring its dual role in modulating inflammation and survival under physiological stress.

Atherosclerosis-Associated Immune Remodeling in the Pathogenesis of Benign Prostatic Hyperplasia

Investigator: Alina Moriarty, Ph.D.
Mentor: Elena Galkina, Ph.D.
Co-Authors(s):
Petra Popovics, Macon & Joan Brock Virginia Health Sciences Eastern Virginia Medical School
Department(s): Biomedical and Translational Sciences
Poster #: 60B

INTRODUCTION

Benign prostatic hyperplasia (BPH) is a common non-malignant condition in men over 50, defined by prostate enlargement that can lead to urinary symptoms. Although evidence suggests androgens are involved in BPH development, the underlying mechanisms of BPH remain elusive.

Atherosclerosis, a multifactorial chronic inflammatory disease of aging, is characterized by arterial wall inflammation, lipid accumulation, endothelial damage, and a dysregulated immune response. Atherosclerosis contributes to the development of multiple diseases and can result in multiorgan dysfunction. Emerging evidence suggests a strong association between systemic and local atherosclerosis of the prostatic artery, chronic inflammation, and BPH. However, it remains unclear whether the mechanisms driving atherosclerosis also support the development of BPH in aging men.

The low-density lipoprotein receptor-deficient (Ldlr-/-) mouse is a well-established model for studying atherosclerosis. It produces sustained hyperlipidemia and an atherosclerotic milieu that more closely mimics human dyslipidemia-associated prostatic inflammation than does feeding C57BL/6 mice a high-fat diet alone. However, this approach is insufficient to induce robust atherosclerosis or the full spectrum of metabolic and immune perturbations required to study BPH pathogenesis.

METHODS

Male Ldlr-/- mice were fed a standard chow diet (CD) or a high-fat, high-cholesterol diet (DDC) for 16-18 weeks to induce atherosclerosis. Spectral Flow cytometry of the postate was performed.

RESULTS

Spectral flow cytometry analysis of prostate lobes revealed changes in immune cell composition in DDC-fed mice compared to CD-fed Ldlr-/- mice. Importantly, leukocyte distribution in the prostate differed by diet and lobe.

CONCLUSION

Our data suggesting atherosclerosis affects the prostate microenvironment in a region specific manner. Further analysis will determine whether changes in the prostatic immune landscape could accelerate pathological urinary dysfunction.

Androgen Receptor Dysfunction Compromises Ovarian Angiogenic Responses in Polycystic Ovary Syndrome (PCOS)

Investigator: Megan A. G. Sage, Ph.D., M.S.
Mentor: Diane M. Duffy, Ph.D.
Co-Authors(s):
Arielle Yeshua, Macon & Joan Brock Virginia Health Sciences Eastern Virginia Medical School
Department(s): Biomedical and Translational Sciences
Poster #: 59B

INTRODUCTION

Ovarian follicles require a robust vascular supply to grow and ovulate. Dysfunction of ovarian vasculature impairs follicle growth and ovulation. The ovarian vasculature is in close proximity to theca cells, which produce androgens. Women with PCOS have altered macrovascular and microvascular function as well as elevated androgens. We hypothesize that the response of ovarian microvascular endothelial cells to androgens may be impaired in PCOS.

METHODS

Ovarian microvascular endothelial cells from healthy oocyte donors (HOMECs) and PCOS patients (PCOMECs) were isolated from discarded follicular aspirates. HOMEC and PCOMEC expression of classical androgen receptor AR and plasma membrane androgen receptor SLC39A9 mRNA was determined via qPCR, and protein was assessed through immunostaining of fixed cells and Western blot of cell lysate. HOMEC and PCOMEC response to androgens via AR was determined using gradient-driven migration and live cell tracking assays. Response to androgens via SLC39A9 was determined by zinc influx using Zinquin ethyl ester and proliferation via BrdU incorporation.

RESULTS

HOMECs and PCOMECs expressed mRNA and protein for AR and SLC39A9. PCOMEC AR mRNA expression was 138% greater than that of HOMECs ($p < 0.05$), with no difference in SLC39A9 mRNA between HOMECs and PCOMECs. HOMEC migration was increased by 62% in the presence of testosterone (T; $p < 0.05$), but not the membrane impermeable bovine serum albumin-conjugated T (BSA-T), whereas PCOMEC migration was not altered by any stimulus. siRNA knockdown of AR blocked T-stimulated migration in HOMECs ($p < 0.05$) while siRNA knockdown of SLC39A9 had no impact on basal or T-stimulated migration. PCOMEC migration in the presence of T was not affected by siRNA knockdown of SLC39A9 or AR. Live cell tracking showed that T increased speed and distance traveled by migrating HOMECs, while T had no impact on migrating PCOMECs. T stimulated zinc influx in a dose dependent manner in HOMECs (93% increase, $p < 0.05$), but not in PCOMECs. Additionally, T, BSA-T, and the SLC39A9-selective agonist (-)-epicatechin each increased proliferation in HOMECs by 300-500% ($p < 0.05$), with no change in PCOMEC proliferation. siRNA knockdown of SLC39A9 blocked T-stimulated proliferation in HOMECs ($p < 0.05$) while siRNA knockdown of AR had no impact on basal or T-stimulated proliferation. PCOMEC proliferation in the presence of T was not affected by siRNA knockdown of SLC39A9 or AR. These findings indicate that androgens stimulate migration via AR and increase zinc influx and proliferation via SLC39A9 in HOMECs, but not in PCOMECs.

CONCLUSIONS

Overall, androgens act via both SLC39A9 and AR at HOMECs to stimulate proliferation and migration, which are key processes in angiogenesis. Importantly, although PCOMECs express SLC39A9 and AR, androgens do not stimulate angiogenic responses via SLC39A9 or AR in PCOMECs. Local androgen action may be central to ovarian vascular remodeling and ovulatory angiogenesis in healthy ovarian function. Absent or aberrant function of androgen signaling in PCOMECs may contribute to ovarian vascular dysfunction and may ultimately play an important role in the pathology of PCOS. This work was supported by the Ryan Translational Research Fund and the Jones Family Foundation.

An open pipeline for measuring immune infiltration in multiplex images of triple-negative breast cancer

Investigator: Peter Scheible, B.S.
Mentor: Amy H. Tang, Ph.D.
Co-Authors(s):
Jonathan Baker, Macon & Joan Brock Virginia Health Sciences Eastern Virginia Medical School
Department(s): Biomedical and Translational Science
Poster #: 72A

INTRODUCTION

In triple-negative breast cancer (TNBC), checkpoint immunotherapy helps some patients and not others, and the protein stain used to select them, programmed death-ligand 1 (PD-L1), predicts response only loosely. Where immune cells sit may explain some of the gap: lymphocytes stalled in surrounding tissue behave differently from those touching tumor cells. Multiplex immunofluorescence can measure that, staining one section for eight proteins so every cell is typed and placed. The catch is the analysis. Cell counts rest on a chain of software decisions. Reproducibility studies show those decisions can shift the fraction of cells called positive by more than 25 percent, and they are rarely reported. We built an open pipeline that makes each decision explicit and measured what each one costs.

METHODS

The pipeline runs in four stages: assemble the image, outline every nucleus with a deep learning model, measure and type each cell, then describe where the cells sit. Three choices depart from common practice. Positivity for a protein is decided per image, at the dip between that image's stained and unstained cells, rather than by a fixed cutoff or a fixed percentage. Tumor regions follow the real outline of the tumor, gaps and all, and each stretch of boundary is checked against the stain underneath before it is accepted. A cell carrying both tumor and immune signal keeps both labels and lands in a dual-identity category, infiltrated tumor or tumor-resident immune, according to which evidence is stronger. The pipeline also labels any measurement it cannot support, so unreliable numbers travel with the warning attached.

RESULTS

We processed 279 images from 43 patients plus seven tonsil controls, typing 1,018,945 cells in one run with no failures. Each departure changed the answer. A fixed cutoff, still the common default, discarded 55 to 74 percent of visibly stained tumor cells on tumor dense images. Approximating a tumor boundary with a simple convex outline swept connective tissue immune cells inside the tumor and inflated measured infiltration nearly fourfold. Counting them all as immune mislabeled a median 76 percent of supposed infiltrating immune cells, which were tumor cells. The warning system flagged two measurements as unusable. Read from a rendered image, one protein marked 1 percent of cells positive, against 23 percent on the original unmixed signal and a published normal range of 5 to 30 percent. A second protein came from a neighboring slice never aligned to the panel, so the pipeline reports it per image only, never per cell. In the TNBC samples, immune cells were two and a half to three times denser outside tumors than inside. Suppressive T cells concentrated within the tumor mass. Neither pattern appears in tonsil.

CONCLUSION

The analysis steps behind a multiplex image can change a result more than the biology being compared, and most stay invisible once the numbers are written down. This tool makes them explicit and checkable. The pipeline, its tests, and the per cell measurements for all 279 images are available for reuse.

From Pilot to Partnership: Two-Year Implementation of Comprehensive Sexuality Education for Hampton Roads Youth in Group Homes

Investigator: Keeley Yokley, MPH, B.S.W.
Mentor: Hongyun (Tracy) Fu, Ph.D.
Co-Authors(s):
Luwam Abeselom,
Chinenye Udemba, Norfolk State University
Haley Hunsaker, Macon & Joan Brock Virginia Health Sciences Eastern Virginia Medical School
Dylan Jack, Macon & Joan Brock Virginia Health Sciences Eastern Virginia Medical School
Jessi Bates, Old Dominion University
Sarah Wray, Tidewater Youth Services
Department(s): Department of Pediatrics
Poster #: 71A

INTRODUCTION
Adolescents in crisis or foster care settings may lack access to inclusive, developmentally appropriate comprehensive sexuality education (CSE) due to stigma, inconsistent instruction, and limited opportunities for trusted dialogue. In 2025, Teen Health 360, in partnership with Tidewater Youth Services, piloted Get Real: Comprehensive Sex Education That Works at two group homes in Hampton Roads, Virginia, returning in 2026 following positive initial findings. This quality improvement initiative examined two years of implementation to assess feasibility, knowledge outcomes, and youth perspectives on CSE in group home settings.

METHODS
During summers 2025 and 2026, Teen Health 360 delivered five sets of Get Real academy sessions, with each set consisting of 11 45-minute Get Real high school lessons to 33 adolescents aged 13–18 at group homes in Portsmouth and Virginia Beach. Topics included anatomy, healthy relationships, gender and sexual identity, consent, sexually transmitted infections (STIs), contraception, communication, and decision-making. Trauma-informed, interactive strategies included discussions, demonstrations, hands-on activities, anonymous questions, and communication skill-building. Mixed-methods evaluation included pre/post knowledge assessments, post-program evaluations, and focus group discussions (FGDs) with participants. Data were examined within and across implementation years.

RESULTS
Thirty-three participants completed the pre-assessment, and twenty-seven completed the post-survey. Using post-survey data, participants had a mean age of 15 years (SD=1.27); 83% identified as male, 54% as Black, and 83% as straight. Attendance improved in 2026, when 62.5% completed all 11 lessons and 87.5% attended at least half, compared with 53% and 71%, respectively, in 2025.

Knowledge increased significantly from pre to post assessment. Mean knowledge scores (range: 0-14) increased from 6.48 (SD=2.16) to 8.67 (SD=4.32; p=.025), while the proportion correctly answering at least 11 items increased from 0% to 46.7% ($p < .001$). Six individual items improved significantly, including HIV transmission (8.0% to 50.0%, $p < .001$), legal consequences of sending nude images of minors (32.0% to 76.7%, $p < .001$), and understanding of the term transgender (28.0% to 66.7%, $p<0.01$).

Program experiences were highly positive: over 80% felt safe, viewed facilitators as knowledgeable, and felt comfortable expressing themselves and asking questions; 89% felt engaged. In 2026, 100% endorsed a safe environment, knowledgeable facilitators, and comfort expressing themselves and asking questions, compared with 61.5% in 2025 (all $p < .010$).

Qualitative findings from FGDs indicated that youth valued interactive learning about STI prevention, condom use, healthy relationships, consent, and communication. Participants described actionable skills, including checking condom expiration dates, discussing STI testing with partners, communicating consent, and seeking support from trusted adults. They also identified gaps in peers' sexual health knowledge and a need for accessible resources when approaching adults feels difficult.

CONCLUSION
Two years of implementation support the feasibility, acceptability, and educational benefit of interactive, trauma-informed CSE in group home settings. Consistent knowledge gains, positive feedback, and youth perspectives demonstrate the value of providing medically accurate information alongside practical prevention, communication, and help-seeking skills.
Sustained partnerships between health education programs and youth-serving organizations may help address gaps in access to trusted sexual health information. Future implementation should prioritize experiential learning, open discussion, and connections to trusted adults and preventive sexual health resources.

Beyond Negative Serology: Neurocysticercosis Mimicking an Intracranial Malignancy

Investigator: Raeed W. Bari, MD
Mentor: Saad Mussarat, MD
Co-Authors(s):
Raeed Bari, Macon & Joan Brock Virginia Health Sciences Eastern Virginia Medical School
Department(s): Internal Medicine
Poster #: 64A

INTRODUCTION

Neurocysticercosis (NCC), caused by the larval form of Taenia solium, is a leading infectious cause of acquired seizures worldwide but may be overlooked in non-endemic regions. Diagnosis can be challenging when neuroimaging findings mimic malignancy and serologic testing is negative. We present a young man with recurrent seizures and enhancing intracranial lesions initially concerning for malignancy, in whom epidemiologic history and subsequent radiographic response supported a clinical diagnosis of NCC despite negative serology.

CASE INFORMATION

A 22-year-old man who emigrated from Guatemala with a history of a seizure two years earlier presented after a witnessed seizure at home followed by confusion. In the emergency department, he developed a focal seizure progressing to a generalized tonic-clonic seizure. Initial metabolic evaluation, urine drug screening, and computed tomography of the head were unrevealing. Seizure activity was controlled with lorazepam and levetiracetam.

Brain MRI demonstrated an $8 \times 7 \times 7$ mm rim-enhancing cortical lesion in the left frontoparietal region with approximately 2.4×1 cm of adjacent subcortical edema. There was no associated hemorrhage or diffusion restriction. Additional imaging review identified a rim-enhancing left occipital lesion without surrounding edema and a 3-mm solid-appearing enhancing right frontal nodule without associated reactive signal. The dominant lesion and surrounding edema initially raised concern for malignancy; however, the patient lacked constitutional symptoms, and systemic imaging failed to identify a primary malignancy.

Given his prior residence in Guatemala, a region endemic for Taenia solium, previous seizure history, and compatible intracranial lesions, NCC was considered. Taenia solium IgG antibody testing by ELISA was negative. Despite negative serology, clinical suspicion remained high, and he was treated with albendazole and dexamethasone while levetiracetam was continued.

The patient experienced no further seizures or focal neurologic deficits. Follow-up MRI demonstrated complete interval resolution of the previously enhancing posterior left frontal lesion and associated edema, with no residual pathologic enhancement or intracranial mass. At outpatient neurology follow-up, he remained asymptomatic and seizure-free.

DISCUSSION

This case highlights the diagnostic challenge of NCC when serologic testing is negative and neuroimaging initially suggests malignancy. Enhancing intracranial lesions with surrounding edema have a broad differential, including neoplastic and infectious etiologies. In this patient, the radiographic appearance initially favored malignancy; however, the absence of an identified primary malignancy and his epidemiologic history prompted reconsideration of NCC.

Negative serologic testing should not be interpreted in isolation to exclude NCC when clinical suspicion remains high. Prior residence in an endemic region, recurrent seizures, compatible neuroimaging, and complete resolution of the enhancing lesion and associated edema following antiparasitic and corticosteroid therapy supported NCC as the clinical diagnosis despite negative serology

CONCLUSION

For patients presenting with seizures with unexplained enhancing intracranial lesions, a detailed country-of-origin and exposure history can provide a critical diagnostic clue even years after immigration from an endemic region. This case emphasizes the importance of integrating epidemiologic history, neuroimaging, serologic testing, and longitudinal radiographic response when individual diagnostic studies are inconclusive.

When Common Symptoms Reveal a Hematologic Emergency: Acute Myeloid Leukemia Presenting With Nonspecific Symptoms

Investigator: Nicholas B. D'Alessandro, MD
Mentor: Sami G. Tahhan, MD
Co-Authors(s):
Ahmed Ismail, Macon & Joan Brock Virginia Health Sciences Eastern Virginia Medical School
Department(s): Department of Medicine
Poster #: 65A

INTRODUCTION

Acute myeloid leukemia (AML) may initially present with vague, nonspecific symptoms that can be attributed to chronic illness, medication effects, or common outpatient conditions. Recognizing constitutional symptoms and promptly reviewing basic labs are critical to prevent delays in diagnosis and treatment.

CASE INFORMATION

A 74-year-old man with type 2 diabetes mellitus, hereditary hemochromatosis (C282Y/H63D compound heterozygosity), and obstructive sleep apnea presented with several weeks of fatigue, polyuria, subjective postural hypotension, abdominal discomfort, and some tachypnea. One month prior, he was active, exercising regularly, and reported feeling well. Previous blood counts were overall unremarkable. Initially, his symptoms were ascribed to the recent addition of empagliflozin or possible infection, as he recently recovered from an ear infection.

Urinalysis was negative, no other medication changes were noted, and the physical exam was unremarkable. Subsequent testing demonstrated a white blood cell count of 11.3×10^9/L, hemoglobin of 14.3 g/dL, platelets of 22×10^9/L, and 31% circulating blasts on differential. Peripheral smear showed marked thrombocytopenia and large irregular blasts, prompting emergency department referral and hospitalization with expedited oncological workup. Repeat testing showed 23–37% peripheral blasts with progressive thrombocytopenia. Flow cytometry identified 39% myeloblasts with a CD34-negative, dim CD117-positive, HLA-DR-negative, cytoplasmic myeloperoxidase-positive phenotype concerning for acute promyelocytic leukemia. However, PML:RARA [t(15;17)] fluorescence in situ hybridization (FISH) was negative.

Bone marrow biopsy demonstrated 98% hypercellular marrow with 86% blasts/monoblasts and myeloid maturation arrest. Molecular testing identified FLT3 internal tandem duplication with high allelic ratio (0.82), two additional FLT3 insertions, NPM1 mutation, and IDH2 R140Q mutation; karyotype and AML/MDS FISH panels were normal. His diagnosis was AML with FLT3, NPM1, and IDH2 mutations and promyelocytic features. He began azacitidine and venetoclax, with gilteritinib added for FLT3-mutated AML. A day-21 marrow showed no morphologic, immunophenotypic, or flow-cytometric evidence of residual AML, although low-level FLT3-ITD molecular residual disease persisted. Subsequent marrow assessments remained morphologically negative for AML.

DISCUSSION

This case highlights the insidious onset and rapid progression of AML. Weeks before his clinic visit, he went to urgent care twice and an otolaryngologist with each visit noting apyrexia, negative constitutional symptoms, and localized otitis media treatment. In the clinic, the presenting symptoms were non-specific and confounded by recent illness and comorbidities. High clinical suspicion for underlying malignancy is paramount, especially in the elderly population. Fortunately, rapid workup and treatment by oncology led to a favorable response, with his most recent marrow biopsy without evidence of residual/recurrent AML.

CONCLUSION

AML is a rare, yet increasingly treatable hematologic malignancy emerging rapidly despite previously normal labs and apparent clinical stability. As such, the differential diagnosis for new or progressive constitutional symptoms must include malignancy, especially in the elderly population, as these may be the only presenting symptoms. A simple, inexpensive test such as a complete blood count with differential must be performed, as it can identify life-threatening hematologic disease and facilitate early intervention.

Pseudohyperkalemia Secondary to Thrombocytosis in CALR-Mutated Essential Thrombocythemia

Investigator: Ahmed Ismail, MD
Mentor: Sami G. Tahhan, MD
Co-Authors(s):
Mikaela Kcomt, Macon & Joan Brock Virginia Health Sciences Eastern Virginia Medical School
Sami G. Tahhan, Macon & Joan Brock Virginia Health Sciences Eastern Virginia Medical School
Department(s): Department of Medicine
Poster #: 61A

INTRODUCTION

Pseudohyperkalemia is an in vitro elevation in measured serum potassium caused by cellular potassium release during clot formation or specimen processing. It should be considered in patients with marked thrombocytosis and otherwise unexplained hyperkalemia to prevent unnecessary and potentially harmful potassium-lowering treatment.

CASE INFORMATION

A 73-year-old female with CALR exon 9 double-mutated, JAK2 V617F-negative, MPL-negative, and BCR:ABL1-negative essential thrombocytosis was followed for recurrent thrombocytosis and intermittent hyperkalemia. She had previously developed severe pancytopenia while receiving hydroxyurea, with a marrow biopsy showing marked hypocellularity (5–10%) without fibrosis or blast excess, prompting subsequent cautious cytoreductive management. After hydroxyurea was held because of treatment-associated cytopenias, her platelet count increased from 408×10^3/µL to 791×10^3/µL. Concurrent potassium levels were repeatedly borderline elevated at 5.3 mmol/L. After hydroxyurea reinitiation at 500 mg daily, platelet counts trended down to 603×10^3/µL. Potassium levels also trended down to 4.7 mmol/L.

Throughout this period, kidney function was preserved, and bicarbonate remained normal at the highest potassium measurement, with no evidence of renal failure or metabolic acidosis. The recurrent elevation in potassium, temporally associated with marked thrombocytosis and with no alternative metabolic explanation, was most consistent with thrombocytosis-associated pseudohyperkalemia.

DISCUSSION

In thrombocytosis, platelets release potassium during coagulation, which can artifactually increase serum potassium despite normal in vivo potassium concentration. Pseudohyperkalemia is supported by a serum-to-plasma potassium difference greater than 0.4 mmol/L; confirmation requires paired plasma potassium collected in a lithium-heparin tube and/or rapidly analyzed whole-blood potassium. This case was complicated by concurrent Lisinopril exposure, which could contribute to true hyperkalemia; however, potassium elevations were documented before angiotensin-converting-enzyme inhibitor initiation and occurred despite stable renal function and normal bicarbonate. The temporal relationship between recurrent thrombocytosis and potassium elevation therefore raised strong concern for pseudohyperkalemia.

CONCLUSION

Apparent hyperkalemia in patients with essential thrombocythemia and substantial thrombocytosis should prompt evaluation for pseudohyperkalemia before treatment escalation. Paired serum and plasma or whole-blood potassium testing is essential to establish the diagnosis, avoid inappropriate therapy, and prevent iatrogenic hypokalemia.

When the Tube, Not the Patient, Is Hypoglycemic: Filgrastim-Related Hyperleukocytosis Causing Artifactual Hypoglycemia

Investigator: Ahmed Ismail, MD
Mentor: Sami G. Tahhan, MD
Co-Authors(s):
Narges Khalili, Macon & Joan Brock Virginia Health Sciences Eastern Virginia Medical School
Sami G. Tahhan, Macon & Joan Brock Virginia Health Sciences Eastern Virginia Medical School
Department(s): Department of Medicine
Poster #: 61B

INTRODUCTION

Hypoglycemia is a potentially life-threatening condition. However, a low laboratory glucose value does not always represent true systemic hypoglycemia. Artifactual hypoglycemia is a preanalytical phenomenon caused by ongoing in vitro glucose consumption by metabolically active blood cells before sample processing. It is particularly likely with marked leukocytosis and delayed separation of serum or plasma from cellular components.

CASE INFORMATION

A 54-year-old man with a history of HIV and rectal adenocarcinoma on chemotherapy presented to our outpatient clinic for routine follow-up. He had seen his HIV Nurse Practitioner the day before and had routine lab monitoring ordered to include a CBC and BMP. Laboratory evaluation from the previous day revealed an elevated WBC of 653000/µL, increased from a baseline of ~4,000/µL (normal range of 4000 to 11000 /uL) with predominant neutrophilia. A basic metabolic panel showed low serum glucose of 32 mg/dL (normal range 70-99 mg/dL), raising concern for level 2 hypoglycemia.

Discussion with his oncologist revealed that the patient had received prophylactic Filgrastim (G-CSF) to support his Bone marrow a few days earlier. He was asymptomatic with normal vital signs and denied diaphoresis, palpitations, weakness, confusion, or altered sensorium.

Repeat point-of-care fingerstick capillary glucose measured immediately was normal at 97 mg/dL. The patient was diagnosed with artifactual hypoglycemia related to marked leukocytosis due to G-CSF. No intervention was required, and glucose values remained normal on subsequent testing.

DISCUSSION

Hypoglycemia is an important clinical condition that can lead to autonomic and neuroglycopenic symptoms, which can be life-threatening. Hypoglycemia can be categorized as Level 1 hypoglycemia (Blood sugar <70 mg/dL but ≥54 mg/dL), Level 2 hypoglycemia (Blood sugar <54 mg/dL), or Level 3 hypoglycemia (requiring assistance).

Artifactual hypoglycemia is a false low blood glucose reading that can occur due to improper blood sample collection or consumption of glucose from an abundance of cells in the blood, such as leukocytes or erythrocytes. Risk factors for artifactual hypoglycemia include delayed sample processing and extreme leukocytosis. Our patient, unfortunately, did not have his CMP tube processed for about 8 hours, compounding the risk of artifactual hypoglycemia due to his leukocytosis.

G-CSF can induce marked neutrophilic leukocytosis. When leukocyte counts rise to 50,000–100,000/µL, rapid glycolysis by metabolically active leukocytes, as in our patient, can artifactually lower measured serum glucose, especially if blood samples are not processed promptly. This artifactual hypoglycemia is well described in leukemic blasts but can also occur with reactive neutrophilia.

Bedside fingerstick capillary glucose, which was normal in our patient, or immediate plasma fluoride-oxalate tube processing helps confirm the diagnosis. Capillary glucose fingerstick circumvents delayed processing and glucose consumption by Leukocytes, whereas Fluoride acts as a preservative and can inhibit glycolysis in leukocytes.

CONCLUSION

Artifactual hypoglycemia from leukocytosis is solely an in vitro phenomenon. It should be recognized promptly to avoid unnecessary dextrose administration, endocrine evaluation, and Emergency Department visits and hospitalizations, which can be costly.

Caught Between the Heart and the Kidneys: A Challenging Case of Statin-Induced Rhabdomyolysis

Investigator: Mikaela Kcomt, MD
Mentor: Kelly Thomson, MD
Co-Authors(s):
Jeevitha Prativadi, Macon & Joan Brock Virginia Health Sciences Eastern Virginia Medical School
Department(s): Palliative Medicine, Internal Medicine
Poster #: 66A

INTRODUCTION

Statins are widely prescribed due to their proven benefit in reducing cardiovascular event risk. Statin use comes with the potential for myopathy. Rhabdomyolysis is a rare (<0.1%) but serious adverse effect, most often occurring within the first year of therapy. Acute kidney injury (AKI) is the most severe complication of rhabdomyolysis and significantly increases mortality. Management includes statin discontinuation, aggressive fluid resuscitation, urine alkalization, and occasionally dialysis.
We present a case of severe statin-induced rhabdomyolysis causing AKI, in which fluid resuscitation was limited by a complex cardiac history.

CASE INFORMATION

A 73-year-old woman with a history of cardiogenic shock following acute myocardial infarction and resulting ischemic cardiomyopathy and systolic heart failure, presented with two weeks of myalgias, progressive weakness, and fatigue, along with two days of dark urine. She had recently lifted heavy furniture at home. Her medications included rosuvastatin 40 mg and ezetimibe 10 mg. Exam revealed hypotension (BP 90/60 mmHg) and new bilateral lower extremity weakness (3/5).

Initial labs showed creatinine 6.8 mg/dL (baseline 1.1) and anion gap metabolic acidosis. Muscle enzymes were markedly elevated: CPK 74,916 U/L, myoglobin >30,000 ng/mL, aldolase 196.9 U/L, AST 938 U/L, and ALT 531 U/L. Urinalysis revealed blood without RBCs, consistent with myoglobinuria. Autoimmune workup was negative, including anti–3-hydroxy-3-methylglutaryl–coenzyme A reductase (anti-HMGCR) and myositis-specific antibodies.

She was diagnosed with statin-induced rhabdomyolysis complicated by AKI, with recent physical exertion possibly contributing. Management included discontinuation of rosuvastatin, cautious intravenous hydration (starting at 125 mL/h, tapered based on urine output and volume status), a bicarbonate infusion later transitioned to oral therapy, and midodrine to support renal perfusion. Urine output improved to ~3 L/24h by day three, while creatinine peaked at 8.0 mg/dL on day four and declined to 4.1 mg/dL at discharge.

DISCUSSION

Statin-induced rhabdomyolysis is characterized by rapid skeletal muscle breakdown with release of intracellular components, including CPK (often >40-fold above normal), aldolase, myoglobin, and electrolytes.

Statins inhibit HMGCR, decreasing cholesterol synthesis while also reducing production of coenzyme Q, a component of the mitochondrial electron transport chain. The resulting coenzyme Q depletion impairs ATP generation, leading to myocyte injury. AKI results from volume depletion and myoglobin-induced tubular obstruction and cytotoxicity. Statin users engaging in strenuous exercise may face a higher risk of rhabdomyolysis, though definitive evidence is lacking.

The "classic" triad of muscle pain, weakness, and dark-colored urine is not always present, and diagnosis often requires a high index of suspicion.

Fluid resuscitation, given early and in high volumes with targeted urine output, is the cornerstone of management. Our patient's complex cardiac history limited fluid administration. Bicarbonate was added to initial fluids based on evidence that urine alkalization can mitigate myoglobin-induced tubular injury. Although dialysis is often required to manage volume overload and severe metabolic disturbances, it was ultimately not needed in this case.

CONCLUSION

Early recognition and management of rhabdomyolysis are essential to prevent AKI and improve outcomes. Evidence-based guidelines for fluid management or adjunctive therapies have not yet been established. Our case contributes to clinical experience in managing this condition, particularly in complex and high-risk scenarios.

The Platelet–Potassium Paradox: Pseudohyperkalemia in Essential Thrombocythemia

Investigator: Mikaela Kcomt, MD
Mentor: Sami G. Tahhan, MD
Co-Authors(s):
Ahmed Ismail, Macon & Joan Brock Virginia Health Sciences Eastern Virginia Medical School
Department(s): Internal Medicine
Poster #: 66B

INTRODUCTION

Pseudohyperkalemia is an artifactual elevation in serum potassium resulting from in vitro release of potassium during blood cell lysis. It should be suspected when hyperkalemia occurs in the absence of renal dysfunction, other electrolyte abnormalities, or relevant medications. Marked thrombocytosis, particularly in essential thrombocythemia (ET), can cause pseudohyperkalemia through platelet-mediated potassium release during clotting.

Distinguishing pseudohyperkalemia from true hyperkalemia is critical, as untreated hyperkalemia can cause life-threatening cardiac arrhythmias, while unnecessary treatment of pseudohyperkalemia may result in iatrogenic complications.

Although hematologic causes of pseudohyperkalemia are well recognized, this condition remains underappreciated in clinical practice. We report a case of pseudohyperkalemia in a patient with marked thrombocytosis, later diagnosed with essential thrombocythemia.

CASE INFORMATION

A 75-year-old man with a history of hypertension, ischemic stroke, adrenal incidentaloma, left peroneal deep vein thrombosis, and treated hepatitis C was found to have hyperkalemia on routine outpatient laboratory testing, prompting his primary care team to recommend evaluation in the emergency department (ED).

Laboratory testing revealed a serum potassium of 6.3 mmol/L in the setting of marked thrombocytosis (platelet count 807,000/µL). Renal function was at baseline (creatinine of 1.1 mg/dL), and there were no other electrolyte or acid-base abnormalities. The patient was asymptomatic and was not taking medications known to cause hyperkalemia. The critical result was relayed to the on-call resident, and the patient was instructed to seek immediate evaluation given the potential risk of cardiac arrhythmias. The patient declined evaluation in the ED and was subsequently contacted by the primary care office and instructed to return for repeat laboratory testing.

Repeat testing 10 days later demonstrated normalization of serum potassium to 4.3 mmol/L. No potassium-lowering therapy was administered. At the time of the hyperkalemia episode, the patient had persistent thrombocytosis. His platelet count had increased from 504,000/µL in 2023 to 807,000/µL at the time of the episode and ultimately peaked at 958,000/µL. Hematologic evaluation revealed a positive JAK2 V617F mutation, and bone marrow biopsy demonstrated findings consistent with ET. He was started on hydroxyurea and aspirin, with progressive improvement in his platelet count. Following treatment, his platelet count decreased to 385,000/µL, while serum potassium remained normal.

DISCUSSION

Pseudohyperkalemia may result from preanalytical factors, including improper blood collection, sample handling, transport, or storage, but can also occur despite appropriate specimen collection in the setting of marked leukocytosis or thrombocytosis. Among hematologic causes, pseudohyperkalemia is most frequently associated with ET but may also occur with reactive thrombocytosis. The mechanism involves potassium leakage into the serum from the numerous platelets trapped within the clot.

When unexplained hyperkalemia occurs in a patient with thrombocytosis, the potassium level should be reassessed using an anticoagulated plasma sample or venous whole blood. A normal potassium concentration in a simultaneously collected plasma or whole-blood sample supports pseudohyperkalemia.

CONCLUSION

In our patient, the temporal association between treatment of ET and normalization of serum potassium supported pseudohyperkalemia. Recognition of this association is important to prevent unnecessary diagnostic evaluation and potentially harmful treatment, including inappropriate administration of potassium-lowering therapies or dialysis.

Infection Prevention, Surveillance, and Bar Salvage Following Minimally Invasive Repair of Pectus Excavatum

Investigator: Karen Elizabeth Kennamer, B.S.
Mentor: Robert Obermeyer, MD
Co-Authors(s):
Kai Rossbach, Macon & Joan Brock Virginia Health Sciences Eastern Virginia Medical School
Rihannon Torres, Children's Hospital of the King's Daughters
Turaj Vazifedan, Children's Hospital of the King's Daughters
Franklin Margaron, Children's Hospital of the King's Daughters
Michael Goretsky, Children's Hospital of the King's Daughters
Department(s): Pediatric Surgery
Poster #: 64B

INTRODUCTION

Minimally invasive repair of pectus excavatum (MIRPE) involves the implantation of metal hardware for chest wall remodeling. For optimal outcomes, the bars must remain in place for approximately 3 years; however, infection may limit bar retention and necessitate premature removal. From 2005 to 2013, Children's Hospital of The King's Daughters (CHKD) noted an increase in the postoperative infection rate following MIRPE. These findings prompted the development of infection-prevention bundle (IPB) and infection-treatment bundles. This study provides long-term follow-up evaluating the impact of these bundles on the incidence and timing of superficial and deep bar infections, as well as bar salvage.

METHODS

A single-institution, institution review board (IRB) approved retrospective cohort study (IRB No. 14-03-WC-0034) was conducted among patients undergoing MIRPE from 2005 to 2025. Infection-prevention and infection-treatment pathways were implemented in 2013, and patients were stratified into pre- and post-implementation cohorts. Postoperative infections were classified by timing (early, ≤90 days; late, >90 days) and severity (superficial or deep). Deep infections were further assessed for bar salvage and retention. Data was summarized by descriptive statistics and compared between cohorts using univariable analysis.

RESULTS

During the study period 1,695 patients underwent MIRPE. There were 854 patients in the pre-bundle cohort and 841 patients in the post-bundle cohort. Following infection prevention bundle implementation early (3.0% to 1.5%, p=0.02) and superficial infections (2.1% to 0.8%, p=0.01) decreased significantly while late (0.4% versus 0.7%, p=0.74), deep (1.4% versus 1.4%, p=0.52) and overall infection incidence (3.51% versus 2.26%, p=0.06) did not significantly change between cohorts.

Among patients with deep bar infections there was a significant increase in bar salvage (75% versus 100%, p=0.03), length of preservation (2.2 versus 2.8 years, p=0.05), and median time to infectious presentation (33.0 versus 64.0 days p=0.03). Median time from infection presentation to operative intervention decreased 10.5 to 3.0 days, although this did not reach statistical significance (p=0.06). There was no significant difference in the operative techniques used to treat infection.

CONCLUSION

Infection after MIRPE is rare. Implementation of an infection prevention bundle was associated with a significant reduction in early and superficial infections. Despite these measures, the incidence of deep bar infection remained unchanged. Deep infections presented significantly later, with some occurring beyond the Centers for Disease Control and Prevention recommended 90-day surveillance period. This supports the need for extended surveillance matching the life of the implant. Although deep bar infections were not prevented with the infection prevention bundle, early antibiotic and surgical therapy allowed successful treatment with preservation of bars.

An Evaluation of the Effect of Baseline Ovarian Cysts on IVF and FET Outcomes

Investigator: Kyle Nguyen Le, MD
Mentor: Benjamin Harris, MD, MPH
Co-Authors(s):
Kyle Le, Macon & Joan Brock Virginia Health Sciences Eastern Virginia Medical School
Benjamin Harris, Shady Grove Fertility
Department(s): Obstetrics and Gynecology, Division of ReprOld Dominion Universityctive Endocrinology and Infertility
Poster #: 67B

INTRODUCTION

The utilization of assisted reproductive technologies (ART) is often a high stakes process for patients that requires significant investment of time and finances. Patients who undergo IVF and frozen embryo transfer (FET) cycles may have their treatment cycle cancelled if there are ovarian cysts present on the initial ultrasound scan. Ovarian cysts detected on baseline ultrasonography warrant careful consideration. A non-functional simple cyst can have an association with a low baseline estradiol (E2) and thus thought not to affect the clinical response to a controlled ovarian hyperstimulation cycle. A functional cyst which releases E2, on the other hand, can adversely alter ovarian response to gonadotropin stimulation. Baseline E2 levels are often used in clinical decision making of whether to proceed with the cycle or not and the cutoff levels may be practice dependent. Further, complex cysts are another type of ovarian cyst which may have a profound negative impact on ovarian reserve and thus also be a cause for suboptimal oocyte and/or embryo quality The objective of this study was to evaluate the impact of the cyst type and baseline E2 levels on IVF and FET outcomes.

METHODS

This was a retrospective cohort comparing patients, 18-45 years old undergoing IVF/FET at a multi-center fertility network with baseline ovarian cysts to no ovarian cysts from Oct '22 to Dec '25. Patients with donor egg cycles, uterine factor, and intact hydrosalpinx were excluded. Primary outcomes were oocytes retrieved and live birth per transfer. Secondary outcomes were mature oocytes (MIIs), 2 pronuclei (2PN) embryos, usable blastocysts, euploidy and clinical pregnancy. Poisson regression evaluated the association between cyst status and reproductive outcomes, adjusting for age and BMI. E2 level was stratified into four groups and evaluated for differences in primary and secondary outcomes.

RESULTS

There were 1,962 simple, 2,405 complex, and 12,097 no cyst cycles. Oocytes retrieved were lower in simple (11, aRR 0.81 [0.78, 0.85]) and complex (11, aRR 0.78 [0.74, 0.81]) versus no cyst cycles (15). Simple (2, aRR 0.83 [0.78, 0.89]) and complex (2, aRR 0.74 [0.69, 0.78]) had less usable blastocysts compared to no cyst cycles (3). Euploidy rate was similar across groups. Clinical pregnancy was lower in simple (51.6%, aRR 0.89 [0.81, 0.98]), but similar in complex (52.6%; aRR 1.06 [1, 1.13]) and no cyst cycles (57.1%). Live birth per transfer were similar in simple (39.1%, aRR 0.89 [0.79, 1.01]) and no cyst cycles (45.4%), but higher in complex cycles (52.6%, aRR 1.08 [1.01, 1.16]). Increasing E2 >50 was associated with fewer oocytes retrieved, MIIs, 2PN embryos, usable blastocysts and a dose-response was not seen with E2 levels. Clinical pregnancy and live birth were similar across E2 groups.

CONCLUSION

Baseline ovarian cysts were associated with reduced oocyte and blastocyst yields. Simple cysts are linked to lower clinical pregnancy, while complex cysts had similar clinical pregnancy and higher live birth. Elevated E2 >50 predicts poorer oocyte and blastocyst yield, but pregnancy outcomes were similar between groups. Overall, baseline cysts and elevated E2 reduce oocyte yield, but do not compromise live birth per transfer.

Review of Amyloid Brain PET in Alzheimer's Disease Including Pearls and Pitfalls of Quantification Using Cenitloid Score

Investigator: John Paul Lyons, MD
Mentor: Lester Johnson, MD, Ph.D.
Co-Authors(s):
Allonna Walker, Philadelphia College of Osteopathic Medicine
David Johnson, Macon & Joan Brock Virginia Health Sciences Eastern Virginia Medical School
Kathy Byun, Medical Center Radiologists
Department(s): Radiology
Poster #: 63A

INTRODUCTION
Amyloid deposition in the brain is associated with neurodegenerative disorders, most notably Alzheimer's disease. Efforts to assess the amyloid burden of patients are increasingly impactful with the advent of anti-amyloid therapies. One method for examining the density of amyloid deposits in the brain is amyloid positron emission tomography (PET), utilizing radiopharmaceutical compounds such as florbetapir, flutemetamol, and florbetaben which have high affinity for aggregates of fibrillar amyloid. This bound structure of radiotracer and amyloid plaques can then be detected by PET imaging and seen visually as increased tracer uptake in the cerebral cortex in patients with Alzheimer's disease. Until recent years, amyloid PET has been interpreted visually as positive or negative, with no scale for quantifying the degree of uptake of radiotracer. Moreover, comparison between different amyloid PET studies was complicated by the different radiopharmaceuticals used.

DISCUSSION
These limitations prompted the development of Centiloid Score which allowed for quantification of the amount of amyloid disease in the brain on a scale in common among different radiotracers. This scaling method has anchor points at 0 and 100, representing typical young cognitively unimpaired patients versus patients with typical mild to moderate Alzheimer's disease, respectively. The Centiloid scale employs standardized uptake value ratios (SUVR) and Z-scores to quantify the amyloid plaques. The SUVR compares the average uptake in the target regions of interest (ROI) to that of the uptake in the reference region, generally the cerebellum or pons. Given the Centiloid score's reliance on comparison, it is of the utmost importance that the system chooses appropriate regions for both the areas of interest and control. However, due to factors such as high background noise, prominent brain tissue atrophy, or non-standard positioning of the head, the Centiloid values can be misrepresentative of the actual degree of amyloid deposition, which can in turn affect patients' abilities to access anti-amyloid therapies. In this educational exhibit, cases of amyloid PET with inaccurate and unreliable Centiloid values will be presented to demonstrate how these factors can result in quantification that is misrepresentative of patients' actual amyloid disease burden.

CONCLUSION
This information is important because the reader of amyloid PET must assess the validity of the computer automated ROI and Centiloid values with awareness of these pitfalls to avoid misinterpretations from inaccurate data. The increasing use of anti-amyloid therapies has necessitated quantifying amyloid disease and tracking response with amyloid PET and Centiloid scores. Further improvements in the systems used to generate quantitative assessments of the studies would be beneficial.

Androgen Receptors in the Human Oocyte

Investigator: Bijan Morshedi, MD
Mentor: Diane Duffy, MD
Co-Authors(s):
Megan Sage, Old Dominion University
Nicole Banks, Shady Grove Fertility
Department(s): Biomedical and Translational Science
Poster #: 68B

INTRODUCTION
Androgens play a critical role in female reproduction. Two major receptors, the classical androgen receptor (AR) and solute carrier family 39 member 9 (SLC39A9), have been shown to regulate androgen function in animal studies. Specifically, mouse AR knockout studies showed impaired follicular development, fewer ovulated oocytes, and diminished fertilization rates, whereas SLC39A9 knockout studies in zebrafish showed impaired oocyte germinal vesicle breakdown, meiotic resumption, and early embryogenesis. However, the presence of these receptors in human oocytes has not been studied. The purpose of this study is to investigate the presence and localization of AR and SLC39A9 in human oocytes.

METHODS
Discarded deidentified oocytes were obtained with consent from participants undergoing in vitro fertilization, as approved by the Old Dominion University Institutional Review Board. Oocytes were fixed in 4% paraformaldehyde, incubated with primary and labeled secondary antibodies, and mounted on slides using mounting medium with DAPI. Oocytes were imaged using the BioTek Cytation C10 Confocal Imaging Reader. Human granulosa cells and sperm that were bound to the zona pellucida were used as positive controls since previous studies have demonstrated the presence of AR and SLC39A9 on these cells. Oocytes exposed only to secondary antibodies were negative controls.

RESULTS
A total of 60 oocytes were labeled from 19 different participants with a mean age of 34.1 years (range 22 – 42). Of the 33 oocytes labeled for SLC39A9, 100% displayed SLC39A9 in the cytoplasm. Of the 17 MII oocytes labeled for SLC39A9, 6 (35.3%) displayed SLC39A9 in the polar body. AR labeling was performed on 24 oocytes, with 100% displaying AR in the cytoplasm. Of the 9 MII oocytes labeled for AR, only 1 (11.1%) displayed AR in the polar body.

CONCLUSIONS
SLC39A9 and AR are both present in the cytoplasm of human oocytes at the GV, M1, and M2 stages of maturity, without polarity to the polar body or nucleus. This is expected for AR, which is typically located in the cytoplasm when not bound to androgens. However, SLC39A9 is a transmembrane protein and is typically found on the plasma membrane, not commonly within the cytoplasm. Ongoing studies focus on the subcellular localization of each protein, with the goal of providing insight into the function of oocyte AR and SLC39A9 in human fertility.

Support: This project was supported by the Jones Family Reproductive Medicine Research Fund.

Acute Kidney Injury as a Predictor of Mortality in Heart Failure-Related Cardiogenic Shock: A Systematic Review and Meta-Analysis with Reconstructed Individual Participant Data

Investigator: Juan Munoz-Moreno, MD
Mentor: Johanna Contreras, MD
Co-Authors(s):
Amin Yehya, Sentara
Raymond Benza, Macon & Joan Brock Virginia Health Sciences Eastern Virginia Medical School
Department(s): Cardiology
Poster #: 62B

INTRODUCTION
Acute kidney injury (AKI) is common in cardiogenic shock (CS), but its prognostic significance has been defined mainly in myocardial infarction-related CS and may not generalize to heart failure-related CS (HF-CS), a critical gap in risk stratification.

METHODS
MEDLINE, Embase, and Web of Science were searched through November 2025 for cohort studies comparing mortality with versus without AKI in HF-CS, excluding myocardial infarction- or post-cardiotomy-related CS. Primary outcome was all-cause mortality (ACM) at 30, 90, and 180 days. Crude hazard ratios (cHRs) were pooled via random-effects models; when unavailable, individual participant data were reconstructed from Kaplan-Meier curves and analyzed via Cox regression. Leave-one-out analysis was performed.

RESULTS
Of 4,926 screened studies, four cohort studies (N=1,333) met inclusion criteria. AKI was associated with significantly higher ACM at 30 days (cHR 2.31; 95% CI 1.44–3.71; p=0.0005), 90 days (cHR 2.34; 95% CI 1.33–4.14; p=0.003), and 180 days (cHR 2.14; 95% CI 1.16–3.96; p=0.01). Pooled reconstructed Kaplan-Meier curves confirmed sustained survival divergence favoring no-AKI patients at 30 days (HR 1.72; 95% CI 1.46–2.04; p<0.001) and 90 days (HR 2.48; 95% CI 1.47–4.17; p<0.001). Substantial 30-day heterogeneity, driven by Sundermeyer et al., resolved on its exclusion (I^2=0%). AKI stage 3 showed the highest pooled mortality risk (cHR 3.26; 95% CI 0.68–15.65; p=0.14), consistent with Sundermeyer et al. (aHR 1.97; 95% CI 1.56–2.48; p<0.001).

CONCLUSION
AKI predicts sustained higher mortality in HF-CS, a clinically meaningful prognostic marker warranting larger prospective studies on optimal AKI management.

Essential Thrombocythemia Presenting as STEMI: A Case of Multivessel Coronary Thrombosis Managed with Emergency Thrombocytapheresis

Investigator: Juan Munoz-Moreno, MD
Mentor: Johanna Contreras, MD
Co-Authors(s):
None listed.
Department(s): Cardiology
Poster #: 62A

INTRODUCTION

Essential thrombocythemia (ET) is a myeloproliferative neoplasm marked by a paradoxical thrombotic and hemorrhagic risk, and rarely presents as ST-elevation myocardial infarction (STEMI). Prompt recognition is essential to guide tailored antithrombotic, cytoreductive, and thrombocytapheresis-based management.

CASE INFORMATION

A 68-year-old man with hypertension presented with chest tightness and dyspnea. ECG showed anterior ST-elevation with troponin T of 1,000 ng/L, and platelets were 708,000/µL. After aspirin and clopidogrel loading, angiography revealed thrombi in the proximal LAD and mid RCA. LAD flow was restored with two drug-eluting stents. Echocardiography showed LVEF 40% with an apical thrombus, prompting heparin and guideline-directed medical therapy. Platelets rose to 1,055,000/µL, raising suspicion for ET, and hydroxyurea was started. CT was unremarkable. JAK2 mutation was detected, and marrow biopsy confirmed ET with hyperlobulated megakaryocytes, grade 1 reticulin fibrosis, and CD61 positivity. Despite cytoreduction, platelets escalated to 1,224,000/µL, above the threshold for acquired von Willebrand syndrome, prompting emergency thrombocytapheresis that achieved counts below 600,000/µL after four sessions. Staged RCA revascularization added three more stents, conferring high ischemic risk. Repeat echocardiography showed thrombus resolution and LVEF improvement to 46%. He completed one month of triple therapy, two months of vitamin K antagonist plus clopidogrel, then transitioned to indefinite clopidogrel and hydroxyurea, with no thrombotic or hemorrhagic events after one year.

DISCUSSION

Hypercoagulable states increasingly reflect acquired rather than inherited factors with advancing age, and myeloproliferative neoplasms are a key acquired driver of extreme, persistent thrombocytosis capable of triggering multivessel coronary thrombosis, distinguishing this presentation from reactive thrombocytosis, which rarely exceeds 1,000,000/µL. Diagnosis followed International Consensus Classification criteria: sustained platelet count above 450,000/µL, marrow megakaryocytic hyperplasia with hyperlobulated nuclei and grade 1 fibrosis, JAK2 mutation, and exclusion of reactive causes and other myeloproliferative neoplasms (polycythemia vera, chronic myeloid leukemia, primary myelofibrosis) through normal erythropoietin, cytogenetics, and marrow morphology. Platelet counts rising despite hydroxyurea prompted platelet-lowering apheresis, which lowers counts 30% to 60% per session toward a target below 600,000/µL and served as an effective bridge, allowing safe staged revascularization. Extreme thrombocytosis also unmasked acquired von Willebrand syndrome, reflected in impaired ristocetin-induced platelet aggregation and suboptimal P2Y12 inhibition, which required increasing the clopidogrel dose and underscores the paradoxical thrombotic-hemorrhagic balance inherent to this disease. The antithrombotic strategy followed a time-limited triple therapy transitioning to dual and then single antiplatelet therapy, consistent with contemporary acute coronary syndrome guidelines favoring bleeding-reduction strategies after percutaneous intervention. Evidence guiding anticoagulation duration for left ventricular thrombus is limited to expert consensus, and no dedicated data exist for essential thrombocythemia specifically, highlighting a persistent knowledge gap. This case reinforces that unexplained or refractory thrombocytosis accompanying acute coronary thrombosis warrants hematologic evaluation, and that management requires close cardiology-hematology collaboration to balance ischemic and hemorrhagic risk.

CONCLUSION

ET should be suspected in multivessel coronary thrombosis, and emergency thrombocytapheresis can serve as a critical bridge to safe revascularization when cytoreductive therapy alone is insufficient. Tailored antithrombotic therapy and multidisciplinary follow-up remain essential given ET's paradoxical thrombohemorrhagic risk.

When the Atrium Is No Longer an Option: Rescue Leadless Ventricular Pacing After Right Atrial Angiosarcoma Resection

Investigator: Yara Bassam Mohammed Nawaiseh, MD
Mentor: Saad Mussarat, MD
Co-Authors(s):
None listed.
Department(s): Internal Medicine
Poster #: 68A

INTRODUCTION

Primary cardiac tumors are exceedingly rare, with a reported autopsy incidence of 0.0001-0.030%, of which approximately 25% are malignant. Angiosarcoma is the most common primary malignant cardiac tumor, predominantly arising in the right atrium, with a five-year survival of approximately 14%. Its aggressive, infiltrative behavior often necessitates extensive surgical resection, which may significantly alter right atrial anatomy and disrupt the sinoatrial node. We present a case of delayed sinus node dysfunction following right atrial angiosarcoma resection in which postsurgical anatomic alteration precluded atrial leadless pacemaker implantation, necessitating rescue ventricular leadless pacing.

CASE INFORMATION

A 65-year-old woman with a history of breast cancer treated with lumpectomy and radiation was diagnosed with a large infiltrative right atrial angiosarcoma measuring $4.9 \times 4.6 \times 5.7$ cm, extending into the caval inflow region and right coronary artery territory. She underwent surgical resection with right atrial reconstruction.

Approximately five months later, she developed recurrent lightheadedness and near-syncope. Ambulatory monitoring demonstrated symptomatic sinus pauses up to seven seconds with junctional escape rhythm, and inpatient telemetry confirmed intermittent sinus node dysfunction with sinus exit block. Echocardiography showed preserved left ventricular systolic function (ejection fraction 58%). Her sinus node dysfunction was attributed to either surgical injury or residual infiltrative tumor near the sinoatrial node.

Given symptomatic sinus node dysfunction, permanent pacing was indicated. With an indwelling mediport, upcoming chemotherapy, and infection risk from additional transvenous hardware, a leadless strategy was favored; with intact atrioventricular conduction, atrial leadless pacing was initially pursued.

However, intraprocedural angiography and intracardiac imaging revealed no suitable right atrial appendage for stable device deployment, and atrial leadless implantation was aborted. The procedure was converted to successful femoral-vein implantation of a leadless ventricular pacemaker programmed for backup pacing at 40 beats per minute.

At 18-month follow-up, she remained predominantly in sinus rhythm with intact intrinsic atrioventricular conduction and a ventricular pacing burden of only 3%. She experienced no recurrent lightheadedness and had returned to an active lifestyle.

DISCUSSION

This case illustrates two consequences of extensive right atrial tumor resection: delayed sinus node dysfunction and loss of the anatomic substrate required for atrial leadless pacemaker implantation. Although atrial leadless pacing was attractive given her isolated sinus node dysfunction, preserved atrioventricular conduction, and infection risk, successful implantation ultimately depended on preserved right atrial anatomy.

In this patient, the surgery that likely caused her sinus node dysfunction also created the anatomic barrier that prevented the intended atrial pacing strategy. Intraprocedural imaging demonstrated that prior resection and reconstruction had eliminated a suitable implantation site, necessitating an alternative approach. Ventricular leadless pacing provided effective rescue therapy, and a low backup rate preserved intrinsic conduction and sustained symptom resolution.

CONCLUSIONS

As atrial leadless pacing becomes increasingly utilized, clinicians should recognize that prior right atrial surgery may fundamentally alter device feasibility. Careful review of operative anatomy, along with targeted preprocedural imaging, may help anticipate these limitations. When atrial implantation is anatomically precluded in a patient with preserved atrioventricular conduction, low-rate ventricular leadless backup pacing may offer a practical and effective alternative.

Trends in Pediatric Craniofacial Injuries Associated with Electric Bicycle and Scooter Use in the United States 2016-2025: An Emerging Public Health Challenge

Investigator: Alyssa Reese, MD
Mentor: Lambros Viennas, MD
Co-Authors(s):
None listed.
Department(s): Department of Surgery, Division of Plastic Surgery
Poster #: 63B

INTRODUCTION

Electronic bicycles (e-bikes) and scooters (e-scooters) have become increasingly popular throughout the United States (U.S.) in the past decade. With an increase in use, the number of injuries secondary to use of these devices has also sharply risen. The purpose of this study was to ascertain the frequency and types of craniofacial injuries associated with e-bike and e-scooter use in the pediatric population.

METHODS

The National Electronic Injury Surveillance System (NEISS) database was queried from 2016 to 2025 for craniofacial injuries associated with e-bike and e-scooter use in pediatric patients ≤17 years of age. Cases were identified using dedicated e-bike/e-scooter product codes, with narrative-text keyword review for years predating consistent device-specific coding. Craniofacial injuries were identified by body part codes corresponding to the head, face, eye, mouth, and ear. Patient demographics, injury characteristics, disposition, season, and year of injury, as well as helmet use were extracted. National injury estimates were calculated using NEISS statistical sample weights.

RESULTS

A total of 2,547 injuries were initially identified. After manual narrative review and exclusion of unrelated injuries, 722 patient encounters were ultimately included. NEISS sampling weights were applied to generate a weighted national estimate of 24,766 pediatric craniofacial e-bike/e-scooter injuries in the United States between 2016 and 2025. No cases were identified in 2016 and 2017. Case volume increased approximately 2.2-fold per year over the included study period of 2018 to 2025 (log-linear trend, R^2=0.99, $p<0.0001$). There were an estimated 55 cases in 2018, which rose to 2,313 by 2023 and ultimately reached 12,815 during 2025. 41.6% (N=10,294) of the injuries took place on the street/highway and 38.9% (N=9,639) took place during the summer months. Median age was 14 years and there was a predominance of males (N=20,174, 81.5%). Injuries were most frequently in the head (49.8%) and face (31.2%). 6.3% (N=1,558) sustained craniofacial fractures. The mouth (4.4%), ear (0.6%), and eye (0.06%) were rarely involved. Helmet use was documented as absent in 24.0% of cases (N=5,956). Most patients were treated and released from the emergency room (N=20,189, 81.5%), but 16.5% (N=4,131) were admitted or transferred.

CONCLUSION

Craniofacial injuries related to e-bike and e-scooter use among pediatric patients have increased substantially from 2016 to 2025. There is an ongoing need for pediatric-specific public health initiatives, including helmet-use counseling and age restrictions. Craniofacial and trauma surgeons, emergency physicians, and pediatricians should be aware of this evolving injury pattern to aid in prevention, counseling, and management of these injuries.

Robotic Left Cardiac Sympathetic Denervation for Refractory Ventricular Tachycardia – A case report.

Investigator: Hira Sarfraz, MD
Mentor: Sami G. Tahhan, MD
Co-Authors(s):
Usman Javed, Riverside Regional Medical Center
Department(s): Internal Medicine
Poster #: 65B

INTRODUCTION
Ventricular tachycardia (VT) storm in patients with advanced structural heart disease remains a challenging clinical problem, particularly when ventricular arrhythmias persist despite antiarrhythmic therapy and catheter ablation. Cardiac sympathetic denervation (CSD) is an adjunctive neuromodulatory strategy that reduces sympathetic input contributing to ventricular arrhythmogenesis. We describe successful robotic left cardiac sympathetic denervation (LCSD) for refractory VT storm in a patient with severe ischemic cardiomyopathy.

CASE INFORMATION
A 69-year-old man with severe ischemic cardiomyopathy (left ventricular ejection fraction 15%), prior coronary artery bypass grafting, mechanical aortic valve replacement, mitral valve repair, permanent atrial fibrillation, and a cardiac resynchronization therapy defibrillator (CRT-D) developed recurrent VT requiring multiple ICD therapies. Despite extensive substrate-based VT ablation, he subsequently experienced recurrent VT and nonsustained ventricular arrhythmias while receiving mexiletine. Amiodarone had been discontinued because pulmonary function testing demonstrated reduced diffusing capacity and a restrictive ventilatory defect concerning for underlying parenchymal lung disease. Several months later, he presented with VT storm requiring multiple ICD therapies, including 11 shocks in a single day. He remained hemodynamically stable without evidence of acute ischemia and was initially treated with intravenous lidocaine.

DISCUSSION
Given recurrent ventricular arrhythmias despite antiarrhythmic therapy and prior catheter ablation, CSD was pursued. The patient underwent robotic-assisted LCSD under general anesthesia. The left sympathetic chain was mobilized from immediately below the stellate ganglion through the T4 level and transected, with cauterization of surrounding tissue to interrupt accessory sympathetic fibers, including the nerves of Kuntz. The procedure was uncomplicated.

Sympathetic activation can facilitate ventricular arrhythmias by increasing myocardial excitability and dispersion of repolarization. Recurrent VT and ICD shocks may further increase adrenergic activation, creating a self-perpetuating cycle of ventricular arrhythmias. CSD targets this autonomic contribution without eliminating the underlying scar-mediated substrate and therefore represents a complementary strategy to catheter ablation. Following LCSD, the patient continued mexiletine. Subsequent device interrogation demonstrated no recurrent ventricular high-rate events, VT, or ICD therapies. At one-year follow-up, he remained free of recurrent ventricular tachyarrhythmias and ICD therapies.

CONCLUSION
Robotic LCSD may provide effective and durable suppression of ventricular arrhythmias in carefully selected patients with advanced structural heart disease and refractory VT despite antiarrhythmic therapy and catheter ablation. This case adds to the existing literature supporting cardiac sympathetic denervation as an adjunctive strategy for refractory ventricular arrhythmias, particularly given the limited evidence from large prospective trials.

When the Kidney Mass is missing: High-grade Renal Cell carcinoma Presenting As Extensive Cavoatrial Tumor Thrombus

Investigator: Muhammad Tamoor Shaikh, MD
Mentor: Saad Mussarat, MD
Co-Authors(s):
Zahra Tasneem, Macon & Joan Brock Virginia Health Sciences Eastern Virginia Medical School
Department(s): Internal Medicine
Poster #: 67A

INTRODUCTION

Renal cell carcinoma (RCC) has a recognized propensity for venous invasion, with tumor thrombus extending from the renal vein through the inferior vena cava (IVC) and occasionally into the right atrium. A renal primary is usually identifiable on cross-sectional imaging. We present an unusual case of high-grade RCC presenting predominantly as extensive Cavo atrial tumor thrombus without a definite renal mass.

CASE INFORMATION

A 69-year-old man with chronic kidney disease stage 3b and cirrhosis complicated by portal hypertension and recurrent ascites presented with progressive abdominal distention. Imaging demonstrated extensive thrombosis of the intrahepatic and suprahepatic IVC extending into the right atrium, thrombosed hepatic veins, bilateral renal-vein involvement, and bilateral lower-extremity deep vein thromboses. CT angiography showed only an equivocal right renal abnormality without a discrete mass. MRI confirmed extensive thrombus involving the IVC, right atrium, and right renal vein; enhancement within the right renal-vein thrombus raised concern for tumor thrombus. Echocardiography demonstrated large echogenic structures within the right atrium and IVC concerning for mass versus thrombus. Mechanical thrombectomy of the IVC and bilateral iliac veins was performed. Histopathologic examination unexpectedly demonstrated metastatic high-grade renal cell carcinoma, favouring high-grade papillary RCC. Immunohistochemistry was positive for PAX8, RCC, AMACR, CD10, and vimentin and negative for CK7, CK20, GATA3, and CD117, supporting renal origin despite the absence of a radiographically apparent primary. The patient had concomitant extensive venous thromboembolic disease requiring anticoagulation. He was treated initially with heparin and subsequently apixaban, but recurrent bilateral deep femoral thromboses prompted therapeutic enoxaparin. Pembrolizumab and Lenvatinib were initiated. His course was complicated by recurrent ascites, hepatic encephalopathy, progressive renal dysfunction, pancytopenia, recurrent thrombosis, and bleeding. With progressive multiorgan dysfunction and advanced malignancy, care transitioned to comfort-focused management and hospice.

DISCUSSION

This case illustrates the diagnostic challenge of RCC presenting primarily as extensive Cavo atrial tumor thrombus without an identifiable renal mass. Enhancement within thrombus and contiguous involvement of the renal veins, IVC, and right atrium should raise suspicion for malignant vascular invasion. Importantly, tumor thrombus must be distinguished from concomitant bland venous thromboembolism because anticoagulation does not treat the malignant component. Histopathologic examination of thrombectomy material may be decisive when imaging is inconclusive.

CONCLUSION

High-grade RCC can rarely present with extensive Cavo atrial tumor thrombus despite the absence of a radiographically identifiable renal mass. In patients with unexplained extensive venous thrombosis, particularly with renal-vein involvement or thrombus enhancement, tumor thrombus should remain an important diagnostic consideration. Histopathologic evaluation of thrombectomy tissue can be critical when imaging is inconclusive, enabling definitive diagnosis and guiding appropriate oncologic management.

Beyond Heat: Histotripsy as an Emerging Nonthermal Option for Liver Tumors

Investigator: Dillon Woody, MD
Mentor: Adam Lustig, MD
Co-Authors(s):
Oleksandra Melchers, Macon & Joan Brock Virginia Health Sciences Eastern Virginia Medical School
Department(s): Interventional Radiology
Poster #: 69A

INTRODUCTION
Primary and metastatic liver tumors remain an important cause of cancer-related morbidity and mortality. Surgical resection offers the best opportunity for cure in appropriately selected patients, but many patients are not surgical candidates because of tumor location, multifocal disease, limited hepatic reserve, comorbidities, or extrahepatic disease. Liver-directed therapies such as microwave ablation (MWA), chemoembolization, and radioembolization therefore play an important role in treating unresectable tumors. Histotripsy is an emerging noninvasive, nonthermal ablation technique that uses focused ultrasound to mechanically destroy targeted tissue. Unlike conventional thermal ablation, histotripsy does not rely on heat and requires no needle or applicator placement within the tumor. These differences may provide advantages in selected patients and introduce the possibility of biologic effects beyond local tumor destruction.

DISCUSSION
Mechanism and Potential Advantages Histotripsy delivers high-amplitude focused ultrasound pulses that generate microscopic cavitation bubble clouds within targeted tissue. Rapid expansion and collapse of these bubbles mechanically fractionate tumor tissue into acellular debris. Treatment can be targeted and monitored using real-time ultrasound. Because tissue destruction is mechanical rather than thermal, histotripsy avoids the conventional heat-sink limitation that can reduce the effectiveness of MWA near large blood vessels. Preclinical studies have also demonstrated sharply defined treatment zones with relative preservation of collagen-rich structures such as major vessels and bile ducts. Additionally, histotripsy does not require tumor puncture, potentially avoiding complications associated with percutaneous applicator placement. Clinical Evidence and Immunologic Effects Early human studies, including the first-in-human THERESA trial and multicenter HOPE4LIVER trial, have demonstrated the feasibility and short-term safety of histotripsy for primary and metastatic liver tumors. More recent clinical experience has shown encouraging local tumor control, although long-term survival data and randomized comparisons with established therapies remain limited. Histotripsy may also have immunologic effects. Mechanical tumor destruction can release tumor-associated antigens and inflammatory signals without thermal denaturation. Preclinical studies have demonstrated immune-cell recruitment, tumor-specific T-cell responses, effects on untreated distant tumors, and enhanced responses when combined with immune checkpoint inhibition. These findings have raised interest in histotripsy as a potential immune primer, although this effect has not yet been established clinically. Histotripsy also has limitations. Successful treatment requires adequate ultrasound visualization and an unobstructed acoustic window. Tumors obscured by ribs, lung, or bowel gas may be difficult to target, and long-term oncologic outcomes remain under investigation.

CONCLUSION
Histotripsy represents a fundamentally different approach to liver tumor ablation through noninvasive, nonthermal mechanical tissue destruction. Early clinical results demonstrate promising feasibility and safety, while avoidance of heat-sink effects and potential immune activation may provide advantages in selected patients. Histotripsy is unlikely to replace established liver-directed therapies but may expand treatment options, particularly for tumors in anatomically challenging locations. Larger comparative studies and longer follow-up are needed to establish long-term efficacy, define appropriate patient selection, and determine whether its potential immunologic effects translate into meaningful clinical benefit.

Validity Evidence for the Otosurgical Technical Instruction & Competency (OTIC) Rubric using Longitudinal Assessment of Resident Surgical Performance

Investigator: Gabriella Marie Adams, B.S.
Mentor: Peter Volsky, MD
Co-Authors(s):
None listed.
Department(s): Otolaryngology-Head and Neck Surgery
Poster #: 19B

INTRODUCTION
Valid and reliable assessments of operative performance are essential to competency-based surgical education. The Otologic Technical Instruction and Competency (OTIC) Rubric was created to assess technical performance of essential otologic procedures; it scores global Procedure and Component performance and classifies errors. To study construct validity, Procedure and Component scores were examined in relation to experience, level of training, and operative components.

METHODS
We conducted a longitudinal validation study of intraoperative OTIC assessments collected from October 2022 through June 2026 at an academic otolaryngology residency program. Twenty-two residents (PGY-1 to PGY-5) were evaluated during postauricular approach with canal incisions (PAA group 1), postauricular approach without canal incisions (PAA group 2), tympanotomy, mastoidectomy, stapedotomy, facial recess approach, and tympanoplasty. Cumulative procedure-specific attempts, interval between attempts, and postgraduate year (PGY) were analyzed by multivariable mixed-effects ordinal logistic regression. Spearman correlations and procedural-step models evaluated relationships between Component Skills and Procedure scores; unstable multivariable step models were summarized using Spearman correlations. Trainees' response to Rubric implementation was obtained by anonymous survey.

RESULTS
A greater number of procedure-specific attempts were independently associated with higher Procedure scores for PAA group 1 (OR 1.58, 95% CI 1.14–2.18; p=.007), PAA group 2 (OR 1.20, 95% CI 1.04–1.39; p=.011), tympanotomy (OR 1.59, 95% CI 1.14–2.21; p=.007), and tympanoplasty (OR 2.48, 95% CI 1.25–4.94; p=.011). Facial recess demonstrated a similar positive association that was not significant (OR 1.75, 95% CI 0.95–3.19; p=.069). PGY experience was independently associated with competency only for mastoidectomy (OR 2.70 per year of training, 95% CI 1.20–6.04; p=.017). Time between consecutive attempts was not independently associated with competency for any procedure.

Procedural-step models identified independent predictors of competency: PAA Group 1-canal incision (OR 3.33, 95% CI 1.59–6.99; p=.002) and deep dissection (OR 8.65, 95% CI 2.95–25.39; p< .001); tympanotomy-lateral mallear ligament disarticulation (OR 74.15, 95% CI 2.75–2002.15; p=.010); and mastoidectomy-tegmen (OR 10.89, 95% CI 3.55–33.40; p< .001) and antrum dissection (OR 44.74, 95% CI 10.91–183.53; p< .001). Significant component–Procedure correlations were observed for PAA Group 2 (ρ=.750–.786), stapedotomy (ρ=.764–.807), facial recess (ρ=.441–.711; p≤.006), and tympanoplasty (ρ=.672–.906; all p< .001), with graft placement showing the strongest association (ρ=.906).

Participants (n=13) evaluated rubric-based appraisals. All agreed or strongly agreed that appraisals help identify deficiencies, set practice goals, enhance awareness of errors/near-misses, and add value to residency training. Additionally, 92.3% agreed or strongly agreed that appraisals enhance intra-operative learning and assist in planning and executing procedural steps. All agreed or strongly agreed that the rubric is easy to understand and scoring anchors are clear; 92.3% agreed or strongly agreed that it can be effectively applied across all training levels.

CONCLUSION
The OTIC Rubric is a practical tool for competency-based education in otologic surgery. This study supports its construct validity by demonstrating expected relationships with increasing procedural experience, progression through residency, and performance of key operative components. Trainees' responses were an overwhelming endorsement of its operational clarity, appraisal value, coverage of core constructs, and practical utility. These findings support further development of the OTIC Rubric as a formative and summative assessment.

Investigating the Impact of Demographic and Socioeconomic Factors on GIST Outcomes

Investigator: Adam Akari, M.S.
Mentor: Marybeth Hughes, MD, FACS
Co-Authors(s):
Daniel Montero, Macon & Joan Brock Virginia Health Sciences Eastern Virginia Medical School
Fang Fang, Old Dominion University
Matvey Karpov, Old Dominion University
Rachel Burke, Macon & Joan Brock Virginia Health Sciences Eastern Virginia Medical School
Eric Feliberti, Macon & Joan Brock Virginia Health Sciences Eastern Virginia Medical School
Winifred Lo, Macon & Joan Brock Virginia Health Sciences Eastern Virginia Medical School
Department(s): Surgery
Poster #: 03A

INTRODUCTION
Gastrointestinal stromal tumors (GISTs) are the most common mesenchymal tumors of the gastrointestinal tract. Imatinib and later-line tyrosine kinase inhibitors have transformed management, yet outcomes still vary widely. Social determinants of health are well established drivers of cancer outcomes, influencing both access to care and survival. In GIST, these factors remain far less studied than tumor biology. This study examines how demographic, socioeconomic, and clinical factors shape treatment and survival.

METHODS
We conducted a population-based retrospective cohort study of adults diagnosed with GIST in SEER from 2010 to 2024. Patients missing grade, T stage, or treatment status, and seven receiving intraoperative systemic therapy, were excluded. Outcomes were overall (OS) and disease-specific survival (DSS). Multivariable Cox proportional hazards models estimated the independent associations of demographic (age, sex, race/ethnicity, marital status), socioeconomic and health-system (income, urban residence, Commission on Cancer accreditation), tumor (grade, T/N/M stage), and treatment factors with each outcome.] Interactions between the treatment sequence and survival time were also evaluated to account for time-varying treatment effects.

RESULTS
Among 2,857 patients, 53.8% were female, 49.8% non-Hispanic White, 23.7% non-Hispanic Black, and 60.5% married. Overall, 96.6% received surgery, systemic therapy, or both, and 72.6% underwent surgery alone. At last follow-up 89.5% were alive, with GIST-specific and non-GIST deaths nearly equal (5.3% vs 5.2%). Non-Hispanic Black patients had higher overall (HR 1.77, 95% CI 1.31-2.38) and disease-specific mortality (HR 1.52, 95% CI 1.00-2.31) than non-Hispanic White patients. Unmarried patients had approximately twice the hazard of death (OS HR 1.95, 95% CI 1.52-2.50; DSS HR 2.12, 95% CI 1.49-3.01). Cases reported by Commission on Cancer-accredited facilities had lower disease-specific mortality (HR 0.55, 95% CI 0.35-0.88). Income, urban residence, and time from diagnosis to treatment were not associated with either outcome. Distant metastasis (OS HR=3.96, 95% CI=2.80-5.60; DSS HR=4.67, 95% CI=3.08-7.08), high grade (OS HR=1.62, 95% CI=1.17,1.96; DSS HR=1.76, 95% CI=1.23-2.53), male sex, and older age (OS HR=1.32, 95% CI=1.25-1.39; DSS HR=1.11(1.04-1.19) predicted worse survival outcomes. Excluded patients with missing values of the study variables differed significantly across demographic, clinical, and health-system factors.

CONCLUSION
Demographic and health-system factors were independently impact survival in GIST after adjustment for tumor burden and treatment. Being non-Hispanic Black, unmarried, and older age were the strongest demographic predictors of adverse survival outcomes, whereas income and rurality were not, indicating disparities in GIST is not primarily driven by area-level economics. These differences persisted in the surgically treated cohort, indicating access to operation alone may not close outcome gaps. Notably, care at Commission on Cancer accreditation significantly improved disease-specific survival, and adjuvant systemic therapy conferred significant early survival benefits. Findings should be interpreted considering selection bias inherent to complete-case analysis and short follow-up.

The Price of Pelvic Floor Therapy: Financial Toxicity in Caregivers of Children with Refractory Dysfunctional Voiding

Investigator: Kevin Alterman, B.A.
Mentor: Sarah H. Williamson, MD
Co-Authors(s):
Malea Drummond, Children's Hospital of the King's Daughters
Laura Cartino, Children's Hospital of the King's Daughters
Reyna Nikolaus, Children's Hospital of the King's Daughters
Janelle Fox, Children's Hospital of the King's Daughters
Jasilyn Wray-Jordan, Children's Hospital of the King's Daughters
Turaj Vazifedan, Children's Hospital of the King's Daughters
Department(s): Children's Surgical Specialty Group, Division of Urology
Poster #: 20B

INTRODUCTION
Dysfunctional voiding (DV) is a pediatric bladder–bowel disorder managed with timed voiding and constipation treatment, with pelvic floor physical therapy (PFPT) reserved for refractory cases. PFPT may create financial strain through visit frequency, copays, and caregiver work absences. This study assesses financial toxicity (FT) among caregivers of children with refractory DV and evaluates PFPT as a contributing factor.

METHODS
Patients aged 5-17 years with DV and ≥2 urology visits were included. Exclusion criteria were neurogenic bladder, cerebral palsy, chronic catheterization, prior bladder surgery, or structural anomalies. Caregivers completed a demographics survey, FACIT-COST financial toxicity instrument, and time/travel questionnaire; patients ≥8 years assented to chart review for PFPT utilization. Two-sided Pearson correlation, t-test, ANOVA, chi-square, and Fisher's exact tests were performed with $p<0.05$ considered significant.

RESULTS
Among 34 patient–caregiver dyads, median patient age was 10 years (IQR 7-14). Most patients were Caucasian (67.6%, n=23) and female (67.6%, n=23). Median FACIT-COST score for caregivers was 29 (IQR 18-38; range 3-44). PFPT was used by 31.3% (n=10). Dyads not attending PFPT had significantly higher FACIT-COST scores (greater financial well-being) than those attending (31.7 vs 18.5; $p=0.002$). FACIT-COST scores negatively correlated with number of PFPT visits ($r = -0.44$; $p=0.012$), indicating that more sessions predicted more FT. Neither FT nor PFPT use was significantly associated with race, ethnicity, or sex.

CONCLUSION
Considerable financial toxicity exists in pediatric DV management, particularly among families utilizing PFPT. While PFPT is non-invasive and non-pharmacologic, providers should be mindful of its potential financial burden on families.

Gestational weight gain and maternal-neonatal dyadic outcome desirability

Investigator: Chase Armstrong, B.S.
Mentor: Tetsuya Kawakita, MD, M.S.
Co-Authors(s):
None listed.
Department(s): Obstetrics and Gynecology
Poster #: 01A

INTRODUCTION
Reported optimal gestational weight gain (GWG) differs across analyses of similar data. We estimated the GWG range associated with the most favorable maternal-neonatal dyadic outcome in each prepregnancy BMI class, and tested whether that range depends on which outcomes are counted.

METHODS
This was a cross-sectional analysis of term singleton live births without prior cesarean using National Center for Health Statistics (NCHS) linked birth/infant death files, 2016–2023. Births were ranked into 8 maternal-neonatal dyadic categories and scored with partial credit. GWG was standardized to a 40-week equivalent and grouped into 2-kg categories, the highest open-ended (30 kg or more). Expected desirability was g-computed over 20 covariates within BMI class. The favorable range comprised GWG categories exceeding the BMI class average (bootstrap 95% CI excluding 0). Prespecified sensitivity analyses varied the ranking (dropping small-for-gestational-age [SGA]; penalizing large-for-gestational-age), and the exposure (subtracting birthweight, alone and with placental and fluid mass).

RESULTS
Among 21,724,087 births, the favorable range was +15 to 30 kg (underweight), +13 to +29 (normal weight), +11 to +21 (overweight), +7 to +19 (obesity class I), +1 to +13 (class II), and -1 to +11 (class III). The 2009 National Academy of Medicine (NAM) range overlapped it in all BMI classes, all 4 sensitivity analyses, and with that category excluded. Dropping SGA from the ranking produced the largest change: the favorable range fell by up to 14 kg (for example, normal weight, +13 to +29 became -1 to +15 kg), yet all still overlapped NAM.

CONCLUSION
NAM recommendations lie within the favorable GWG range in every BMI class and under every specification tested. Its location, however, was sensitive to which outcomes were counted.

Beyond the Negative Biopsy: Recurrent Pericardial Effusion Unmasking Mediastinal Lymphoma

Investigator: Aravindan Balaguru, B.S.
Mentor: Zahra Tasneem, MD
Co-Authors(s):
None listed.
Department(s): Internal Medicine
Poster #: 10A

INTRODUCTION

Pericardial effusion is a recognized complication of mediastinal lymphoma, particularly with bulky disease. However, establishing malignancy as the underlying etiology can be challenging when repeated fluid analysis and tissue sampling are nondiagnostic. We present a case of recurrent, hemodynamically significant pericardial effusion in which multiple negative diagnostic studies delayed the diagnosis of an aggressive mediastinal lymphoma.

CASE INFORMATION

A 26-year-old man with a remote history of resected unifocal Langerhans cell histiocytosis presented with chest pressure and bilateral cervical lymphadenopathy. He was found to have a large pericardial effusion with tamponade physiology requiring urgent pericardiocentesis. Despite drainage, the effusion repeatedly reaccumulated, necessitating two subsequent pericardial window procedures.

An extensive evaluation across multiple hospitalizations including pericardial fluid cytology and flow cytometry, pericardial and pleural biopsies, and repeated cervical lymph node sampling with cytology, flow cytometry, and FISH was negative or nondiagnostic for malignancy. Inflammatory pericarditis was considered, and colchicine was initiated without improvement.

The patient was subsequently readmitted with recurrent pericardial effusion. Cardiac MRI revealed a 15 × 11-cm anterior mediastinal mass encroaching on the right atrium, and PET imaging demonstrated extensive hypermetabolic cervical, supraclavicular, mediastinal, hilar, axillary, and pericardial adenopathy. Prior lymph node pathology demonstrating inflammatory lymphadenitis with a T-cell and histiocytic infiltrate, along with leukopenia and rash, raised concern for Kikuchi disease. Erdheim-Chester disease was also considered given his history and recurrent pericardial involvement. He was treated empirically with prednisone.

Following steroid taper, he was readmitted with persistent bulky mediastinal disease, progressive pericardial and cardiophrenic adenopathy, and a recurrent circumferential pericardial effusion measuring up to 4.5 cm. Repeat pericardiocentesis yielded 550 mL of serous fluid. Given progressive radiographic disease despite repeatedly nondiagnostic studies, CT-guided core biopsy of the anterior mediastinal mass was pursued. Pathology demonstrated an aggressive CD30+/CD20+ mediastinal B-cell lymphoid malignancy with overlapping features of mediastinal gray zone lymphoma and classical Hodgkin lymphoma. He was initiated on dose-adjusted R-EPOCH. Following treatment, the pericardial effusion decreased to a small residual collection without further need for drainage.

DISCUSSION

This case illustrates the diagnostic challenge of malignancy presenting as recurrent pericardial effusion despite repeatedly negative cytology and tissue sampling. Although negative studies appropriately broadened the differential toward inflammatory and histiocytic disorders, the patient's recurrent effusions, failure of anti-inflammatory therapy, progressive adenopathy, and bulky mediastinal mass remained discordant with a benign inflammatory process.

For patients with recurrent admissions, the longitudinal clinical trajectory can be as important as an individual diagnostic result. Negative pericardial cytology or limited lymph node sampling does not definitively exclude lymphoma, particularly when diagnostic tissue architecture is not adequately captured. When recurrent pericardial disease remains unexplained and imaging demonstrates progressive adenopathy or a suspicious mediastinal mass, the working diagnosis should be reassessed and repeat tissue acquisition from the highest-yield target pursued. This case emphasizes the importance of recognizing discordance between negative diagnostic testing and a progressively malignant clinical phenotype to avoid diagnostic delay.

National Football League Hand Injuries: Return to Sport and Performance

Investigator: Madison Baldauf, B.S.
Mentor: Kate Nellans, MD
Co-Authors(s):
Chloe Heiting, Donald and Barbara Zucker School of Medicine at Hofstra/Northwell
Gabriella Chin, Donald and Barbara Zucker School of Medicine at Hofstra/Northwell
George Economou, Northwell Orthopedics
Priya Duvvuri, Northwell Orthopedics
Carolina Herrera, Biomedical & Translational Sciences
Department(s): Orthopedic Surgery
Poster #: 18B

INTRODUCTION
Injuries sustained by professional athletes have the potential to severely impact performance and abilities. While lower extremity injuries have dominated the literature, upper extremity trauma represents a significant source of morbidity in football players. The aim of this study is to characterize the impact of hand injuries on the performance of athletes in the National Football League (NFL). This is significant, due to the highly variable functional demands for each position.

METHODS
NFL players who sustained phalanx, thumb, metacarpal, or carpal injuries from the 2012-2013 season to 2022-2023 season were identified using Pro Sports Transactions. Performance data was extracted from Pro Football Reference including player position and number of games missed, as well as number of games played, games started, and snap counts in the seasons prior to and following injury. Players were excluded if the injury occurred during the player's rookie or final season or if additional injuries were sustained at the time of the upper extremity injury. Data was analyzed using ANOVA single factor test (alpha=0.05.)

RESULTS
304 players sustained a phalanx, thumb, metacarpal, or carpal injury, with three players having injuries in two of these categories: metacarpal, n = 110 (35.8%); carpal, n = 80 (26.1%); thumb, n = 78 (25.4%); and phalangeal, n = 39 (12.7%). Linebackers (14.6%) and wide receivers (12.8%) were most likely to sustain one of these injuries. Most occurred during the preseason or in September ($p < 0.001$). The average number of games missed due to injury was 5.5; carpal: 6.4, phalangeal: 5.8, thumb: 5.4, and metacarpal: 4.3 ($p = 0.02$). Sixty-five players were injured in their rookie season and 58 in their final season. The average change in games played in the preceding season to those in the following season was +1.0, with no significant difference when stratified by injury. The average change in games started was +0.5. The average change in snap counts was +72.8; by injury, phalangeal: +120.1, carpal: +31.5, thumb: +125.7, and metacarpal: +50.0. Safeties had the greatest decrease in games played (0.8 fewer), and the greatest decrease in games started (2.0 fewer). Safeties also had the largest decline in snap counts, with an average of 94.9 fewer snaps after injury.

CONCLUSION
Phalanx, thumb, metacarpal, and carpal injuries are common injuries in NFL players, with an average of about 25 recorded per season, and they have a measurable impact on player performance. Players missed an average of more than 5 games due to these injuries, which is nearly a third of a normal season. Fifty-eight players did not return to the NFL, suggesting that hand injuries may be costly to both players and organizations and should be carefully managed by trainers and medical staff. However, there was an overall improvement in performance among the players who returned the following season, which varied greatly depending on the position of the player. This study should help guide team physicians in anticipating the impact on players after a hand injury based on their position.

Acellular Fish Skin Substitute Use in the Management of an Open Mid-Foot Dislocation: A Case Report

Investigator: Madison Baldauf, B.S.
Mentor: David Zupruk, DO
Co-Authors(s):
Christian Busch, Macon & Joan Brock Virginia Health Sciences Eastern Virginia Medical School
Department(s): Orthopedic Surgery
Poster #: 18A

INTRODUCTION

Standard management of open fractures includes irrigation and debridement of the wound followed by skeletal stabilization and often skin grafting over the defect. Skin grafting is associated with complications such as infection, hematoma, contracture, and potential failure. A novel alternative is acellular fish skin substitute, derived from North Atlantic codfish, requiring very minimal processing. We sought to explore it's use and effectiveness in the management of an open mid-foot dislocation.

CASE INFORMATION

A 35 year old man with notable history including class II obesity and a previous left tibia fracture presented to the emergency department after suffering multiple injuries in a motorcycle crash. Imaging and operative findings identified a complex open right midfoot/forefoot fracture-dislocation (Lisfranc injury) classified as Gustilo-Anderson Type I/II open fracture along with compartment syndrome. He was immediately taken to the operating room for fasciotomies of the right leg and foot as well as skeletal stabilization with an external fixation device. Approximately 5 weeks following injury, the patient underwent open reduction and internal fixation of the fractures and acellular fish skin substitute was applied to the open wounds following sharp debridement. At this point the wounds measured 4 x 3 cm medially, 9 x 4 cm dorsally, and 3 x 5 cm laterally. The AFSS mesh was applied over each wound, secured with 3-0 Monocryl suture, and covered with a non-adherent dressing and a wound vac to facilitate negative pressure healing. Antibiotics were administered for 24 hours postoperatively. At his 1 week follow up appointment, the AFSS was incorporating appropriately and a second layer was then applied. Subsequent appointments continued to confirm appropriate incorporation and healing. Seven months after initial injury, complete re-epithelialization was achieved and the patient was continuing physical therapy exercises at home.

DISCUSSION

This patient suffered a devastating open fracture injury with extensive soft tissue defects. These injuries are a challenge to manage and in this case, extremity amputation was a concern from initial presentation. In contrast to the majority of these injuries, this patient did not require a skin graft. There was no infection, hematoma formation, scar contracture, or other complications throughout the healing process.

CONCLUSION

Acellular fish skin substitutes are a novel tool in the management of open fractures and this case demonstrates an excellent outcome. The major benefits of this product include its ease of application, long shelf life of nearly three years, room temperature storage, low risk of viral or prion disease transmission, and affordability. Though there is no head to head comparison of total cost, skin grafting for open fractures costs over $25,000 on average in the US. AFSS costs approximately $127 per square inch, and shorter hospital stay. Surgeons managing these injuries should consider AFSS application before pursuing skin grafting.

Reassessing Resource Utilization in Pediatric Low-Grade Blunt Renal Trauma

Investigator: Alexis Boscia, B.S.
Mentor: Jamie Golden, MD, Ph.D.
Co-Authors(s):
Karen Kennamer, Macon & Joan Brock Virginia Health Sciences Eastern Virginia Medical School
William Rice, Macon & Joan Brock Virginia Health Sciences Eastern Virginia Medical School
Rhiannon Torres, Children's Hospital of the King's Daughters
Katherine Davenport, Children's Hospital of the King's Daughters
Department(s): Pediatrics
Poster #: 21B

INTRODUCTION
Pediatric blunt renal trauma (BRT) is rare but consumes substantial health care resources. Though evidence-based guidelines exist for pediatric blunt liver and spleen injuries, a lack of renal pathways results in variable, potentially unnecessary resource use. We hypothesized that management of low-grade pediatric BRT utilizes resources disproportionate to injury severity.

METHODS
We retrospectively reviewed patients 1-17 years old admitted to a level 1 pediatric trauma center with BRT from 2014-2024. Injuries were classified using American Association for the Surgery of Trauma (AAST) guidelines as low-grade (LGI; I-III) or high-grade (HGI; IV-V). Demographic, injury, management, intervention, and outcome data were collected. Management variables included ICU admission, urinary catheterization, laboratory monitoring, activity restriction, and repeat imaging. Interventions included angioembolization, ureteral stenting, nephrectomy, and blood transfusion. Analyses were performed using Mann-Whitney U or Kruskal-Wallis tests for continuous and Chi-square or Fisher's exact tests for categorical variables. Data are presented as medians unless otherwise specified. Subset analysis was performed for patients with non-renal injuries increasing bleeding risk or ICU admission (complicating injuries).

RESULTS
Fifty-six patients presented with BRT. Two were excluded for immediate operative management of complicating injuries. Of the remaining 54 patients, 38 (70%) had LGI and 16 (30%) had HGI. Groups did not differ in gender (66% vs 56% male), age (12 vs 10 years), or weight (44.3 vs 34.4 kg) ($p>0.05$). HGI patients had higher ISS (16.5 vs 9.5, $p=0.011$) and were more likely to have gross hematuria (94% vs 53%, $p=0.004$). Complicating injuries were present in 8 (21%) LGI and 1 (6%) HGI patient. Resource utilization was high, but less so for LGI than HGI patients. HGI patients were more likely to undergo urinary catheterization (50% vs 18%, $p=0.018$) and be admitted to the ICU (56% vs 26%, $p=0.035$). HGI patients had more hemoglobin draws (8 vs 4.5, $p=0.012$), more CT scans (2 vs 1, $p<0.001$), longer total bedrest (3 vs 1 days, $p=0.007$), and longer lengths of stay (4 vs 3 days, $p=0.007$). Operative intervention was less common in LGI (0% vs 25%; $p=0.006$). All 4 operations were ureteral stent placements. No patients required nephrectomy or angiography. Blood transfusion rates were similar for LGI and HGI (5% vs 19%; $p=0.15$). All transfused LGI patients had complicating injuries; no uncomplicated LGI patient required intervention. Survival to discharge was similar between LGI and HGI (97% vs 100%). The only mortality was secondary to severe hypoxic brain injury.

CONCLUSION
BRT patients in our study had excellent outcomes and low rates of intervention. LGI patients required fewer resources and interventions than HGI patients, and uncomplicated LGI did not require intervention. Serial labs, ICU admission, inpatient observation, and bedrest remained high despite the absence of intervention, supporting de-escalation in this low-risk group.

Targeting Stress Induced Senescence in Lung Fibrosis

Investigator: Ethan S. Casto, B.S.
Mentor: Yan Sanders, MD
Co-Authors(s):
Sara Palega, Macon & Joan Brock Virginia Health Sciences Eastern Virginia Medical School
Department(s): Biomedical and Translational Sciences
Poster #: 07B

INTRODUCTION

Idiopathic Pulmonary Fibrosis (IPF) is an age-related disease characterized by the pathologic deposition of extracellular matrix (ECM) caused by chronic fibroblast activation and aberrant wound repair. There is no cure for IPF, and the disease carries a median survival of 3-5 years. While different cell lineages are implicated, lung fibrosis specifically is characterized by the over-accumulation and activation of fibroblasts, including senescent lung fibroblasts with a pathological senescence-associated secretory phenotype (SASP). The senescent cells drive IPF by disrupting lung epithelium, myofibroblast activation, ECM remodeling, and creating a pro-inflammatory environment through secretion of cytokines. In this project, we established an in vitro-cell model of bleomycin inducing cellular senescence in IMR90 human lung fibroblasts. The senescence markers p21, β-gal, and apoptosis markers BAX, XIAP were evaluated, as well as pro-fibrotic and inflammatory markers α-SMA, and IL-1B.

METHODS

IMR90 human lung fibroblasts were exposed to bleomycin at 0, 10, 20, 30, 40, and 50 ug/mL for 24 hrs. Whole cell lysate was harvested 3 days following bleomycin exposure. Various markers to characterize the cell phenotypes were examined by Western blots. β-Gal staining was performed 3 days after exposure to bleomycin at 0, 10, and 40 ug/mL to examine cellular senescence.

RESULTS

As bleomycin concentration increased, the expression of p21, a growth arrest marker; BAX and XIAP, markers of apoptosis; and α-SMA, a fibrotic marker, increased as well. The cell senescence marker, β-Gal expression, also increased with bleomycin concentration.

CONCLUSION

The established protein markers of senescence: p21 and β-Gal, inflammation: IL-1B, profibrotic: α-SMA, and apoptosis: BAX, XIAP, were evaluated by Western Blotting. Bleomycin exposure induced the upregulation of senescent, fibrotic, and apoptotic markers, with 10 ug/mL and 20 ug/mL being the most effective at inducing cellular senescence while limiting cell death. The effects of bleomycin on cellular proliferation are under investigation, along with the effects of antioxidants and epigenetic modifiers in the presence of genotoxic drugs. This project will further our understanding of underlying mechanisms of the development of IPF and possible therapies that could be used to treat the disease.

Association of Cervical Spine Pathology with Acromioclavicular Joint Pain and Distal Clavicle Excision: A TriNetX Database Study

Investigator: Wayne Jay Cochran, II, B.S.
Mentor: Kevin Bonner, MD
Co-Authors(s):
Zachary Krumm, Macon & Joan Brock Virginia Health Sciences Eastern Virginia Medical School
Madison Baldauf, Macon & Joan Brock Virginia Health Sciences Eastern Virginia Medical School
Julia Pittaluga, Jordan-Young Institute
Department(s): Orthopedics
Poster #: 04A

INTRODUCTION
Distal clavicle excision (DCE) is commonly performed with rotator cuff repair (RCR) for symptomatic acromioclavicular (AC) joint pathology. While the indications and outcomes of RCR and DCE are well established, the influence of concomitant cervical spine pathology on shoulder pain, surgical decision-making, and postoperative outcomes remains incompletely understood. This study evaluated the association between cervical spine pathology and surgery with outcomes related to AC joint pain, DCE, and RCR using the TriNetX database.

METHODS
A retrospective cohort study was performed using the TriNetX database from 2015–2025. Patients older than 18 years and alive at analysis were included. The postoperative window for all outcomes was at least 1 day following surgery. To reduce confounding, propensity score matching was performed using age at index event and baseline comorbidities including diabetes mellitus, hypertension, and tobacco use, with three independent matched cohort analyses conducted.

The first analysis compared rates of DCE and postoperative AC joint pain in patients undergoing RCR with and without preexisting cervical spine pathology, identified using ICD-10 code M50 series, not requiring a clinical encounter for diagnosis. Postoperative AC joint pain was identified using ICD-10 code M25.51 series. The second analysis evaluated rates of subsequent cervical spine surgery following RCR in patients with and without concomitant DCE; cervical spine surgery included anterior cervical decompression and fusion, total disc replacement, and posterior extradural laminotomy or foraminotomy. The third analysis assessed rates of subsequent RCR and DCE following shoulder arthroscopy in patients with and without cervical spine pathology.

RESULTS
Matched cohorts included 16,266 patients per group in the first analysis, 28,172 per group in the second, and 25,181 per group in the third. Patients with cervical spine pathology demonstrated significantly higher rates of AC joint pain following RCR (62.70% vs 56.19%; RR 1.12, 95% CI 1.10–1.14; $P < 0.0001$). There was no difference in rates of DCE following RCR (2.89% vs 2.56%; RR 1.13, 95% CI 0.99–1.28; $P = 0.0712$). Patients undergoing DCE at the time of RCR had a minimally increased risk of subsequent cervical spine surgery compared with RCR alone (1.12% vs 0.88%; RR 1.26, 95% CI 1.07–1.49; $P = 0.066$). Patients with preexisting cervical spine pathology had increased rates of DCE (3.05% vs 2.68%; RR 1.14, 95% CI 1.03–1.26; $P = 0.01$) following shoulder arthroscopy. There was no difference in subsequent RCR (6.91% vs 6.62%; RR 1.04, 95% CI 0.98–1.11; $P = 0.21$).

CONCLUSION
In patients undergoing RCR, preexisting cervical spine pathology was associated with increased postoperative AC joint pain with no significant influence on rate of DCE. Patients who underwent RCR with concomitant DCE had higher rates of subsequent cervical spine surgery. Preexisting cervical spine pathology was associated with increased rates of DCE following shoulder arthroscopy, but did not influence rates of RCR. These findings suggest that underlying cervical spine pathology may be associated with persistent or overlapping shoulder symptoms in patients who undergo RCR and should be considered during patient evaluation, surgical decision-making, and preoperative counseling.

Global Trends in Orthoplastic Research: A Bibliometric Analysis (1993-2026)

Investigator: Wayne Jay Cochran, II, B.S.
Mentor: Scott Levin, MD
Co-Authors(s):
Elizabeth Card, Perelman School of Medicine
Department(s): Orthoplastic Surgery
Poster #: 48B

INTRODUCTION

The orthoplastic approach to reconstruction incorporates multidisciplinary collaboration and principles from both orthopedic and plastic surgery in the management of complex limb trauma and oncologic defects. This integrated approach has been shown to improve clinical outcomes. Although research on orthoplastic surgery has increased substantially, there remains a need for a comprehensive characterization of publication trends, thematic focus areas, and gaps within the literature.

DISCUSSION

Articles detailing the orthoplastic approach were analyzed from the Web of Science Core Collection (WOSCC) database from 1993 to 2026. We assessed publication trends, citation analysis, co-authorship networks, and keyword co-occurrence mapping.
A total of 279 publications were identified. Annual publication output increased from 7 articles in 2018 to 45 in 2025, demonstrating substantial growth in orthoplastic research. The most productive countries were the United Kingdom and the United States, while the leading institutions included Southmead Hospital and the University of Pennsylvania. The most prominent authors were L. Scott Levin, Khan U, and Kovach SJ.

Keyword analysis revealed several major research clusters, including management, limb salvage, trauma, and microsurgery. Additionally, citation burst analysis identified emerging areas of interest, particularly in pressure wound therapy and microsurgery.

CONCLUSION

Orthoplastic surgery has experienced substantial growth since its inception, with research increasingly shifting from technical reconstructive considerations toward multidisciplinary care pathways, limb salvage, functional outcomes, and patient-centered management. Despite continued reliance on a core group of foundational publications, opportunities remain to strengthen international collaboration and expand the evidence base through prospective, multicenter investigations.

Access to Sleep Apnea Care in Hampton Roads: Analysis of the Local Sleep Health Care Landscape, Referral Pathways, and Oral Appliance Therapy Treatment Patterns

Investigator: Avin Ryan Curtis, B.S.
Mentor: Sara Rothenberg, M.S.
Co-Authors(s):
None listed.
Department(s): Pediatrics Research
Poster #: 22B

INTRODUCTION
OSA (Obstructive Sleep Apnea) affects nearly 1 billion people worldwide, carrying risks such as cardiovascular disease, neurological disorders, and motor vehicle accidents. Military populations are disproportionately affected due to frequent travel, stimulant and sedative use, trauma exposure, and chronic sleep deprivation. Although CPAP (continuous positive airway pressure) is the current standard of care, it lacks adherence amongst military members due to poor portability, practical issues, and psychological challenges. This study evaluates accessibility and success of OAT (oral appliance therapy) to assess whether it should be considered first line for military populations.

METHODS
Medical records of 213 Tricare-insured patients aged 22-66 prescribed OAT by a private dental sleep medicine practice in the Hampton Roads area were reviewed. Themes of data gathered included severity of OSA, prior CPAP use, pathway/timeline of treatment, and success of OAT. Success was measured both via self-report as well as clinically via changes in AHI.

RESULTS
186 patients initiated treatment, with an average of 10.6 weeks from referral to initiation. 32 patients experienced a delay in care, with 20 reporting a cost barrier. Self-reports demonstrated 129 patients experienced some improvement, compared to 18 denying any improvement. Objective clinical data was limited to 24 patients, with an average improvement/decrease in AHI by 4.7 ($p<0.01$), with a range of -25.2 (improvement) to +4 (worsening), and 8 patients experiencing a decrease of AHI to below 5 (diagnostic threshold).

CONCLUSION
Overall, OAT is highly effective at improving OSA symptoms and AHI, although for some patients it does not provide complete resolution. Although there are possibilities for delays in care, they were limited to 15% for this study population. The findings of this study prompt the need for further direct comparisons of timeline, cost, and efficacy of the two treatments. In particular, more post-treatment sleep studies are required to determine objective success of OAT relative to CPAP in this population, however, these initial results are promising.

Effect of SGLT-2 inhibitor (SGLT-2i) on glycemic management and cardiovascular outcomes in the immediate post-op period in patients with Type 2 diabetes mellitus (T2DM) undergoing Coronary Artery Bypass Graft (CABG) surgery

Investigator: Ethan Ding, B.S.
Mentor: Manasi Shah, MD
Co-Authors(s):
Michael Bittner, Macon & Joan Brock Virginia Health Sciences Eastern Virginia Medical School
Amanda Graves, Macon & Joan Brock Virginia Health Sciences Eastern Virginia Medical School
Ann Harper, Sentara
Amin Yehya, Sentara
Department(s): Department of Endocrinology
Poster #: 05A

INTRODUCTION

Sodium-glucose cotransporter 2 inhibitors (SGLT2-I), a commonly prescribed antihyperglycemic agent for patients with type 2 diabetes mellitus (T2DM), have proven efficacy in managing T2DM and its common cardiovascular comorbidities. The increased risk of coronary artery disease in T2DM patients makes them more likely candidates for coronary artery bypass graft (CABG) surgery. SGLT2-I improve long-term cardiovascular outcomes, but evidence of their effects in the immediate post-op period is limited.

METHODS

We collected medical records of patients with T2DM who underwent CABG surgery (N = 765) from 2019 to 2025 at our hospital from the EPIC system. Of the population studied, patients who received dapagliflozin (N = 166) during their hospital stay were compared to those who did not receive this drug (N = 599). Patients with prior use of any SGLT2-I were included, but only dapagliflozin use was studied due to formulary restrictions in our hospital. We performed Chi-square, t-tests, and logistic regression to investigate relationships between inpatient SGLT2-I use and baseline characteristics, insulin requirements, mean glucose values, occurrence of arrhythmias, 90-day readmission rates, and post-op mortality.

RESULTS

The average age of the population was 64 years, with a majority being male (n=557), White (n=506), and an average BMI of 31.3 kg/m2. Of 765 patients, 97% received insulin during their hospitalization; 22% received dapagliflozin with mean initiation on post-op day 3. Among variables studied, several showed statistically significant association with SGLT2-I use, including BMI, baseline creatinine, glargine and lispro insulin dosing (on the day before discharge), heart failure with preserved ejection fraction (HFpEF), and 90-day readmissions (all $p < 0.05$). In the multivariable logistic regression model, only HFpEF and baseline creatinine remained significantly associated with dapagliflozin use after adjusting for covariates. Patients with HFpEF had significantly lower odds of receiving dapagliflozin (OR 0.48, $p = 0.0458$). Treatment with dapagliflozin did not affect mean glucose values, total and ICU lengths of stay, occurrence of major arrhythmia during admission, 90-day readmission rates, or post-op mortality.

CONCLUSION

Our study showed that patients who received dapagliflozin during their hospital stay for CABG surgery required lower basal and bolus insulin doses at discharge compared to those who did not receive dapagliflozin. On average, dapagliflozin was initiated 3 days after surgery. While patients with HFpEF were less likely to receive this drug in our study, further studies are required in this specific population post-CABG surgery.

The Effectiveness of Arthroplasty as a Salvage Tool for Proximal Humerus Nonunion/Malunion: A Systematic Review

Investigator: Moumen Elbakary, B.S.
Mentor: Claire Simpson, BS
Co-Authors(s):
Parsa Sedaghat, Virginia Commonwealth University
Matt Smith, Virginia Commonwealth University
Charles Reiter, Virginia Commonwealth University
Haileigh Hooper, Virginia Commonwealth University
Erica Brody, Virginia Commonwealth University
Jimmy Satalich, Virginia Commonwealth University
Jennifer Vanderbeck, Virginia Commonwealth University
Department(s): Eastern Virginia Medical School
Poster #: 46B

INTRODUCTION
Proximal humerus fractures are some of the most common fractures in adults. First line treatment is typically conservative, however sequelae including nonunion and malunion are possible and can cause considerable instability, pain, and loss of function. The purpose of this systematic review was to evaluate the usage of shoulder arthroplasty as a salvage tool for proximal humerus nonunion and malunion, providing insight on its effect on various outcome measures.

METHODS
In adherence to PRISMA (Preferred Reporting Items for Systematic Review) guidelines, Medline, Embase, Cochrane, and Web of Science were searched through March 2026 to include in this systematic review. Studies that evaluated the usage of shoulder arthroplasty as a salvage tool in nonunion and malunion were included. Patient demographics, procedure type, range-of-motion (ROM), complications, and surgical outcome measures including ASES, Constant Murley, VAS, and patient satisfaction were recorded and analyzed.

RESULTS
Of the 1,960 studies identified in our search, 8 studies comprising 5,568 patients met the inclusion criteria. The mean patient age was 68.78 years and mean follow-up was 56.28 months. Of the studies included, five evaluated solely reverse shoulder arthroplasty, one with both reverse and anatomic arthroplasty, and two solely anatomic arthroplasty. Clinical outcomes improved when both preoperative and postoperative data were available. Mean Constant Murley scores increased from 19.7 to 59.45 in combined nonunion/malunion cohorts, 15 to 68 in nonunion cohorts, and 22 to 63.9 cohorts. Flexion and external rotation (ER) were the most heavily reported ROM values, included in 7 of the 8 studies. Mean gain of flexion in combined nonunion/malunion cohorts was 56.2°, 29° for nonunion, and 41° for malunion. Mean gain of ER in combined nonunion/malunion cohorts was 25.9°, 9.5° in nonunion, and 20° in malunion. The most frequent complications reported in the combined study population were dislocation (3.35%), infection (2.85%), and fracture (2.80%).

CONCLUSIONS
The findings of this systematic review suggest that shoulder arthroplasty can be an effective salvage tool in patients with nonunion and malunion of PHFs. Increases in CM scores and patient satisfaction, as well as improved ROM, give evidence for the improved quality-of-life that salvage arthroplasty can provide. This review also relayed complication rates for surgeons, showing the risks associated with the intervention. However, limited homogeneity and preoperative data across studies limit our comparisons. Future studies without these hindrances will provide more insight on how to best treat proximal humerus nonunion and malunion.

Development of a New Primary Melanoma During Pembrolizumab Therapy for Metastatic Urothelial Carcinoma

Investigator: Julia Feord, B.S.
Mentor: Marybeth Hughes, MD, FACS
Co-Authors(s):
None listed.
Department(s): Surgical Oncology
Poster #: 17A

INTRODUCTION

Pembrolizumab is a programmed cell death protein 1 (PD-1) inhibitor used to treat multiple malignancies, including advanced melanoma and urothelial carcinoma. Although pembrolizumab has demonstrated substantial antitumor activity against melanoma, the development of a new primary melanoma during treatment is unexpected and has not been reported to our knowledge. We present a patient who developed an advanced primary melanoma while receiving pembrolizumab for metastatic urothelial carcinoma.

CASE INFORMATION

A 68-year-old woman with metastatic urothelial carcinoma was receiving maintenance pembrolizumab every six weeks. Approximately three years after initiating therapy, she developed an exophytic polypoid lesion on the left anterior distal thigh. Histopathologic examination demonstrated an ulcerated, exophytic polypoid melanoma with a Breslow depth of 12.6 mm and a high mitotic rate, consistent with a T4b primary melanoma. She subsequently underwent wide local excision and sentinel lymph node biopsy. Final pathology demonstrated no residual melanoma, clear surgical margins, and a left inguinal sentinel lymph node negative for metastatic melanoma, consistent with stage 2C disease. She remains without evidence of melanoma recurrence and undergoes surveillance computed tomography every six months.

DISCUSSION

This case demonstrates that a new primary melanoma may arise despite ongoing systemic PD-1 inhibition. Possible explanations include tumor-intrinsic or microenvironmental mechanisms of resistance, insufficient immune recognition of the emerging tumor, or coincidental melanoma development unrelated to pembrolizumab therapy. The temporal association alone does not establish that pembrolizumab contributed to the development of the melanoma. Instead, this presentation illustrates that treatment with an immune checkpoint inhibitor does not eliminate the risk of a new primary malignancy, even when that therapy has established activity against the same cancer type.

CONCLUSION

Continued routine skin examinations and age- and risk-appropriate cancer surveillance remain important for patients receiving long-term immunotherapy. New or changing cutaneous lesions warrant prompt evaluation regardless of concurrent PD-1 inhibitor treatment.

Duchenne Muscular Dystrophy: A Case Highlighting Imaging Findings and Supportive Care

Investigator: Juan Emilio Ferrando, B.S.
Mentor: Shashidhara Murthy, MD
Co-Authors(s):
Juan Ferrando, Macon & Joan Brock Virginia Health Sciences Eastern Virginia Medical School
Trenton Taros, Macon & Joan Brock Virginia Health Sciences Eastern Virginia Medical School
Department(s): Radiology
Poster #: 11A

INTRODUCTION

Duchenne muscular dystrophy (DMD) is a severe X-linked recessive genetic disease that affects approximately 1 in 5,050 males at birth. Although most cases are hereditary and diagnosed in males, de novo mutations and symptomatic female carriers have been described. Mutations in the DMD gene result in reduced or absent dystrophin protein. Dystrophin acts as a molecular shock absorber, protecting the sarcolemma during routine muscle contraction. Due to a lack of dystrophin, tears accumulate in the sarcolemma, leading to muscle fiber necrosis. Early symptoms begin during childhood, presenting initially with muscle weakness and difficulty ambulating. This then progresses to involve other organ systems, leading to gastroparesis, urinary dysfunction, respiratory failure/ventilation, dilated cardiomyopathy, and death. Currently, the life expectancy for someone diagnosed with DMD is between 20-40 years, with a median of 28.1 years if born after 1990. We report a case of a 27-year-old male previously diagnosed with DMD presenting to the emergency department for a painful, erythematous skin rash on his distal right leg. We will also discuss the role of imaging studies in the management of DMD and radiological findings often seen in those diagnosed with DMD.

CASE INFORMATION

A 27-year-old male with a past medical history of DMD requiring a wheelchair and 24/7 assistance with activities of daily living, dilated cardiomyopathy, restrictive lung disease, and osteoporosis presents to the ED with a painful, erythematous, warm, and edematous skin rash overlying the right distal tibia/fibula. These symptoms began 2 days ago, causing him to initially present to another hospital, where he was prescribed cephalexin and doxycycline before being discharged. Despite adhering to his antibiotics, his symptoms have continued to worsen.

Vital signs are 98.1 F, heart rate 108, respiratory rate 18, blood pressure 117/60, and SpO2 98%. WBC count, lactate, and procalcitonin are within normal limits. Metabolic panel demonstrates mild hyperglycemia, and hepatic function panels show mild ALT elevation but are otherwise unremarkable. At this moment, he does not meet SIRS criteria. Differential diagnosis initially includes cellulitis, DVT, and peripheral artery disease. An X-ray of the tibia, duplex vascular ultrasound, two chest X-rays, and a lower extremity CT with contrast were ordered during his hospital visit.

DISCUSSION

Several radiologic findings are commonly seen in those diagnosed with DMD. These include muscle with progressive fatty replacement and atrophy, calf pseudohypertrophy, spine/skeletal findings like lordosis, scoliosis, and osteoporosis, reduced lung volumes, and atelectasis. The patient in this case report demonstrates many of these findings. These include a low lung volume with atelectasis, severe diffuse fatty infiltration into the gastrocnemius, and skeletal changes including osteoporosis. Additionally, edema of the right lower extremity with stranding on the dorsum of the foot is identified.

CONCLUSION

The patient was diagnosed with cellulitis and discharged home on Linezolid after notable improvement in his cellulitis symptoms while on IV antibiotics. Although radiographic studies are not used for diagnosing DMD, several imaging modalities are used to aid with supportive measures and monitor disease progression.

Internal Hernia After Roux-en-Y Gastric Bypass: A Case Report and Review of CT Findings

Investigator: Juan Ferrando, B.S.
Mentor: Adam Lustig, MD
Co-Authors(s):
Juan Ferrando, Macon & Joan Brock Virginia Health Sciences Eastern Virginia Medical School
Trenton Taros, Macon & Joan Brock Virginia Health Sciences Eastern Virginia Medical School
Department(s): Radiology
Poster #: 39B

INTRODUCTION

Post-gastric bypass-associated internal hernia is a well-described complication associated with laparoscopic Roux-en-Y bypass surgery. The incidence of internal hernia in this population ranges from around 2% for those who had their mesenteric defect closed vs. 6% if the mesenteric defect was not closed. Different possible hernia sites include Petersen's space, Jejunojejunostomy mesenteric defect, and the transverse mesocolon defect. Timely identification of internal hernias is extremely important, as they can become obstructed or incarcerated, leading to necrosis. Having a structured approach to CT reporting has been shown to improve diagnostic accuracy. We report a case of a 65-year-old woman who presented to the emergency department and was later diagnosed intraoperatively with an internal hernia after contrast-enhanced CT identified key diagnostic signs. Additionally, we will review other important signs not identified in this case that can be used to help healthcare providers identify internal hernia more accurately.

CASE INFORMATION

A 65-year-old female with a past medical history of gastric bypass, abdominoplasty, and cholecystectomy, with all surgeries occurring around 15 years ago, presents to the emergency department for severe cramping abdominal pain, nausea, and vomiting. Vital signs are stable; there is no leukocytosis, and a CT without contrast is performed due to deferral of contrast. CT demonstrates mesenteric edema and nonspecific changes. Her pain resolves, and she is again able to tolerate food. A diagnosis of Dumping syndrome was made, and she was discharged.

Two days later, she returns to the emergency department with similar symptoms. Metabolic panel shows elevated BUN and creatinine along with a mild anion gap of 18. Liver function tests, lipase, and magnesium are within normal limits. A CT with contrast is performed, and bariatric surgery is consulted.

DISCUSSION

Contrast-enhanced CT demonstrated prior Roux-en-Y bypass, swirling and edema of the mesentery with a questionable transition point of the biliary limb in the midline upper abdomen. Signs of post-laparoscopic Roux-en-Y gastric bypass-associated internal hernia on CT include: (1) swirl sign, (2) small-bowel obstruction, (3) clustered loops, (4) mushroom sign, (5) hurricane eye sign, (6) small bowel behind the superior mesenteric artery, (7) right-sided anastomosis, (8) enlarged nodes, (9) venous congestion, and (10) mesenteric edema. The presence of the swirl sign is considered to have the highest combination of sensitivity and specificity for detecting a post-gastric bypass internal hernia on CT.

CONCLUSION

An intraoperative diagnosis of incarcerated partially obstructed internal hernia of the biliopancreatic limb through Peterson's space is made and immediately repaired. The patient was discharged home the following day.

Ureteral obstruction due to sloughed fatty tissue following embolization of angiomyolipoma: A Case Report

Investigator: Peter Andrew Gahan, B.S.
Mentor: Sarah Shaves, MD
Co-Authors(s):
Peter Gahan, Macon & Joan Brock Virginia Health Sciences Eastern Virginia Medical School
Trenton Taros, Macon & Joan Brock Virginia Health Sciences Eastern Virginia Medical School
Department(s): Department of Radiology
Poster #: 12A

INTRODUCTION

Angiomyolipoma (AML), a form of benign renal neoplasm, generally occurs either spontaneously or due to tuberous sclerosis. Although AML is often asymptomatic and found incidentally, there are cases where spontaneous hemorrhage occurs and causes a wide variety of symptoms, sometimes progressing to shock. Angioembolization is a potentially life-saving treatment in such cases and is generally successful as a treatment. Here, we describe a patient who underwent two AML embolization procedures and was later found to have a portion of the mass in her renal collecting system.

CASE INFORMATION

A 46-year-old female with no pertinent past medical history presented to the emergency department with fever and worsening left lower quadrant (LLQ) abdominal pain. Physical exam showed LLQ tenderness and guarding, 39.2 °C fever, and mild tachycardia. A CT Abdomen/Pelvis with IV Contrast was ordered, showing trace pelvic free fluid, left retroperitoneal/pelvic varicosities, and a 10.9 by 8.2 cm heterogeneously enhancing left renal mass containing fat compatible with AML. Urology consult suggested high bleeding risk given the size. The patient was admitted and treated with antibiotics. After discharge, the decision was made to pursue embolization as definitive treatment. Approximately 15 cc of a 7:3 EtOH to lipiodol mixture was injected proximal to tortuous arterial vasculature supplying the AML. Post-procedure CT for new symptoms showed a large retroperitoneal hematoma surrounding the left lower pole AML, which required transfusion. CTA further demonstrated persistent arterial phase blood flow in the superior aspect of the mass. Lateral and medial left lower pole renal artery branches were successfully embolized using n-BCA glue. The remainder of the patient's post-operative course was largely unremarkable. Approximately 8 months later, the patient presented to the ED with a recurrence of her left flank pain, with tenderness noted on physical exam. CT Abdomen/Pelvis with IV Contrast showed a small fat density within the left ureter and mild hydronephrosis, believed to be obstruction secondary to fat from the inferior pole AML sloughing off into the collecting system. The patient excreted the fat before further follow-up, noting an "oily" appearance to her urine.

DISCUSSION

AML embolization is a highly effective procedure with a low major complication rate, though minor complications frequently occur. The most common minor complication is post-embolization syndrome. While definitions of this syndrome vary, hallmarks include fever, pain, nausea, and vomiting following the procedure. However, AML sloughing into the renal collecting system is incredibly rare, with seemingly only three cases of lipiduria following the procedure being published. These cases agree that tissue disruption during the embolization procedure is potentially contributory, and all of the cases involved an AML of 10 cm or greater. This case appears to be consistent with that assessment, though current evidence is far from conclusive.

CONCLUSION

Although minor complications are common, lipiduria is not typically seen following AML embolization. This may be due to underreporting by patients, especially given that the fat can be passed with urination. However, more cases are needed to truly gain an understanding of this rare complication.

Student Perceptions of Critical Elements in the Proficiency Enhancement Program (PEP)

Investigator: Jillian Gallardo, B.S.
Mentor: Julie Kerry, Ph.D.
Co-Authors(s):
Natascha Heise, Macon & Joan Brock Virginia Health Sciences Eastern Virginia Medical School
Laurie Wellman, Macon & Joan Brock Virginia Health Sciences Eastern Virginia Medical School
Department(s): Biomedical and Translational Sciences
Poster #: 14B

INTRODUCTION

Condensed preclinical timelines in medical education create high workload, necessitating efficient, active learning strategies to maximize knowledge retention and long-term understanding. To address these concerns, PEP was developed utilizing evidence-based scaffolding, from the "Make it Stick" cognitive framework. PEP incorporates weekly faculty led supplemental sessions featuring open-ended practice questions emphasizing peer-to-peer instruction. Prior data showed high voluntary student participation, with 92.9% (26/28 students) of Medical Masters (MM) and 86% (130/151 students) of Medical Doctor (MD) students enrolled. Because broad meta-analytic data previously established a positive correlation between high engagement and academic success, PEP's high participation shows significant academic promise. However, less is known about which specific elements drive engagement. This study investigates which elements PEP students identify as most critical to their academic performance.

METHODS

A mixed-methods study evaluated student perceptions of PEP. An attendee feedback survey (27.6% response rate) underwent quantitative and qualitative analyses. Institutional course evaluation comments including "PEP" were also extracted. Qualitative data were coded using an inductive and deductive approach using a framework encompassing eight core domains from the "Make it Stick" principles: effort, retrieval practice, interleaving, peer-to-peer learning, reflection, growth mindset, learning tools, and psychological safety.

RESULTS

Analysis of PEP course evaluations and survey revealed that among the evaluated metrics, retrieval practice (n=4.72/5.0) and creating a safe space (n=4.20/5.0) emerged as the most critical elements, receiving the highest frequency of "extremely important" designations. Peer-to-peer learning (n=4.12/5), reflection (n=4.17/5), and interleaving (n=4.17/5) were rated as highly or moderately important. Furthermore, most respondents agreed that PEP sessions provided a collaborative and supportive learning environment (4.79/5), using "safe space" and "inclusive" in comments and strongly agreed that the program successfully encouraged higher-order thinking (n =4.74/5) using coding such as "integrate material" and "apply knowledge".

CONCLUSION

PEP drives high voluntary engagement by reducing the cognitive load of condensed learning timelines through retrieval, fostering higher-order thinking within a collaborative, psychologically safe space. Unboxing student preferences provides actionable insights for accelerated medical curriculum design. A future longitudinal study is planned to further explore these findings and objectively evaluate PEP participation on academic outcomes.

Validating a prognostic biomarker, SIAHHigh/Low , a downstream gatekeeper of TNBC-driven EGFR/RAS pathway activation to risk stratify TNBC patients in a Sentara/VOA/EVMS clinical cohort

Investigator: Hailey M. Gauck, B.S.
Mentor: Amy H. Tang, Ph.D.
Co-Authors(s):
Mark Matta, Macon & Joan Brock Virginia Health Sciences Eastern Virginia Medical School
Zach Bouker, Macon & Joan Brock Virginia Health Sciences Eastern Virginia Medical School
Claire Piatak, Macon & Joan Brock Virginia Health Sciences Eastern Virginia Medical School
Taylor Drake, Macon & Joan Brock Virginia Health Sciences Eastern Virginia Medical School
Billur Samli, Sentara
Janet Winston, Sentara
Rick Jansen, Mayo Clinic
Michael Danso, Sentara
Richard Hoefer, Sentara
Amy Tang, Old Dominion University
Department(s): Biomedical and Translatioal Sciences, Microbiology and Molecular Cell Bio
Poster #: 23B

BACKGROUND

Breast cancer is the 2nd leading cause of cancer death among women in the United States. Triple-negative breast cancer (TNBC) accounts for 15-20% of all breast cancers. TNBC has 40-50% relapse and 22% survival rates. With extensive genetic diversity, tumor heterogeneity, and genomic instability, many similarly treated TNBC patients with identical clinicopathological characteristics (TNM/RCB) experience treatment disparity and disparate survival. Current methods fall short in predicting relapse/resistance/survival with high accuracy. Seven in Absentia Homologue (SIAH) is an evolutionarily highly conserved RING-domain E3 ligase that is the most downstream signaling gatekeeper of a major tumor-driving EGFR/RAS/RAF/MEK/ERK pathway, whose activation/inactivation was reflected in SIAHhigh/low expression. We propose that SIAH is a new prognostic biomarker for patient risk stratification and relapse/survival prediction in TNBC post-neoadjuvant chemotherapy (NACT).

METHOD

A retrospective chart review was conducted using Sentara/EPIC and VOA iKnowMedicine portals to update clinical data in a large cohort of 553 TNBC patients. The IHC staining of SIAH, Ki67, EGFR, and H&E was performed in primary and residual tumors. Representative IHC images were captured. Statistical analyses, including Kaplan-Meier survival curves, were conducted to determine whether SIAHHigh/Low expression pre- and post-NACT, and NACT-induced reduction of SIAH expression in pair-matched TNBC tumor specimens is prognostic of relapse/chemoresistance/survival in high-risk TNBC.

RESULTS

Among 553 TNBC patients, 180 high-risk patients received NACT. 51 of them have pair-matched primary and residual tumor biospecimens. 41 of them had Grade 3 tumors, and 21 of them had Stage II diseases. The statistical analyses demonstrated that high SIAH expression in residual tumors reflects persistent EGFR/K-RAS/SIAH pathway activation following ineffective NACT, predicting tumor relapse and poor survival. Conversely, no or low SIAH expression in residual tumors reflects EGFR/K-RAS/SIAH pathway shutdown by effective NACT, predicting tumor remission and improved survival. ($p<0.05$)

CONCLUSION

High SIAH expression in residual tumors post-NACT was associated with TNBC malignancy and poor survival. We aim to develop a SIAH-centered biomarker panel to risk-stratify TNBC patients and predict relapse/resistance/survival at 1st-line neoadjuvant settings. This project aims to delineate the molecular underpinnings of the EGFR/RAS/SIAH pathway-driven treatment disparity and the persistently high mortality in TNBC in Virginia.

Assessing healthcare utilization and primary care follow-up among patients attending an integrated primary care clinic as part of pregnancy and postpartum care

Investigator: Angela Goyal, B.S.
Mentor: Michael Kopec, MD
Co-Authors(s):
Alison Patev, Sentara
Thien-Phuoc (Janesah) Ngo, Macon & Joan Brock Virginia Health Sciences Eastern Virginia Medical School
Department(s): Family Medicine
Poster #: 24B

INTRODUCTION

Despite advances in obstetric care, maternal morbidity and mortality remain significant public health concerns in the US. Approximately 50% of pregnancy-related deaths occur after the traditional 42-day postpartum period after patients transition out of obstetric care, creating a "postpartum cliff." Fragmented communication between obstetric and primary care providers and underemphasis on longitudinal care may delay management of chronic medical conditions that persist beyond pregnancy. To address this gap, an integrated Family Medicine (FM) clinic was established within the EVMS MFM practice in January 2025 and expanded to General Obstetrics in February 2026. This study evaluated whether the integrated clinic improved postpartum continuity of care by increasing follow-up attendance.

METHODS

We conducted a retrospective cohort study of adults receiving prenatal and postpartum care within the EVMS OB-GYN Department. The sample included 29 patients who attended at least one integrated FM clinic visit between June 2025 and April 2026, compared with 12 eligible patients receiving standard obstetric care. Demographics, attendance at a postpartum PCP visit, and number of postpartum PCP visits were obtained through retrospective chart review.

RESULTS

The mean age at most recent delivery was 30.1 years (SD = 5.9), with delivery occurring at a mean gestational age of 36.3 weeks (SD = 4.4). Nineteen patients (46.3%) identified as White and 20 (48.8%) as Black. Most patients (75.6%) had Medicaid, while 19.5% had Tricare and 4.9% had another form of insurance or no insurance. Among patients seen in the integrated clinic, 20 of 29 (69.0%) had at least one postpartum PCP visit, compared with 3 of 12 (25.0%) patients in the comparator group. Fisher's Exact test demonstrated a significant difference in attendance at any postpartum PCP visit between groups ($p = .03$), with patients in the integrated clinic more likely to have at least one postpartum visit. Mann-Whitney U analysis also demonstrated a significant difference in the number of postpartum PCP visits between groups ($p = .04$), with the integrated clinic group having more visits.

CONCLUSION

Patients receiving care through the integrated FM clinic had significantly greater postpartum PCP follow-up than patients receiving standard obstetric care, both in likelihood of attending a postpartum visit and in number of visits. These findings suggest that embedding primary care within obstetric practice may help address barriers to postpartum continuity and facilitate transition to longitudinal care. Although the small sample size and retrospective design limit our conclusions, integrated obstetric-primary care models may represent a promising strategy to reduce fragmentation of care and support ongoing maternal health after pregnancy.

Genomic characterization of intrahepatic and extrahepatic cholangiocarcinoma identifies distinct and unique molecular signatures

Investigator: Austin Grove, B.S.
Mentor: Winifred Lo, MD
Co-Authors(s):
Luisel Ricks-Santi, Macon & Joan Brock Virginia Health Sciences Eastern Virginia Medical School
Kylie Lopez, Macon & Joan Brock Virginia Health Sciences Eastern Virginia Medical School
Department(s): Surgery
Poster #: 08B

INTRODUCTION

Cholangiocarcinomas (CCA) are epithelial malignancies categorized as intrahepatic cholangiocarcinoma (iCCA) or extrahepatic cholangiocarcinoma (eCCA). 20-30% of iCCA and more than 65% of eCCA are unresectable. Of the resectable tumors, 5-year survival is ~30% for both cancers. Currently, they are managed using the same treatment algorithm, but studies show different possible gene targets. In this study, we aim to identify clinical and molecular differences between iCCA and eCCA to better differentiate tumor subtypes and potential treatment targets.

METHODS

The Cancer Genome Atlas (TCGA) cholangiocarcinoma dataset was accessed through cBioPortal and cases were classified as iCCA (n=384) or eCCA (n=420). Clinicopathologic characteristics, including tumor stage, grade, recurrence, and overall survival, and genomic characteristics, including tumor mutational burden (TMB), fraction of the genome altered (FGA), and gene-specific alterations, were compared between groups using the cBioPortal analytical platform. Statistical analyses were performed to evaluate differences between iCCA and eCCA. A two-sided P value of <0.05 was considered significant.

RESULTS

Compared with eCCA, iCCA was characterized by larger mean tumor size (p=<10-10), higher mean FGA ($p=9.807\times10^{-6}$), and higher mean BMI (p=0.002), as well as more frequent stage IV disease at diagnosis (p=0.0397), poorer tumor differentiation (p=4.239x10-3), multifocal disease (p=<10-10), and underlying cirrhosis (p=4.8x10-4). Compared with iCCA, eCCA had a higher TMB ($p=3.372\times10^{-4}$). Genomic alterations enriched in iCCA include BICC1, IDH1, BAP1, IDH2, FGFR2, NRBF2, and FOXP1. Those enriched in eCCA include TP53, SMAD4, KRAS, NSD2, BRCA2, STK11, and AMER1. Survival was not different between iCCA and eCCA.

DISCUSSION

iCCA is harder to detect, thus allowing time to dedifferentiate and progress in stage, causing multifocal disease and increased FGA. Genes associated with iCCA and eCCA are mutually exclusive. Currently, three FDA-approved, targeted therapies for CCA act on FGFR2 and IDH1, which are associated with iCCA. No therapy acts on genes associated with eCCA. If targeted therapies progress, genomic diagnosis of CCA could lead to better patient outcomes. iCCA and eCCA are clinically and genomically different cancers. Their mutually exclusive genes can be used diagnostically, improving treatment for patients by using potential targeted therapies. Moving forward, mutant-vs-wild type gene analysis will cross-examine mutations with clinical outcomes.

Changing Practice Trends in Antibiotic Prophylaxis and Voiding Cystourethrogram Utilization for Prenatal Hydronephrosis: A 17-Year Multicenter Experience

Investigator: Elizabeth Harvie, B.A.
Mentor: Sarah H. Williamson, MD
Co-Authors(s):
Jasilyn Wray-Jordan, MPH, Children's Hospital of the King's Daughters
Malea Drummond, DNP, Children's Hospital of the King's Daughters
Kevin Alterman, Macon & Joan Brock Virginia Health Sciences Eastern Virginia Medical School
Amira Elzarea, Macon & Joan Brock Virginia Health Sciences Eastern Virginia Medical School
Phillip Poppas, Macon & Joan Brock Virginia Health Sciences Eastern Virginia Medical School
Janelle Fox, MD, Children's Hospital of the King's Daughters
Peter Stuhldreher, MD, Children's Hospital of the King's Daughters
Louis Wojcik, MD, Children's Hospital of the King's Daughters
Department(s): Pediatrics Urology
Poster #: 06A

INTRODUCTION
The utility of continuous antibiotic prophylaxis (CAP) and voiding cystourethrograms (VCUG) in prenatal hydronephrosis is highly debated. Using data from a multicenter cohort, we trended CAP prescription, VCUG utilization, and urinary tract infection (UTI) rates across hydronephrosis subgroups.

METHODS
A multicenter cohort data analysis was performed using patients with prenatal hydronephrosis and ≥3 months of urology follow-up. Patients were stratified into groups: isolated hydronephrosis (n=1,636) and hydroureteronephrosis (≥7mm ureteral dilation (n=308)). CAP was defined as any prescription during the follow-up period. Confirmed UTI required fever, pyuria, a single-organism positive culture from catheterization or clean-catch specimen, and antibiotic treatment. Temporal trends were analyzed by year of first visit across six cohorts spanning 2007-2024.

RESULTS
1,944 patients met inclusion criteria. Among patients with isolated hydronephrosis, CAP prescription ($p<0.0001$) and VCUG utilization ($p<0.0001$) showed significantly decreasing trends over the study period, while UTI rates remained stable (range 1.6–4.5%; $p=0.24$).

In contrast, CAP rates ($p=0.52$) and VCUG utilization ($p=0.46$) remained stable over time in hydroureteronephrosis patients. UTI rates were similarly unchanged ($p=0.21$), though this group's UTI rate was substantially higher (overall 14.6%).

CONCLUSION
Since 2007, CAP prescription and VCUG utilization have decreased significantly in patients with isolated hydronephrosis without an increase in confirmed UTI rates, supporting the safety of conservative management in this population. Meanwhile, hydroureteronephrosis management remained consistent, reflecting higher infection risk in this group. These findings support reduction of antibiotic prophylaxis and invasive imaging in isolated hydronephrosis with continued need for surveillance in hydroureteronephrosis.

Primary and Secondary Inferior Vena Cava (IVC) Masses: Multimodality Imaging Review

Investigator: Eric C. Hayes, B.S.
Mentor: Swachchhanda Songmen, MD
Co-Authors(s):
Virang Kumar, Macon & Joan Brock Virginia Health Sciences Eastern Virginia Medical School
Department(s): Radiology
Poster #: 29A

INTRODUCTION
True masses of the inferior vena cava (IVC) are uncommon and present a diagnostic challenge, even to experienced clinicians. IVC pathology spans a spectrum of primary neoplastic, secondary neoplastic, and non-neoplastic processes, including frequent pseudo-lesions posed by inconsistent delayed contrast imaging. As clinical presentation is often non-specific and symptom severity more dependent on mass location within the IVC than disease severity, the recognition of sometimes subtle imaging differences plays a key role in narrowing differentials, timely diagnosis, and appropriate treatment of patients. In this literature review, we will review how to approach imaging of IVC masses based on their location/features, discuss imaging techniques, and mass differentiation based on imaging features.

DISCUSSION
Primary IVC masses are exceedingly rare in comparison to secondary involvement as part of caval extension or thrombus formation from neighboring abdominal malignancies. Additionally, non-neoplastic processes—including postsurgical changes in transplant patients, IVC stents, and fistula formation—are common mimics of neoplastic pathology. Differentiating these pathologies is critical, as definitive diagnosis of suspected neoplastic IVC masses often requires invasive tissue biopsies. Accurate diagnosis is contingent upon a proper understanding of IVC anatomy, selection of proper imaging modalities, and imaging characteristics of respective masses. Patient prognosis is often a function of mass location, where earlier mass effect and/or compressive symptoms can lead to earlier presentation to medical attention. Unfortunately, if a mass occurs in a location that does not produce more significant symptoms, identification may be largely incidental and risks worse outcomes. Imaging techniques can vary based on patient age, initial versus supplemental study, and level of concern for malignant processes. While ultrasound is often the initial modality employed, especially in children, contrast-enhanced computed tomography (CECT) generally serves as the most commonly utilized technique. Magnetic resonance imaging (MRI), especially magnetic resonance venography (MRV), offers superior reliability in the detection and delineation of tumor thrombus extent when compared with CT. Multimodal imaging, including ultrasound with doppler, CECT, and MRI provide complimentary information regarding continuity with adjacent organs, vascular invasion, enhancement pattern, and possible metastatic activity to assist in distinguishing pathology. Important distinguishing characteristics for intraluminal IVC masses are an expansile appearance, positive "embedded sign," and "imperceptible caval lumen sign."

CONCLUSION
IVC masses are rare, with symptoms often dependent on their location, and require knowledge about their anatomical relationships, imaging features, and common presentations to accurately diagnose them. The utilization of multimodal imagining techniques enables clinicians to appropriately differentiate primary, secondary, and non-neoplastic masses, thus enabling accurate diagnosis and suitable therapeutic interventions.

Occipital condyle fracture with hypoglossal canal involvement presenting as delayed dysarthria after e-bike trauma, a case report

Investigator: Lauren Hill, B.S.
Mentor: Rhorie Kerr, MD
Co-Authors(s):
Jason Acheampong, Macon & Joan Brock Virginia Health Sciences Eastern Virginia Medical School
Department(s): Otolaryngology
Poster #: 13A

INTRODUCTION
Occipital condyle fractures are rare injuries resulting from high-energy blunt trauma. Due to their anatomic relationship to the hypoglossal canal, injury to the occipital condyle can result in hypoglossal nerve (CN XII) injury. This case report describes a rare case of delayed hypoglossal nerve palsy associated with an occipital condyle fracture involving the hypoglossal canal following electric bicycle trauma.

CASE INFORMATION
A 38-year-old man presented following an electric bicycle accident with multiple facial and skull base fractures, including a nondisplaced left occipital condyle fracture extending into the hypoglossal canal. Initial examination by the otolaryngology service demonstrated midline tongue positioning with intact mobility. The occipital condyle fracture was managed nonoperatively with rigid cervical immobilization.

DISCUSSION
Twelve days after the injury, the patient returned for otolaryngology follow-up and reported new-onset dysarthria characterized by a lisp that had begun to improve. Examination demonstrated leftward deviation of the tongue on protrusion, decreased leftward tongue mobility, preserved rightward mobility, and mild left tongue fasciculations, consistent with a partial left hypoglossal nerve palsy. The delayed development of ipsilateral tongue weakness in the setting of fracture extension into the hypoglossal canal was consistent with delayed traumatic hypoglossal neuropathy. The patient reported poor compliance with cervical immobilization.

CONCLUSION
Hypoglossal nerve injury is a rare complication of occipital condyle fractures involving the hypoglossal canal and may present in a delayed fashion despite an initially normal cranial nerve examination. Serial cranial nerve examinations and careful evaluation of the hypoglossal canal on imaging are important following skull base trauma. Otolaryngology follow-up may facilitate recognition of subtle delayed neurologic deficits and allow for appropriate counseling and rehabilitation.

Exposure to Galactic Cosmic Rays Results in Damage of Ovarian Follicles and Loss of Corpora Lutea Development

Investigator: Gavin C. Hughes, B.S.
Mentor: Diane M. Duffy, Ph.D.
Co-Authors(s):
Anyah Skipwith, Macon & Joan Brock Virginia Health Sciences Eastern Virginia Medical School
Mitch Warren, Macon & Joan Brock Virginia Health Sciences Eastern Virginia Medical School
Rebecca Duncan, Macon & Joan Brock Virginia Health Sciences Eastern Virginia Medical School
James Vettichira, Macon & Joan Brock Virginia Health Sciences Eastern Virginia Medical School
Richard Britten, Macon & Joan Brock Virginia Health Sciences Eastern Virginia Medical School
Department(s): Biomedical and Translational Sciences
Poster #: 09B

INTRODUCTION

NASA's planned Mars missions will result in astronaut exposure to galactic cosmic rays (GCR) on both the outbound and return journeys. GCR may harm the female reproductive system which is uniquely susceptible to damage. Damage to the ovary may reduce fertility and induce early menopause, increasing risk for cardiovascular disease, osteoporosis, and early death for female astronauts. Altered ovarian function may also impact decision-making by female astronauts. We hypothesize that GCR will harm rat ovaries leading to reduced corpora lutea development, follicle loss, and follicle damage.

METHODS

Female Wistar rats were exposed to no irradiation (sham) or exposed to 20 cGy of simulated GCR (G/G) delivered in two doses separated by 6 months. At 4 months after the last exposure, rats were euthanized in diestrus. Ovaries from sham and G/G exposed rats were embedded in paraffin, sectioned, and every 5th was stained with H&E. Corpora lutea and follicles were manually counted. Corpora lutea counts was assessed by Mann-Whitney U Test. Follicles were categorized as primordial, primary, secondary, or antral based on surrounding granulosa cells and compared using one tailed t-test. Pyknosis and mitosis were assessed by counting pyknotic and mitotic nuclei in secondary and antral follicles and compared using one tailed t-test.

RESULTS

While 75% of sham rats showed signs of active ovulation (containing >11 corpora lutea), only 17% of G/G exposed ovaries had comparable corpora luteal numbers, with the rest containing no corpora lutea. An inter-group comparison revealed significantly fewer corpora lutea within the ovaries of GCR exposed rats than in those from sham rats ($p=0.046$). GCR exposure reduced the number of secondary follicles ($p=0.048$), but not follicles at other stages ($p>0.05$). There was a significant increase in pyknotic nuclei ($p=0.028$) and significant decrease in mitotic nuclei ($p=0.028$) in antral follicles exposed to GCR. These rats were part of a study that established the impact of GCR exposure on decision making (attentional set-shifting, ATSET) performance. During the compound discrimination reversal (CDR) stage of that task, rats without corpora lutea took significantly ($P=0.026$) longer to make decisions when compared to rats with corpora lutea.

CONCLUSION

Our results showed that low dose GCR exposure resulted in decreased corpora luteal, indicating that GCR exposed rats were not actively ovulating. This is consistent with a disruption of LH signaling following GCR exposure, suggesting that the hypothalamus may be radiosensitive. Our results also showed a significant loss in follicles at the secondary stage along with an increase in pyknosis and decrease in mitosis at the antral stage, consistent with radiation-induced follicle damage. There was a correlation between the ovulation status (presence or absence of corpora lutea) and processing speed in the CDR task (ATSET). Overall, space radiation is damaging to the structure of the ovary, with likely consequences for both ovarian function and executive performance. Should similar effects occur in humans, GCR exposure during the mission to Mars could lead to early menopause in female astronauts, and the associated clinical conditions.

Shock Anxiety Following ICD Electrical Storm in Arrhythmogenic Right Ventricular Dysplasia/ Cardiomyopathy: A Case Report

Investigator: Emily Inzer, B.S.
Mentor: David Spiegel, MD
Co-Authors(s):
None listed.
Department(s): Psychiatry and Behavioral Sciences
Poster #: 37B

INTRODUCTION

Arrhythmogenic right ventricular dysplasia/cardiomyopathy (ARVD/C) is an inherited cardiomyopathy characterized by progressive fibrofatty replacement of the right ventricular myocardium, predisposing patients to ventricular arrhythmias, heart failure, and sudden cardiac death. Implantable cardioverter-defibrillators (ICDs) are implanted for prevention of sustained ventricular arrhythmias and sudden cardiac death, often around age 40. Early implantation exposes patients to decades of ICD therapy and psychological burden, yet evidence guiding management of shock anxiety in ARVD/C remains limited.

CASE INFORMATION

We present a patient with ARVD/C who developed severe shock anxiety and phobic avoidance following an ICD electrical storm after 10 years of complication-free device function. Three months after hospitalization for five high-rate ventricular arrhythmias requiring ICD therapy, she was referred to psychiatry for inability to leave home because of fear of future ICD shocks. She had no prior psychiatric or substance/alcohol use history. Her symptoms progressed to panic attacks, hypervigilance, and avoidance of cardiologist-recommended physical activity.

DISCUSSION

Evaluation for reversible precipitants of electrical storm and ICD malfunction was unrevealing except for metoprolol nonadherence. Electrophysiology reprogrammed the ICD to reduce future shock episodes. Despite cardiac management, the patient developed disabling shock anxiety with panic, hypervigilance, and phobic avoidance. Given her marked functional impairment and limited evidence for pharmacologic treatment of shock anxiety, CBT was selected based on evidence supporting its use in ICD recipients. Treatment incorporated ICD-specific psychoeducation, cognitive restructuring, relaxation techniques, development of a shock-management plan, and systematic desensitization to feared activities. Her FSAS score decreased from 33 to 14, with return to occupational, social, and recreational activities.

CONCLUSION

Shock anxiety affects 20%–84% of ICD recipients, and experiencing more than five lifetime ICD shocks increases anxiety risk. This case highlights the importance of recognizing the psychiatric sequelae of ICD therapy in ARVD/C and supports CBT as a promising nonpharmacologic intervention. Early collaboration between cardiology and psychiatry may improve outcomes, although larger prospective studies are warranted.

Project Success: A Qualitative Investigation of Factors Influencing Families of Late Talkers to Pursue Communication Evaluations Before Age Three

Investigator: Kirsten Johnson, M.S.
Mentor: Danika Pfeiffer, Ph.D., CCC-SLP
Co-Authors(s):
None listed.
Department(s): Speech-Language Pathology
Poster #: 03B

INTRODUCTION

Late-talking, defined as fewer than 50 spontaneous words and no two-word combinations at 24 months, affects between 10% and 20% of toddlers. Early intervention is important for supporting children's language development and preventing persistent challenges. While there are several barriers reported in the literature related to pursuing speech/language evaluations before age three, there is currently limited literature focused on success stories. The purpose of this study is to identify factors that helped families successfully receive a speech/language evaluation before the age of 3.

METHODS

A purposive sampling strategy was used to recruit 7 English-speaking caregivers for the first of two focus groups. The first virtual focus group was conducted using a semi-structured protocol and audio-recorded and transcribed using Zoom recording technology. The data are currently being consensus coded by trained coders using an inductive conventional content analysis approach.

RESULTS

As of September 2026, coders have coded approximately 50% of the first English focus group and 100 % is expected to be completed by Research Day. To date, a codebook has been established with 72 codes for the English focus group. Preliminary analysis has identified recurring topics discussed by caregivers who navigated the speech/language evaluation process. These topics include: (a) caregivers' uncertainty regarding the evaluation process, prompting them to take initiative and seek out information from a variety of resources; (b) how caregivers' religious and geographic communities perceived speech/language delays; and (c) the behaviors their child displayed that made the caregiver recognize their child was having difficulty with communication and how the caregiver navigated these concerns. Ongoing analysis will continue to refine the initial codes to identify overarching categories capturing the factors that impacted caregivers' success with receiving a speech/language evaluation early for their child.

CONCLUSION

Findings are expected to improve understanding of caregivers' experiences navigating the speech/language evaluation process by informing development of a theoretical framework summarizing factors that influence caregivers' success in obtaining an early speech/language evaluation. Insights from this study will be used to inform the design of supports to help more families obtain an early speech/language evaluation by identifying key barriers, resources, and/or gaps in information.

Oral Nicotine Pouches, Other Substance Infractions, and Educational Responses in K-12 School Settings

Investigator: Ria Kapoor, B.S.
Mentor: Paul T. Harrell, Ph.D.
Co-Authors(s):
Ann Edwards, Macon & Joan Brock Virginia Health Sciences Eastern Virginia Medical School
Kelli England, Macon & Joan Brock Virginia Health Sciences Eastern Virginia Medical School
Amy Paulson, Macon & Joan Brock Virginia Health Sciences Eastern Virginia Medical School
Hannah Savage, Macon & Joan Brock Virginia Health Sciences Eastern Virginia Medical School
Erica Mcdonald, Macon & Joan Brock Virginia Health Sciences Eastern Virginia Medical School
Department(s): Pediatrics
Poster #: 06B

INTRODUCTION

K-12 schools are experiencing changes in the substance use landscape. In particular, oral nicotine pouches (ONP) are increasingly used by youth. Nicotine exposure during adolescence can contribute to dependence and continued tobacco use. Limited information is available on the presence of ONP-related infractions in K-12 schools or how schools are responding to student use. Understanding how emerging nicotine products are appearing in school settings may help inform more effective prevention and response strategies. This study aimed to characterize nicotine-related infractions across Virginia K-12 school settings and evaluate the school responses being used, including their perceived effectiveness.

METHODS

Educational professionals were recruited across Virginia using Qualtrics with electronic gift cards provided to validated work e-mail addresses. Participants (N=202, M age=45.2, SD=9.7, 69.4% female, 60.2% White, 26.7% African American) included Vice Principals/Deans (35.4%), Guidance Counselors (24.3%), Principals/Headmasters (17.0%), and other school personnel (23.3%); experience in educational system averaged 18 (SD=9.2) years. Survey assessed school setting, substances implicated in infractions, responses to use, and perceived effectiveness of responses (rated from 0-100). Among respondents reporting school setting, 35.5% represented rural schools, 36.1% suburban schools, and 28.4% urban schools. Logistic regression and paired sample t-tests were used to compare responses.

RESULTS

Vaped nicotine was commonly reported across all three school settings, ranging from 84.8% of suburban schools to 78.8% of urban schools. ONP infractions were less common overall, but more common in rural (20.8%) than non-rural (10.1%) settings, OR: 2.34, 95% CI: 1.06-5.18. In contrast, cigarette infractions were highest in urban schools (17.3%), followed by rural (7.7%) and suburban (6.1%) schools. The most endorsed disciplinary responses were out-of-school suspension (90.8% endorsement; M=55.9 perceived effectiveness, SD=29.9), parent conferences or notification (88.3%; M=56.7, SD=26.5), and in-school suspension (77.7% M=46.2, SD=25.3). Referral for treatment (47.6%; M = 58.5, SD=30.6) and diversion programs (29.6%; M = 59.7, SD=27.8) were less used but perceived as more effective than these disciplinary responses. Among a subsample that reported both in-school suspensions and diversion programs (n=51), diversion programs were perceived as significantly more effective, M=62.0, SD=27.9 vs. M=45.9, SD=28.2, $p < .001$.

CONCLUSION

Nicotine-related infractions remain common across Virginia K-12 schools, with vaping reported most frequently. ONP infractions are less common, occurring primarily in rural settings. Cigarette-related infractions were highest in urban settings. Educational responses are primarily punitive despite perceptions that supportive responses would be more effective. These findings suggest a mismatch between current practice and perceived effectiveness, and support incorporation of treatment-oriented approaches as nicotine products evolve.

Radiographic Patterns of Methotrexate Neurotoxicity and Mechanistic Correlates

Investigator: Ria Kapoor, B.S.
Mentor: Alberto E. Musto, MD, Ph.D.
Co-Authors(s):
None listed.
Department(s): Biomedical and Translational Science
Poster #: 27A

INTRODUCTION

Methotrexate (MTX) is widely used in the treatment of hematologic malignancies and can produce acute, subacute, and chronic neurotoxicity following systemic or intrathecal administration. Clinical manifestations include stroke-like deficits, seizures, encephalopathy, myelopathy, leukoencephalopathy, and posterior reversible encephalopathy syndrome (PRES). Although characteristic magnetic resonance imaging (MRI) abnormalities have been described, the basis for their recurrent localization to specific neuroanatomic regions remains incompletely understood. Existing literature has largely characterized MTX neurotoxicity by clinical syndrome, timing, or imaging appearance, while comparatively less attention has been directed toward why particular cerebral regions appear repeatedly susceptible. This study aimed to characterize recurring MRI phenotypes of MTX-associated neurotoxicity and develop an integrated mechanistic framework linking these radiographic patterns to regional neuroanatomic vulnerability.

DISCUSSION

Published case reports, case series, imaging studies, and mechanistic literature related to MTX-associated neurotoxicity were reviewed. Representative MRI cases were selected to illustrate recurring patterns of lesion distribution and imaging characteristics, and three recurring radiographic phenotypes were identified: diffusion-restrictive deep white-matter injury, fluid-attenuated inversion recovery (FLAIR)-dominant leukoencephalopathy, and posterior cortical/subcortical injury consistent with PRES. Mechanistic literature was then examined for regional factors that might account for these distributions, including cerebral perfusion and medullary arterial anatomy, oligodendrocyte and myelin biology, folate and homocysteine metabolism, N-methyl-D-aspartate (NMDA) receptor-mediated excitotoxicity, adenosine-dependent vascular regulation, and deep medullary venous drainage. These findings were integrated into a proposed model of regional susceptibility. The first phenotype was an acute diffusion-restrictive deep white-matter pattern involving the centrum semiovale, corona radiata, and adjacent deep white matter, with minimal or absent early FLAIR abnormality. This pattern is proposed to reflect regional perfusion vulnerability related to low baseline white-matter blood flow and distal medullary arterial supply, predisposing these territories to cytotoxic injury. The second phenotype was FLAIR-dominant leukoencephalopathy involving periventricular and deep white matter, with extension into the centrum semiovale, corona radiata, and corpus callosum. This distribution is consistent with increased susceptibility of heavily myelinated, oligodendrocyte-rich regions to sustained metabolic and cellular injury. Deep medullary venous anatomy may further increase periventricular vulnerability by limiting interstitial clearance and prolonging local exposure to homocysteine and adenosine. The third phenotype was a posterior cortical/subcortical pattern consistent with PRES, characterized by bilateral parieto-occipital involvement and vasogenic edema. This pattern may reflect MTX-associated increases in adenosine with disruption of cerebral vasodilation and autoregulatory control, promoting vasogenic edema in posterior regions. Across all three phenotypes, homocysteine-mediated NMDA receptor excitotoxicity may act as a shared molecular stressor.

CONCLUSION

MTX neurotoxicity demonstrates recurring rather than random MRI distributions. The observed phenotypes support a model in which systemic metabolic and vasoregulatory injury interacts with region-specific vascular, cellular, molecular, and venous characteristics. This framework links established MTX-associated biochemical disturbances with the neuroanatomic distribution of injury and provides an explanation for the heterogeneous but reproducible MRI manifestations of MTX neurotoxicity. Improved understanding of the mechanisms underlying MTX neurotoxicity may help identify strategies to prevent neurologic complications and guide management when MTX remains clinically necessary.

Papaverine-Soaked Surgicel as a Topical Adjunct for Vasospasm in Vascular Anastomosis: A case series

Investigator: Alden I. Kaufman, M.S.
Mentor: Amber Carrier, MD, Ph.D.
Co-Authors(s):
Alyssa Reese, Macon & Joan Brock Virginia Health Sciences Eastern Virginia Medical School
Department(s): Transplant surgery
Poster #: 30A

INTRODUCTION

Intraoperative vasospasm is a challenge in large-vessel and microsurgical anastomosis alike. In response to mechanical manipulation, dissection, and temperature changes, blood vessels respond through calcium channel-mediated smooth muscle contraction, resulting in vasospasm and increased risk of thrombosis. Vasodilators have shown promising effects in reducing intraoperative vasospasm.

Papaverine is one vasodilator that has shown promising efficacy in reducing vasospasm. Papaverine is an opium alkaloid that acts as a phosphodiesterase inhibitor and calcium channel blocker to reverse vasospasm. Typically, vessels are directly irrigated with the drug via a syringe or soaked sponge; however, limited contact with the vessel may theoretically reduce the drug's efficacy in sustaining vasospasm reduction over time.

To address the vessel contact time limitation, alternative vasodilator delivery mechanisms have been tested, including electrospun polymer fibers, fibrin glue, thermosensitive hydrogels, and polymer membranes, mostly in animal models. We propose that Surgicel, as a hemostatic, biodegradable delivery reservoir, increases papaverine's contact duration and, as a result, its efficacy in reversing vasospasm.

MAIN BODY

Surgicel is a hemostatic, resorbable, woven cellulose mesh, which, upon contact with blood, forms a gel-like matrix serving as a reservoir for liquid. Surgicel is widely available and has been utilized by the authors to prolong papaverine delivery in renal transplant anastomoses. Papaverine is prepared as a dilute solution of 60 mg in 8 mL of intravenous normal saline (7.5 mg/mL). A piece of Surgicel is cut to approximate the vessel diameter and gently wrapped circumferentially around the vessel in the area of the intended arteriotomy or venotomy. Papaverine is applied by syringe directly to the vessel and over the Surgicel wrap before clamping. Following reperfusion and visual resolution of vasospasm, the Surgicel is removed, and the field is irrigated with saline prior to closure, thereby limiting tissue contact time.

Increasing papaverine's local application via Surgicel is not without theoretical risk. An ex vivo study applying papaverine to the outer surface of internal thoracic arteries for 15 to 45 minutes, a route and duration similar to our technique, found impaired endothelial function not explained by acidity alone, while contractile function was preserved. Despite this, topical papaverine remains standard practice at concentrations that have greatly exceeded in-vitro half-maximal inhibitory concentration (IC50) thresholds, including the concentration used here, without a significant pattern of anastomosis or graft failure.

CONCLUSION

Current literature largely focuses on novel extended-delivery systems and comparative in vitro efficacy and toxicity studies. Our technique is an initial step toward evaluating how a short-term drug-carrier delivery method might impact vasospasm before, during, and directly following anastomosis. Because Surgicel and papaverine are each independently approved for clinical use, further study of this technique is highly accessible compared to more novel biomaterials. Studies to prospectively quantify vessel response to this technique and retrospectively assess outcomes in patients who had Surgicel-soaked papaverine versus papaverine irrigation alone are next steps. More broadly, this approach suggests a novel biomaterials opportunity: a hemostatic matrix pre-embedded with a vasodilatory agent, applicable across all vascular anastomoses.

Open Globe Injuries in U.S. Trauma Centers: A 2024 Trauma Quality Program Study

Investigator: Zaid S. Khan, M.S.
Mentor: Albert Y. Cheung, MD
Co-Authors(s):
Zaid Khan, Macon & Joan Brock Virginia Health Sciences Eastern Virginia Medical School
Giovanni DiSandro Jr, Macon & Joan Brock Virginia Health Sciences Eastern Virginia Medical School
Albert Cheung, Virginia Eye Consultants, CVP Physicians
Rebecca Britt, Macon & Joan Brock Virginia Health Sciences Eastern Virginia Medical School
Department(s): Ophthalmology
Poster #: 32B

INTRODUCTION
Open globe injuries require urgent surgical repair. Whether trauma center verification level influences the care pathway has not been characterized using national data.

METHODS
Multinomial logistic regression evaluated care pathways among 2,282 eligible direct arrivals at Level I -III centers, adjusting for demographics, injury severity, and clinical factors. Secondary analyses evaluated globe closure and arrival-to-closure timing. The main outcome measures included on-site definitive surgery (closure or enucleation), transfer without documented on-site definitive surgery, or neither.

RESULTS
Compared with Level I, Level II and III centers had higher adjusted relative risk ratios for transfer versus on-site surgery: 12.96 (95% CI, 9.74 -17.25) and 71.17 (40.81 -124.13), respectively. Adjusted probabilities of on-site surgery were 63.8%, 30.7%, and 10.7% at Levels I, II, and III. Globe-closure odds were lower at Level II (adjusted OR, 0.227; 95% CI, 0.179 -0.286) and Level III (0.045; 0.026 -0.079). Lower closure odds persisted across 14 binary sensitivity analyses while five separate multinomial sensitivity analyses supported the transfer association. Concerning timed direct arrivals and incoming transfers, 92.7% and 95.1%, respectively, underwent closure within 24 hours of reporting-hospital arrival.

CONCLUSION
Care pathways varied substantially by trauma center verification level, consistent with regionalized ophthalmic trauma care.

Photoactivated Chromophore for Keratitis-Corneal Cross-Linking: A Scoping Review & Bibliometric Analysis

Investigator: Zaid S. Khan, M.S.
Mentor: Albert Y. Cheung, MD
Co-Authors(s):
Zaid Khan, Macon & Joan Brock Virginia Health Sciences Eastern Virginia Medical School
Mehron Kouhestani, Macon & Joan Brock Virginia Health Sciences Eastern Virginia Medical School
Giovanni DiSandro Jr., Macon & Joan Brock Virginia Health Sciences Eastern Virginia Medical School
Albert Cheung, Virginia Eye Consultants, CVP Physicians
Department(s): Ophthalmology
Poster #: 32A

INTRODUCTION
Photoactivated Chromophore for Keratitis-Corneal Cross-linking (PACK-CXL) as a topic of research is gaining momentum. We sought to characterize the related scholarly literature utilizing a big-data text-mining approach, identifying gaps in clinical reporting, outcome focus, and therapeutic positioning.

METHODS
A highly sensitive search was performed using the Lens.org scholarly aggregator (encompassing PubMed, Crossref, and OpenAlex). To isolate modern clinical applications, records underwent automated temporal restriction (post-2000) and ophthalmic scope filtering to exclude industrial photochemical noise. Bibliometric visualization was conducted using Python-based natural language processing and VOSviewer. Clinical variables were tagged using a non-deterministic, multi-label text-mining framework to eliminate subjective classification bias.

RESULTS
The search identified 10,352 records; after deduplication and screening, 1,429 records (13.8%) were included in the final analysis. Evaluation of explicit clinical positioning revealed a distinct paradigm shift: comparative framing (n=332; 23.2%) overwhelmingly dominated the literature, far exceeding adjunctive (n=77; 5.4%) or rescue/refractory applications (n=47; 3.3%). Regarding pathogen targets, bacterial keratitis was the most frequently represented etiology (n=352; 24.6%), followed by fungal (n=290; 20.3%) and Acanthamoeba (n=120; 8.4%). Riboflavin/UVA remained the primary explicitly discussed modality (11.1%) compared to Rose Bengal/Green light (3.1%). Abstract-level reporting of clinical outcomes remained structurally focused, with mentions of healing/epithelialization (40.4%) consistently outpacing explicit functional mentions of visual acuity (20.4%).

CONCLUSIONS
The PACK-CXL literature demonstrates exponential growth with a definitive shift toward comparative study framing, possibly signaling a transition from a 'salvage' therapy to standard-of-care evaluation. Regardless, abstract-level reporting remains inconsistent and weighted toward structural endpoints; future work would benefit from standardized reporting of visual acuity, epithelial healing, microbiologic cure, and keratoplasty outcomes.

Igniting Potential: Observations and Insights into High School Healthcare Pathway Programs

Investigator: Sarah A. King, B.S.
Mentor: Amanda Burbage, Ph.D.
Co-Authors(s):
Katie Liu, Macon & Joan Brock Virginia Health Sciences Eastern Virginia Medical School
Kela Cowan-Gant, Macon & Joan Brock Virginia Health Sciences Eastern Virginia Medical School
Amanda Burbage, Macon & Joan Brock Virginia Health Sciences Eastern Virginia Medical School
Department(s): Eastern Virginia Medical School, School of Health Proffessions, Doctor of Medical and Health Professional Education
Poster #: 15B

INTRODUCTION

High school healthcare pathway programs play an important role in shaping the future healthcare workforce by providing students with opportunities to envision themselves in the field and offering tools to support their progression into the profession. Since the repealing of affirmative action, barriers to admission for applicants of underrepresented backgrounds have been rising. There is a growing need to support students on their path into a healthcare career. This study aimed to develop a map of high school pathway programs across the United States to identify common program features and document promising practices in program operation.

METHODS

This sequential mixed methods study first used environmental scan procedures to evaluate U.S. programs (n = 90) across structural frameworks, curriculum development, length, cost, and other defining features. After the environmental scan was completed, interviews with purposefully selected program directors (n = 6) were conducted on Zoom, lasting 45-60 minutes following a standardized protocol developed from the results of the environmental scan. Interviews were transcribed and an iterative coding procedure using inductive descriptive coding, and a secondary coding review was done prior to development of themes.

RESULTS

Among the 90 external programs identified, summer-only programming was the most common structure (52.2%), while only 11.1% were clearly multi-year. Hands-on activities were the most frequently documented program component (85.6%), followed by exposure to multiple health professions (77.8%) and mentoring (61.1%). Academic support was documented in approximately half of programs (46.7%), while shadowing (31.1%), research (30.0%), and service (12.2%) were less common. Most programs used an application-based entry process (78.9%), and no participant fee was reported for 57.8%. Formal academic credit or a degree pathway was uncommon (13.3%). Across programs, three themes were identified: long-term mentorship, life-skill development, and academic support. These themes were embedded within broader, cross-cutting practices, including hands-on experiences that made health careers tangible, exposure to multiple professions and potential career pathways, and relationships with near peers, professionals, alumni, and program staff that helped students envision and navigate those pathways. Programs operationalized these elements differently according to their populations, local workforce needs, institutional contexts, and available resources. Directors also described challenges maintaining longitudinal connections and measuring student outcomes after program completion.

CONCLUSION

Ultimately, this study differentiated the key aspects between a "healthcare experience" program and a true "pathway" program. The environmental scan and director interviews suggest that healthcare pathway programs share common goals but use different structures and strategies to achieve them. Understanding the framework of these programs helps program directors develop their structure and better support their students along the path to entering the healthcare field.

Clinical Characteristics and Outcomes of Ambulatory Bloodstream Infections in Pediatric Hematology/Oncology Patients

Investigator: Emily E. Lessard, B.S.
Mentor: Eric Werner, MD, MMM
Co-Authors(s):
Renee Brown, Macon & Joan Brock Virginia Health Sciences Eastern Virginia Medical School
Department(s): Division of Hematology/Oncology
Poster #: 25B

INTRODUCTION

Central line-associated bloodstream infections (CLABSIs) cause significant morbidity in pediatric hematology/oncology (PHO) patients. While inpatient CLABSIs have been the focus of prevention efforts, ambulatory bloodstream infections (ABSIs) remain less studied. Since December 2011, Children's Hospital of The King's Daughters (CHKD) Division of PHO has maintained a database of ABSI events in PHO patients with CLs to support quality improvement initiatives. This study aimed to categorize ABSI events, identify patient and CL characteristics, and describe clinical outcomes (CO).

METHODS

We performed a retrospective chart review of PHO patients with ABSI identified between December 2011 and December 2024. Demographic characteristics, CL type, CL access location, neutropenia, recent transfusions and anesthesia, microbiology, and COs were collected from the electronic medical record. COs included hospitalization, pediatric intensive care unit (PICU) admission, and mortality.

RESULTS

A total of 122 ABSIs were identified among 101 unique patients. Age, sex, and insurance status were comparable to those of the Hampton Roads pediatric population. Of these infections, 108 (89%) were CLABSIs, 12 (10%) were single positive blood infections (SPs), and 2 (2%) were secondary bloodstream infections. Most patients experienced a single infection (84%), while 13% had two infections and 3% had three. CL types included implanted ports (63%), Hickman/Broviac catheters (20%), peripherally inserted central catheters (12%), and other devices (4%). CLs were most commonly last accessed in the outpatient PHO clinic (59%) and the home setting (30%). 18% were last accessed ≥7 days before infection. Neutropenia (ANC <500 cells/μL) was present in 57% of infections. The median hospital length of stay (LOS) was 8 days, 26% of events required PICU admission, 28% required line removal, and overall mortality was 2%. 37% of patients had received a transfusion (mean 3.38 days) and 12% had undergone anesthesia (mean 3.36 days) before infection. COs were similar between CLABSIs and SPs, with a median LOS of 8 days and a PICU admission rate of 25% in both groups. No deaths occurred in SP patients.

CONCLUSION

ABSIs in PHO patients remain an important source of morbidity, with frequent hospitalization and intensive care needs and merit targeted prevention strategies in the outpatient setting.

Distance to Diagnostic Imaging as a Predictor of Late-Stage Cancer Diagnosis Across 16 US States

Investigator: Shinjer Li, B.S.
Mentor: Jose Morey, MD
Co-Authors(s):
Imad Haque, Sentara
Department(s): Radiology

INTRODUCTION
Access to diagnostic imaging varies widely across the United States, but whether distance to imaging facilities independently predicts cancer screening and diagnosis at advanced stages has not been tested across multiple states. This study assessed that relationship for seven cancer outcomes across 16 states.

METHODS
We analyzed 1,304 counties across 16 states (166.1 million population), grouped into five geographic tiers. The primary exposure was median distance from county centroids to the nearest imaging center. Outcomes included mammography and colorectal screening rates (CDC PLACES) and late-stage incidence for breast, lung, colorectal, prostate, and cervical cancers (NCI State Cancer Profiles). Ordinary least squares regression with robust standard errors was run for each state separately, adjusting for poverty, racial composition, age, rurality, and uninsurance.

RESULTS
Median imaging distance ranged from 2.3 miles (New Jersey) to 46.2 miles (North Dakota). In adjusted models, imaging distance significantly predicted higher late-stage colorectal cancer in 6 of 15 states (40%), lung cancer in 4 of 15, cervical cancer in 3 of 6, prostate in 2 of 15, and breast in only 1 of 14. Every significant association was positive. Across all outcomes and states, imaging distance reached significance in 21 of 112 state-outcome pairs. When all counties were pooled, every bivariate correlation between imaging distance and each outcome was statistically significant.

CONCLUSION
Imaging distance independently predicts lower screening and more advanced diagnoses, with colorectal cancer showing the strongest evidence. The minimal effect for breast cancer likely reflects the success of mobile mammography. These findings support expanding mobile imaging for other cancers and targeting facility placement to imaging deserts.

Comparative Genomic Characterization of Cholangiocarcinoma and Gallbladder Adenocarcinoma

Investigator: Kylie Alise Lopez, B.S.
Mentor: Winifred Lo, MD
Co-Authors(s):
Austin Grove, Macon & Joan Brock Virginia Health Sciences Eastern Virginia Medical School
Luisel Ricks-Santi, Macon & Joan Brock Virginia Health Sciences Eastern Virginia Medical School
Department(s): Surgery
Poster #: 33B

INTRODUCTION

Cholangiocarcinoma (CCA) and gallbladder adenocarcinoma (GBC) are rare, aggressive epithelial malignancies that are clinically classified together as biliary tract cancers (BTCs). Recent single-institution studies suggest they possess distinct molecular characteristics and therapeutic vulnerabilities. However, comprehensive genomic comparisons between these malignancies remain limited. This study compares the genomic landscapes of CCA and GBC for disease classification and identification of actionable treatment targets.

METHODS

Genomic and clinical data were obtained from The Cancer Genome Atlas through cBioPortal. CCA (n = 984 patients) and GBC (n = 932 patients) cases were selected using cancer type and primary tumor site classifications excluding metastatic disease and mixed histologies. Clinicopathologic characteristics, including nonsynonymous tumor mutational burden (TMB), TMB score, fraction genome altered (FGA), somatic mutations, copy number alterations (CNAs), co-mutation frequencies, gene enrichments, and survivorship were compared between cohorts. Statistical comparisons were performed using Kaplan-Meier (KM), Wilcoxon, two-sided Fisher exact, and Cox proportional hazards tests, with $P < 0.05$ considered significant. Potentially actionable targets were referenced using OncoKB. For survivorship analyses, cohorts were further stratified to include only patients with overall survival calculated from the date of diagnosis to death or last follow-up (CCA, n = 176; GBC, n = 112). The most frequently altered genes within each cohort were binarized (mutant = 1, wild-type = 0) for KM and Cox hazards analyses.

RESULTS

Patients with CCA demonstrated significantly longer median overall survival than GBC ($P < 0.01$). GBC exhibited significantly higher median nonsynonymous TMB and TMB scores than CCA ($P < 0.01$), whereas FGA and CNAs did not differ significantly. CCA demonstrated genomic enrichments involving receptor tyrosine kinase signaling, DNA repair, and cellular metabolism, whereas GBC demonstrated enrichments in tumor suppressor loss, TGF-β signaling, PI3K pathway alterations, and cell-cycle dysregulation. CCA was enriched for concurrent co-mutations involving chromatin remodeling, DNA repair, and receptor tyrosine kinase signaling, whereas GBC demonstrated co-occurring alterations involving tumor suppressor loss, chromatin remodeling, TGF-β signaling, and PI3K pathways. Survivorship analyses identified ARID1A mutations, PBRM1 mutations, and concurrent ARID1A-TP53 alterations as significantly associated with poorer overall survival in CCA, whereas no significant survival-associated genomic alterations were identified in GBC.

CONCLUSION

CCA and GBC demonstrate distinct clinical and genomic characteristics despite their current classification as BTCs. These findings support recognition of CCA and GBC as biologically distinct malignancies that may benefit from disease-specific therapeutic strategies.

Physical Activity Interventions for Children and Adolescents with Obesity: A Scoping Review

Investigator: Haley Lundeen, B.S., B.A.
Mentor: Ellen Pudney, Ph.D., M.S.
Co-Authors(s):
Charlotte Dawson, Macon & Joan Brock Virginia Health Sciences Eastern Virginia Medical School
Becky Blanton, Macon & Joan Brock Virginia Health Sciences Eastern Virginia Medical School
Esther Sarino, Macon & Joan Brock Virginia Health Sciences Eastern Virginia Medical School
Department(s): Pediatrics, Division of Community Health and Research
Poster #: 47B

INTRODUCTION

Weight stigma, or weight-based teasing or discrimination, has been experienced in physical activity settings by as many as 73% of youth with overweight or obesity and commonly results in decreased fitness regardless of weight status and decreased lifetime participation in physical activity. Despite its well-documented high prevalence and negative effects, it is unknown whether interventions aiming to increase physical activity among youth with obesity consider the barrier of experienced or anticipated weight stigma. To guide researchers and public health officials in designing effective physical activity interventions, this scoping review describes existing physical activity interventions and highlights the extent, if any, that they consider weight stigma in their design or implementation.

DISCUSSION

The protocol for this scoping review was prospectively registered on the Open Science Framework and conducted in accordance with the Preferred Reporting Items for Systematic Reviews and Meta-Analysis extension for scoping reviews (PRISMA-ScR). Reference librarians conducted a literature search to capture published physical activity interventions targeting youth ages 11 to 18 with obesity in the United States since 2013. The databases searched were APA PsychInfo, CINAHL, Cochrane Libraries, PubMed, and Web of Science, resulting in 3,283 references. Using Covidence software, two reviewers blindly screened titles/abstracts and then completed a full text screen of the 301 publications that passed the initial screening process, discussing discrepancies until a consensus was reached. Reviewers identified 50 publications (describing a total of 40 interventions) that fit the inclusion criteria and were included in data extraction. One reviewer extracted data from the articles and a second reviewer confirmed the extractions to ensure accuracy. In addition to evaluating whether and how the interventions considered weight stigma, other elements that were extracted included details regarding the components of the intervention (e.g., content, setting, mode of delivery, targeted level of intervention, length), targeted outcomes (e.g., weight loss, fitness, self-efficacy), and sample characteristics (e.g., distribution of body mass index, age, gender, race/ethnicity).

CONCLUSION

Findings from this review showcases the various approaches that have been taken to encourage physical activity among youth with obesity, identifying the common characteristics of recent interventions to inform future intervention development. Findings demonstrate that very few of the interventions considered weight stigma in their design and/or implementation, highlighting an important gap that warrants attention in future studies.

Beyond the vaginal septum: An unusual case highlighting MRI evaluation of uterine anomalies

Investigator: Brian Luong, B.S.
Mentor: Sarah Shaves, MD
Co-Authors(s):
Jacob Graham, Macon & Joan Brock Virginia Health Sciences Eastern Virginia Medical School
Department(s): Radiology
Poster #: 19A

INTRODUCTION
Occurring in 5.5% of the general population, uterine anomalies are the result of abnormalities in the genesis, fusion, and resorption phases of paramesonephric duct development. These abnormalities are more prevalent in women with infertility and recurrent pregnancy loss. Accurate classification can be performed via 3D ultrasound or MRI and is important as management differs among the uterine anomaly types. Although a longitudinal vaginal septum is more commonly associated with abnormalities in the fusion phase that can cause bicornuate and didelphys uterus, it may also rarely occur with a septate uterus.

CASE INFORMATION
A 34-year-old G0P0 woman with a 10 year history of infertility and ultrasound revealing two endometrial cavities had an MRI of her pelvis. Her MRI demonstrated two endometrial cavities with a complete septum in her uterus and vagina. This vaginal septum initially pointed her diagnosis towards bicornuate or didelphys uterus. However, measurement of the external uterine contour demonstrated a fundal cleft measuring less than 1 cm. This supported a diagnosis of complete longitudinal vaginal septum with complete septate uterus rather than a bicornuate or didelphys uterus. She was offered the option of surgical resection of the septum and chose to defer intervention. She conceived several months later without surgical intervention and was counseled regarding complications associated with a septate uterus.

DISCUSSION
Anchoring on a longitudinal vaginal septum may lead to misdiagnosis of bicornuate or didelphys uterus due to stronger association with these anomalies. MRI allows for measurement of the external fundal contour, fundal cleft, intercornual distance, and endometrial cavity angle, all of which are helpful in classification of the uterine anomaly type. This distinction is clinically important as a septate uterus may be amenable with hysteroscopic septum resection. This is not the case for bicornuate or didelphys uterus as surgical correction would be much more invasive. Additionally, septate uterus has also been associated with an increased risk of spontaneous abortion. For patients with multiple pregnancy losses, accurate diagnosis is particularly important.

CONCLUSION
Complete longitudinal vaginal septum can occur in association with a septate uterus and should not be considered diagnostic of a uterine fusion anomaly. Careful measurement of radiographic features such as fundal cleft is essential to avoid misclassification and ensure appropriate clinical management.

Confronting Death in Training: Changes in Medical Students' Response to Patient Death across Clerkship Phase

Investigator: Camilla Macia, B.S.
Mentor: Kelly Thomson, MD
Co-Authors(s):
Remy Lloyd, Macon & Joan Brock Virginia Health Sciences Eastern Virginia Medical School
Hannah Haberkorn, Macon & Joan Brock Virginia Health Sciences Eastern Virginia Medical School
Simone Schuemaecker, Macon & Joan Brock Virginia Health Sciences Eastern Virginia Medical School
Department(s): Internal Medicine
Poster #: 16B

INTRODUCTION

Medical students may encounter patient death during clinical training, yet formal education on processing these experiences remains limited. Witnessing patient death can evoke a range of emotional responses and concerns, requiring effective coping strategies during an already demanding period of training. The extent to which clinical clerkships alone prepare students to navigate patient death remains unclear. We analyzed pre- and post-clerkship survey data to assess changes in medical students' confidence, emotional responses, coping strategies, and concerns related to patient death.

METHODS

We conducted pre- and post-clerkship surveys of MD2027 students at Eastern Virginia Medical School at Old Dominion University. Anonymous REDCap surveys administered at the beginning and end of the clerkship year assessed expectations and experiences regarding patient death. Outcomes included confidence in managing patient death, emotional responses, coping strategies, and related concerns.

Paired and aggregate responses were compared using paired analyses and chi-square tests. Free-text responses were independently reviewed and categorized into themes within three domains: emotions, concerns, and coping strategies. Responses could be assigned to multiple categories. Cohen's κ was used to assess inter-rater reliability.

RESULTS

Twenty-one students completed the pre-clerkship survey, and 13 completed the post-clerkship survey, yielding 13 paired responses. Ten respondents (76.9%) experienced the death of a patient during clerkship.

Confidence was measured using a 5-point Likert scale. Five students gained confidence (38.5%), six lost confidence (46.2%), and two reported no change (15.4%). No students reported complete confidence before clerkship, whereas four did afterward. Students experiencing their first patient death gained a median of 1 point in confidence, while those with prior exposure lost a median of 0.5 points.

Emotional themes included grief/sadness, guilt/empathy, anger/distress, and shock/emotional detachment. Grief/sadness was the most common anticipated and experienced emotion. Shock/emotional detachment remained uncommon (3 pre-clerkship vs. 2 post-clerkship responses). Inter-rater agreement was nearly perfect ($\kappa=0.98$).

Coping themes included physical self-care, mindfulness/reflection, social support, and avoidance/suppression. Social support was anticipated more often than utilized, while mindfulness/reflection was the most frequently reported coping strategy. Inter-rater reliability was nearly perfect ($\kappa=0.98$).

Concerns centered on family communication, emotional impact, desensitization, and effects on patient care. Reported concerns decreased across all categories after clerkship. Inter-rater reliability was substantial ($\kappa=0.80$).

CONCLUSIONS

Clinical exposure to patient death had a variable impact on students' confidence. While some students gained confidence, others lost confidence, suggesting that clinical experience alone may not adequately prepare students for the emotional, practical, and professional challenges of patient death. Despite limited statistical power, findings suggest increased variability in confidence following clinical exposure, differences between anticipated and experienced emotions, stable coping patterns, and fewer concerns related to patient death. These results indicate that formal education may be needed to complement clinical experience. We developed a targeted educational intervention addressing grief normalization, emotional responses, coping strategies, healthcare team roles, postmortem care, family communication, and interdisciplinary support. Future evaluation will assess its impact on student confidence, preparedness, and ability to process patient death.

Class IV Obesity Versus Lower-Class Obesity: Mortality and Complications After Emergent Trauma Laparotomy

Investigator: Ryan Mancoll, B.S.
Mentor: Samantha Olafson, MD
Co-Authors(s):
William Rice, Macon & Joan Brock Virginia Health Sciences Eastern Virginia Medical School
Spencer White, Macon & Joan Brock Virginia Health Sciences Eastern Virginia Medical School
Department(s): Surgery
Poster #: 07A

INTRODUCTION

Obesity affects over 40% of U.S. adults, with class IV (Body Mass Index (BMI) ≥ 50) rising substantially. The relationship between obesity and emergent trauma laparotomy outcomes is established, yet the literature collapses obesity class I–IV under a single category. However, physiology differs by obesity class, and no study has stratified morbidity and mortality across these classes. We aimed to characterize this relationship to more accurately represent each class. We hypothesized that as BMI increases, so do major adverse outcomes.

METHODS

This was a retrospective cohort study using data from the American College of Surgeons (ACS) Trauma Quality Improvement Program (2017-2024). Inclusion criteria were age >18 years, BMI ≥30 kg/m2, abdominal AIS ≥3, and emergent laparotomy within 6 hours of ED arrival. Patients who died before or on ED arrival and those with non-blunt/penetrating mechanism were excluded. Groups for analysis were stratified by obesity class, I-II (BMI 30-39.9), III (BMI 40-49.9), and IV (BMI >= 50). Unweighted statistics characterized demographics and outcomes. Multivariate regression analyzed mortality, discharge disposition, LOS, infectious, and pulmonary complications.

RESULTS

Of 18,583 patients included, there were 15,580 (83.8%) class I-II, 2,448 (13.2%) class III, and 555 (3.0%) class IV and above patients. Class III/IV patients were younger, more female, and more often black than class I-II ($p < 0.001$), with higher rates of penetrating trauma ($p = 0.041$), and shock index ($p < .001$). After regression, class IV was the largest independent predictor of mortality (OR 2.78, 95% CI 2.04–3.79). Class III also predicted mortality (OR 1.41, 1.18–1.70). Class III and Class IV had higher odds of non-home discharge (OR 1.38,1.19-1.60), (OR 1.93, 1.46-2.56). Class III was associated with 1.5x odds of unplanned reoperation. Obesity class predicted pulmonary complications dose-dependently with (OR 1.27, 1.05-1.52) for Class III and (OR 1.55, 1.11-2.16) for Class IV. Although BMI class was not associated with surgical site infectious complications, class IV independently predicted severe sepsis (OR 1.68, 1.03–2.75).

CONCLUSIONS

Risk stratification in obese trauma patients undergoing laparotomy should extend beyond obese vs. non-obese. These findings highlight a dose-response relationship between escalating BMI class and mortality risk, unfavorable discharge disposition, and pulmonary complications. Contrary to current literature, surgical site infection was not associated with BMI class. BMI class carries independent prognostic significance and should not be treated as binary in trauma care.

Whippet Induced Functional Vitamin B12 Deficiency and the Neurological Effects: A Case Report

Investigator: Baylee Marin, B.S.
Mentor: Jean-Philippe Daniel, MD
Co-Authors(s):
Keti Gvazava, Macon & Joan Brock Virginia Health Sciences Eastern Virginia Medical School
Department(s): Neurology
Poster #: 40B

INTRODUCTION

Vitamin B12, known as cobalamin, is a water soluble vitamin that plays a role in the formation of DNA and myelin. There are four main etiologies of vitamin B12 deficiency, including autoimmune antibodies to intrinsic factor, structural malabsorptive disorders, lack of dietary intake, and toxin mediated deficiency. Deficiency can cause a length-dependent peripheral neuropathy or myelopathy. The central nervous system can be affected in a condition known as subacute combined degeneration, hallmarked by damage to the dorsal columns, corticospinal tracts, and spinocerebellar tracts. This results in sensory ataxia and loss of proprioception. A recent leading cause of B12 deficiency with secondary neurological dysfunction is the recreational use of nitrous oxide, colloquially known as "whippets".

CASE INFORMATION

We present the case of a 45 year old female with a past medical history of bipolar 1 disorder, anxiety disorder, and migraines who presented for recurrent falls associated with bilateral lower extremity weakness, sensory changes, and worsening back pain. She had diffuse lower extremity weakness (4/5), mild hyporeflexia at the Achilles tendons, and length-dependent sensory loss to all modalities. She had a shuffling gait with reduced foot clearance. MRI of the cervical, thoracic, and lumbar spine revealed no abnormal cord signal or structural etiology. Laboratory evaluation revealed a vitamin B12 level of <150, with a markedly elevated methylmalonic acid level of 16,242, consistent with severe functional vitamin B12 deficiency. On further history, the patient reported recreational nitrous oxide ("whippet") use earlier in the year. The clinical presentation, laboratory findings, and absence of structural findings were felt to be most consistent with vitamin B12 deficiency-associated polyneuropathy (versus imaging-negative myelopathy), likely related to nitrous oxide-induced depletion. Her symptoms improved with aggressive vitamin B12 supplementation.

DISCUSSION

While B12 deficiency related neurological damage is historically taught as two distinct entities, peripheral neuropathy vs central subacute combined degeneration, in actuality there is often overlap between polyneuropathy and myelopathy. Findings have shown more significant axonal dysfunction of motor neurons in nitrous oxide abusing patients than sole vitamin B12 deficiency patients, suggesting that there may be pathologic changes unique to nitrous oxide in the pattern of neuronal dysfunction. The degree of motor neuron damage seems to have a disproportionally higher effect on lower distal muscles than proximal muscles, a presentation that differs from the more proximal and minimal loss in those with isolated vitamin B12 deficiency. Spinal cord involvement is also more prevalent in nitrous oxide use than pure vitamin B12 deficiency.

CONCLUSION

The exact pathophysiologic mechanism of damage from nitrous oxide abuse may be more nuanced than simple induction of vitamin B12 deficiency. While our patient presented with a polyneuropathy and lack of radiologic findings, the literature shows there is no obvious proportion of one or the other associated with nitrous oxide use. Furthermore, the frequently overlapping symptomatology of peripheral neuropathy and central nervous system damage can make a diagnosis even more challenging. Our case highlights the importance of considering nitrous oxide abuse as a possible etiology of vitamin B12 deficiency and neurological impairment.

Measuring AI Health Literacy: A Factor Analytic Approach

Investigator: Mariana Meade, B.S.
Mentor: Rehan Qayyum, MD
Co-Authors(s):
Mariana Meade, Macon & Joan Brock Virginia Health Sciences Eastern Virginia Medical School
Atiq Bhatti, Macon & Joan Brock Virginia Health Sciences Eastern Virginia Medical School
Department(s): Department of Medicine
Poster #: 17B

INTRODUCTION
Generative AI tools (e.g., ChatGPT) are increasingly used by patients seeking health information, yet no validated instrument measures patients' capacity to use these tools effectively. This study aimed to identify the latent factor structure of a novel Generative AI Health Literacy questionnaire using exploratory and confirmatory factor analysis.

METHODS
This cross-sectional study distributed a 57-item questionnaire to 653 adult patients (interim analysis toward a target n=880) at the department of medicine clinics. Skip logic produced two analytic blocks: Block 1 (all 653 respondents; 17 items on digital literacy and trust) and Block 2 (372 AI users; 37 items on AI-specific domains). Exploratory factor analysis (EFA), using polychoric correlations with promax rotation, was conducted separately per block, with parallel analysis guiding factor retention. EFA-informed confirmatory factor analysis (CFA) followed via structural equation modeling.

RESULTS
Mean age was 53 ± 16.6 years; 53% were female, 50.4% White, 38.7% Black, and 46.7% college graduates. Overall, 57.1% used AI for health information, of whom 45% used ChatGPT. For Block 1, parallel analysis supported a two-factor solution: Digital Literacy (8 items; variance 0.47) and Trust in AI (4 items; variance 0.85); CFA showed reasonable fit (χ^2=94.6, p<0.001; CFI=0.990; RMSEA=0.042; SRMR=0.040). For Block 2, parallel analysis supported four factors: AI Use Frequency (5 items; variance 0.32), AI Competency (13 items; variance 0.6), Impact of AI on Health Understanding (3 items; variance 0.84), and Cognitive Evaluation of AI Output (3 items; variance 0.22). The four-factor CFA showed moderate fit (χ^2=520, p<0.001; CFI=0.930; RMSEA=0.062; SRMR=0.084). There is not currently a significant difference in AI use between gender groups (p=0.330) or pooled race groups (p=0.228).

CONCLUSIONS AND RELEVANCE
This analysis revealed a parsimonious four-factor structure, with AI Use Frequency demonstrating excellent psychometric properties. These preliminary findings will be cross-validated in the full sample. Once validated, this instrument could help identify patients—particularly older adults and those with lower digital literacy—who may benefit from targeted support navigating AI for health information.

Cocaine-Associated Pulmonary Vasoconstriction Mimicking Pulmonary Embolism on Perfusion Lung Scintigraphy

Investigator: Oleksandra Melchers, M.S.
Mentor: Fiora McRae, MD
Co-Authors(s):
Kyle Bonner, Macon & Joan Brock Virginia Health Sciences Eastern Virginia Medical School
Department(s): Radiology
Poster #: 14A

INTRODUCTION

Cocaine is associated with acute cardiopulmonary toxicity, including vasospasm-mediated ischemia. In patients with elevated D-dimer and renal impairment limiting CT pulmonary angiography (CTPA), pulmonary perfusion scintigraphy may be used to evaluate suspected pulmonary embolism (PE). We describe a case in which a high-probability perfusion scan following recent cocaine use mimicked PE, which was subsequently excluded by magnetic resonance angiography (MRA).

CASE INFORMATION

A 59-year-old woman with chronic obstructive pulmonary disease, stage III chronic kidney disease, remote PE, and polysubstance use presented with several days of chest pain and dyspnea. She reported crack cocaine use two days prior. Laboratory evaluation demonstrated an elevated D-dimer (6.07 mg/L FEU), mildly elevated troponin, and acute-on-chronic renal dysfunction (creatinine 2.7 mg/dL; eGFR 19.7 mL/min/1.73 m^2). Chest radiography was unremarkable. Because renal dysfunction limited CTPA, pulmonary perfusion scintigraphy was performed; ventilation imaging could not be completed. The study demonstrated multiple bilateral moderate-to-large peripheral wedge-shaped perfusion defects without corresponding radiographic abnormalities, interpreted as high probability for PE and new compared with a remote baseline study.

Anticoagulation was initially considered but ultimately discontinued after multidisciplinary evaluation given the discordant clinical picture and recent cocaine exposure. Bronchodilator therapy produced symptomatic improvement. Subsequent contrast-enhanced pulmonary MRA demonstrated no pulmonary arterial filling defect to suggest acute PE. The patient remained stable without anticoagulation and was discharged.

DISCUSSION

Cocaine-associated pulmonary vasoconstriction has been reported to produce regional perfusion abnormalities that can mimic thromboembolic disease on lung scintigraphy. In this patient, recent crack cocaine exposure, multiple apparent perfusion defects, and absence of emboli on subsequent pulmonary MRA suggest transient pulmonary vasoconstriction as a potential explanation for the discordant imaging findings. Underlying COPD may further complicate interpretation through regional alterations in ventilation and perfusion. This case highlights the importance of correlating scintigraphic findings with clinical history and confirmatory imaging rather than interpreting a high-probability perfusion pattern in isolation.

CONCLUSION

Recent cocaine exposure should be considered a potential confounder when pulmonary perfusion imaging suggests PE, particularly when confirmatory vascular imaging is discordant. Recognition of this uncommon imaging mimic may help prevent unnecessary anticoagulation and its associated risks.

Multimodality Imaging of a Jugular Paraganglioma: A Case Report

Investigator: Cynthia L. Monroe, B.S.
Mentor: John Campbell, MD
Co-Authors(s):
Seong Lee, Macon & Joan Brock Virginia Health Sciences Eastern Virginia Medical School
Department(s): Radiology
Poster #: 43B

INTRODUCTION

Jugular paraganglioma is a rare, highly vascular neuroendocrine tumor arising from paraganglia of the head and neck that is located at the jugular fossa. Because of their complex location, early diagnosis and assessment are important for treatment planning. This case report demonstrates jugular paraganglioma, with an enhancing right jugular-foramen mass on MRI, bone erosion on CT, and intense radiotracer uptake on 68Ga-DOTATATE PET/CT.

CASE INFORMATION

The patient was a 92-year-old man with profound right-sided sensorineural hearing loss managed with a CROS hearing aid and lacked symptoms of hormone hypersecretion. Imaging demonstrated a right jugular foramen mass consistent with a jugular paraganglioma. The mass involved the vertical and horizontal portions of the carotid canal and tympanic cavity, with small extension into the neck and no intracranial extension. T2 FLAIR demonstrated mild hyperintense signal with associated right sided mastoid effusion, while T2 had few punctate signal voids. Pre-contrast T1 showed mild hyperintensity, which may be due to slow flowing blood, hemorrhage, or proteinaceous content. Post-contrast T1 revealed avid enhancement of the tumor measuring 28 x 18mm and mildly increased in size since 2017. Additionally, CT temporal bone demonstrated erosive changes at the anterior and medial walls of the right jugular foramen. 68Ga-DOTATATE PET/CT showed intense abnormal radiotracer uptake corresponding to the known mass, confirming jugular paraganglioma. Given his high level of functioning, absence of cranial neuropathies, and age, observation of the tumor was pursued.

DISCUSSION

Paragangliomas, or glomus tumors, are divided into sympathetic and parasympathetic groups. Sympathetic paragangliomas, located in the chest and abdomen, present with symptoms of catecholamine excess. Parasympathetic paragangliomas, located in the head and neck, present with tinnitus, hearing loss, cranial nerve palsies or a palpable neck mass. The most common head and neck paraganglioma is the carotid body tumor and second most common is jugular paraganglioma. This patient had a jugular paraganglioma, a locally infiltrative tumor that may be bilateral or coexist with other tumors but rarely metastasizes.

For imaging of jugular paragangliomas, CT is best for assessing irregularly eroded bony margins and moth-eaten appearance. Angiography shows intense tumor blush commonly from the ascending pharyngeal artery. MRI demonstrates low T1 signal, high T2 signal, and marked intense enhancement on post-contrast T1. On T1 and T2, the salt and pepper appearance is visible, with salt describing blood products from hemorrhage or slow flow and pepper representing flow voids due to high vascularity. Lastly, 68Ga-DOTATATE PET/CT is useful for detecting paragangliomas because these tumors overexpress somatostatin receptors, particularly SSTR2, resulting in intense radiotracer uptake.

Differential diagnosis includes jugular schwannoma, bony metastases, meningioma, normal anatomic variation, jugular bulb thrombosis, and endolymphatic sac tumor. In this patient, the combination of irregular bone erosion, avid enhancement, vascular flow voids, and intense 68Ga-DOTATATE uptake supported jugular paraganglioma over these other diagnoses.

CONCLUSION

Jugular paraganglioma is a rare, highly vascular tumor that can be differentiated from other head and neck lesions by its characteristic findings on CT, MRI, and 68Ga-DOTATATE PET/CT. Recognizing these imaging features is important for diagnosis and treatment planning.

Thoracic Lymphoma: A Spectrum of Imaging Findings

Investigator: Cynthia L. Monroe, B.S.
Mentor: Sarah Shaves, MD
Co-Authors(s):
Kyle Bonner, Macon & Joan Brock Virginia Health Sciences Eastern Virginia Medical School
Department(s): Radiology
Poster #: 20A

INTRODUCTION
Thoracic lymphoma may include nodal, lung, pleural, pericardial and chest wall involvement. Imaging is often ordered for staging of disease and to assess response to therapy. Recognition of the spectrum of possible findings that may simulate other diseases can lead to earlier suspicion and diagnosis. Radiologists should be familiar with the types of thoracic involvement that may be seen with lymphoma.

CASE INFORMATION
A series of patients with thoracic lymphoma demonstrated a broad range of clinical presentations and imaging findings. Case A is a patient that presented with chest pain and impending superior vena cava syndrome; imaging showed a lobulated soft tissue mass in the anterior mediastinum, consistent with an anterior mediastinal lymphoma. Case B was an example of pulmonary lymphoma, where CT showed a solitary pulmonary nodule in the left lower lobe. In case C, a patient with endobronchial lymphoma presented with a cough, while CT revealed a mass in the left mainstem bronchus. Case D was a patient with esophageal lymphoma, who presented with chest pain and dysphagia. CT demonstrated diffuse esophageal wall thickening and an intraluminal soft tissue mass within the mid to distal esophagus. Case E involved a patient experiencing dysrhythmia. CT showed a heterogeneously enhancing lobulated soft tissue mass within the right atrium and a pericardial effusion, which later proved to be cardiac lymphoma. In case F, a patient presented with shortness of breath and CT showed left-sided pleural effusion. Pleural fluid analysis later revealed pleural lymphoma. Case G was a patient that presented with an anterior chest wall palpable lump. CT chest showed a left sternal lytic lesion with a soft tissue component infiltrating the anterior chest wall. Subsequent tissue sampling revealed chest wall lymphoma.

DISCUSSION
Thoracic lymphoma most commonly involves anterior and middle mediastinal lymphadenopathy with or without hilar disease. Extranodal lymphoma occurs when proliferation of lymphoid cells infiltrates outside of the lymph nodes and is less common but can mimic other diseases on imaging, making diagnosis difficult. Pulmonary lymphoma commonly occurs in immunosuppressed patients and features nodules, infiltrates with air bronchograms, ground glass opacities, perilymphatic nodularity, and cavitation. Endobronchial lymphoma is rare and can have a polypoid mass, postobstructive hyperinflation, atelectasis, consolidation, and involve internal mammary nodes. Esophageal lymphoma has a polypoid or circumferential mass, submucosal lesions, diffuse thickening, and ulceration. Cardiac lymphoma occurs rarely as a primary cardiac tumor and is characterized by a bulky epicardial or myocardial mass, typically right atrium involvement, epicardial encasement, and occasionally tamponade. Pleural lymphoma is also rarely a primary tumor and can manifest as an effusion or have soft tissue masses. Lastly, chest wall lymphoma is rare and includes chest wall masses, breast masses, and skeletal lesions. These cases demonstrate the various locations and appearances of lymphoma in the chest and raise awareness of potential disease mimics.

CONCLUSION
Thoracic lymphoma can involve various structures, including the lungs, pleura, chest wall, pericardium, lymph nodes, bones, and breasts and present with diverse features on imaging. Knowledge of the manifestations of thoracic lymphoma is important for early diagnosis and treatment.

Implementation of an MRI/MRA-First Pathway for Suspected Transient Ischemic Attack: A Pre-Post Imaging Utilization Study

Investigator: Kevin Moran, M.S.
Mentor: Peter Van Geertruyden, MD
Co-Authors(s):
Kevin Moran, Macon & Joan Brock Virginia Health Sciences Eastern Virginia Medical School
Phillip Poppas, Macon & Joan Brock Virginia Health Sciences Eastern Virginia Medical School
Joseph Sisti, Macon & Joan Brock Virginia Health Sciences Eastern Virginia Medical School
Department(s): Radiology
Poster #: 02A

INTRODUCTION
Brain MRI with diffusion-weighted imaging provides sensitive detection of acute cerebral ischemia in patients with suspected transient ischemic attack (TIA), while MRA permits evaluation of the intracranial and cervical vasculature. Despite these advantages, CTA head and neck is frequently obtained in patients with resolved neurologic symptoms who subsequently undergo MRI, potentially resulting in duplicative imaging and unnecessary exposure to ionizing radiation and iodinated contrast. We evaluated the effect of implementing a structured MRI/MRA-first pathway for suspected TIA on institutional neurovascular imaging utilization.

METHODS
In August 2025, an MRI/MRA-first imaging pathway was implemented at a single hospital for non-stroke-alert patients undergoing evaluation for suspected TIA in the Observation Unit. The pathway utilized brain MRI with diffusion-weighted imaging, MRA of the head, and MRA of the neck, collectively termed the "triple rule-out" protocol. CTA head/neck remained available when MRI could not be completed within the targeted 12-hour timeframe. Monthly MRI/MRA triple-rule-out and CTA head/neck examination volumes were retrospectively reviewed for the 12 months before implementation (August 2024–July 2025) and 12 months after implementation (August 2025–July 2026). Because available CTA data included examinations performed for all clinical indications, CTA volume was evaluated as an institutional utilization measure rather than as a TIA-specific cohort. Differences in the relative utilization of MRI/MRA versus CTA head/neck between periods were assessed using the chi-square test.

RESULTS
MRI/MRA triple-rule-out volume increased from 760 examinations during the preimplementation period to 1,483 examinations after implementation, representing a 95.1% increase. Mean monthly MRI/MRA volume increased from 63.3 to 123.6 examinations. Monthly volume ranged from 39–82 before implementation and 93–171 afterward, with every postimplementation month exceeding the highest monthly volume observed before implementation. MRI/MRA accounted for 50.3% of combined MRI/MRA and CTA head/neck examinations before implementation compared with 67.3% afterward, an increase of 17.0 percentage points ($p < 0.001$). Overall CTA head/neck volume remained relatively stable, decreasing from 752 to 720 examinations (4.3%).

CONCLUSION
Implementation of a structured MRI/MRA-first pathway for suspected TIA was associated with a nearly twofold and sustained increase in utilization of the dedicated MRI/MRA triple-rule-out protocol and a significant shift in institutional neurovascular imaging utilization toward MRI/MRA. The persistence of increased MRI/MRA utilization throughout the 12-month postimplementation period suggests sustained adoption of the pathway. Because CTA head/neck data included examinations performed for all clinical indications, the effect of the intervention on CTA utilization specifically among patients with suspected TIA cannot be determined from the available data. Patient-level analysis would be required to assess changes in TIA-specific CTA utilization and duplicative imaging.

Use of a Pressure-Directed Valve Microcatheter for Yttrium-90 Radioembolization in Complex Hepatogastric Arterial Anatomy

Investigator: Kevin Moran, M.S.
Mentor: Shashidhara Murthy, MD
Co-Authors(s):
Kevin Moran, Macon & Joan Brock Virginia Health Sciences Eastern Virginia Medical School
Chris Myers, Macon & Joan Brock Virginia Health Sciences Eastern Virginia Medical School
Department(s): Radiology
Poster #: 41B

INTRODUCTION

Yttrium-90 (Y-90) radioembolization requires selective hepatic arterial delivery while minimizing nontarget embolization, particularly to the gastrointestinal tract, where inadvertent microsphere deposition can cause clinically significant radiation injury. Prophylactic coil embolization of extrahepatic branches can reduce this risk but is not always feasible when nontarget gastric vessels are too numerous, too small, or otherwise inaccessible to catheterization. Pressure-directed valve microcatheters may offer an alternative by altering local flow dynamics to eliminate reflux into nontarget branches while preserving delivery to the intended hepatic territory.

CASE INFORMATION

A 77-year-old woman with biopsy-proven cecal adenocarcinoma and hepatic metastases was referred for liver-directed therapy after a left hepatic metastasis progressed despite systemic treatment. She had completed 12 cycles of folinic acid, fluorouracil, and oxaliplatin plus bevacizumab (FOLFOX–bevacizumab) and was subsequently receiving folinic acid, fluorouracil, and irinotecan plus bevacizumab (FOLFIRI–bevacizumab), which was held periprocedurally. Computed tomography (CT) demonstrated interval enlargement of the left hepatic lesion from 2.8 × 3.0 cm to 3.4 × 3.4 cm.

On mapping angiography, the tumor was supplied by the left hepatic artery, and numerous small branches supplied the adjacent gastric wall. Mapping with a conventional 2.8-French Progreat microcatheter (Terumo Medical Corporation, Somerset, NJ) demonstrated substantial gastric wall perfusion on cone-beam CT (CBCT). Because these branches were too numerous and small for practical coil embolization, mapping was repeated with a TriNav pressure-generating, one-way-valve, intermittently occlusive microcatheter (TriSalus Life Sciences, Westminster, CO). Repeat CBCT demonstrated elimination of visible gastric wall perfusion while tumor perfusion was maintained. Technetium-99m macroaggregated albumin (Tc-99m MAA) was then administered via the segment 2/3 hepatic artery through the TriNav catheter. Subsequent single-photon emission CT/CT (SPECT/CT) showed no extrahepatic intra-abdominal activity and a pulmonary shunt fraction of 3.3%.

DISCUSSION/CLINICAL FINDINGS

Radioembolization of segments 2/3 was performed using Y-90 resin microspheres (SIR-Spheres; Sirtex Medical, Woburn, MA) delivered through the TriNav catheter. Intraprocedural CBCT demonstrated appropriate tumor blush without extrahepatic uptake, and the prescribed activity of 39.3 mCi was fully delivered. Post-treatment SPECT/CT showed intense localization of activity within the left hepatic mass without extrahepatic activity.

Shortly after the procedure, the patient developed abdominal discomfort, nausea, and vomiting and was admitted for overnight observation and supportive care with antiemetics, acid suppression, analgesia, and hydration. By the following morning she reported marked improvement, denied further nausea or vomiting, and was discharged with only mild residual left upper quadrant soreness. The rapid onset of symptoms may reflect a greater degree of embolization achieved with the TriNav catheter and a correspondingly earlier onset of post-embolization syndrome. These symptoms were readily managed, and use of the TriNav catheter enabled treatment of a lesion that would not otherwise have been feasible. This case illustrates how pressure-directed delivery can provide a technical solution when conventional coil protection is not feasible.

CONCLUSIONS

Pressure-directed valve microcatheter technology may facilitate selective radioembolization in patients with complex hepatogastric arterial anatomy when numerous small nontarget vessels cannot feasibly be coil embolized. In this case, the TriNav catheter eliminated visible gastric perfusion on mapping CBCT while preserving tumor targeting and enabling successful Y-90 delivery without post-treatment extrahepatic activity.

Laryngeal Involvement in United Airway Disease: Voice Symptoms in Adults with Chronic Rhinosinusitis and/or Allergic Rhinitis

Investigator: Joel Moses, B.A.
Mentor: Kent Lam, MD
Co-Authors(s):
Victoria Reynolds, Old Dominion University
Department(s): Otolaryngology
Poster #: 26B

INTRODUCTION
United airway disease (UAD) describes shared inflammatory processes involving the upper and lower respiratory tract, including allergic rhinitis (AR), chronic rhinosinusitis (CRS), and asthma. Although anatomically positioned between the upper and lower airway, the larynx remains relatively under-characterized within this framework. Emerging evidence suggests that allergic upper-airway inflammation may extend to the larynx and contribute to dysphonia; however, existing literature is largely retrospective, and prospective characterization of laryngeal symptoms and vocal function in UAD remains limited. This study prospectively evaluates laryngeal involvement in adults with AR and/or CRS using patient-reported symptoms, voice-related quality of life, and objective acoustic measures of vocal quality.

METHODS
Adults aged 18–89 years presenting to a rhinology clinic were enrolled into AR, CRS, or combined AR+CRS groups according to clinical diagnostic criteria. Participants completed the Vocal Tract Discomfort Scale (VTDS) and Voice-Related Quality of Life (V-RQOL) questionnaire and underwent standardized voice recording. Acoustic analysis in Praat included jitter, shimmer, harmonic-to-noise ratio (HNR), and smoothed cepstral peak prominence (CPPs). Clinically significant patient-reported findings were defined as VTDS >15 and/or total V-RQOL <90; objective positivity was defined as ≥1 acoustic measure exceeding its prespecified criterion. Current analyses include 45 participants with complete patient-reported data, 48 voice samples with adequate HNR for acoustic analysis, and 42 with both.

RESULTS
Clinically significant subjective findings were present in 60.0% (27/45) of participants, while 35.6% (16/45) met both VTDS and V-RQOL criteria. Among usable recordings, 52.1% (25/48) demonstrated ≥1 dysphonia-associated acoustic finding; CPPs was the most frequently positive individual measure (43.8%). Among participants with paired data, objective abnormalities were more frequent among those with clinically significant subjective findings than among those without (61.5%, 16/26 vs 37.5%, 6/16), although this association was not statistically significant (Fisher exact p≈0.204). VTDS differed across diagnostic groups (Kruskal-Wallis p=0.040), with greater discomfort in AR than CRS after Bonferroni correction (adjusted p=0.046). Overall acoustic positivity did not significantly differ among diagnostic groups.

CONCLUSION
Clinically meaningful laryngeal symptoms, voice-related impairment, and acoustic abnormalities were common in this preliminary AR/CRS cohort. Subjective and objective findings showed incomplete overlap, suggesting complementary but potentially distinct dimensions of laryngeal involvement and effects on participants' quality of life in the social and physical domains. Exploratory differences in VTDS by diagnosis further suggest that laryngeal symptom burden may vary across UAD phenotypes. These findings support continued investigation of the larynx as an underrecognized component of UAD. Completion of comparison-group recruitment, analysis of the perceptual presence, nature, and severity of dysphonia, and analysis of sinonasal disease severity and relevant covariates will further clarify these relationships.

Congenital Agenesis of the Corpus Callosum Presenting with Chronic Cognitive Impairment: A Case Report

Investigator: Emily Mungovan, B.A.
Mentor: Yoonah Kim, MD
Co-Authors(s):
Seong Lee, Old Dominion University
Department(s): Radiology
Poster #: 21A

INTRODUCTION

Neuropsychiatric symptoms that are atypical in severity or pattern for an established diagnosis may warrant further evaluation for an underlying neurologic etiology. In this case, a patient who had been diagnosed with both attention-deficit/hyperactivity disorder (ADHD) and autism spectrum disorder (ASD) was found to have complete congenital agenesis of the corpus callosum (AgCC), which may contribute to his constellation of emotional, behavioral, and memory symptoms. AgCC may occur as an isolated malformation or in association with other congenital abnormalities and genetic syndromes, with prognosis influenced substantially by the presence of additional malformations.

CASE INFORMATION

This patient is a 21-year-old male with a past medical history of ADHD and ASD who was referred to neurology for evaluation of chronic memory impairment. He reported poor memory and concentration beginning in second grade, with persistent effects on his daily functioning. He received a Montreal Cognitive Assessment (MoCA) score of 21/30 and a memory index score of 12/15 at his neurology intake appointment. Neuropsychological testing demonstrated memory deficits substantially greater than typically expected with ADHD, which the evaluating neuropsychologist described as resembling a pattern seen in dementia. The patient subsequently underwent MRI of the brain without contrast, which revealed a complete absence of the corpus callosum with colpocephaly. Additional findings included subependymal gray matter heterotopia along the right temporal horn. The posterior horns of the lateral ventricles were symmetrically dilated, with mild displacement of the third ventricle.

The patient continues to undergo psychotherapy and supportive counseling, and he takes bupropion and methylphenidate daily. He has not undergone further workup at this time.

DISCUSSION

Further evaluation may help determine whether AgCC is isolated or associated with a broader genetic or congenital syndrome. The presence of additional CNS abnormalities can increase suspicion for an underlying syndromic or genetic etiology. In this patient, gray matter heterotopia represents an additional CNS malformation warranting consideration of further evaluation. A comprehensive assessment may include a three-generation family history, detailed developmental and physical examination, evaluation for associated abnormalities, and genetic testing such as chromosomal microarray.

Given the additional CNS abnormality identified on MRI, further clinical and genetic evaluation may help determine whether the patient's AgCC represents an isolated malformation or part of a broader congenital syndrome.

CONCLUSION

Agenesis of the corpus callosum is a congenital malformation with a highly variable clinical presentation. When identified on imaging, careful evaluation for associated CNS abnormalities and other congenital or genetic findings can help distinguish isolated AgCC from a broader syndromic process and guide appropriate management.

Nanobodies in Neurological Disease: Advances in Engineering, Delivery, and Therapeutic Applications

Investigator: Raj Vinayak Nair, B.S.
Mentor: Alberto E. Musto, MD, Ph.D.
Co-Authors(s):
Alberto E. Musto, Macon & Joan Brock Virginia Health Sciences Eastern Virginia Medical School
Viviana Parreno, National Institute of Agricultural Technology INTA
Shinjer Li, Macon & Joan Brock Virginia Health Sciences Eastern Virginia Medical School
Shirish Yasa, Macon & Joan Brock Virginia Health Sciences Eastern Virginia Medical School
Blake Pierpoint, Macon & Joan Brock Virginia Health Sciences Eastern Virginia Medical School
Department(s): Biomedical and Translational Science
Poster #: 31A

INTRODUCTION

Nanobodies, or single-domain antibodies derived from camelid heavy-chain-only antibodies, have emerged as powerful tools in biomedical research and therapeutic development. Their small size, high specificity, tissue penetration capacity, stability, and production capacity can offer advantages over traditional therapeutic antibodies for neurological treatments.

DISCUSSION

This review provides an overview of nanobody structural and biochemical features, new selection and engineering strategies, and current advances in nanobody humanization. We discuss the role of nanobodies in diagnostics, imaging, and therapeutics for neurological disorders, including Alzheimer's disease, Parkinson's disease, multiple sclerosis, epilepsy, and brain tumors. Special attention is given to recent breakthroughs enabling nanobody delivery to the central nervous system, including receptor-mediated transcytosis, intranasal administration, and intrabody engineering. In addition, we explore in silico nanobody discovery platforms powered by artificial intelligence, which accelerate the design of nanobody-antigen complexes.

CONCLUSION

These developments underscore the transformative potential of nanobodies as diagnostic probes and therapeutic agents for a broad range of neurodegenerative, inflammatory, infectious, and neoplastic diseases of the brain.

Evaluating Obstetric Provider Needs Alignment and Patient Engagement Associated with an Integrated Primary Care Clinic as Part of Longitudinal OB Care

Investigator: Thien-Phuoc (Janesah) Dang Ngo, B.S.
Mentor: Michael Kopec, MD
Co-Authors(s):
Angela Goyal, Macon & Joan Brock Virginia Health Sciences Eastern Virginia Medical School
Alison Patev, Macon & Joan Brock Virginia Health Sciences Eastern Virginia Medical School
Department(s): Family and Community Medicine
Poster #: 27B

INTRODUCTION
Fragmented transitions from obstetric (OB) to primary care after delivery may contribute to unmet non-OB healthcare needs and adverse maternal outcomes. To improve care coordination and support for OB patients, a Family Medicine provider was embedded within Maternal Fetal Medicine (MFM) and General OB practices to create an integrated clinic. This study evaluated sociodemographic factors associated with patient engagement, patient needs, and provider-clinic alignment.

METHODS
A retrospective cohort study compared 29 pregnant and postpartum patients who utilized the integrated clinic with 12 referred patients who did not utilize clinic services. Eligible patients delivered between June 2025 and April 2026 and met predefined prenatal/postpartum visit criteria. Manual chart review of Epic collected demographic characteristics, pregnancy outcomes, and the three primary diagnoses addressed during integrated clinic visits. Data from a parallel MFM/OB provider needs assessment survey were collected to identify provider-perceived specialty care needs. Study data were managed in REDCap.

RESULTS
The mean maternal age at delivery was 30.1 years (SD = 5.9) with a mean gestational age of 36.3 weeks (SD = 4.4). The sample was 46.3% Black and 48.8% White, with two patients missing racial data. 75.6% of patients had Medicaid, 19.5% had Tricare, and 4.9% had private insurance or no insurance. The top three patient needs addressed during integrated clinic visits were 1) psychiatric needs such as depression or anxiety, 2) OB-related conditions such as history of Cesarean section and pre-eclampsia, and 3) cardiology concerns such as myocardial infarction and history of cardiac arrest. The MFM/OB provider needs assessment survey responses aligned with patient needs addressed during integrated clinic visits. The specialty with the highest perceived need was psychiatry (n = 24), followed by cardiology (n = 17), and then primary care (n = 13). No significant differences in age, race, gestational age at delivery, or insurance type were observed between patients who utilized the integrated clinic and those who did not (all $p > .05$).

CONCLUSION
Integrated primary care services addressed diverse healthcare needs that aligned with MFM/OB provider-identified needs. While no significant demographic differences were observed between patients who utilized the integrated clinic and those who did not, larger studies are needed to identify factors influencing patient engagement.

Digital cognitive behavioral therapy (dCBT-I) for psychiatrically acute adolescents with suicidal ideation and co-occurring insomnia: An open pilot of intervention feasibility and acceptability

Investigator: Ca Nguyen, B.A.
Mentor: Cassie Glenn, Ph.D.
Co-Authors(s):
Kathryn Loschert, Old Dominion University
Abigail Luce, Old Dominion University
Emelyn Auad, Old Dominion University
Evan Kleiman, Rutgers
Department(s): Psychology
Poster #: 34B

INTRODUCTION

Suicide is a leading cause of death among adolescents in the U.S., with especially high rates among adolescents recently discharged from acute psychiatric care. Insomnia has been linked to increased suicidal ideation (SI) and serves as a promising treatment target to reduce SI in adolescents. Cognitive behavioral therapy for insomnia (CBT-I) has proven efficacious at reducing insomnia, but few people have access to this intervention. Digital versions have the potential to be scaled to reach vulnerable populations, such as those during high risk periods. This open pilot tested the feasibility and accessibility of a smartphone-based version of dCBT-I (SleepioTM) among high-risk adolescents for reducing insomnia and SI.

METHODS

This open pilot included twelve adolescents, ages 14-18 (M=15.8, SD=1.2), recently (past 90 days) hospitalized (inpatient or emergency department) for suicide risk and had co-occurring insomnia. In this project, all adolescents were offered Sleepio, which delivers core CBT-I components (i.e., sleep hygiene, sleep restriction, stimulus control, cognitive therapy, relaxation) through 6 sessions in a smartphone app. This study assessed the feasibility (sessions attended) and acceptability of the intervention from both adolescents and caregivers (post-treatment assessments).

RESULTS

All 12 adolescents completed at least one Sleepio session, and three adolescents (25%) completed all six sessions (i.e., the full treatment package). Partial intervention completion rates were as follows: one session (n=3), two sessions (n=1), three sessions (n=3), and four sessions (n=2).

Adolescents' post-treatment survey ratings (n=10; Scale 0=not at all to 4=very) indicated that they somewhat liked the program (M=2.10, SD=1.10), it was mostly easy to use (M=2.80, SD=1.23), convenient (M=2.90, SD=1.10), and easy to understand (M=3.20, SD=0.79). In addition, adolescents rated that it was moderately useful for improving their sleep (M=2.30, SD=1.42). The lowest ratings were for the program's ability to keep their interest and attention (M=1.60, SD=1.07). Finally, in a post-treatment interview, all teens identified at least one dCBT-I skill they used to improve their sleep (e.g., relaxation).

Caregivers' post-treatment survey ratings indicated that their adolescents, overall, liked the intervention (Scale: 1=low to 5=high; M=3.45, SD=0.69). Most (64%) observed a notable improvement in their adolescent's sleep patterns, and 82% reported an improvement in their adolescent's mood.

CONCLUSION

This pilot study shows preliminary feasibility and acceptability of dCBT-I among high-risk adolescents, as most completed at least one session and were able to identify new skills learned. However, adolescents on average reported that the intervention did not hold their attention, and only 25% completed the full treatment package. Limitations of this study include small sample size and lack of a control group. A small randomized control trial is currently in progress to address these limitations.

Rare Presentation of Appendicitis Within a Ventriculoperitoneal Shunt Associated Hernia: A Radiological Perspective

Investigator: Himali Patel, M.S.
Mentor: Amy Farkas, MD
Co-Authors(s):
Marie Mack, Macon & Joan Brock Virginia Health Sciences Eastern Virginia Medical School
Department(s): Radiology
Poster #: 22A

INTRODUCTION

Acute appendicitis is a common surgical emergency, typically resulting from luminal obstruction and subsequent inflammation. However, appendicitis within a hernia sac is uncommon, with ventral and incisional hernia involvement only reported sporadically in the literature. We present a rare case of appendicitis associated with an incisional hernia from ventriculoperitoneal shunt (VPS) placement.

CASE INFORMATION

A 16-year-old male with a complex medical history including prematurity, hydrocephalus with VPS placement, and spastic quadriplegic cerebral palsy with baclofen pump placement presented to the emergency department with right lower quadrant abdominal pain. The patient was evaluated the day prior for emesis, right lower extremity pain, anxiety, and agitation. Imaging of the right extremity was unremarkable, though labs were significant for leukocytosis (17x10^3/uL), and elevated ANC and CPK. Symptoms improved with pain management, but the patient subsequently returned with abdominal pain. Physical exam revealed right lower quadrant tenderness without peritoneal signs. Computed tomography (CT) demonstrated a dilated (1.2 cm) fluid-filled appendix extending through the abdominal wall musculature within 2 mm of the VPS catheter. The appendix demonstrated inflammatory change without evidence of gross perforation.

Pediatric surgery was consulted for management of appendicitis. Given the proximity of the appendix to the VPS, neurosurgery was also consulted pre-operatively to externalize the shunt. The patient underwent emergent laparoscopic appendectomy with debridement of the abdominal wall incision and shunt externalization. Intraoperative findings included contained appendiceal rupture with purulence contacting the VPS. Cultures obtained from the VPS subsequently grew E. coli. The patient's postoperative course included intensive care for hypoxia and fevers, and repair of a brief shunt disconnection. He was hospitalized for 18 days between shunt externalization and reinternalization.

DISCUSSION

Abdominal complications of VPS include pseudocysts, bowel-related complications, ascites, catheter migration, and hernias. Inguinal hernias occur in approximately 13% of pediatric VPS patients aged 0–5 years, with greatest risk within two years of placement. Incisional hernias, in contrast, are a recognized but poorly characterized complication, with fewer than 10 cases reported.

Appendices within hernia sacs have been extensively described for inguinal (Amyand's) and femoral (de Garengeot) hernias, a small percentage of which present with acute appendicitis. Appendicitis within an incisional hernia is uncommon, reported only sporadically in the literature. CT is crucial for diagnosis and preoperative planning, as presentation varies with the entrapped appendix's location, as demonstrated by our patient. Management of concurrent hernia repair depends on contamination: using mesh repair for clean fields and tissue repair for contamination.

VPS presence further complicated surgical decision making for our patient. Shunt externalization or removal must be considered in a patient with potential for VPS contamination. CT can help assess proximity of infection to a VPS, while intraoperative findings may further inform decision making.

CONCLUSION

Appendicitis within a VPS–associated incisional hernia is, to our knowledge, previously unreported. CT guided diagnosis and treatment, as incision debridement and management of VPS contamination were required in addition to appendectomy. Awareness of this case reinforces the importance of recognizing atypical variations of common disease presentations, and how recognition of imaging findings can facilitate coordination of multidisciplinary care.

Supernumerary Testes Beyond Triorchidism: A Case of Tetraorchidism and Its Management

Investigator: Himali Patel, M.S.
Mentor: Amy Farkas, MD
Co-Authors(s):
Marie Mack, Macon & Joan Brock Virginia Health Sciences Eastern Virginia Medical School
Maria Aguiar, Children's Hospital of the King's Daughters
Sarah Williamson, Children's Hospital of the King's Daughters
Department(s): Radiology
Poster #: 42B

INTRODUCTION

Polyorchidism is a rare congenital genitourinary anomaly defined by more than two histologically confirmed testes. Triorchidism predominates, whereas tetraorchidism — four testes — is exceedingly rare, with fewer than 10 reported cases. We present a case of tetraorchidism, emphasizing imaging findings.

CASE INFORMATION

An 11-year-old male with ADHD, atopic dermatitis, and resolved hydronephrosis presented with two months of intermittent right groin pain. The episodes of pain occurred multiple times per week with occasional radiation to the right lower quadrant. Symptoms improved with ibuprofen but often required school absences. Physical exam revealed bilateral scrotal testes, tenderness of the right groin and scrotum, and a right inguinal hernia with an inguinal bulge. Ultrasound revealed the right testis in the inguinal canal with a moderate hydrocele and a mobile left testis in the inguinal canal and scrotum. Additional bilateral scrotal masses with the same vascularity and echogenicity as testes were identified, consistent with supernumerary testes. The supernumerary right testicle was noted to be atrophic.

Urology consultation recommended right inguinal hernia repair, orchiopexy, and hydrocelectomy. Prior to scheduled surgery, the patient experienced an episode of severe pain and increased right scrotal swelling, concerning for an incarcerated hernia and requiring urgent surgical intervention. Exploration confirmed four distinct testes located as follows: right testis in the inguinal canal with inguinal hernia, right type A3 supernumerary testis in the scrotum, left testis in the scrotum, and left type A3 supernumerary testis in the scrotum.

Intervention included right inguinal orchiopexy, removal of the atrophic right supernumerary testis, and left scrotal orchiopexy of both testes. Histopathology of the removed right supernumerary testis confirmed testicular tissue with seminiferous tubules, germ cells, and Sertoli cells. At six-month follow-up, the patient had recovered well without complication. He will continue monitoring for pain or concerns following self-examination or puberty.

DISCUSSION

Fewer than ten histologically confirmed cases of tetraorchidism have been reported. It is thought to result from anomalous transverse division of the genital ridge. Epididymal and vas deferens anatomy vary in supernumerary testes. Testes without connection to an epididymis and vas deferens lack reproductive potential. Scrotal ultrasound is the first-line imaging modality. MRI can further characterize supernumerary or extrascrotal testes. Given misdiagnosis rates of approximately 22% based on ultrasound alone, accurate imaging is essential.

Management is individualized using the Bergholz classification. Asymptomatic, scrotal testes with favorable anatomy may be observed, while extrascrotal location, cryptorchidism, or torsion may warrant surgery. Neoplasm occurs in approximately 6.4% of cases, with malignancies occurring predominantly in cryptorchid supernumerary testes. Thus, cryptorchidism is an important factor when considering surveillance, orchiopexy, or orchiectomy. Given the rarity of tetraorchidism, management should be individualized to the patient's history and clinical symptoms, finding balance between preservation of reproductive function and malignancy risk.

CONCLUSIONS

Tetraorchidism is an exceedingly rare anomaly. Management depends on the location and anatomy of each supernumerary testis. The Bergholz functional classification guides individualized care, favoring surveillance for scrotal, asymptomatic, imaging-confirmed testes and surgery for extrascrotal location, cryptorchidism, or torsion. Because cryptorchidism is the principal malignancy risk factor, accurate characterization of each testis is essential.

Successful Treatment of Refractory Long COVID Headache with Staged Peripheral Nerve Decompression: A Case Report

Investigator: Anjani Patibandla, B.S.
Mentor: Yifan Guo, MD
Co-Authors(s):
Robin Bai, Texas Tech University Health Sciences Center at the Permian Basin
Adam Evans, Macon & Joan Brock Virginia Health Sciences Eastern Virginia Medical School
Department(s): Plastic and Oral Maxillofacial Surgery
Poster #: 15A

INTRODUCTION

Headache is a frequent neurologic manifestation of Long COVID, defined as persistent or newly developed symptoms following acute SARS-CoV-2 infection. However, the mechanisms underlying persistent headache and effective treatments remain uncertain. Headaches may develop after infection in patients without a prior headache disorder and can resemble migraine, tension-type headache, or mixed phenotypes. Management is generally directed toward the presenting phenotype and may provide limited relief in refractory cases. Although peripheral nerve dysfunction has increasingly been recognized in Long COVID, the role of focal nerve compression in post-COVID headache remains unclear. We describe a young woman with new-onset, treatment-resistant chronic daily headache following COVID-19 who experienced sustained resolution after peripheral nerve decompression.

CASE INFORMATION

A 19-year-old woman with postural orthostatic tachycardia syndrome and complex regional pain syndrome type I of the left lower extremity, but no history of migraine or other primary headache disorder, developed severe headaches approximately three weeks after SARS-CoV-2 infection. Symptoms included diffuse head pain, retro-orbital pressure, visual changes, photophobia, and phonophobia. Over two years, headaches became continuous and significantly impaired school attendance and daily functioning. Multiple medications, botulinum toxin injections, and repeated peripheral nerve blocks provided inadequate or temporary relief. Severe nausea and poor oral intake resulted in a 25-pound weight loss and temporary nasogastric feeding. Brain and spine magnetic resonance imaging and rheumatologic evaluation were unrevealing. Targeted blocks of the bilateral supraorbital, supratrochlear, and greater occipital nerves produced substantial temporary relief, prompting staged peripheral nerve decompression. Surgical exploration demonstrated vascular compression, fascial scarring, and muscular fibrosis surrounding the affected nerves. Following decompression, headache severity and frequency progressively declined, with complete resolution by one-year follow-up. The Pediatric Migraine Disability Assessment (PedMIDAS) score improved from >50 to 0, and the Headache Impact Test-6 (HIT-6) score was 42. She reported only mild headaches approximately once weekly and returned to school and subsequently college.

DISCUSSION/CLINICAL FINDINGS

The pathophysiology of Long COVID headache is likely multifactorial, with proposed contributions from inflammation, altered pain signaling, autonomic dysfunction, and peripheral nerve abnormalities. Recent studies demonstrating small-fiber dysfunction in Long COVID provide increasing evidence of peripheral nervous system involvement in persistent post-COVID pain. Peripheral nerve compression has also been implicated in other refractory headache syndromes and may respond to surgical decompression. In this patient, improvement after targeted nerve blocks and direct evidence of nerve compression at surgery suggest that focal peripheral pathology contributed to her symptoms. This response raises the possibility that diagnostic nerve blocks could identify patients with Long COVID headache who have a surgically addressable peripheral pain source. Further investigation is warranted to evaluate this potential treatment pathway.

CONCLUSION

This case demonstrates a novel therapeutic approach to refractory Long COVID headache in a patient without a pre-existing headache disorder. Targeted nerve blocks identified potential sites of peripheral involvement, while staged decompression was followed by sustained resolution of chronic daily headache and substantial functional recovery. Peripheral nerve evaluation may warrant consideration in selected patients with treatment-resistant Long COVID headache.

Low-Dose Buprenorphine Induction for 7-Hydroxymitragynine Dependence in a Twin Pregnancy: A Case Report

Investigator: Katherine Pepper, B.S.
Mentor: Alana Dopp, MD
Co-Authors(s):
None listed.
Department(s): Psychiatry and Behavioral Sciences
Poster #: 16A

INTRODUCTION

7-Hydroxymitragynine (7-OH), a mu-opioid receptor partial agonist derived from kratom, is increasingly marketed as a concentrated recreational analgesic and was recently placed under temporary DEA scheduling. Evidence to guide management of 7-OH dependence in pregnancy is essentially absent. We present the first published case of a pregnant patient seeking 7-OH cessation, treated with low-dose buprenorphine induction.

CASE INFORMATION

A 36-year-old woman, gravida 5, at 20 weeks' gestation with a dichorionic-diamniotic twin pregnancy, ADHD, and anxiety was referred by her obstetric provider to stop 7-OH. She reported a two-year history, currently 15 mg six times daily (90 mg/day) from an online distributor, with escalating doses to maintain effect and avoid withdrawal, consistent with tolerance and dependence. An intake drug screen did not detect 7-OH, as routine immunoassays do not identify mitragynine or metabolites. She underwent a 7-day low-dose buprenorphine/naloxone protocol, titrating from 0.5 mg/day to 12 mg/day, then continued titration to 32 mg/day, above the FDA-labeled maximum, discontinuing 7-OH 18 days after completing induction. She was maintained on 16 mg/day at cesarean delivery at 38 weeks. Neither twin developed neonatal opioid withdrawal syndrome (NOWS) (birth weights 2670 g and 2830 g; Apgars 8 and 9; both appropriate for gestational age; length of stay 4 days). Postoperatively she took two kratom capsules for pain and was maintained on 24 mg/day.

DISCUSSION

Low-dose buprenorphine induction enabled 7-OH cessation in pregnancy without a pre-initiation withdrawal period, with a favorable neonatal course and no NOWS in either twin. The requirement of 32 mg/day reflects both the increased buprenorphine metabolism of pregnancy and the dependence liability of concentrated 7-OH products, which differ substantially from traditional whole-leaf kratom. The buprenorphine-naloxone combination product was used, consistent with cohort data showing comparable or more favorable outcomes relative to buprenorphine alone. Because standard immunoassays do not detect 7-OH, a negative screen does not exclude use.

CONCLUSION

Clinicians should screen for kratom/7-OH use in pregnancy, counsel on withdrawal risk, and consider low-dose buprenorphine induction as a viable strategy for transitioning patients onto medication for opioid use disorder (MOUD). Standardized protocols and reporting are needed.

MRI-Derived Subcutaneous Thigh Fat Measurements as a Surrogate for DEXA-Derived Adiposity in Dermatomyositis patients

Investigator: Christian Pfeffer-Kleemann, B.A.
Mentor: Rebecca Brown, MD, MHSc
Co-Authors(s):
Rasimcan Meral, National Institutes of Health
Mahlon Dyer, National Institutes of Health
Department(s): National Institute of Diabetes and Digestive and Kidney Diseases
Poster #: 09A

INTRODUCTION

Juvenile Dermatomyositis is frequently associated with lipodystrophy, characterized by abnormal adipose tissue distribution. Although DEXA scans are useful in providing quantitative measures of regional and total body adiposity composition, MRI allows for greater anatomical detail in assessing specific regional adiposity. We investigated the relationship between DEXA-derived measures of adiposity and MRI derived measurements of subcutaneous thigh fat in patients with dermatomyositis.

METHODS

This cross-sectional analysis assessed 41 patients with juvenile and adult-onset dermatomyositis, who underwent DEXA scans and thigh MRIs within hours or days of each other. Subcutaneous fat thicknesses, cross sectional area, and segmented fat volume were measured at sections corresponding to 25%, 50%, and 75% of the femur length bilaterally. Simple linear regression analyses were run to compare MRI-derived measurements with DEXA-derived leg fat mass, DEXA leg fat percentage, BMI, and total body fat %. Multiple linear regression investigated proximal thigh thickness and cross- sectional area simultaneously in relation to DEXA leg fat percentage.

RESULTS

All MRI-derived measurements demonstrated significant associations with the DEXA derived adiposity values ($p<0.05$). The proximal (25%) thigh thickness demonstrated the strongest associations with total body fat percentage and DEXA derived leg fat percentage. When proximal thickness and cross-sectional area were considered simultaneously, proximal thickness remained significantly associated with DEXA leg fat percentage.

CONCLUSION

DEXA-derived adiposity measures correspond significantly with regional MRI-derived measurements of subcutaneous thigh fat in dermatomyositis. Simple proximal thigh thickness performed particularly well and may represent a useful candidate MRI measure for objectively characterizing adipose tissue distribution. Future studies should determine whether these measurements can identify clinically significant lipodystrophy and monitor changes in fat distribution longitudinally.

The effects of differing insulin signal pathways on fibrinolysis in severe insulin resistance syndromes

Investigator: Christian Pfeffer-Kleemann, B.A.
Mentor: Marissa Lightbourne, MD, MPH
Co-Authors(s):
Rebecca Brown, National Institutes of Health
Department(s): National Institute of Diabetes and Digestive and Kidney Diseases
Poster #: 31B

INTRODUCTION

Insulin resistance is associated with impaired fibrinolysis and increased cardiovascular risk. Elevated plasminogen activator inhibitor-1 (PAI-1), a major inhibitor of fibrinolysis, has been associated with insulin resistance and hyperinsulinemia. However, whether PAI-1 elevation stems from hyperinsulinemia or requires intact downstream insulin signaling remains unclear. We compared blood levels of certain metabolic factors in several groups of patients with severe insulin resistance. One group had insulin receptor mutations (INSR), characterized by receptor-level signaling binding defects, while another groups of patients had lipodystrophy (LD), characterized by severe insulin resistance with relatively preserved/overstimulated downstream pathways, and the final group consisted of healthy volunteers (HV).

METHODS

We performed a cross-sectional analysis of adults ≥18 years with pathogenic INSR variants (n=10), non-HIV lipodystrophy (n=15), or healthy controls (n=14). Patients were age and sex matched. Plasma was collected at baseline, 30 and 120 minutes following a 75-g oral glucose tolerance test (OGTT). Total and active PAI-1, tissue plasminogen activator (tPA), PAI-1–tPA complex, plasmin, plasminogen, fibrin, fibrin monomer, fibrinogen, thrombin, and urokinase were measured by ELISA. Insulin and glucose were measured concurrently. Between-group and within-group differences and associations with insulin were evaluated using regression models.

RESULTS

At baseline, patients with LD demonstrated significantly higher total PAI-1, active PAI-1, tPA, and PAI-1–tPA complex concentrations compared with INSR patients and healthy volunteers. Despite severe hyperinsulinemia, INSR patients demonstrated fibrinolytic factor concentrations similar to the healthy volunteers. During the oral glucose tolerance test, total and active PAI-1 decreased from baseline to 120 minutes in LD despite increasing insulin and glucose, whereas active PAI-1 increased in INSR. Correlational analysis showed that changes in insulin did not consistently predict changes in most fibrinolytic components.

DISCUSSION

Patients with lipodystrophy demonstrated marked elevations in PAI-1 and related fibrinolytic factors, whereas patients with receptor-level insulin resistance had profiles similar to healthy controls despite severe hyperinsulinemia. These findings suggest that hyperinsulinemia is insufficient to explain PAI-1 elevation and that preserved or overactive post-receptor insulin signaling may contribute to impaired fibrinolysis in insulin-resistant states. Further investigation of insulin signaling pathways regulating PAI-1 should utilize larger cohorts and analyze non-plasma paracrine changes. This may help clarify mechanisms contributing to increased cardiovascular risk in insulin resistance.

Characteristics and Sociodemographic Determinants of Oral Immunotherapy Utilization among Food-Allergic Children in Hampton Roads, 2020–2026.

Investigator: Nicholas J. Popolizio, B.A.
Mentor: Angela D. Hogan, MD
Co-Authors(s):
Lindsey Moore, Children's Hospital of the King's Daughters
Department(s): Allergy, Asthma, and Immunology
Poster #: 28B

INTRODUCTION
Food allergy affects approximately 8% of U.S. children. While allergen avoidance remains the standard of care, it can significantly impact quality of life. Oral immunotherapy (OIT) is an established treatment option that induces desensitization through gradual allergen exposure. Prior studies have reported racial and socioeconomic disparities in OIT utilization. This study aimed to characterize pediatric patients receiving OIT in Hampton Roads and identify potential disparities in access to care.

METHODS
We conducted a retrospective cohort study of pediatric patients who underwent OIT at Children's Hospital of The King's Daughters (CHKD) Allergy & Immunology clinics between January 1, 2020, and February 10, 2026. Patients were identified through a secure database. Demographic, clinical, treatment, and socioeconomic data were collected, including race/ethnicity, atopic comorbidities, insurance status, home value, OIT food, use of Palforzia or omalizumab, and adverse reactions. Home values were compared with the June 2026 Hampton Roads median sale price ($395,000).

RESULTS
Ninety-two patients underwent OIT. Most identified as White (82.6%), non-Hispanic (97.8%), and male (54.3%). Atopic dermatitis (72.8%), allergic rhinitis (44.6%), and asthma (23.9%) were common comorbidities. Peanut OIT was the most frequently prescribed therapy (67.4%), followed by milk (13.0%) and Palforzia (12.0%).

A total of 108 OIT-related reactions occurred; 52 patients (56.5%) experienced at least one reaction with 15 reactions occurring in clinic on up-dosing. Twenty-four reactions (22.2%) required epinephrine, and 5 patients required emergency department evaluation, all following home dosing. Eight patients received omalizumab prior to OIT initiation, and none experienced OIT-related reactions.

Potential socioeconomic disparities were identified. Mean home value among OIT patients was $644,072, substantially above the regional median sale price, with 83.0% of patients residing in homes valued above regional median. Most patients had private insurance (73.9%) or Tricare (22.8%), while only 5.4% had Medicaid coverage.

CONCLUSION
Pediatric OIT patients in Hampton Roads were predominantly White, non-Hispanic, and from relatively affluent backgrounds. OIT was generally safe, with few severe reactions and no reactions among patients receiving omalizumab prior to treatment. These findings suggest potential racial and socioeconomic disparities in OIT utilization and highlight the need to improve access to food allergy therapies for underserved populations.

MRI Diagnosis of Bilateral Corporal Cavernosal Herniations Following Corporal Tunneling for Ischemic Priapism: A Rare Delayed Complication

Investigator: Phillip Jennings Poppas, B.S.
Mentor: Swachchhanda Songmen, MD
Co-Authors(s):
Damon Scolari, Macon & Joan Brock Virginia Health Sciences Eastern Virginia Medical School
Stephanie Harper, Macon & Joan Brock Virginia Health Sciences Eastern Virginia Medical School
Department(s): Diagnostic Radiology
Poster #: 23A

INTRODUCTION

Corporal tunneling is reserved for refractory ischemic priapism and carries known risks of fibrosis and erectile dysfunction. Corporal cavernosal herniation is an exceedingly rare and underreported complication characterized by focal outpouching of the cavernosal tissue following corporal intervention. We present a case of bilateral corporal herniations diagnosed by MRI 10 months after corporal tunneling.

CASE INFORMATION

A 28-year-old male presented to the emergency department with 24 hours of priapism refractory to aspiration, irrigation, and phenylephrine. Urology performed corporal tunneling with irrigation and intracavernosal phenylephrine, achieving detumescence. At one-month follow-up, he had palpable, nontender induration at the surgical sites and new erectile dysfunction, attributed to expected postsurgical change with fibrosis. Follow up examinations at five and nine months revealed similar physical exam findings and discomfort associated with the indurations. This prompted dedicated penile MRI to delineate fibrosis vs corporal herniation. MRI revealed bilateral corporal cavernosal herniations with intact tunica albuginea, measuring $2.7 \times 1.6 \times 2.2$ cm on the right and $2.1 \times 2.4 \times 2.9$ cm on the left. Incidental findings of absent enhancement with T1 hypointensity in the anterior right corpus cavernosum concerning for infarction were also noted. He was scheduled for hernia excision with corporal body reconstruction.

DISCUSSION

The mechanism of corporal cavernosal herniation is uncertain but may relate to focal disruption or weakening of the corporal architecture following tunneling. Because initial induration may mimic expected postsurgical fibrosis on physical exam alone, diagnosis is frequently delayed. MRI can help distinguish herniation from postoperative fibrotic change and identify associated complications such as ischemia or infarction, providing valuable anatomic characterization when postoperative induration persists or evolves.

CONCLUSION

This case highlights corporal cavernosal herniation as a rare, delayed complication of corporal tunneling and demonstrates the essential role of MRI in diagnosis when postoperative induration persists or evolves beyond the expected postsurgical course.

Evaluating Baseline Serum IgE and Eosinophil Levels as Predictors of Omalizumab Response in Chronic Spontaneous Urticaria

Investigator: Maria Puglese, B.S.
Mentor: April Pace, D.H.Sc., B.S.M.L.S.
Co-Authors(s):
Daniella Gurovich, Macon & Joan Brock Virginia Health Sciences Eastern Virginia Medical School
Paul Sinno, Macon & Joan Brock Virginia Health Sciences Eastern Virginia Medical School
Kyunghyun Kim, Macon & Joan Brock Virginia Health Sciences Eastern Virginia Medical School
Department(s): Eastern Virginia Medical School Brickell Medical Sciences Library
Poster #: 28A

INTRODUCTION
Chronic spontaneous urticaria (CSU) is a debilitating inflammatory skin disease characterized by recurrent wheals, angioedema, or both without an identifiable trigger. Omalizumab is an effective treatment for antihistamine-refractory CSU; however, treatment response varies among patients. Baseline serum immunoglobulin E (IgE) and eosinophil levels have been proposed as potential biomarkers of treatment response. This systematic review evaluated the association between baseline serum IgE and eosinophil levels and response to omalizumab in patients with CSU.

DISCUSSION
A systematic review was conducted using PubMed, Web of Science, Cochrane Library, and Google Scholar. Following duplicate removal, 606 unique records underwent title and abstract screening. 48 full-text articles were assessed for eligibility, and 10 studies met inclusion criteria for qualitative synthesis. Studies with extractable responder versus non-responder data using validated clinical response measures were included in the primary meta-analysis. Pooled mean differences (MD) with 95% confidence intervals (CI) were calculated, and heterogeneity was assessed using I^2. Of the 10 studies included in the systematic review, two met criteria for the primary quantitative synthesis of baseline IgE and eosinophil levels. Responders demonstrated significantly higher baseline serum IgE concentrations than non-responders (MD +109.1 IU/mL, 95% CI 54.1–164.2; $I^2 = 0\%$; $p < 0.001$). In contrast, baseline eosinophil counts were not significantly different between responders and non-responders (MD −14.1 cells/μL, 95% CI −98.1 to 69.8; $I^2 = 44\%$; $p = 0.74$). Sensitivity analyses incorporating studies with less comparable response definitions attenuated the association between IgE and treatment response (MD +79.6 IU/mL, 95% CI −4.4 to 163.6; $I^2 = 51\%$; $p = 0.063$), while eosinophil results remained nonsignificant (MD −21.2 cells/μL, 95% CI −53.0 to 10.6; $I^2 = 0\%$; $p = 0.19$). The remaining eligible studies were included in the qualitative synthesis because they lacked comparable quantitative data for meta-analysis.

CONCLUSION
Higher baseline serum IgE appears to be associated with improved response to omalizumab in CSU when analyses are restricted to studies with comparable responder definitions, whereas baseline eosinophil counts were not predictive of treatment response. The limited number of studies eligible for quantitative synthesis highlights an important evidence gap and underscores the need for standardized outcome reporting in future studies.

The discordance between pCR rate and survival benefit following immuno-oncology (IO) therapy in TNBC

Investigator: Niya Lucille Rhodes, M.S.
Mentor: Amy H. Tang, Ph.D.
Co-Authors(s):
Hailey Gauck, Macon & Joan Brock Virginia Health Sciences Eastern Virginia Medical School
Mary Guye, Sentara
Richard Hoefer, Sentara
Department(s): Biomedical and Translational Science
Poster #: 26A

INTRODUCTION

Triple-negative breast cancer (TNBC) is the most aggressive subtype of breast cancer. Although TNBC accounts for approximately 15% of all breast cancers, it contributes disproportionately to all breast cancer-related mortality (approximately 40%). Its molecular aggressiveness, genetic diversity, genomic instability, and biological heterogeneity make relapsed, multidrug-resistant, and metastatic TNBC particularly challenging to treat. TNBC patients experience 40-50% relapse and 22% mortality rates in general. Before 2021, chemotherapy was the mainstay of standard-of-care (SOC) treatment in both neoadjuvant and adjuvant settings. On July 26, 2021, the FDA approved pembrolizumab (Keytruda), an immune checkpoint inhibitor, in combination with chemotherapy as a new SOC regimen to treat high-risk early-stage TNBC in the neoadjuvant setting. Despite remarkable improvements in pathological complete response (pCR) rates with immuno-oncology (IO) therapy, patients with similar clinicopathological characteristics, including tumor-node-metastasis (TNM) stage and residual cancer burden (RCB), still experience different clinical outcomes. Historically, pCR has been used as an important and reliable prognostic marker to predict event-free survival (EFS), progression-free survival (PFS), and overall survival (OS) in TNBC. Whether the prognostic significance of pCR remains equivalent post-IO-therapy warrants further investigation.

METHODS

We reviewed landmark findings from the KEYNOTE-522 and I-SPY 2 clinical trials and related high-profile publications from 2020 through 2025. We also reviewed all the clinical prognostic markers recognized or utilized by NCI, NCCN, and FDA in the evaluation and management of TNBC. The pCR and long-term survival rates reported in KEYNOTE-522 and I-SPY 2 were extracted and compared to evaluate the relationship between pCR rate and survival benefit following neoadjuvant IO-therapy in TNBC.

RESULTS

The results from KEYNOTE-522 and I-SPY 2 demonstrate marked increases in the pCR rates following IO-therapy, with the reported pCR rates increasing from approximately 40–45% with conventional chemotherapy to approximately 60–65% with IO-therapy. This represents an approximately 40–50% percentage-point absolute increase in the pCR rate. In contrast, improvements in 3/5-year survival rate appear comparatively modest. In KEYNOTE-522, the EFS rate increased from 76.8% to 84.5%, representing a 7.7-percentage-point absolute increase. Thus, the magnitude of improvement in pCR was substantially greater than the corresponding improvement in EFS/PFS/OS. This apparent discordance raises the question that the prognostic relationship between pCR and survival may differ following the new IO-therapy when compared with conventional neoadjuvant chemotherapy (NACT).

CONCLUSION

The new IO-therapy has produced a substantial increase in pCR rates in early-stage TNBC, whereas the corresponding improvement in 5-year survival rate appears comparatively limited/modest. These findings suggest that an increase in pCR does not necessarily translate into a proportional improvement in patient survival following IO-therapy. We propose the concept of "pseudo-pCR" to describe the discrepancies in which the pCR rate following IO-therapy may overestimate its traditional prognostic value in predicting survival benefit in TNBC. Since pCR may become discordant and incongruent with survival benefit post-IO therapy, this "pseudo-pCR" concept is hypothesis-generating and requires further investigation and integrated analyses of tumor/TME/TIME biology, host immune response, residual disease burden, new molecular biomarkers, and long-term clinical outcomes.

Examining associations between sexual orientation acceptance and mental health symptoms among sexual minority adolescents

Investigator: Samantha D. Riley, B.S.
Mentor: Catherine R. Glenn, Ph.D.
Co-Authors(s):
Camille Kissinson, Old Dominion University
Rena Ferrara, Old Dominion University
Richard Liu , Mass General Brigham
Evan Kleiman, Rutgers
Department(s): Department of Psychology
Poster #: 08A

INTRODUCTION

Lesbian, gay, bisexual and queer+ (LGBQ+) youth are more likely to experience depression, anxiety, and suicidal ideation (SI) than their heterosexual peers. These disparities, and increasing rates of poor mental health among LGBQ+ adolescents, make it important to identify protective factors for their mental health. It is unclear how LGBQ+ identity acceptance from others impacts the mental health of LGBQ+ adolescents. This study aims to evaluate whether greater initial (i.e., first learning of identity) and current acceptance of identity from caregivers, close friends, and other peers predict lower depression, anxiety, and SI among LGBQ+ adolescents.

METHODS

Participants for this study were recruited from three collaborating sites within 90 days of discharge from acute psychiatric care units following hospitalization for suicide risk. Adolescents (ages 12-18) participated in a baseline assessment in which they completed validated measures of past-week depression symptom severity (PROMIS pediatric depression scale), past-week anxiety symptom severity (PROMIS pediatric anxiety scale), past-week SI severity (Passive and Active Suicide Ideation Scale: PASIS), as well as perceptions of close others' (i.e., caregivers, friends, peers) acceptance of their sexual orientation identity both when the other first learned of the adolescent's LGBQ+ identity, and currently. Separate multiple linear regression models examined associations between each source (person) and timing (past or current) of acceptance and depression, anxiety and SI severity, controlling for age and whether youth identified as transgender or gender diverse (TGD).

RESULTS

118 adolescents identified as LGBQ+ (55.9% of the full study sample). Higher initial peer acceptance of adolescent sexual orientation was significantly associated with less severe current adolescent anxiety (β=-2.08, p=.001). Conversely, higher current close friend acceptance was associated with more severe adolescent depression (β=2.71, p=.025). Higher current peer acceptance was associated with less severe anxiety at a trend level (β=-1.08, p=.076). All other linear regression models examining associations between initial and current acceptance of adolescents' sexual orientation and mental health outcomes, controlling for age and TGD identity, were not significant.

CONCLUSIONS

Among LGBQ+ adolescents recently hospitalized for suicide risk, greater initial peer acceptance of sexual orientation was associated with lower current anxiety, with a similar trend emerging for current peer acceptance. This suggests peer acceptance may be particularly relevant to anxiety among high-risk LGBQ+ adolescents. In contrast, current acceptance from close friends was unexpectedly associated with increased depression, warranting further investigation. Acceptance from parents, peers, and friends was not associated with past two-week SI severity. However, caregiver and close friend sexual orientation acceptance was relatively high and showed limited variability in this sample, which may have contributed to null results. Further research should examine additional factors related to both acceptance and LGBQ+ adolescent mental health, such as victimization and the presence of LGBQ+ peers, to further characterize the relationship between variables assessed in this project.

Identifying and De-Labeling Inappropriate Penicillin Allergies in a Primary Care Clinic: A Student-Driven Feasibility Study

Investigator: Owen Matthew Rolph, B.S.
Mentor: John E. Snellings, MD
Co-Authors(s):
Christian Busch, Macon & Joan Brock Virginia Health Sciences Eastern Virginia Medical School
Department(s): Family & Community Medicine
Poster #: 44B

INTRODUCTION

Penicillin (PCN) is one of the most common drug allergies reported in the U.S., though evidence suggests that most documented cases are not true IgE-mediated hypersensitivity reactions. Mislabeled allergies can stem from misattribution of infection symptoms and over-reliance on family history, and are associated with poor antibiotic stewardship and worsened health outcomes for patients. Although validated allergy de-labeling protocols exist, they remain underutilized in primary care settings. This student-led study evaluated the implementation of a primary care-based PCN de-labeling protocol, including patient eligibility, acceptance of testing, and the role of medical students in coordinating these efforts.

METHODS

Interviewer-administered questionnaires were used to obtain allergy histories from patients with documented PCN allergies in a primary care clinic. The questionnaires included the PEN-FAST clinical decision rule (score range 0–5), which estimates the likelihood of a positive direct oral challenge (DOC). Patients scored a 0 (<1% risk) if their allergy occurred more than five years ago, their history did not include symptoms of anaphylaxis or severe cutaneous adverse reactions, and they did not require treatment. These individuals qualified for allergy de-labeling without challenge, though optional testing was offered. Patients who scored 1–2 (5% risk) were eligible for a DOC with oral amoxicillin. To assess patient acceptance of de-labeling and identify potential barriers to implementation, participants were asked about their willingness to undergo DOC and, when testing was declined, their reasons for hesitancy. The timing of allergy-related discussion relative to study consent was also recorded to evaluate whether prior discussion influenced participation.

RESULTS

139 of 157 (89.5%) patients consented to participate in the study. Patients who discussed their allergy before consenting were significantly less likely to enroll than those who did not (77.1% vs. 92.2%, $p = 0.018$). Among participants who did consent, 44 scored 0, and 43 scored 1-2. Grouped analysis (0, 1-2, 3-5) demonstrated no significant association between PEN-FAST score and willingness to undergo a DOC ($p = 0.26$). Among patients who declined testing, the most commonly cited reason was concern about another allergic reaction ($n = 11$).

CONCLUSION

Primary care-based PCN allergy screening identified 32.1% of participating patients as eligible for DOC. Although PEN-FAST score was not significantly associated with willingness to undergo DOC, concerns about experiencing another allergic reaction were the most commonly reported barrier to testing. These findings highlight both the potential for structured PCN allergy screening to expand access to de-labeling and the importance of addressing patient concerns during the process. The successful coordination of screening by medical students, initiation of DOCs at the original clinic, and expansion of recruitment to a second facility further demonstrate the feasibility of integrating a student-led de-labeling approach into primary care.

Utilizing Quantitative Magnetic Resonance Imaging Features to Characterize Seizure Status in Glioblastoma Patients

Investigator: Andrei Sanda, B.A.
Mentor: Alberto E. Musto, MD, Ph.D.
Co-Authors(s):
Ibrahima Wann, Old Dominion University
Md Shibly Sadique, Old Dominion University
Michael Evans, Old Dominion University
Khan Iftekharuddin, Old Dominion University
Department(s): Biomedical and Translational Sciences
Poster #: 29B

INTRODUCTION
Glioblastoma Multiforme(GBM) is an aggressive, incurable brain tumor that presents with seizures in roughly one-third of patients. Quantitative MRI features have emerged as promising imaging markers for predicting glioma-associated epilepsy, but evidence in glioblastoma remains limited. In this study, we analyzed MRI scans of GBM patients to uncover relationships between the tumor core, peritumoral edema, and cerebrospinal fluid(CSF) according to seizure status.

METHODS
Preoperative MRI scans from 22 patients in the publicly available Ivy Glioblastoma Atlas Project (Ivy GAP) were obtained through The Cancer Imaging Archive (TCIA) in the modalities of T1-weighted(T1w), T1-post contrast(T1-CE), T2-weighted(T2w), and T2 fluid attenuated inversion recovery(T2 FLAIR). Variables were compared using two-sided exact permutation Mann-Whitney U tests, exact Wilcoxon signed-rank tests, and Fisher's exact tests, with a $p < 0.05$ considered statistically significant.

RESULTS
The analysis compared several volumetric ratios involving the tumor core, peritumoral edema, and CSF stratified by seizure history. Patients with a seizure history(n=5) had higher median edema-to tumor core and edema-to-CSF ratios compared to patients without a seizure history, though these findings were not statistically significant.

CONCLUSIONS
Although no volumetric ratios differed significantly between the seizure-history and no-seizure-history groups, the numerical differences in edema-related ratios warrant validation in larger, more balanced cohorts. Future studies should integrate these quantitative imaging features with relevant clinical and molecular markers to better understand their potential relationship with seizure status in GBM.

A Quality Improvement Project to Improve Patient Flow in the Children's Hospital of the King's Daughters Emergency Department

Investigator: Eleanor (Ellie) Schonberg, M.S.
Mentor: Bejamin Klick, MD
Co-Authors(s):
Courtney Jacobs, Children's Hospital of the King's Daughters
James Burhop, Children's Hospital of the King's Daughters
Gracyn Burhop, Maury High School
Department(s): Emergency Medicine
Poster #: 30B

INTRODUCTION

Long wait times represent a common complaint of patients and their families in the pediatric emergency department (ED). Online reviews of the CHKD ED specifically indicate patients feeling "forgotten about" and waiting for multiple hours without clear reasoning. Group decision making and participation among patients, families and providers are all critical parts of care at CHKD, and negative ED experiences limit care effectiveness and patient feelings of care quality. To better understand the limitations affecting ED flow and efficiency, we performed a retrospective chart review to inform future quality improvement (QI) initiatives.

METHODS

Data related to arrival and departure time, time from order to completion of x-rays, ultrasound, CT scans and lab studies, as well as demographic data such as race, insurance type, age, and gender was collected from 200 patient charts at varying timepoints between January 10, 2024, and April 10, 2026. Length of stay (LOS) was evaluated via quantile regression for different groups. Pearson correlation was used to assess the correlation between age and length of stay. All statistical tests were performed using SPSS 31.0. In addition, surveys of patient and provider feedback were collected via QR code to identify further opportunities for improvement.

RESULTS

Among the variables collected, race, day of the week, arrival time, CT scan, ultrasound imaging and pharmacy orders did not significantly affect LOS. X-rays, room placement, lab studies, increasing age, female sex and increased acuity were all significantly associated with increased LOS. LOS varied based on admission status, with admitted patients having an average 6-hour LOS versus 3-hour average LOS for discharged patients. In surveys, both families and providers reported frustration with long wait times for radiology studies specifically, as well as a desire for more staff and improved communication about expected wait times.

CONCLUSION

While limited in sample size, this study allows for further targeted QI improvement projects, particularly related to significantly increased LOS for x-ray imaging and lab studies. A better understanding of patient flow, sources of delay and inefficiency within the CHKD ED will help identify opportunities to improve existing systems, enhance the patient experience, and increase provider satisfaction.

A Comparison of Relative Value Units in Various Pediatric Surgical Specialties

Investigator: Matthew Serrata, B.S.
Mentor: Yifan Guo, MD
Co-Authors(s):
Alyssa Reese, Macon & Joan Brock Virginia Health Sciences Eastern Virginia Medical School
Jason Pham, Macon & Joan Brock Virginia Health Sciences Eastern Virginia Medical School
Department(s): Plastic and Oral Maxillofacial Surgery
Poster #: 45B

INTRODUCTION

The Relative Value Unit (RVU) is one metric for assessing clinician productivity. A 2023 study revealed that compared to other surgical specialties, plastic surgery had the lowest RVU per hour and the highest operating time. Additionally, pediatric operations have been underrepresented in the annual reassessment of RVUs. The goal of our study was to investigate the relationship between RVU and operating time in pediatric surgical care.

METHODS

The American College of Surgeons National Surgical Quality Improvement Program Pediatric (NSQIP-P) datasets from 2019 to 2023 were compiled. Cases were sorted by CPT code strings, and the top 10 most common CPT codes for each specialty were isolated. CPT codes with non-zero RVUs were included (N = 16,840). Pearson correlation coefficients were calculated for total RVUs versus total operating room time for each case.

RESULTS

Results of the correlation analyses across seven surgical specialties are illustrated in Figure 1. On average, pediatric orthopedic surgery procedures had the greatest RVU per operative hour (R = 0.84), while pediatric surgery and plastic surgery had the lowest (R = 0.10 and 0.19, respectively). Orthopedic surgery's average operative time was near the median (234 minutes), while plastic surgery was higher (290 minutes).

CONCLUSION

Plastic surgery procedures again demonstrated some of the lowest RVU-per-hour and highest operating-time values among the specialties studied, now replicated in a pediatric population. These findings suggest RVU valuations may not adequately capture the operative burden of pediatric plastic surgery, warranting reassessment of how productivity is measured in this field.

The Reproductive Cost of Deep Space: Galactic Cosmic Radiation Impairs Ovarian Function and Is Associated With Prolonged Decision-Making in Female Rats

Investigator: Anyah Skipwith, M.S.
Mentor: Diane M. Duffy, Ph.D.
Co-Authors(s):
Gavin Hughes, Macon & Joan Brock Virginia Health Sciences Eastern Virginia Medical School
Mitch Warren, Macon & Joan Brock Virginia Health Sciences Eastern Virginia Medical School
Rebecca Duncan, Macon & Joan Brock Virginia Health Sciences Eastern Virginia Medical School
James Vettichira, Macon & Joan Brock Virginia Health Sciences Eastern Virginia Medical School
Richard Britten, Macon & Joan Brock Virginia Health Sciences Eastern Virginia Medical School
Department(s): Biomedical and Translational Science
Poster #: 10B

INTRODUCTION

Long-duration Mars missions will expose female astronauts to galactic cosmic radiation (GCR), a deep-space radiation environment that cannot be fully shielded. Ovarian follicles are finite and highly susceptible to ionizing radiation, yet GCR's effects on the ovary remain unknown. We hypothesize that GCR will negatively impact follicular development and ovulation.

METHODS

GCRSim mimics the GCR encountered during Mars missions. Female Wistar rats were assigned to GCRSim/GCRSim (G/G, n=8) and Sham (n=8) treatment groups. Irradiated animals received 20 cGy of space radiation delivered in two doses separated by 6 months, sham animals received no radiation. Ovaries were collected during diestrus, embedded in paraffin, sectioned, and stained with H&E. Follicles were classified as primordial (squamous granulosa cells), primary (single cuboidal layer), secondary (multiple cuboidal layers), or antral (visible antrum). Follicle populations and corpora lutea were counted and analyzed. In a subset of five animals per group, secondary and antral follicles were assessed for mitotic figures and pyknotic nuclei as indicators of follicular proliferation and atresia. These animals were part of a study evaluating GCR effects on attentional set-shifting (ATSET) performance, which measures cognitive flexibility.

RESULTS

G/G ovaries had fewer secondary follicles than Sham ovaries ($p=0.048$, Welch's t-test). However, primordial, primary, and antral follicle counts were similar in both treatment groups. Sham ovaries contained more corpora lutea than G/G ovaries ($p=0.046$, Mann-Whitney U), and the proportion of ovaries lacking corpora lutea trended higher in the G/G group than in the Sham group ($p=0.066$, Fisher's exact). Corpora lutea were present in 2/8 G/G ovaries and 6/8 Sham ovaries. G/G antral follicles had fewer mitotic figures than Sham follicles ($p=0.028$, Welch's t-test), with a trend toward reduced mitosis in secondary follicles ($p=0.061$). G/G antral follicles had more pyknotic nuclei than Sham follicles ($p=0.028$, Welch's t-test), with a trend toward increased pyknosis in secondary follicles ($p=0.065$). During the compound discrimination reversal (CDR) stage of the ATSET, which requires response updating following a change in learned contingencies, rats lacking corpora lutea took longer to make decisions than rats with corpora lutea ($p=0.026$).

CONCLUSION

GCRSim exposure reduced secondary follicle and corpora lutea counts, suggesting impaired follicular development and ovulation. Reduced mitotic activity and increased pyknosis in G/G follicles suggest that impaired follicular proliferation and increased atresia may contribute to reduced follicle development. Reduction of corpora lutea may decrease progesterone production and alter reproductive cycling, which is associated with early menopause, cardiovascular disease, osteoporosis, and early mortality. Additionally, absence of corpora lutea was associated with prolonged decision-making time. This suggests an association between ovarian function and cognitive flexibility following GCR exposure. Prolonged response times may be consequential during long-duration spaceflight, where timely decision-making and cognitive performance are critical to mission success. Further longitudinal studies are needed to determine whether these ovarian and cognitive changes are transient or permanent, and their implications for performance and female reproductive health after long-duration spaceflight.

Luminal Lipid Oxidation & Foam Cell Formation in Benign Prostatic Hyperplasia: Evidence for an Atherosclerosis-like Mechanism

Investigator: Darel Connor Snead, B.S.
Mentor: Petra Popovics, Ph.D., M.S.
Co-Authors(s):
Thaissa Horne, Macon & Joan Brock Virginia Health Sciences Eastern Virginia Medical School
Alicia Malewska, University of Texas Southwestern
Douglas Strand, University of Texas Southwestern
Petra Popovics, Macon & Joan Brock Virginia Health Sciences Eastern Virginia Medical School
Department(s): Biomedical and Translational Science
Poster #: 11B

INTRODUCTION

Benign Prostatic Hyperplasia (BPH) is characterized by nonmalignant enlargement of glandular and stromal compartments, inflammation, and tissue remodeling. BPH progression can produce lower urinary tract symptoms (LUTS) through urethral compression. However, the mechanisms driving BPH progression remain incompletely understood, highlighting the need to identify pathological mechanisms that may provide additional therapeutic targets beyond symptom management. Recent studies identified increased lipid accumulation and lipid-laden macrophages (foam cells) within the prostatic lumen as previously underrecognized pathological features. These findings raise an important mechanistic question: what drives macrophage recruitment and foam-cell formation within the prostatic lumen? In atherosclerosis, oxidation of retained lipids promotes macrophage recruitment and foam-cell formation within the arterial intima. We therefore hypothesize that oxidative modification of locally retained lipids may similarly promote macrophage recruitment, foam-cell formation, and tissue remodeling within the prostatic lumen.

METHODS

Whole-mount prostate tissues were obtained from organ donors (n=5) and patients undergoing simple prostatectomy for BPH (n=6) at UT Southwestern Medical Center. Global protein oxidative stress was assessed using the OxyIHC kit, while lipid peroxidation was evaluated using 4-hydroxynonenal (4-HNE) immunohistochemistry. Epithelial 4-HNE staining intensity was quantified with ImageJ and group differences were assessed by an unpaired t-test in GraphPad Prism. 7-ketocholesterol (7-KC), a product of cholesterol oxidation, and CD68+ macrophages were evaluated by immunofluorescence microscopy. Spatial localization of oxidative markers and CD68+ macrophages was evaluated in both donor and BPH prostate tissues.

RESULTS

Quantitative analysis demonstrated significantly increased epithelial 4-HNE staining intensity in BPH compared with donor prostate tissue ($p<0.001$). In contrast, OxyIHC revealed no apparent differences in global protein oxidative stress between donor and BPH tissues. Immunofluorescence demonstrated 7-KC immunoreactivity in both donor and BPH tissues. In one obstructed BPH specimen, intraluminal accumulation of 4-HNE, 7-KC, and CD68+ macrophages was observed, consistent with a localized oxidative microenvironment; however, this pattern was not found in the remaining specimens.

CONCLUSION

These findings support preferential epithelial lipid peroxidation as a feature of BPH despite no apparent increase in global protein oxidative stress likely due to differences in the sensitivity of these techniques. The intraluminal accumulation of oxidized lipids and CD68+ macrophages in an obstructed BPH specimen, but not in specimens without ductal obstruction, raises the possibility that localized oxidative-inflammatory microenvironments within the prostatic lumen may be associated with ductal obstruction. Together, these findings are consistent with a model in which selective lipid oxidation may contribute to an atherosclerosis-like inflammatory pathway in BPH. Further studies examining oxidized lipid-macrophage co-localization and lipidomic differences between donor and BPH prostate tissues will help determine which oxidized lipid species are associated with BPH and whether they serve primarily as markers of disease or actively contribute to macrophage recruitment, foam-cell formation, and BPH progression.

Upper Extremity Revascularization with Radial Recurrent Artery-to-Deep Palmar Arch Bypass Using a Lesser Saphenous Vein Graft: A Case Report

Investigator: Laura Snow, B.S.
Mentor: Manas Nigam, MD
Co-Authors(s):
Adam Akari, Macon & Joan Brock Virginia Health Sciences Eastern Virginia Medical School
Jason Pham, Macon & Joan Brock Virginia Health Sciences Eastern Virginia Medical School
Department(s): Plastic and Reconstructive Surgery
Poster #: 38B

INTRODUCTION

Upper extremity bypass is a rare surgery performed in cases of chronic ischemia affecting the hand, forearm, or arm. Interventions for critical ischemia can include bypass, sympathectomy, endarterectomy with patch angioplasty, venous arterialization, or amputation1. Ultimately, bypass can lead to significant improvements in ischemia symptoms2. We present a unique case of right upper extremity revascularization using a lesser saphenous vein graft to connect the radial recurrent artery to deep palmar arch for ischemia and ulceration.

CASE INFORMATION

A 46-year-old, left-hand-dominant woman with a history of end stage renal disease, two renal transplants, and chronic DVT of the right lower extremity managed with apixaban presented with worsening right-hand pain and ulceration of the small finger. She was previously evaluated by vascular surgery, who recommended cilostazol and nitroglycerin without improvement of her symptoms. Digital pressures showed critical insufficiency with dampened or flat-lined waveforms in each digit. Arterial duplex showed bilateral upper extremity small vessel disease. Angiogram showed radial/ulnar artery occlusion at the level of the forearm and perfusion of the deep palmar arch via anterior interosseous artery.

DISCUSSION

The patient underwent a right upper extremity bypass in which the right radial recurrent artery was anastomosed to the deep palmar arch using the reversed contralateral lesser saphenous vein graft tunneled superficial to the carpal tunnel. Intraoperatively, the ulnar artery was thrombosed, and both the ulnar and radial artery were heavily calcified as evidenced by the angiogram. The radial recurrent artery was found to have the least calcifications, and an end-to-end anastomosis was performed using 9-0 nylon sutures. The superficial palmar arch was incomplete. The deep palmar arch was chosen as the outflow vessel through an end-to-side anastomosis using 9-0 nylon sutures. Postoperatively, she was kept on a therapeutic heparin drip, and biphasic signals were visualized on Doppler up to the metacarpophalangeal joint of the volar thumb and the PIP joints of all the fingers, followed by outpatient apixaban. In the two months following the procedure, the patient was found to have significant improvement in the ulceration of her small finger.

CONCLUSION

This unique case presents the novel technique of bypass connecting the radial recurrent artery to the deep palmar arch and highlights the utilization of lesser saphenous vein grafts in patients with vasculopathy. Among conduit options, a single paper found the lesser saphenous vein to have 87% patency after 12 months3.

Bioinformatics Analysis of Disrupted Intercellular Communication Networks in TNBC Immune Evasion

Investigator: Manas Tiwari, B.S.
Mentor: Lifang Yang, MD, Ph.D.
Co-Authors(s):
Paul Cheddie, Macon & Joan Brock Virginia Health Sciences Eastern Virginia Medical School
Linsong Zhang, Macon & Joan Brock Virginia Health Sciences Eastern Virginia Medical School
Department(s): Biomedical and Translational Sciences, Division of Microbiology & Molecular Cell Biology
Poster #: 12B

INTRODUCTION

Triple Negative Breast Cancer (TNBC) is an aggressive cancer with fewer targeted therapies.

Chemotherapy combined with anti–PD-1/PD-L1 immunotherapy is currently the standard of care for TNBC patients; however, fewer than 50% of patients achieve a durable response, pointing to additional immunosuppressive mechanisms within the tumor microenvironment (TME). TNBC progression is shaped by reciprocal signaling among malignant, immune, stromal, and vascular cells, which can establish protumorigenic and immunosuppressive circuits. We hypothesize that TNBC tumors harbor non-cell-autonomous intercellular communication networks that facilitate immune evasion through specific ligand-receptor signaling pathways.

METHODS

We conducted an exploratory bioinformatics analysis using publicly available scRNA-seq and spatial transcriptomics data of 10 TNBC patients. Quality control filtered out cells with <20 features or >15% mitochondrial reads. Single-cell data were processed in Seurat to annotate major tumor, stromal, and immune lineages using canonical marker expression. CellChat was used to infer cell-cell communication networks and identify dominant ligand-receptor interactions. Spatial transcriptomics data were analyzed in R to map gene expression and evaluate the spatial co-localization of predicted interacting cell populations and ligand-receptor pairs within tumor tissues.

RESULTS

Single-cell analysis identified diverse cell populations, including cancer epithelial cells, cancer-associated fibroblasts (CAFs), myeloid cells, and lymphocytes, within the TNBC TME. CellChat analysis revealed multi-lineage signaling networks, with CAFs showing the strongest outgoing signaling intensity and myeloid cells the greatest incoming communication. Across stromal-epithelial and immune-epithelial communication axes, the PPIA–BSG emerged as a prominent, recurrent ligand–receptor signaling bridge linking CAFs and myeloid cells to cancer epithelial cells. Comparative CellChat analysis revealed key tumor-specific signaling shifts: cancer cells gained myeloid-derived EGFR signaling and a broad CAF/myeloid receptor switch toward Syndecan-1 (SDC1) matrix interactions, alongside the loss of CAF-derived IGF signaling. Spatial transcriptomic analysis confirmed the co-enrichment of cancer epithelial cells, CAFs, and myeloid populations along with the spatial co-localization of PPIA and BSG transcripts at dense tumor–stroma interfaces

CONCLUSION

TNBC intercellular communication is coordinated across a complex multi-lineage network rather than driven by a single cell type. The altered communication in TNBC involves both tumor-specific gains (EGFR activation and SDC1 receptor rewiring) and conserved stroma–tumor drivers. The pervasive recurrence and spatial colocalization of the PPIA–BSG matrix-remodeling axis represents a high-priority candidate for functional validation and novel therapeutic targeting.

1.5-Ventricle Repair of Double Inlet Left Ventricle with S,D,S Segmental Anatomy and a Functional Hypoplastic Right Ventricle in an Infant

Investigator: Jhobani Torres-Gomez, B.S.
Mentor: Umar S. Boston, MD
Co-Authors(s):
Jacob Chen, Macon & Joan Brock Virginia Health Sciences Eastern Virginia Medical School
Kaitlin Hardy, Children's Hospital of the King's Daughters
Department(s): Cardiac Surgery
Poster #: 24A

INTRODUCTION

Double-inlet left ventricle (DILV) is a rare form of a functionally univentricular heart typically managed through staged single-ventricle palliation. In selected patients with a hypoplastic but morphologically developed and functionally preserved right ventricle (RV), a 1.5 biventricular repair can be considered by septating the ventricles.

CASE INFORMATION

A 5-month-old female with prenatally diagnosed DILV and S,D,S segmental anatomy. Preoperative transesophageal echocardiography demonstrated a large inlet ventricular septal defect, a small-to-moderate secundum atrial septal defect. The RV was moderately hypoplastic however demonstrated tripartite morphology, prominent trabeculation, significant hypertrophy, and preserved systolic function. Moderate pulmonary valve stenosis was also present, with a peak gradient of 42 mm Hg. Given the preserved RV morphology and function, a 1.5-ventricle strategy was selected. This entailed septating the ventricle with a 3mm fenestrated patch of the 18mm ventricular septal defect and bidirectional Glenn shunt. The ASD was closed primarily leaving a 3mm fenestration as well. Postoperative echocardiography demonstrated preserved RV and LV systolic function, good Glenn flow with additional antegrade pulmonary blood flow, and pulmonary valve gradient of 26mmHg. The postoperative course was complicated by complete heart block requiring permanent epicardial dual-chamber pacemaker placement on postoperative day 7. The patient's postoperative saturations were greater than 95% on room air.

DISCUSSION

Although DILV is generally treated through a single-ventricle pathway, ventricular size alone may not fully characterize the functional potential of a hypoplastic RV. Assessment of RV morphology and systolic function may identify selected patients who are amenable to ventricular septation with or without a Glenn. In this patient, tripartite RV morphology supported the decision to pursue a 1.5 ventricular repair rather than perform a Glenn with a Pulmonary Artery (PA) band as would be done if single ventricle palliation was pursued. The addition of a bidirectional Glenn reduced systemic venous preload on the RV. It is anticipated that with future RV growth the VSD fenestration can be closed via a percutaneous route in the cauterization lab. The development of complete heart block illustrates the potential complexity of this approach to septet the heart.

CONCLUSION

A 1.5-ventricle repair may be a feasible alternative to conventional single-ventricle palliation in carefully selected patients with DILV and a hypoplastic but functional RV. Evaluation of RV morphology and function is critical to guide surgical strategy. Long-term follow-up is necessary to assess RV growth and function and to determine if the complications associated with long term Fontan physiology can be avoided.

Lyme Neuroborreliosis with Bilateral Bell's Palsy

Investigator: James Sajeev Vettichira, B.S.
Mentor: Catherine Derber, MD
Co-Authors(s):
Salma Yousuf, Macon & Joan Brock Virginia Health Sciences Eastern Virginia Medical School
Department(s): Infectious Disease
Poster #: 25A

INTRODUCTION

Facial nerve palsy is the most common cranial neuropathy of Lyme neuroborreliosis (LNB), and bilateral involvement occurs in roughly 30% of Lyme facial palsy. Erythema migrans lacking central clearing is readily mistaken for cellulitis.

Lyme neuroborreliosis is a neurologic manifestation of Lyme disease that may present with meningitis, radiculopathy, or cranial nerve palsy. Facial nerve involvement is common, but rapidly progressive bilateral facial palsy is uncommon and may complicate diagnosis, particularly when the characteristic erythema migrans rash is absent or mistaken for cellulitis.

CASE INFORMATION

A 22-year-old man with recent military training in North Carolina and Indiana presented with headache, neck pain, intermittent limb paresthesias, and a confluent erythematous rash of the right neck without central clearing. Three weeks earlier, the rash had been diagnosed as cellulitis on CT and treated with cephalexin, with apparent improvement that reinforced the initial diagnosis. He recalled no tick bite and was afebrile, with a white cell count of 10.2×10^9/L and ESR of 17 mm/h. Left facial weakness present on admission progressed to right-sided weakness on hospital day 3 the second day of intravenous ceftriaxone. Lyme serology was positive, and CSF showed lymphocytic pleocytosis with elevated protein and normal glucose. MRI of the internal auditory canals demonstrated enhancement of cranial nerves III, V, VI, and VII, yet the deficit remained confined to the facial nerves, with no ophthalmoplegia, diplopia, or trigeminal sensory loss. Corticosteroids were withheld. He received intravenous ceftriaxone followed by oral doxycycline, with complete resolution documented 14 days after discharge.

DISCUSSION

Three lessons. Erythema migrans without central clearing mimics cellulitis, and response to an agent inactive against Borrelia is not reassurance. Contralateral progression after appropriate therapy is expected and is not treatment failure. Radiologic involvement may substantially exceed the clinical deficit, suggesting the inflammatory process is more extensive than bedside examination reveals a dissociation not previously described in bilateral LNB facial palsy.

CONCLUSION

Lyme neuroborreliosis should be considered in patients presenting with aseptic meningitis and progressive facial nerve palsy, particularly when the weakness is bilateral. This case demonstrates how Lyme disease may initially resemble bacterial cellulitis and highlights the importance of recognizing evolving neurologic findings, obtaining appropriate serologic and cerebrospinal fluid testing, and initiating targeted antimicrobial therapy. It also signifies that radiologic involvement of the cranial nerves can be more extensive than the bedside examination suggests. It also reminds us that steroids offer no benefit in Lyme neuroborreliosis.

A Retrospective Review of Injury Patterns Associated with Manuel and Light Electric Vehicles In Pediatric Patients

Investigator: Jonah Wright, B.S.
Mentor: Katherine Davenport, MD
Co-Authors(s):
Madison Baldauf, Macon & Joan Brock Virginia Health Sciences Eastern Virginia Medical School
Rhiannon Torres, Children's Hospital of the King's Daughters
Jamie Golden, Children's Hospital of the King's Daughters
Department(s): Pediatrics Trauma Surgery
Poster #: 35B

INTRODUCTION
Light electric vehicles (electric bikes and scooters) are becoming increasingly accessible as a transportation method for children. Despite their high attainable speeds, there are no age, weight, training, or protective equipment requirements. Current literature on pediatric injuries associated with light electric vehicles is quite limited. This study sought to compare injury patterns and clinical characteristics of pediatric patients injured while riding light electric versus manual vehicles (manual bikes and scooters).

METHODS
A retrospective review was conducted of 262 pediatric patients treated at Children's Hospital of The King's Daughters following injuries involving light electric vehicles or manual vehicles from May 1st, 2018 to May 1st, 2025. Demographics, injury severity score (ISS), prehospital transport, trauma activation, protective equipment use, injury type, operative management, intensive care unit (ICU) admission, and hospital length-of-stay (LOS) were collected for each patient and compared between light electric and manual vehicle groups.

RESULTS
A smaller proportion of riders injured on light electric vehicles were female compared to male (13% female vs 28% male, $p = 0.035$). Overall, mean ISS was similar between light electric and manual vehicle groups (6 electric vs 6 manual). Light electric vehicle injuries, however, were significantly more likely to result in trauma activation (71% electric vs 46% manual, $p = 0.008$), head or facial injury (74% electric vs 50% manual, $p = 0.006$), and extremity injury (73% electric vs 52% manual, $p = 0.02$). Protective equipment use was low for both groups (9.7% electric vs 15.7% manual). Prehospital transport by emergency medical services (EMS) (74% electric vs 77.6% manual), ICU admission (6% electric vs 8% manual), and LOS in the hospital (1.5 days electric vs 1.9 days manual) were comparable between light electric and manual vehicle groups. Operative management was required in 22.6% of light electric vehicle injuries and 37.4% of manual vehicle injuries ($p = 0.08$).

CONCLUSION
Despite similar overall injury severity, pediatric light electric vehicle injuries exhibited a distinct, worrisome injury pattern that included significantly higher rates of trauma activation, head or facial injury, and extremity injury when compared to manual vehicles. Of particular interest was the high rate of head and facial injury with very low rates of protective equipment use. These findings highlight the importance of pediatric-specific safety regulations for electric bicycles and scooters, including minimum age recommendations, helmet use, speed limitation, and rider education, to help prevent avoidable injuries in children as light electric vehicles continue to become more accessible.

Modeling X-Chromosome Deletions in Skeletal and Gastrointestinal Muscle to Uncover Mechanisms in Duchenne Muscular Dystrophy

Investigator: Ellen Wu, B.S.
Mentor: Alakesh Bera, Ph.D.
Co-Authors(s):
Jane Nguyen, Uniformed Services University of the Health Sciences
Department(s): Anesthesiology
Poster #: 13B

INTRODUCTION

Duchenne muscular dystrophy (DMD) is a lethal X-linked disorder characterized by the dysfunction of the dystrophin protein, resulting in atrophy of skeletal muscles, paralysis, cardiopulmonary complications, and premature death. Current literature emphasizes skeletal and cardiac muscle pathology in DMD, while the role of dystrophin dysfunction in smooth muscle biology remains poorly understood. Moreover, the potential link between DMD-associated genomic instability and susceptibility to cellular transformation, or gastrointestinal cancers, has not been systematically explored. This study pinpoints novel relationships between DMD and gastrointestinal (GI) and gastroesophageal (GE) cancers. We hypothesize that the deletion or mutation of the DMD gene results in compensatory activation of oncogenic pathways (e.g., MYC) in skeletal muscle and GI or GE tissues.

METHODS

A bioinformatics model for DMD was developed by integrating multi-omics and functional meta-analyses derived from trusted databases (Human Protein Atlas and cBioPortal for Cancer Genomics). This model revealed that men with gastric cancers frequently exhibit deletions in the DMD gene locus. Key genes on the X-chromosome were selected to incorporate into a genetic panel that features a 'deleted hotspot' region along with compensatory gene loci located on chromosomes 3, 8, and 17. This panel captures pathogenic DMD deletions and compensatory oncogenic mechanisms indicating the novel characterization of a genetic connection between DMD and GI or GE cancers. We profiled seven genes of interest (MECOM, MUC20, MYC, DMD, FOXO4, AGO2, and KDM6A) and determined that they were differentially expressed between a DMD control cell line, human foreskin fibroblasts (HFFs), and gastric cancer cell lines (SNU-1, SNU-16, SNU-407, SNU-C4, GP2d) using PCR, Southern blotting, Western blotting, and immunohistochemical (IHC) staining.

RESULTS

PCR analysis demonstrated upregulation of AGO2 and KDM6A and downregulation of AR in SNU-1, SNU-16, SNU-407, SNU-C4, and GP2d cell lines compared to HFF. MECOM, MUC20, and MYC were upregulated in SNU-16, SNU-407, SNU-C4, and GP2d, but downregulated in SNU-1. DMD was downregulated in SNU-1, while FOXO4 was downregulated in SNU-1 and SNU-16. Southern blot and Western blot analyses demonstrated increased MYC, MUC20, and MECOM expression and decreased DMD and FOXO4 expression in SNU-16 compared to HFF. IHC staining further demonstrated increased MYC expression and decreased DMD expression in cancerous tissue compared to non-cancerous tissue.

CONCLUSION

By identifying shared genomic features between DMD, GI, and GE cancers, this work reveals a novel connection between dystrophin loss and amplification-driven oncogenic pathways, highlighting opportunities for biomarker discovery and targeted therapeutic strategies involving oncogene amplification and tumor suppressor gene downregulation. These findings suggest that DMD mutations may serve as a biomarker for gastric cancer risk and warrant further investigation as potential targets for cancer risk assessment and therapeutic development.

Validating the Clinical Utility of a Novel Prognostic Biomarker, SIAH, to Risk Stratify Operable Pancreatic Cancer Patients at Sentara-EVMS-VOA

Investigator: Stefan Yu, B.S.
Mentor: Amy H. Tang, Ph.D.
Co-Authors(s):
Samantha Vos, Macon & Joan Brock Virginia Health Sciences Eastern Virginia Medical School
Jonathan Baker, Macon & Joan Brock Virginia Health Sciences Eastern Virginia Medical School
Janet Winston, Sentara
Dennis Rowley, Sentara
Richard Hoefer, Sentara
Department(s): Biological and Translational Sciences
Poster #: 36B

INTRODUCTION

Pancreatic ductal adenocarcinoma (PDAC) is the 3rd leading cause of cancer-related death in the United States. The current relative 5-year survival for PDAC is 8%, and the cause of this dismal prognosis is multifactorial, including often late-stage diagnosis and a multidrug-resistant nature. KRAS is a small GTPase and, when oncogenically hyperactivated, is involved in several signaling pathways indispensable for malignant transformation. In 2026, there are an estimated 67,530 new cases of PDAC, with KRAS mutations underpinning 90% of cases. SIAH is an evolutionarily conserved E3 ligase that is the most downstream signaling gatekeeper of the EGFR/KRAS signaling pathway identified thus far. In this clinical study, we aim to determine whether SIAH High/Low expression is a prognostic indicator of relapse and survival in the operable PDAC cohort at Sentara Hospitals.

METHODS

This study's cohort consists of 354 patients diagnosed with PDAC between 2001 and 2016 who underwent surgical resection at Sentara. 148 PDAC tumor specimens were stained for SIAH, Ki-67, and EGFR, including 116 untreated primary tumors and 31 neoadjuvant chemotherapy (NACT)-treated residual tumors. The biomarker expression was scored by two clinical pathologists to ensure IHC accuracy. Pathological TNM classifications were updated following the 8th edition AJCC guidelines. A combination of clinicopathological parameters and biomarkers was used to form groups for statistical analysis. Kaplan-Meier survival curves were generated to determine the prognostic value of SIAH High/Low in predicting overall survival (OS) and relapse-free survival (RFS) in PDAC.

RESULTS

We observed increased survival in the borderline-operable cohort treated with NACT when compared to the upfront surgery primary cohort. Among the primary tumors, we found that high SIAH expression (>15%) is prognostic compared with patients with low SIAH expression (≤15%), in predicting decreased RFS in patients with stage III tumors ($p<0.03$) and in patients with grade 2 tumors ($p<0.05$).

CONCLUSION

We found that high versus low SIAH expression (15% cutoff) in the primary PDAC cohort is prognostic to predict patients' RFS and OS while augmenting the standard clinicopathological parameters. Currently, there is no NCCN recommended pathological biomarker for risk stratification of PDAC tumors comparable to how the measurement of the protein Ki-67 is utilized in breast cancer. Given the limited efficacy of current treatment regimens in the recurrent and metastatic settings, and with the continued development of novel therapies, SIAH has potential as a prognostic biomarker to refine individual risk stratification and treatment planning. We hope that in the future, SIAH-guided risk stratification can inform treatment intensity, potentially reducing unnecessary exposure to chemotherapy and radiation while improving patient outcomes.

Decomposing the Black–White Infant Mortality Gap by Gestational Age, United States, 2016–2023

Investigator: Jessica Zhang, B.A.
Mentor: Tetsuya Kawakita, MD, M.S.
Co-Authors(s):
None listed.
Department(s): Obstetrics and Gynecology
Poster #: 05B

INTRODUCTION

Persistent racial disparities in US infant mortality may reflect both differences in the distribution of gestational age (GA) at birth (GA-distribution) and differences in mortality within GA strata (GA-specific mortality). We decomposed the Black–White infant mortality gap into components attributable to GA-distribution and GA-specific mortality.

METHODS

We analyzed the US live births from 2016 to 2023 using the National Center for Health Statistics Linked Birth/Infant Death restricted file, constrained to maternal race non-Hispanic Black (NHB) or non-Hispanic White (NHW) single-race and gestational age 20 weeks or greater. The cohort includes 19,540,960 births to NHW (n = 15,274,847) and NHB (n = 4,266,113) individuals, with 107,233 infant deaths. A symmetric two-factor Kitagawa/Das Gupta decomposition separated the NHB–NHW infant mortality gap into a GA-distribution component and a GA-specific mortality component. Additionally, we examined stratum-specific contributions and temporal changes in the two components.

RESULTS

The NHB–NHW infant mortality gap was 5.50 per 1,000 births. Of this difference, 4.22 per 1,000 (76.7%; 95% CI, 74.6–79.0) was attributable to differences in GA-distribution, whereas 1.28 per 1,000 (23.3%) was attributable to differences in GA-specific mortality. GA-distribution dominated every GA stratum below 28 weeks; the 22–23-week stratum alone contributed 1.23 per 1,000 to the overall gap. Contrastingly, GA-specific mortality dominated at term, contributing 0.480 per 1,000 at 37–38 weeks and 0.768 per 1,000 at 39–40 weeks.

Notably, NHB infant mortality was lower than NHW mortality at the most immature gestational ages but higher at term, with the mortality curves crossing between 28 and 31 weeks gestation. However, this should not be interpreted as evidence of a survival advantage or as measures of care quality because conditioning on gestational age can induce collider bias.

Temporal analyses revealed that the share of NHB–NHW infant mortality gap attributable to GA-distribution declined by 8.40% in the 2021 birth cohort (95% CI, 6.41–10.39; P = .0002). Furthermore, the two components exhibited distinct temporal shifts: GA-distribution went down in 2020 by 0.404 per 1,000 whereas GA-specific mortality went up in 2021 by 0.507 per 1,000.

CONCLUSION

Most of the US Black–White infant mortality gap during 2016–2023 was attributable to differences in the distribution of gestational age rather than differences in mortality within GA categories. However, the decomposition captured an important shift in the disparity: GA-distribution dominated very preterm births, whereas GA-specific mortality dominated at term births. The distinct 2020 GA-distribution decrease and 2021 GA-specific mortality increase further indicated that the two components followed different temporal trajectories. These findings support treating GA-distribution and GA-specific mortality as distinct dimensions of the disparity rather than as interchangeable explanations.

Piloting the FLASH Comprehensive Sexual Health Curriculum Through a Virtual Summer Academy for Adolescents in Hampton Roads, Virginia

Investigator: Anhthu Cung, M.S.
Mentor: Hongyun (Tracy) Fu, Ph.D.
Co-Authors(s):
Keeley Yokley, Macon & Joan Brock Virginia Health Sciences Eastern Virginia Medical School
Chinenye Udemba, Norfolk State University
Kelly Zeng, Macon & Joan Brock Virginia Health Sciences Eastern Virginia Medical School
Maggie Tu, Brown University
Department(s): Pediatrics, Division of Community Health and Research
Poster #: 46A

INTRODUCTION

Comprehensive sexuality education (CSE) equips adolescents with the knowledge and skills to build healthy relationships and make informed health decisions; however, adolescents in Hampton Roads, Virginia, continue to experience uneven access to medically accurate, inclusive, and comprehensive sexual health education across school and community settings. To address this local need and expand accessible learning opportunities, Teen Health 360 implemented a virtual Summer Academy in 2026 in collaboration with local community partners. The Academy used the evidence-informed, developmentally appropriate Family Life and Sexual Health (FLASH) curriculum developed by Public Health – Seattle & King County.

METHODS

FLASH's middle school curriculum was delivered through a four-day virtual Summer Academy via Zoom in July 2026. Participants attended daily 90-minute sessions covering seven FLASH lessons on healthy relationships, communication, reproductive health, STI prevention, and contraceptive methods. Lesson-specific slides were developed to adapt the curriculum for virtual delivery, incorporating interactive strategies such as Kahoot knowledge checks, peer role-play scenarios, breakout-room activities, group discussions, and Zoom chat. Anonymous questions were collected daily to identify participants' interests and ongoing educational needs. Program outcomes were assessed using pre- and post-surveys, with Pearson chi-square tests examining changes in individual knowledge indicators and analysis of variance (ANOVA) assessing changes in overall knowledge scores.

RESULTS

Nineteen adolescents (aged 10–15 years) enrolled; 84.2% attended all four sessions, 89.5% attended at least three, and 73.7% completed the post-program evaluation. Among participants with available demographic data (n=17), 52.9% were male, 47.1% female, and 88.2% identified as Asian. Mean knowledge accuracy increased significantly from 65.6% at pre-survey (n=17) to 79.2% at post-survey (n=14), a 13.6-percentage-point gain ($p < .01$), with significant improvements across six HIV/STI, reproductive anatomy, and contraceptive knowledge indicators; the largest gain was recognizing that people with HIV/STIs may be asymptomatic (23.5% vs. 92.9%; $p < .001$). Post-program evaluations were highly favorable: 100% reported that FLASH would help them make safe and healthy decisions, 85.7% felt confident recognizing healthy relationships, and 78.6% felt confident discussing condom use with a partner. Open-ended post-survey feedback further suggested that the academy provided an engaging and supportive environment for discussing sensitive sexual health topics.

CONCLUSION

The virtual FLASH Summer Academy demonstrates the feasibility of delivering comprehensive, inclusive sexual health education through a community-based virtual model. FLASH's flexible, evidence-informed design supported medically accurate education while emphasizing communication, informed decision-making, healthy relationships, and personal agency through interactive learning.

Significant improvements in sexual health knowledge, coupled with high participant satisfaction and confidence in applying key skills, provide promising evidence of the program's effectiveness in strengthening adolescents' knowledge and fostering healthy decision-making. Virtual delivery, interactive activities, and anonymous question opportunities also fostered engagement and provided a supportive environment for discussing sensitive topics.

Future implementation will focus on expanding reach, evaluating behavioral and longer-term outcomes, and adapting the model across diverse community settings. Further scaling and evaluation of this virtual academy framework may offer a promising strategy for advancing equitable access to comprehensive sexuality education and bridging gaps in adolescent preventive health education.

Inflammatory and Immunological Biomarkers in Postpartum Depression : a Systematic review

Investigator: Rocio Soledad Maggioni , MD
Mentor: Alberto E. Musto, MD, Ph.D.
Co-Authors(s):
None listed.
Department(s): Center for Integrative Neuroscience and Inflammatory Diseases, Biomedical and Translational Sciences and Neurology, Macon & Joan Brock Virginia Health Sciences at Old Dominion University.
Poster #: 45A

INTRODUCTION
Postpartum depression (PPD), a depressive disorder arising after childbirth, affects approximately one in eight women and is associated with substantial consequences for maternal functioning, infant development, and family well-being, yet its biological basis remains poorly defined. Although immune- inflammatory dysregulation has been proposed as one of the main factors in PPD, its biological mechanism is not clear. Systemic inflammatory signals may communicate with the brain through neuroimmune and neuroendocrine pathways, providing a potential link between peripheral immune dysregulation and depressive symptoms. Accordingly, this systematic review aimed to: (a) characterize peripheral immune- inflammatory biomarkers associated with PPD; (b) examine whether these associations vary according to biomarker type, timing of measurement, and depressive phenotype or severity; and (c) identify gaps in the evidence linking systemic immune dysregulation to PPD.

METHODS
We conducted a systematic review with narrative synthesis in accordance with PRISMA 2020. PubMed, Scopus, Embase, and the Cochrane Library were searched through July 2026, supplemented by manual reference-list searches. Records were screened independently by two reviewers . Included studies evaluated inflammatory or immunological biomarkers during pregnancy or the postpartum period in relation to subsequent or concurrent PPD . Evidence was synthesized across cytokines and chemokines, acute- phase proteins, leukocyte-derived inflammatory indices, and cellular immune markers. Findings were organized according to biomarker pathway, timing of measurement, and whether immune alterations preceded later depressive outcomes or accompanied established PPD.

RESULTS
Fifty-three studies met the inclusion criteria. The evidence indicated timing- and phenotype-dependent immune heterogeneity rather than uniformly increased peripheral inflammation. During pregnancy, IL-6 and C-reactive protein showed limited and inconsistent associations with subsequent postpartum depressive outcomes. Several prospective findings instead implicated reduced anti-inflammatory signaling, particularly lower IL-10, including one cohort in which lower third-trimester IL-10 predicted higher postpartum depression scores ($\beta = -1.28$; $p = 0.006$); however, this pattern remains insufficiently replicated. In contrast, the strongest positive cytokine associations were observed when biomarkers were measured concurrently with established severe PPD. In one clinical sample, higher IL-6 and IL-8 were associated with approximately threefold greater odds of PPD, suggesting a potential state-related signal rather than prospective prediction. Findings during the early postpartum period were less consistent: CRP and IL-6 measured on postpartum day 2 predicted later PPD in one cohort but not others, while urinary IL-1β at day 14 preceded greater depressive symptoms at day 28 in a small prospective sample. Regulatory T cells, TNF-α trajectories, and leukocyte- and platelet-derived inflammatory indices suggested additional pathway-specific patterns, but small samples, heterogeneous outcome definitions, and limited replication prevented identification of a clinically validated immune signature.

CONCLUSIONS
PPD does not appear to correspond to a single state of generalized peripheral inflammation. Instead, the available evidence suggests the potential involvement of interacting cytokine and chemokine pathways that vary across the perinatal timeline, biological pathway, and depressive phenotype. These peripheral immune signals may communicate with the brain through blood–brain barrier, endothelial, neural, and neuroendocrine pathways, potentially affecting neurotransmission and mood regulation. Longitudinal studies integrating peripheral biomarkers with central nervous system measures are needed to clarify systemic-to-brain mechanisms in PPD.

My Body, My Call: Evaluating a Crowdsourcing Open Call to Engage Youth and Community Voices on Bodily Autonomy and Relationship Safety

Investigator: Chinenye Erica Udemba, B.S.
Mentor: Hongyun (Tracy) Fu, Ph.D.
Co-Authors(s):
None listed.
Department(s): Pediatrics
Poster #: 47A

INTRODUCTION
Adolescents continue to face disparities in sexual health education, as traditional approaches often rely on top-down, expert-driven methods that do not reflect youth perspectives and lived experiences. The Teen Health 360 Program promotes adolescent sexual wellness through health education, community engagement, and capacity-building. The program conducted annual crowdsourcing open calls, a structured approach that engages communities in generating innovative solutions, to amplify youth and community voices. The 2026 Open Call, themed "My Body, My Call: How Can Teens Communicate and Set Healthy Boundaries?" invited youth and community members to share their perspectives on communication, consent, bodily autonomy, and relationship safety. This study evaluated the effectiveness of the 2026 Open Call as a youth-centered strategy for community engagement and adolescent sexual health promotion.

METHODS
The open call theme was collaboratively developed by the Teen Advisory Committee and the Community Steering Committee to ensure that both youth and community perspectives shaped the focus of the contest. Following the World Health Organization (WHO) guidelines on crowdsourcing, the open call was promoted through in-person and virtual outreach across schools, community organizations, and social media. Entries were accepted in various formats, including essays, poetry, visual art, music, and videos. Submissions were screened for quality, completeness, authenticity, and responsible use of AI tools before being independently evaluated by 26 judges with diverse backgrounds, using standardized criteria that assessed relevance, innovation, inclusivity, feasibility, and quality. Descriptive statistics were analyzed using Microsoft Excel, while qualitative inductive coding identified themes among top-ranked submissions.

RESULTS
A total of 214 submissions were received, with 91 advancing to the judging round. Of these, 42 (46%) were submitted by youth and 49 (54%) by adults. Thirty entries received top scores (Mean ≥48, Score Range: 24 - 59) and were awarded prizes. Thematic analysis revealed three major themes: (1) judgment-free communication and emotionally safe spaces, (2) trusted adults and peer support, and (3) youth empowerment through consent education and self-advocacy.

CONCLUSION
Crowdsourcing open calls proved to be a feasible, youth-centered strategy for engaging communities on sensitive adolescent health topics and generating actionable insights to enhance sexual health education, outreach, and stigma-reduction efforts.

Save the Date

Research Day is Returning to the 2nd Friday in October!

MARK YOUR CALENDARS NOW!

Research Day 2027

Will be held on
Friday, October 8, 2027

Research Day 2028

Will be held on
Friday, October 13, 2028

Abstracts will be due in late July/early August



MACON & JOAN BROCK
VIRGINIA HEALTH SCIENCES
AT OLD DOMINION UNIVERSITY